DEMOCRATIC AND POPULAR REPUBLIC OF ALGERIA
MINISTRY OF HIGHER EDUCATION
AND SCIENTIFIC RESEARCH
UNIVERSITY M'HAMED BOUGARA OF BOUMERDES
FACULTY OF ENGINEERING
DEPARTMENT OF ELECTRICAL AND ELECTRONIC ENGINEERING

Biometric system: face recognition

Project Report
Submitted in partial fulfillment of the requirements for the Degree of

Magister

In telecommunication

by:

Nadjet RADJI
INGENIEUR D'ETAT

In front of the board of examiners:

President:	Mr Adel Belouchrani	Professor	ENP, Algiers
Members:	Mr Abedelhakim Dahimene	MCB	UMBB, Boumerdes
	Mrs Amina Serrir	MC	USTHB, Algiers
Supervisors:	Mrs Dalila Cherifi	MA	UMBB, Boumerdes
	Mr Hamid Bentarzi	MCA	UMBB, Boumerdes

Year 2010

Abstract

In the last decades, there has been a stronger focus on security around the world. One of the important issues in security is the need of correctly authenticate a person. Traditional methods of establishing a person's identity include passwords, keys or identification cards, but these surrogate representations of identity can easily be lost, shared, manipulated or stolen thereby compromising the intended security. Biometrics provides better security, higher efficiency, and increased user convenience. Among the more acceptable features used in biometrics is the face which provides a more direct, friendly and convenient identification method. Facial research in computer vision can be divided into several areas, such as face recognition, face detection, facial expressions analysis. In our thesis we are interesting on face recognition since it is a biometric method which has become more relevant and needed.

Many methods of face recognition have been proposed. Basically, they can be divided into three categories: Global-Appearance-based methods, local appearance-based methods and hybrid methods. The most successful and well-studied techniques are the appearance-based methods. So, in this thesis some of them are implemented namely: Principle Component Analysis (PCA), Fisher Linear Discriminant (FLD), Singular Value Decomposition (SVD), and Discrete Wavelet Transform (DWT) or Wavelet Packet Decomposition (WPD). The local appearance-based methods can be divided into two groups: The ones that require the use of specific regions and the ones that simply partition the input face image into blocks without considering any specific regions. For the latter type we have implemented the Discrete Cosine Transform (DCT) method.

Furthermore, we have applied DWT and WPD as preprocessing step for PCA, as well DWT for FLD and SVD in order to improve their performances.

Then, we have proposed a new method which combines PCA and WPD in YCbCr color space called (YCbCr-WPD-PCA) **[199]**.

In addition, we have introduced the multibiometrics system particularly multi-algorithm systems. In this thesis we have utilized multi-algorithm systems that consolidate the output of multiple feature extraction algorithms at score levels. We have used the fusion of two types and three types of feature vectors using four fusion rules i.e. minimum, maximum, mean, and product.

Finally, many experiments were conducted using different databases namely YALE, ORL, and FEI databases. The accuracy of each method has been identified and a comparison was performed between them in terms of recognition rates, Equal Error Rates (ERR) or the Receiver Operating Curves (ROC).

Key words: Biometrics, security, face recognition, PCA, FLD, SVD, DCT, DWT, WPD, YCbCr color space, Multibiometrics, fusion.

Résumé

Durant ces dernières années le problème de sécurité est devenu crucial pour l'identification de personnes, d'où la nécessité de développer des systèmes robustes utilisant la biométrie qui permettront une meilleure authentification de personnes remplaçant les méthodes traditionnelles. A rappeler que ces dernières utilisent des moyens d'authentifications tels que les mots de passe, les clés et les cartes d'identifications qui cependant peuvent être facilement perdues, partagées, manipulées ou volées.

En effet, la biométrie fournit une meilleure sécurité, une plus grande efficacité et une meilleure commodité des utilisateurs. Parmi les caractéristiques utilisées dans la biométrie, nous trouvons le visage qu'est plus acceptable par rapport aux autres méthodes biométriques et fournit des informations pertinentes dans les méthodes d'identifications.

La recherche faciale en vision par ordinateur peut être divisée en plusieurs thématiques à savoir l'analyse d'expressions faciales, la reconnaissance et la détection des visages. Plusieurs méthodes de reconnaissance de visages ont été développées. Fondamentalement, elles peuvent être divisées en trois catégories: les méthodes locales, les méthodes hybrides et les méthodes globales. A noter que ces dernières sont très utilisées dans la littérature. Les méthodes locales peuvent être divisées en deux groupes à savoir celles qui exigent l'utilisation de régions spécifiques et celles qui simplement partitionnent l'image en blocs sans envisager de régions spécifiques. Pour ce dernier type nous avons implémenté la transformée en cosinus discrète (DCT) méthode.

Concernant les méthodes globales nous avons implémenté dans notre projet certain d'entre elles qui sont respectivement: analyse en composantes principales (PCA), Fisher linéaire discriminante (FLD), décomposition en valeur singulière (SVD), la transformé en ondelette discrète (DWT) ou la transformée en paquets d'ondelettes (WPD).

Nous avons aussi utilisé DWT et WPD comme prétraitement pour PCA, également DWT pour FLD et SVD afin d'améliorer leurs performances.

Par la suite, nous avons proposé une nouvelle méthode qui combine PCA et WPD dans l'espace de couleurs YCbCr nommée (YCbCr-WPD-PCA) **[199]**.

Nous nous sommes intéressés au système multi-biométriques et plus précisément aux multi-algorithmes utilisant deux ou trois algorithmes afin de consolider les déférents résultats obtenus en niveau des scores. Enfin, plusieurs tests ont été réalisés en utilisant trois bases de données à savoir YALE, ORL, et FEI. Une étude statistique et comparative a été effectuée en prenant des paramètres statistiques tels que le taux d'erreur (ERR) et la courbe caractéristique (ROC).

Mots clés : Biométrie, Sécurité, Reconnaissance des visages, PCA, FLD, SVD DCT, DWT, WPD, YCbCr espace de couleurs, Multibiometrics, Fusion.

الملخص

خلال السنوات الماضية أصبح الأمن محل اهتمام في ميادين شتى في جميع أنحاء العالم, و من بين أهم قضايا الأمن التي ركزت عليها تتمثل في ضرورة توثيق أو تحديد هوية شخص بدقة ,تعتبر الوسائل التقليدية لتحديد هوية الشخص والتي تتضمن استعمال كلمة سر, مفاتيح أو بطاقات الهوية كبدائل لتمثيل الشخص, ولكن هذه الأخيرة يمكن فقدانها بسهولة, أو التلاعب بها أو سرقتها, و بذلك تعرض الأمن المراد للشبهة. مقارنة بالوسائل التقليدية علم المقاييس البيولوجية يوفر أكثر أمان, كفاءة أداء عالية, و يزيد من راحة المستخدمين. ومن بين الخصائص المستخدمة في علم المقاييس البيولوجية, الوجه, الذي يقدم طريقة مباشرة, ودية , مريحة و أكثر قبولا لتحديد هوية الأفراد مقارنة بالأساليب الأخرى. البحث العلمي للوجوه في الكومبيوتر البصري يمكن أن يقسم إلى عدة مجالات: كالتعرف على الوجه, تحديد الوجه, تحليل تعبيرات الوجوه. في السنوات الأخيرة أصبح التعرف على الوجه ضروريا و مطلوبا بكثرة.

اكتشفت العديد من التقنيات للتعرف على الوجوه و التي يمكن تقسيمها إلى ثلاث فئات: الطرق الإجمالية ,الطرق الهجينة و الطرق المحلية. وهذه الأخيرة يمكن أن تقسم إلى مجموعتين: تلك التي تتطلب استخدام مناطق محددة و تلك التي ببساطة تجزئ صورة إلى كتل دون النظر إلى مناطق محددة وفى هذا النوع الأخير أنجزنا محول جيب التمام المنفصل. بالنسبة للطرق الإجمالية طبقنا في هذا البحث عدة طرق هي كما يلي: تحليل المكونات الأساسية, تحليل فيشر الخطي ,تحليل إلى قيم فردية, محول الموجات الصغيرة المنفصل ,تحليل رزمة الموجات الصغيرة و استعملنا كذلك محول الموجات الصغيرة المنفصل و تحليل رزمة الموجات الصغيرة كمرحلة معالجة قبل تطبيق تحليل المكونات الأساسية, محول الموجات الصغيرة المنفصل قبل تطبيق محول جيب التمام المنفصل و تحليل إلى قيم فردية من أجل تحسين فعاليتهم.

و اقترحنا أيضا نظام يجمع بين تحليل المكونات الأساسية و تحليل رزمة الموجات الصغيرة في فضاء الألوان و استعرضنا كذلك المقاييس البيولوجية المتعددة و بشكل خاص نظام متعدد الخوارزميات الذي يدمج بين الناتج من مختلف خوارزميات استخلاص السمات. استخدمنا دمج نوعين ودمج ثلاثة أنواع من استخلاص السمات باستعمال أربع قواعد للدمج :الحد الأدنى ,الحد الأعلى ,المعدل, حاصل الضرب. أجريت اختبارات باستخدام قواعد بيانات مختلفة . حددت دقة كل خوارزمية وأجريت المقارنة بينهم باستخدام نسب التعرف أو معدل الخطأ المتساوي باستخدام منحنيات تشغيل الاستقبال .

الكلمات الأساسية: المقاييس البيولوجية, الأمن ,التعرف على الوجه , تحليل المكونات الأساسية, تحليل إلى قيم فردية, تحليل فيشر الخطي, محول الموجات الصغيرة المنفصل ,محول جيب التمام المنفصل ,تحليل رزمة الموجات الصغيرة, فضاء الألوان , المقاييس البيولوجية المتعددة, ا دماج.

Dedication

This modest work is dedicated

To my beloved mother, who has been a source of inspiration and encouragement to me throughout my life;

To my beloved father who gave everything they ever had, so i could pursue my dream;

To my sisters: Fahima, Rafika, Hanane, Sarah, Chaimaa, Nour- el- houda;

To my brothers: Fouad, Mohamed- Ali, Fahem;

To all my family;

To all my friends without exception

Acknowledgement

First of all, I thank Allah for giving me strength and ability to complete this study. Furthermore, I would like to express my deepest gratitude to my advisors Dr. Cherifi Dalila and Dr. Bentarzi Hamid for their powerful guidance, motivation, valuable suggestions, support and attention throughout this research. I thank all my friends for sharing their experiences and knowledge. Special thank to O.K. Khaddar for his useful help during my research. Finally, I am deeply grateful to my parents for their trust everlasting love, care, and indefectible support morally and materially during all my years of studying.

Table of contents

Table of contents

Table of contents

List of Figures

List of Figures

List of Figures

List of Tables

List of symbols

Symbol	Definition
FAR	False Accept Rate.
FRR	False Reject Rate.
ROC	Receiver Operating Characteristic plots the FRR against the FAR.
EER	Equal Error Rate equal refers to that point in ROC curve where the FAR equals the FRR.
PCA	Principal Component Analysis.
FLD	Fisher Linear Discriminant.
SVD	Singular Value Decomposition.
DCT	Discrete Cosine Transform.
DWT	Discrete wavelet decomposition.
WPD	Wavelet Packet Decomposition.
ICA	Independent Component Analysis.
YCbCr	Color space (Y is luminance Cr and Cb are red and blue chromaticity respectively).
Ψ	Mean face vector.
I_i	Face image matrix.
Γ_i	Face image vector.
ϕ_i	Mean- subtract face vectors.
A	Mean- subtract face matrix by arranging mean- subtract face vectors.
C	Covariance matrix.
U_k , λ_k	Eigenvectors and eigenvalues of C respectively.
RER	Rebuild Error Ratio.
Ω_i	Feature vector of training images.
Ω_{test}	Feature vector of test image.
θ	Threshold.
$\varepsilon_k(\Omega_{test}, \Omega_k)$	Distance between the test face and all the stored faces.
W	Projection matrix.
W_{opt}	Optimal projection matrix.
W_{PCA}	PCA projection matrix.
W_{FLD}	FLD projection matrix.
S_b	Between classes scatter matrix.
S_W	Within class scatter matrix.
$S_T = S_W + S_b$	Total scatter matrix.
SSS	Small sample size problem.
σ_i	Singular values.
$\sum_A$	Diagonal matrix with singular values (SV) on the diagonal.
ORL	Face database from AT&T Laboratories.
Yale	Face database from Yale University.
FEI	Face database from Artificial Intelligence Laboratory of FEI.
GUI	Graphical User Interface.

Introduction

Biometrics is the science of establishing the identity of an individual based on the physical, chemical or behavioral features of the person. Among the features that may be are: face, fingerprints, hand geometry, handwriting, iris, retinal, vein, and voice.

Traditional methods of establishing a person's identity include knowledge- based (passwords) and token-based (keys or ID cards) mechanisms, but these surrogate representations of identity can easily be lost, shared, manipulated or stolen thereby compromising the intended security. Biometric recognition provides better security, higher efficiency, and, in many instances, increased user convenience. By using biometrics, it is possible to establish an identity based on who you are, rather than by what you possess, such as an ID card, or what you remember, such as a password.

Facial research in computer vision can be divided into several areas, such as face recognition, face detection, facial expressions analysis, among others. Face recognition systems have a wide range of application, especially when dealing with security applications, like computer and physical access control, real-time subject identification and authentication, criminal screening and surveillance.

The biggest difficulty in developing a robust face recognizer is that a human face can undergo several transformations. The same person may use different face accessories like glasses, earrings, piercings and makeup. He can change his hair into long/short/skin/fringe and even dye it. He can also wear beard and mustache. Besides, he can be at many facial expressions like smiling, sad or doing a grimace and he can be at many different ages. These facial changes make the recognition task very difficult even human beings do some recognition mistakes from time to time.

Many methods of face recognition for still images have been proposed. Basically they can be divided into three categories:

→ Global-Appearance-based methods, where the whole image is used as a raw input to the learning process.

→ The local appearance-based methods can be divided into two groups: The ones that require the use of specific regions located on a face such as eyes, nose and mouth, as well as their relationships with each other and the ones that simply partition the input face image into blocks without considering any specific regions.

→ Hybrid methods try to use the best of the holistic and feature-based approaches combining local features and the whole face to recognize. The most successful and well-studied techniques to face recognition are the appearance-based methods. So in this thesis several face recognition methods are implemented, among them PCA, FLD, SVD, and DWT.

Introduction

With the increasing availability of color images, approaches have developed for integrating color information into the recognition process. Since the grey-scale approach is sensitive to lighting variations, we have chosen an approach which takes into consideration the intensity information as well as the chromatic information. We have proposed a method that uses color information based on YCbCr color space.

The pronounced need for establishing identity in a reliable manner has spurred active research in the field of biometrics. It is now apparent that a single biometric is not sufficient to meet the variety of requirements including matching performance imposed by several large-scale authentication systems. Multibiometric systems seek to remove some drawbacks encountered by unibiometric systems by consolidating the evidence presented by multiple biometric traits, sources or methods of processing. These systems can significantly improve the recognition performance of a biometric system.

A multibiometric system relies on the evidence presented by multiple sources of biometric information. Based on the nature of these sources, a multibiometric system can be classified into one of the following six categories: multi-sensor, multi-algorithm, multi instance, multi-sample, multimodal and hybrid. And based on the type of information available in a certain module, different levels of fusion may be defined. The various levels of fusion are categorized into two broad categories: pre-classification or fusion before matching, and post-classification or fusion after matching. Pre-classification schemes include fusion at the sensor and the feature levels while post-classification schemes include fusion at the match score, rank and decision levels. In this thesis we have utilized multi-algorithm systems that consolidate the output of multiple feature extraction algorithms at score levels. We have used the fusion of two types and three types of feature vectors.

In this thesis, an overview to biometric system is presented in Chapter I. Chapter II provides a brief background of the field of face recognition, including a description of various existing techniques and then introducing our proposed method and the fusion methods. Chapter III discusses the experimental results of the methods described in chapter II. Chapter IV presents the graphical user interface application for testing the different methods. A conclusion summarizes the realized work and discusses future research directions.

Chapitre I

Biometric system overview

I.1. Introduction:

This chapter provides an overview to the topic of biometric recognition. In the first section, the meaning of biometrics is defined; the types of biometrics are stated as well as factors that determine the suitability of a physical or a behavioral trait to be used in a biometric application. Several biometric modalities are then listed and briefly described. The general concepts related to biometric recognition systems are then introduced in the second section, including identification and definition of the main tasks needing to be performed. Methods for evaluating and comparing the performance of the systems are discussed. The meaning of security is defined in the third section. The relation of biometrics to security is then presented in the last section by giving some applications.

I.2. Biometrics:

I.2.1. Definition:

The generic definitions of biometrics are as follow **[1]**:

- ✓ Biometrics is the science of establishing the identity of an individual based on the physical, chemical or behavioral attributes of the person **[2]**.
- ✓ The term biometrics appears in the early 20th century, and is at first employed as a synonym of biometry, formed from the ancient Greek words **bios** (life) and **metrikos** (measure).
- ✓ Biometrics is the development of statistical and mathematical methods applicable to data analysis problems in the biological sciences.
- ✓ Biometrics is characteristic of the body as a method to code or scramble/ de-scramble data.
- ✓ Biometrics is used to identify people based on their biological traits.
- ✓ Biometrics is the measurement and matching of biological characteristics such as fingerprint images, hand geometry, facial recognition, etc.
- ✓ Biometrics is the application of statistics and mathematics to problems with a biological component.
- ✓ Biometrics uses a unique physical attribute of your body, such as your fingerprint or iris, to identify and verify you.
- ✓ Biometrics is unique personal characteristics
- ✓ Biometrics, or bio-identification, is the practice of measuring physical characteristics of a person to verify their identity.
- ✓ Biometrics = identification/verification of persons based on the unique physiological or behavioral features of humans.
- ✓ Biometrics is defined as the automated recognition of individuals based on their biological or behavioral characteristics.
- ✓ Biometrics any human physical or biological feature that can be measured and used for the purpose of automated or semi-automated identification.
- ✓ Biometrics is strongly linked to a stored identity to the physical person.
- ✓ Biometrics is measurable, physiological and/or behavioral characteristics that verify the identity of an individual.
- ✓ Biometrics is the automated use of physiological or behavioral characteristics to determine or verify identity.

I.2.2. Types of biometrics:

Biometric systems use a variety of physical or behavioral characteristics, including fingerprint, face, hand/finger geometry, iris, retina, signature, gait, palmprints, voice pattern, ear, hand vein, odor or the DNA information of an individual to establish identity. In the biometric literature, these characteristics are referred to as traits, indicators, identifiers or modalities **[2]**. The various biometric modalities can be broadly categorized as **[3]**:

- → **Physical biometrics**: These involve some form of physical measurement and include modalities such as face, fingerprints, iris-scans, hand geometry etc.
- → **Behavioral biometrics**: These are usually temporal in nature and involve measuring the way in which a user performs certain tasks. This includes modalities such as speech, signature, gait, keystroke dynamics etc.
- → **Chemical biometrics**: This is still a nascent field and involves measuring chemical cues such as odor and the chemical composition of human perspiration.

I.2.3. Biometrics Consideration:

Jain et al. have identified seven factors that determine the suitability of a physical or a behavioral trait to be used in a biometric application **[2]**.

- ✓ **Universality:** Every individual accessing the application should possess the trait.
- ✓ **Uniqueness:** The given trait should be sufficiently different across individuals comprising the population.
- ✓ **Permanence:** The biometric trait of an individual should be sufficiently invariant over a period of time with respect to the matching algorithm. A trait that changes significantly over time is not a useful biometric.
- ✓ **Measurability:** It should be possible to acquire and digitize the biometric trait using suitable devices that do not cause undue inconvenience to the individual. Furthermore, the acquired raw data should be amenable to processing in order to extract representative feature sets.
- ✓ **Performance:** The recognition accuracy and the resources required to achieve that accuracy should meet the constraints imposed by the application.
- ✓ **Acceptability:** Individuals in the target population that will utilize the application should be willing to present their biometric trait to the system.
- ✓ **Circumvention:** This refers to the ease with which the trait of an individual can be imitated using artifacts (e.g., fake fingers), in the case of physical traits, and mimicry, in the case of behavioral traits.

I.2.4.Biometric modalities:

Several modalities commonly employed for biometric system are established:

I.2.4.1.Face:

This modality is one of the most commonly used by people to recognize each other. During its evolution, the human brain has developed highly specialized areas dedicated to the analysis of facial images. Indeed, in addition to the once vital necessity of being able to instantly determine whether the unexpectedly encountered individual is a friend or a foe, social interactions also strongly depend on the capability to interpret many subtle facial expressions conveying a great deal of information **[4]**.

I.2.4.2.Fingerprints:

A fingerprint usually appears as a series of dark lines that present the high, peaking portion of the friction ridge skin, while the valleys between these ridges appear as white space and are the low, shallow portion of the friction ridge skin. Fingerprint identification is based primarily on the minutiae, or the location and direction of the ridge endings and bifurcations along a ridge path **[5]**. Minutiae points are the local ridge characteristics that occur either at a ridge ending or a ridge bifurcation.

A ridge ending is defined as the point where the ridge ends abruptly and the ridge bifurcation is the point where the ridge splits into two or more branches. Fingerprints were originally taken using the well-known ink-and-roll technique, and stored on paper cards. This process can now be accomplished using electronic scanners that produce a digital image of the fingerprint pattern. Unlike many other modalities, a great variety of sensors can be employed to acquire fingerprints, such as optical, capacitive, ultrasonic or thermal ones **[4]**.

(a) **(b)**

Figure I.1: Fingerprint recognition **(a)** Optical fingerprint reader **(b)** Fingerprints

I.2.4.3.Hand geometry:

Hand geometry recognition systems are based on a number of measurements taken from the human hand, including its shape, size of palm, the lengths and widths of the fingers **[2] [6]**, distances between joints, and the shape of knuckles **[7]**. The user places his/her hand in a small device, and positions his or her fingers according to a set of pins on the device. Using optical cameras and light-emitting diodes that have mirrors and reflectors, two orthogonal, two dimension images of the back and the sides of the hand are taken. Based on these images, 96 measurements are then calculated and a template created. Most hand readers have pins to help position the hand properly. These pins help with consistent hand placement and template repeatability, so there is a low false positive rate and a low failure to match rate **[7]**.

The large size of the sensor needed to acquire the hand geometry restricts its deployment to stationary access control systems. Moreover, this modality is not very distinctive, and is therefore not very well adapted to identification applications among a large number of users. Finally, some medical conditions like arthritis, that diminishes the mobility of the hand, may prevent accurate measurements, potentially causing a large number of false rejections with affected individuals **[4]**.

(a) **(c)** **(b)**

Figure I.2: Hand geometry recognition **(a)** Hand geometry reader, **(b)** Hand including mirror image as seen by the CCD Camera, **(c)** Distance measurements example

I.2.4.4.Eye (Iris/Retina):

The iris is the colorful part of the eye between the white (sclera) and the pupil. The properties of the iris that enhance its suitability for use in automatic identification include: protection from the external environment, impossibility of surgical modification without risking the vision, and physiological response to light which provides a natural test. Iris recognition is fast, and noninvasive **[8]**.

The retina, the backside of the eyeball, has unique patterns of blood vessels. In the retinal scan, a biometric template is formed by scanning the retina and recording the patterns of capillary blood vessels at the back of the eye. Once the retina is scanned, special software creates a digital profile of the user's unique pattern of blood vessels. The image is processed and saved in the templates, and these templates are stored in user's identification card or in a central database **[8]**.

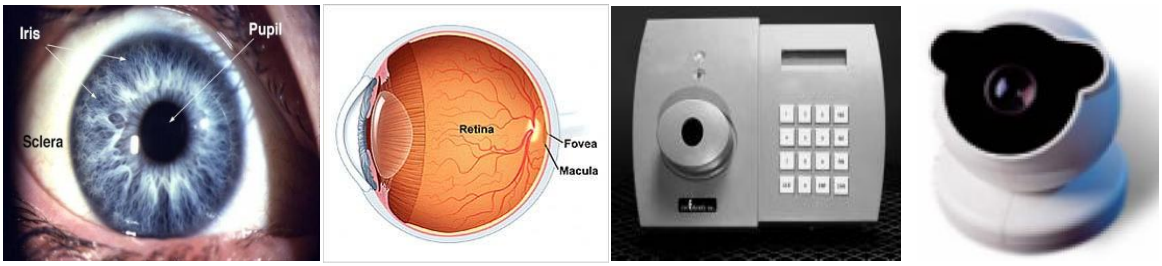

(a) **(b)** **(c)** **(d)**

Figure I.3: Eye recognition **(a)** Iris, **(b)** Retina, **(c)** The retinal eye scanner, **(d)** The iris scanner

I.2.4.5.Signature:

A handwritten signature can be defined as the scripted name or legal mark of an individual, executed by hand for the purpose of authenticating writing in a permanent form **[9]**.

Hilton (1992) notes that the signature has at least three attributes: form, movement, and variation. Since signatures are produced by moving a pen on a paper, movement perhaps is the most important aspect of a signature. Movement is produced by muscles of the fingers, hand, wrist, and, for some writers, arm; these muscles are controlled by nerve impulses. Once a person is used to sign, these nerve impulses are controlled by the brain without any particular attention to detail.

Signatures can be classified as simple, cursive, or graphical based on their form and content, as shown in Figure I.4. A simple signature is one where a person scripts his or her name in a stylish manner. In this type of signature, it is very easy to interpret all the characters in the name. Cursive signatures, on the other hand, are more complex. Though the signatures still contain all the individual characters within the name, they are, however, drafted in a cursive manner, usually in a single stroke. Lastly, the signatures are classified as graphical when they portray complex geometric patterns. It is very difficult to deduce the name of the person from a graphical signature, as it is more of a sketch of the name of the signer.

Type	Genuine	Skilled forgery	Unskilled forgery
Simple			
Cursive			
Graphical	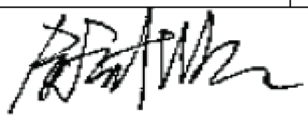		

Figure I.4. Types of signatures

I.2.4.6.Voice:

Voice is a combination of physical and behavioral biometrics. The features of an individual's voice are based on the shape and size of the appendages (e.g., vocal tracts, mouth, nasal cavities, and lips) that are used in the synthesis of the sound **[10]**. Automated biometric systems based on this modality are called automatic speaker verification (ASV) or automatic speaker identification (ASI) systems. They should not be confused with speech recognition systems, which aim at transcribing the information conveyed by the voice into text. If the ASV or ASI system is text dependent, the user is required to speak a selected sequence of words, whereas any kind of words or sentences can be uttered in the case of a text independent system. Typical factors that can contribute to authentication errors are: age, sickness, acoustics, misread or misspoken utterances, words or phrases, emotional states of individual, e.g. stress or duress, and placement of microphone or the use of different microphones.

I.2.4.7.Keystroke dynamics:

It is hypothesized that each person types on a keyboard, he has his own manner. This behavioral biometric is not expected to be unique to each individual but it is expected to offer sufficient discriminatory information that permits identity verification. Keystroke dynamics is a behavioral biometric; for some individuals, one may expect to observe large variations in typical typing patterns. Furthermore, the keystrokes of a person using a system could be monitored unobtrusively as that person is keying in information. However, this biometric permits "continuous verification" of an individual during a period of time **[11]**.

Figure I.5: keystroke dynamics

I.2.4.8.Other biometrics

There exists other biometrics such as: thermogram, smile recognition, lip recognition, ear prints, skin spectroscopy, odor, gait, Electrocardiogram (ECG), and DNA Analysis.

I.3. Biometric system:

I. 3.1. Overview:

The basic block diagram of a biometric system is shown in figure I.6. It comprises a sensor module, feature extraction module, a matching module, and a database module [**6**] **[1]**.

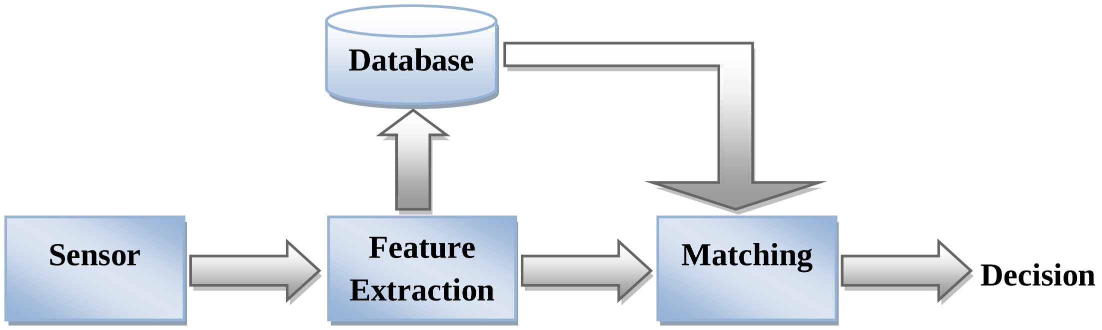

Figure I.6: Basic block diagram of a biometric system.

1. Sensor module: A suitable biometric reader or scanner is required to acquire the raw biometric data of an individual. To obtain fingerprint images, for example, an optical fingerprint sensor may be used to take an image of the friction ridge structure of the fingertip.

2. Feature Extraction module: It is the stage in which the acquired data is processed to extract feature values. For example, the position and orientation of minutiae points in the fingerprint image would be computed in the feature extraction module of a fingerprint system.

3. Matching module: Matching is carried out when the feature values are compared with those in the template by generating a matching score. For example, in this module, the number of matching minutiae between the query and the template can be computed and processed as a matching score.

4. Decision-making module: In decision-making phase, the user's claimed identity is either accepted or rejected based on the matching score generated in the matching module.

5. Database module: The database acts as the repository of biometric information. During the enrollment process, the feature set extracted from the raw biometric sample (i.e., the template) is stored in the database along with some biographic information (such as name, Personal Identification Number (PIN), address, etc.) characterizing the user.

I.3.2. Operations:

In the operation of a biometric system, two distinct phases can be identified: an enrollment procedure and a recognition phase. For the second phase, two modes of operation can further be distinguished: verification, also called authentication, and identification.

I.3.2.1. Enrollment:

Biometric enrollment is the process of registering subjects in biometric databases **[12] [13]**:

- → **Positive enrollment** (enrollment for verification and positive identification): The purpose of enrollment is to construct the database of eligible subjects or members. It has to be somehow determined what makes a subject eligible to be enrolled, and all enrollees must be checked against these criteria. Each subject is enrolled with a biometric template. The subject is issued an ID number or some possession that contains the biometric template.

- → **Negative enrollment** (enrollment for negative identification): The collection of subjects in the database that is ineligible for some application. It has to be determined for what reasons a subject would be ineligible, like membership of a most-wanted list.

I.3.2.2. Verification:

Verification occurs when the biometric system asks and attempts to answer the question, “Is this X?” after the user claims to be X .In verification phase, the biometric system requires input from the user , at which time the user claimed his or her via a password , token identity matches an individual against a claimed identity. The corresponding template is retrieved or a user name, or any combination of the three. This user input points the system to a template in the system also requires a biometric sample from the user it then processes and compares the sample to or against the user-defined template. This is called a "one-to-one" search (1:1). The system will either find or fail to find a match between the two **[14]**.

I.3.2.3. Identification:

In identification phase, the biometric system asks and attempts to answer the question, "Who is X?". In this phase, the biometric device reads a sample, processes it and compares it against every record or template in the database. This type of comparison is called "one-to-many" search (1: N). Depending on how the system is designed it can make a best match, or it can score possible matches, ranking them in order of likelihood **[14]**. Such biometric identification system can be used in two different modes **[13]**.

- → **Positive identification:** In this mode, the system expects there to be a match between the biometric presented and the template. These systems are designed to make sure that a person is in the database. The errors that can be made are false accept and false reject. In fact, positive identification is functionally similar to verification.
- → **Negative identification:** Negative systems are set up to make sure that a person is not in the system. The errors that can be made are false negative errors and false positive errors, i.e., missing a match and false detection of a match.

I.3.3.Performance evaluation:

Unlike passwords and cryptographic keys, biometric templates have high uncertainty. There is considerable variation between biometric samples of the same user taken at different instances of time. Therefore the match is always done probabilistically. This is in contrast to exact match required by password and token based approaches **[3]**. The inexact matching leads to two forms of errors:

I.3.3.1.False Accept Rate (FAR):

False accept rate or the false match rate (FMR) an impostor may sometime be accepted as a genuine user, if the similarity with his template falls within the intra-user variation of the genuine user.

I.3.3.2.False Reject Rate (FRR):

False Reject Rate is often referred to as the false non match rate (FNMR) when the acquired biometric signal is of poor quality, even a genuine user may be rejected during authentication.

Besides, the biometric system can encounter other types of failures such as:

I.3.3.3.The Failure to Capture (FTC):

FTC denotes the proportion of times the biometric device fails to capture a sample when the biometric characteristic is introduced to it. This type of error typically occurs when the device is not able to locate a biometric signal with good quality (e.g., an extremely faint fingerprint or an occluded face image). The FTC rate is also impacted by sensor wear and tear. Thus, periodic sensor maintenance is necessary for the efficient functioning of the biometric system **[2]**.

I.3.3.4.Failure to enroll (FTE):

A system's failure-to-enroll (FTE) rate represents the probability that a given user will be unable to enroll in the biometric system. FTEs occur when users have insufficiently distinctive or replicable biometric data or when the design of the biometric solution is such that providing consistent data is difficult. High failure-to-enroll rates can be particularly problematic for the biometric system, as users unable to enroll must verify through another biometric technology or authentication method **[15]**.

I.3.3.5.Failure to authenticate (FTA):

This error occurs when the system is unable to extract features during verification even though the biometric was legible during enrollment. In case of fingerprints this may be caused due to excessive sweating, recent injury etc. In case of speech, this may be caused by cold, sore throat etc. It should be noted that this error is distinct from false reject where the rejection occurs during the matching phase. However in FTA, the rejection occurs in the feature extraction stage itself.

The performance of biometric system may also be summarized using other single-valued measures such as the Equal Error Rate (EER) and the d-prime value.

I.3.3.6.Equal Error Rate equal or Crossover Error Rate (EER or CER):

The EER refers to that point in a Detection Error Tradeoff (DET) curve or Receiver Operating Characteristic (ROC) curve where the FAR equals the FRR. A lower EER value indicates better performance. DET curve plots the FRR against the FAR at various thresholds on a normal deviate scale and interpolates between these points. When a linear, logarithmic or semi-logarithmic scale is used to plot these error rates, then the resulting graph is known as a (ROC) curve. The main difference between the DET and ROC curves is the use of the normal deviate scale in the former **[2]**.

I.3.3.7.The d-prime value (d'):

The d-prime value (d') measures the separation between the means of the genuine and impostor probability distributions in standard deviation units and is defined as,

$$\boldsymbol{d'} = \frac{\sqrt{2}\left|\boldsymbol{\mu_{genuine}} - \boldsymbol{\mu_{impostor}}\right|}{\boldsymbol{\sigma^2_{genuine}} + \boldsymbol{\sigma^2_{imposter}}} \qquad (\text{I. }1)$$

Where the $\mu's$ and $\sigma's$ are the means and standard deviations, respectively, of the genuine and impostor distributions. A higher d-prime value indicates better performance.

Poh and Bengio introduce another single-valued measure known as F-Ratio which is defined as,

$$F-ratio = \frac{\mu_{genuine} - \mu_{impostor}}{\mu_{genuine} + \mu_{impostor}} \quad (I.2)$$

If the genuine and impostor distributions are Gaussian, then the EER and F-ratio are related according to the following expression:

$$EER = \frac{1}{2} - \frac{1}{2} erf\left(\frac{F-ratio}{\sqrt{2}}\right) \quad (I.3)$$

Where

$$erf(x) = \frac{2}{\sqrt{\pi}} \int_0^x e^{-t^2} dt \quad (I.4)$$

Another more operational measure which combines FAR and FRR into the so-called decision cost function (DCF) given as follows **[16]**:

$$DCF = C_{FR} P_{tar} FRR + C_{FA} P_{imp} FAR \quad (I.5)$$

Where C_{FR} is the cost of false rejection, C_{FA} is the cost of false acceptance, P_{tar} is the a priori probability of targets and P_{imp} is the a priori probability of impostors. A particular case of the DCF is known as the half total error rate (HTER) where the costs are equal to 1 and the probabilities are 0.5 each:

$$HTER = (FAR + FRR)/2 \quad (I.6)$$

I.3.3.8.Ability-to-Verify (ATV) Rate:

ATV is a combination of the failure-to-enroll and false nonmatch rates, and indicates the overall percentage of users who will be capable of authenticating on a daily basis. ATV is given by:

$$ATV = (1 - FTE)(1 - FNMR) \quad (I.7)$$

This metric can be thought of as representing the group of users who cannot enroll (FTE) along with users falsely rejected by the system (FNMR). No system has 100 percent ATV rate, but, in general, a high ATV rate will make for a more effective system **[15]**.

I.4.What is security?

In general, security is the condition of being protected against danger or loss, which is a concept similar to safety. The word "security" as a technical term security means that something that is not only secure but that also has been secured. In the last years, there has been a stronger focus on security in the media all over the world. One of the important issues in security is the need of correctly authenticate a person [**17**]. Traditional methods of establishing a person's identity include passwords, keys or ID cards, but these surrogate representations of identity can easily be lost, shared, manipulated or stolen thereby compromising the intended security [**2**]. Biometric recognition provides better security, higher efficiency, and, in many instances, increased user convenience **[12]**.

I.5. Biometrics and security [1]: The areas where biometrics could be used are:

→ **access and border security**

- Confirming that a passenger boarding a plane is the same individual who checked in. Passengers would be asked to agree to a biometric scan at check-in and again at the gate.
- Providing rapid approval to anyone with immigration clearance, freeing up resources to focus on other travelers.
- Controlling access to restricted areas. This would apply to staff, who would gain access to buildings or rooms either through demonstrating that they matched the biometric stored on their card or through comparison with a database.
- Identifying known terrorists or criminals. Biometrics would be scanned from people passing through airports and compared with a database of known criminals or terrorists.

→ **Police and prison services**

The police and prison services have access to large amounts of sensitive personal information. Biometrics would be an ideal method to make sure that officers can only access information they are authorized to access. The large prisons in UK have installed a hand geometry recognition system to identify the visitors. To meet the requirements of the Learmont and Woodcock reports, visitors have to be identified by two different methods when entering and leaving the prison. This is to ensure that a prisoner does not walk out of the prison in place of the visitor.

→ **Patient management in hospitals**

Most patient records are now held electronically. It is important that anyone who uses the system can only access information that is relevant to the jobs they are doing. Potentially biometrics could be used to keep track of patients, and prevent them from having the wrong procedures carried out or mistakenly be given the wrong drugs. The patient could have their fingerprints taken on admission; the prints would then be checked whenever treatments are administered. This would be especially useful for seriously ill, elderly or mentally ill patients who may have difficulty communicating.

→ **Enterprise network security and web access**

Many companies have internal networks where security of information has to be maintained, with only authorized users able to access it. With the growth of the Internet, there is now a need to restrict access to sensitive data on the web to authorized users only. The web services depend upon the Internet Protocol (IP) name service. If an impostor gains access to the name service, the security based upon correlating names and the network address will fail. The traditional method of authentication involves using usernames and passwords, which are openly transmitted across the network. Passwords can be made more secure by using encryption but not 100 per cent secured. The biometric authentication eliminates the need to remember passwords. The person also needs to be physically present at the time of authentication.

I.6.conclusion:

In this chapter, the definition of biometrics has been provided, and the properties and tasks associated to biometric recognition systems have been introduced. Among the many biometric modalities discussed, face provides a more direct, friendly and convenient identification method and is more acceptable compared with the individual identification methods of other biometrics modalities. Thus, face recognition is one of the most important parts in biometrics. In the next chapter, we will therefore present various methods that have been proposed to perform biometric authentication based on facial images. In addition to methods using fusion, we will propose method by combining principal component, wavelet packet decomposition and YCbCr color space.

Chapitre II

Face recognition methods

II.1.Introduction:

This chapter is dedicated for the face recognition methods. In the first section, we discuss the role of face in modern life. The problematic of the face recognition is given in the second section followed by the steps of a typical face recognition process, where the identification and definition of the main tasks needing to be performed is included. Techniques of recognition for still images are described in the third section. In the fourth, fifth, sixth, seventh and eighth sections we describe the algorithms used, PCA, FDA, SVD, DCT, and DWT respectively. In the ninth section we present the proposed method using WPD and PCA in YCbCr color space. Face recognition using fusion is described in the last section.

II.2.Role of face in modern life:

In the modern life, the need for personal security and access control is becoming an important issue. Biometrics is the technology which is expected to replace traditional authentication methods that are easily stolen, forgotten and duplicated. Fingerprints, face, iris, and voice are commonly used biometric features. Among these features, face provides a more direct, friendly and convenient identification method and is more acceptable compared with the individual identification methods of other biometrics features. Thus, face recognition is one of the most important parts in biometrics **[18]**.

Although face recognition is not as accurate as the other recognition methods such as fingerprints. It still grabs huge attention of many researchers in the field of computer vision. The main reason behind this attention is the fact that the face is the conventional way people use to identify each others**[19**, **20]**.

Face recognition is a non-contact personal identification technique which has advantages over contact identifications such as fingerprints and iris texture **[21]**. Face recognition has many important applications, including security, access control to buildings, identification of criminals and human-computer interfaces. Thus, it has been a well-studied problem despite its many inherent difficulties, such as varying illumination, occlusion and pose **[22]**.

II.3.The Face Recognition Problematic:

A general statement of the problem of machine recognition of faces can be formulated as follows: Given still or video images of a scene, identify or verify one or more persons in the scene using a stored database of faces **[**23, **24**, **25]**.

The steps of a typical face recognition process are given in figure II.1:

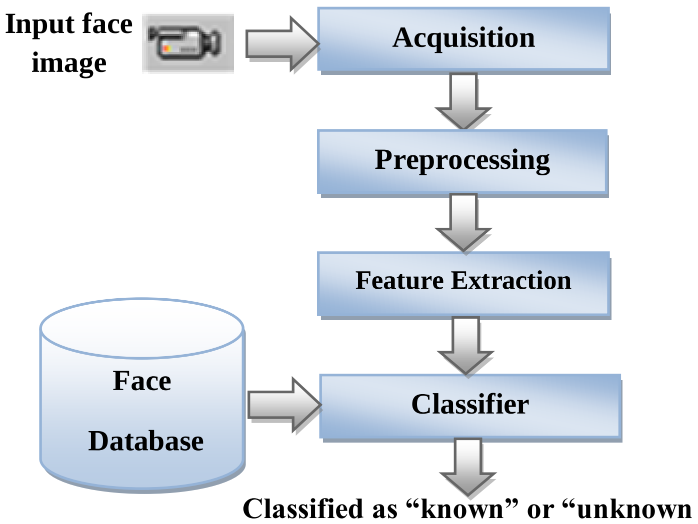

Figure II.1: Steps of a typical face recognition process.

1. Acquisition module:

This is the entry point of the face recognition process. It is the module where the considered face image is presented to the system. The acquisition can be accomplished by digital scanning of an existing photograph or by using an electro-optical camera to acquire a live picture of a subject **[26]**.

2. Pre-processing module:

By using conventional vision techniques, face images are normalized and they are enhanced to improve the recognition performance of the system.

3. Feature extraction module:

Feature extraction is an important step in face recognition. The better features are extracted, the higher recognition rate is. Feature extraction is to analyze and transform input information contained in a pattern, and extract information parameters, which are unsusceptible to random interference as the pattern features. The intention is also to eliminate redundant information, improve recognition precision, reduce calculation quantity, and increase calculation speed. Proper features should possess separability, stability, and independence **[27]**. Separability refers to the fact that there exist differences among features of different class. The greater the differences are the better. Stability means that features of different pattern of same class should be close. The closer, the better is. In addition, the features are less influenced by random interference. Independence refers to the fact that each feature chosen in one pattern is irrelevant to one another. Z. Hong divided image features into:

- **a.** Visual features,
- **b.** Statistical features,
- **c.** Transformation coefficient features and
- **d.** Algebraic features

4. Classification module:

In this module, with the help of a pattern classifier (The most common ones are the nearest-neighbor classifier using either Euclidean or angle distance), extracted features of the face image is compared with the ones stored in face database. After doing this comparison, face image is classified as either known or unknown.

II.4. Techniques of recognition:

Many methods of face recognition for still images have been proposed. Basically, They can be divided into three categories **[23**, **24**, **26**, **28**, **29]**: Holistic or Global-Appearance-based methods **[30]**, Local-feature-based methods or local appearance-based methods, and hybrid methods **[31]**.

a. Global-Appearance-based methods:

In Global-Appearance-based methods, the whole image is used as a raw input to the learning process. Examples of these techniques are Principal Component Analysis (PCA), Independent Component Analysis (ICA) **[32**, **33**, **34**, **35**, **36**, **37]**, Discrete Cosine Transforms (DCT) **[38]**, Linear Discriminate Analysis (LDA), and Neural Network (NN) **[39, 40]** applied to face recognition.

b. Local appearance-based methods:

The local appearance-based methods can be divided into two groups: The ones that require the use of specific regions located on a face such as eyes, nose and mouth, as well as their relationships with each other **[41**, **42**, **43**, **44**, **45**, **46**, **47]**, Dynamic Link Architecture **[48]**, graph matching methods **[49]** and Hidden Markov Models **[50]** and the ones that simply partition the input face image into blocks without considering any specific regions**[51**, **52]**. Effective features that can be used in feature based face recognition can be classified as follows **[26]**:

- **First-order features values:** Discrete features such as eyes, eyebrows, mouth, chin, and nose, which have been found to be important in face identification and are specified without reference to other facial features, are called first-order features.
- **Second-order features values:** Another configurable set of features which characterize the spatial relationships between the positions of the first-order features and information about the shape of the face are called second-order features.
- **Higher-order feature values:** There are also higher-level features whose values depend on a complex set of feature values. For instance, age might be a function of hair coverage, hair color, skin tension, presence of wrinkles and age spots, forehead height which changes because of receding hairline, and so on.

c. Hybrid methods:

In hybrid methods, the best of the holistic and feature-based approaches associated with local features and the whole face to recognize are used. Modular Eigen faces **[53]**, Hybrid Local Feature Analysis (LFA) **[54]** and Component-based 3D Models **[55]** are examples of hybrid models.

Many face recognition techniques have been developed during the past decades. One of the most successful and well-studied techniques to face recognition are the appearance-based methods **[56]**. Appearance-based approaches operate directly on images and process the images as two-dimensional (2-D) holistic patterns. In these approaches, a two-dimensional image of size *w* by *h* pixels is represented by a vector in a *wh* dimensional space. Therefore, each facial image corresponds to a point in this space. This space is called the sample space or the image space, and its dimension typically is very high **[57**, **58]**. A common way to attempt to resolve this problem is to use dimensionality reduction techniques **[59**, **60**, **61**, **62**, **63**, **64]**.

II.5.Principal Component Analysis (PCA):

Principal Component Analysis (PCA) **[65]** is one of the most popular appearance-based methods used mainly for dimensionality reduction in compression and recognition problems **[66]**. Principal component analysis (PCA) also known as Karhunen-Loeve expansion, which has two useful properties when used in face recognition. The first is that it can be used to reduce the dimensionality of the feature vectors. The second useful property is that PCA eliminates all of the statistical covariance in the transformed feature vectors **[67]**.

Sirovich and Kirby **[68**, **69**, **70]** first used PCA to efficiently represent pictures of human faces. They showed that any particular face can be (i) economically represented along the eigenpictures coordinate space, and (ii) approximately reconstructed using just a small collection of eigenpictures and their corresponding projections ('coefficients') **[71]**. Within this context, Turk and Pentland **[72, 73]** presented the well-known Eigenfaces method for face recognition in 1991. Since then, PCA has been widely investigated and has become one of the most successful approaches in face recognition **[74]**.

II.5.2. Face Recognition using PCA (Eigenfaces method):

PCA based approaches typically include two phases**:** training and classification **[75]** as shown in figure II.2.

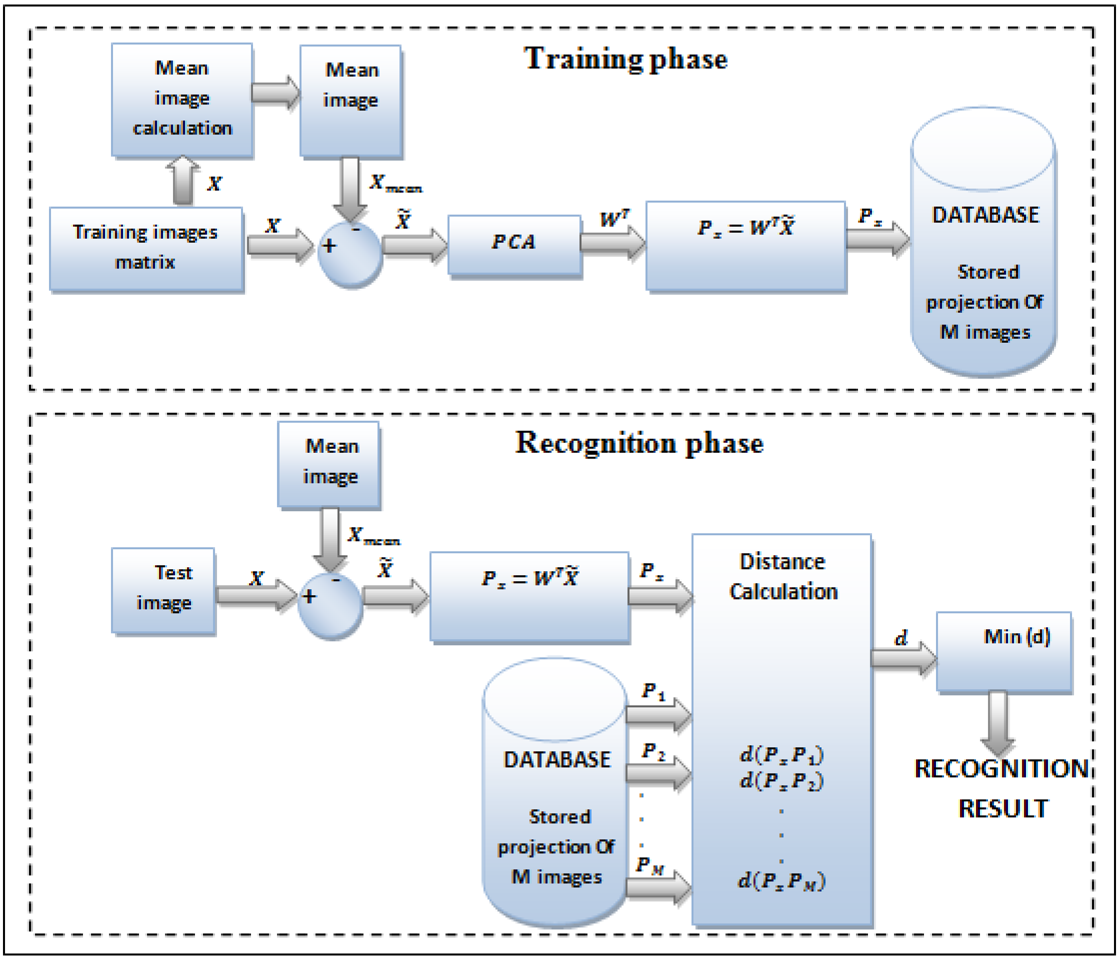

Figure II.2: An illustration of PCA based face recognition system.

I. Training phase:

In the training phase, an eigenspace is established from the training samples using PCA and the training face images are mapped to the eigenspace for classification. The steps involved in this phase are:

Step1: A training set **S** of M face images (I_i; i = 1,. . . ,M) is first acquired.

$$I_i = \begin{bmatrix} \gamma_{11} & \gamma_{12} & \cdots & \gamma_{1N} \\ \gamma_{21} & \gamma_{22} & \cdots & \gamma_{2N} \\ \vdots & \vdots & \ddots & \vdots \\ \gamma_{N1} & \gamma_{N2} & \cdots & \gamma_{NN} \end{bmatrix}_{NXN} \quad for\ i = 1,2,\dots,M \qquad \textbf{(II.1)}$$

Where $[\gamma_{ij}]_{i,j=1,2,\dots,N}$ are the grey values of the pixels.

Step2: Each face image I_i is expressed as a vector $\boldsymbol{\Gamma_i}$ (i=1...M) by concatenating each row (or column) into a long thin vector as shown in figure II.2. Since each image is (NxN) matrix so Γ_i is (N^2x1) vector.

$$I_i = \begin{bmatrix} \gamma_{11} & \gamma_{12} & \cdots & \gamma_{1N} \\ \gamma_{21} & \gamma_{22} & \cdots & \gamma_{2N} \\ \vdots & \vdots & \ddots & \vdots \\ \gamma_{N1} & \gamma_{N2} & \cdots & \gamma_{NN} \end{bmatrix}_{NXN} \xrightarrow{concatenation} \boldsymbol{\Gamma}_i = \begin{bmatrix} \gamma_{11} \\ \gamma_{12} \\ \vdots \\ \gamma_{1N} \\ \gamma_{21} \\ \vdots \\ \gamma_{2N} \\ \gamma_{N1} \\ \gamma_{N2} \\ \vdots \\ \gamma_{NN} \end{bmatrix}_{N^2X1} \quad (\mathbf{II.2})$$

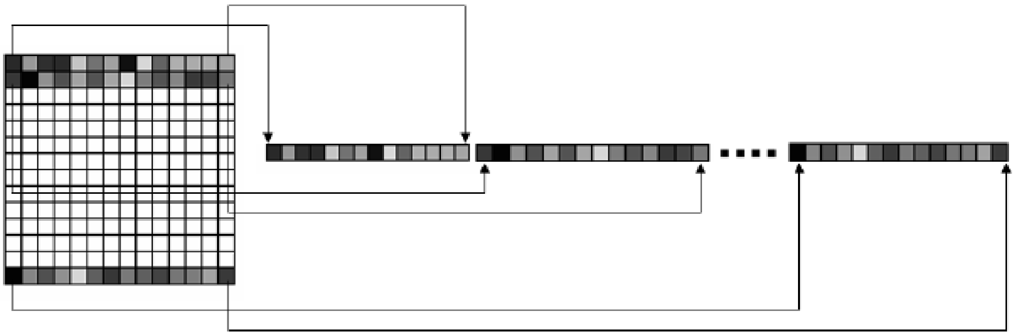

Figure II.3: Construction of face vector.

Step3: Compute the average face vector of the set, which is given by:

$$\boldsymbol{\Psi} = \frac{\mathbf{1}}{\boldsymbol{M}} \sum_{i=1}^{M} \boldsymbol{\Gamma}_i \quad (\mathbf{II.}\,3)$$

$$\boldsymbol{\Psi} = \begin{bmatrix} \psi_{11} \\ \psi_{12} \\ \vdots \\ \psi_{1N} \\ \psi_{21} \\ \vdots \\ \psi_{2N} \\ \psi_{N1} \\ \psi_{N2} \\ \vdots \\ \psi_{NN} \end{bmatrix} = \frac{\mathbf{1}}{\boldsymbol{M}} \begin{bmatrix} {\gamma_{11}}^1 & + & {\gamma_{11}}^2 & + & \dots & + & {\gamma_{11}}^M \\ {\gamma_{12}}^1 & + & {\gamma_{12}}^2 & + & \dots & + & {\gamma_{12}}^M \\ \vdots & \vdots & \vdots & \vdots & \vdots & \vdots & \vdots \\ {\gamma_{1N}}^1 & + & {\gamma_{1N}}^2 & + & \dots & + & {\gamma_{1N}}^M \\ {\gamma_{21}}^1 & + & {\gamma_{21}}^2 & + & \dots & + & {\gamma_{21}}^M \\ \vdots & \vdots & \vdots & \vdots & \vdots & \vdots & \vdots \\ {\gamma_{2N}}^1 & + & {\gamma_{2N}}^2 & + & \dots & + & {\gamma_{2N}}^M \\ {\gamma_{N1}}^1 & + & {\gamma_{N1}}^2 & + & \dots & + & {\gamma_{N1}}^M \\ {\gamma_{N2}}^1 & + & {\gamma_{N2}}^2 & + & \dots & + & {\gamma_{N2}}^M \\ \vdots & \vdots & \vdots & \vdots & \vdots & \vdots & \vdots \\ {\gamma_{NN}}^1 & + & {\gamma_{NN}}^2 & + & \dots & + & {\gamma_{NN}}^M \end{bmatrix}_{N^2X1} \quad (\mathbf{II.4})$$

Where M is the number of images in the training set.

Step 4: The images are mean centered by subtracting the mean image from each image vector.

$$\left[\boldsymbol{\phi_i = \Gamma_i - \Psi}\right]_{N^2 X 1} \qquad \boldsymbol{i = 1, 2, \dots M} \qquad (\textbf{II.}5)$$

The purpose of subtracting the mean image from each image vector is to be left with only the distinguishing features from each face and “removing” in way information that is common.

Step 5: Build the mean- subtract face matrix A.

The mean- subtract faces are arrayed in a matrix **A**, with one column per sample image.

$$\boldsymbol{A} = \begin{bmatrix} \boldsymbol{\Phi_1} & \boldsymbol{\Phi_2} & \boldsymbol{\Phi_3} & \cdots & \boldsymbol{\Phi_M} \end{bmatrix}_{\mathbf{N^2 X M}} \qquad (\textbf{II.6})$$

Step 6: This set of very large vectors is then subjected to principal component analysis, which seeks a set of M orthonormal vectors U_n , which best describes the distribution of the data. The kth vector U_k is chosen such that

$$\boldsymbol{\lambda_k = \frac{1}{M}\sum_{n=1}^{M}\left(U_k^T\phi_n\right)^2} \qquad (\textbf{II.7})$$

is a maximum, subject to

$$\boldsymbol{U_l^T U_k = \delta_{kl} = \begin{cases} 1 & if\ l = k \\ 0 & otherwise \end{cases}} \qquad (\textbf{II.8})$$

Note: The vectors U_k and scalars $\boldsymbol{\lambda_k}$ are the eigenvectors and eigenvalues respectively of C.

Step 7: Getting the eigenvalues and eigenvectors.

The covariance matrix is given as:

$$\boldsymbol{C = \frac{1}{M}\sum_{n=1}^{M}(\phi_n\phi_n^T) = AA^T} \qquad (\textbf{II.}9)$$

Where C is N^2 x N^2

The covariance matrix C however is $N^2 x\ N^2$ real symmetric matrix, and determining the N^2 eigenvectors and eigenvalues is an intractable task for typical image sizes. We need a computationally feasible method to find these eigenvectors.

Consider the eigenvectors $\boldsymbol{V_i}$ of $\boldsymbol{A^T A}$ such that

$$\boldsymbol{A^T\, A\, V_i = \mu_i V_i} \qquad (\textbf{II.10})$$

Premultiplying both sides by A, we have

$$\boldsymbol{AA^T\,A\,V_i = \mu_i AV_i} \qquad (\mathbf{II.11})$$

$$\boldsymbol{C\,AV_i = \mu_i AV_i} \qquad (\mathbf{II.12})$$

$$\boldsymbol{C\,U_i = \mu_i U_i} \qquad (\mathbf{II.13})$$

From which we see that $\boldsymbol{AV_i}$ are the eigenvectors of $\boldsymbol{C = AA^T}$

Thus AA^T and A^TA have the same non zero eigenvalues and their eigenvectors are related as follows:

$$\boldsymbol{U_i = AV_i} \qquad (\mathbf{II.14})$$

Following these analysis, we construct the M x M matrix L

$$\boldsymbol{L = A^TA} \qquad (\mathbf{II.15})$$

Where $\mathbf{L_{mn} = \Phi_m{}^T\,\Phi_n}$.

Step 8: Getting the Eigenfaces.

The M eigenvectors, $\boldsymbol{V_l}$ of L determine linear combinations of the M training set face images to form the eigenfaces $\boldsymbol{U_l}$

$$\boldsymbol{U_l = \sum_{k=1}^{M} V_{lk}\phi_k \qquad l = 1 \ldots M} \qquad (\mathbf{II.16})$$

$\boldsymbol{AV_i}$ need to be normalized in order to be equal to $\boldsymbol{U_i}$. Since we only sum up a finite number of image vectors, *M*, the rank of the covariance matrix cannot exceed *M* -1 (The -1 come from the subtraction of the mean vector ψ) **[76]**.

Because $\boldsymbol{U_l}$ are the eigenvectors of the covariance matrix corresponding to the original face images, and because they are face-like in appearance, we refer to them as “Eigenfaces”.

With this analysis, the calculations are greatly reduced, from the order of the number of pixels in the images (N^2) to the order of the number of images in the training set (M). In practice, the training set of face images will be relatively small ($M << N^2$), and the calculations become quite manageable. The associated eigenvalues allow us to rank the eigenvectors according to their usefulness in characterizing the variation among the images.

Step 9: Compute for each face its projection onto the face space.

All the face images are projected into the subspace spanned by the computed M eigenvectors, the projection weight are found using the following formula:

$$\boldsymbol{W_{ik} = U_k^T(\Gamma_i - \Psi) \quad for\ k = 1, 2, \ldots M\ \ i = 1, 2, \ldots M} \qquad (\mathbf{II.17})$$

$$\boldsymbol{W_{ik} = U_k^T\,\Phi_i} \qquad (\mathbf{II.18})$$

Where U_k^T are the eigenvectors.

These weights form the feature vectors

$$\boldsymbol{\Omega_i}^{\boldsymbol{T}} = [\boldsymbol{W_{i1}}\ \boldsymbol{W_{i2}} \ldots \boldsymbol{W_{iM}}] \qquad \boldsymbol{for\ i = 1, 2, \ldots M} \qquad (\mathbf{II.19})$$

The feature vector describes the contribution of each eigenfaces in representing the input face image, treating the eigenfaces as a basis set for face images.

Step 10: Compute the threshold θ.

A distance threshold θ, that defines the maximum allowable distance from a face class as well as from the face space, is set up by computing half the largest distance between any two face classes **[77]**:

$$\boldsymbol{\theta = \frac{1}{2} max\{d_{ij}\}} \qquad \boldsymbol{i, j = 1 \ldots M} \qquad (\mathbf{II.20})$$

Where $\boldsymbol{d_{ij}}$denotes the distance between training images i and j.

❖ **Rebuilding a face image with Eigenfaces.**

A face image can be approximately reconstructed (see figure II.4) by using the mean image and the eigenfaces as **[26]**

$$\boldsymbol{\Gamma'_i = \Psi + \sum_{k=1}^{M} W_{ik} U_k} \qquad \boldsymbol{i = 1 \ldots M} \qquad (\mathbf{II.21})$$

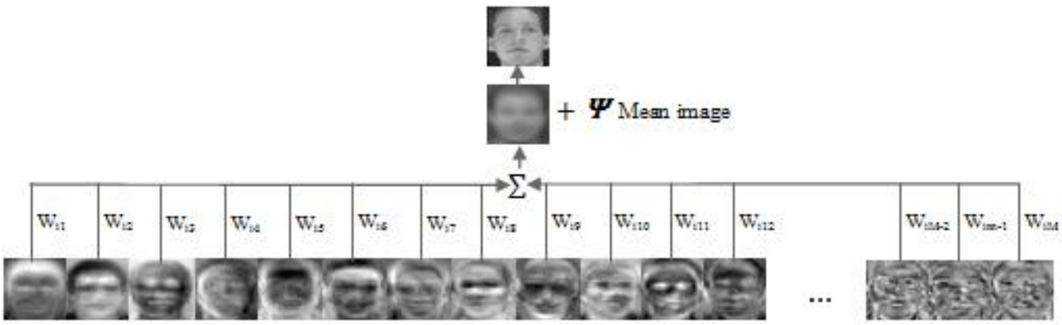

Figure II.4: Reconstruction of face image.

The degree of the fit or the "Rebuild Error Ratio (RER)" can be expressed by means of the euclidean distance between the original and the reconstructed face image as given in:

$$\boldsymbol{RER = \left\| \frac{\Gamma' - \Gamma}{\Gamma} \right\|} \qquad (\mathbf{II.22})$$

It has been observed that, rebuild error ratio increases as the training set members differ heavily from each other. This is due to the addition of the average face image. When the members differ from each other (especially in image background) the average face image becomes messier and this increases the rebuild error ratio.

II. Classification phase:

In the classification phase, an unknown face is presented to the system. The system projects it onto the same eigenspace and computes its distance from all the stored faces. The face is identified as being the same individual as the face which is nearest to it in face space. The steps involved in this phase are:

Step 1:

The test face image to be recognized I_{test} is expressed as a vector Γ_{test} by concatenating each row (or column) into a long thin vector.

$$\boldsymbol{\Gamma}_{test} = \begin{bmatrix} \gamma_{11} \\ \gamma_{12} \\ \vdots \\ \gamma_{1N} \\ \gamma_{21} \\ \vdots \\ \gamma_{2N} \\ \gamma_{N1} \\ \gamma_{N2} \\ \vdots \\ \gamma_{NN} \end{bmatrix}_{N^2X1} \qquad (\mathbf{II.23})$$

Step 2: Subtract the average face from it.

$$\boldsymbol{\Phi}_{\mathbf{test}} = \boldsymbol{\Gamma}_{\mathbf{test}} - \boldsymbol{\Psi} \qquad (\mathbf{II.24})$$

Step 3: Compute its projection onto the face space.

The weight of the test image is determined by the following formula:

$$W_k = U_k^T(\Gamma_{test} - \Psi) \qquad for\ k = 1 \ldots M \qquad (\mathbf{II.25})$$

The weights form a feature vector,

$$\Omega_{test}{}^T = [W_1\ W_2 \ldots W_M] \qquad (\mathbf{II.26})$$

Step 4: Computing the distance between the test face and all known faces.

The simplest method for determining, which face class provides the best description of an input face image is to find the face class k that minimizes the distance between the input face and all the stored faces.

There are several methods of computing the distance between multidimensional vectors. Here, seven different distance measures will be used.

Ω_{test} is the feature vector of the test face and $(\boldsymbol{\Omega_{test}})_i$ is its ith component.

Ω_k is a vector describing the kth face class and $(\boldsymbol{\Omega_k})_i$ is its ith component.

1. Cityblock or L_1 distance

$$\varepsilon_k(\Omega_{\text{test}}, \Omega_{\text{k}}) = |\Omega_{\text{test}} - \Omega_{\text{k}}| = \sum_{i=1}^{M} |(\Omega_{test})_i - (\Omega_k)_i| \quad k = 1, \dots, M \qquad (\text{II}.27)$$

2. Euclidean Distance or L_2 distance: The Euclidean Distance is probably the most widely used distance metric. It is a special case of a general class of norms and is given as:

$$\varepsilon_k(\Omega_{\text{test}}, \Omega_{\text{k}}) = \|\Omega_{\text{test}} - \Omega_{\text{k}}\|^2 = \sum_{i=1}^{M} ((\Omega_{test})_i - (\Omega_k)_i)^2 \quad k = 1, \dots, M \qquad (\text{II}.28)$$

3. Cosine or Negative Angle between feature vectors:

$$\varepsilon_k(\Omega_{\text{test}}, \Omega_{\text{k}}) = -\frac{\Omega_{\text{test}} . \Omega_{\text{k}}}{\|\Omega_{\text{test}}\| . \|\Omega_{\text{k}}\|} = -\frac{\sum_{i=1}^{M} (\Omega_{test})_i (\Omega_k)_i}{\left[\sum_{i=1}^{M} ((\Omega_{test})_i)^2 \sum_{i=1}^{k} ((\Omega_k)_i)^2\right]^{1/2}} \quad k = 1 \dots M \qquad (\text{II}.29)$$

4. The Mahalanobis Distance: The Mahalanobis Distance is a better distance measure when it comes to pattern recognition problems. It takes into account the covariance between the variables and hence removes the problems related to scale and correlation that are inherent with the Euclidean Distance. It is given as:

$$\varepsilon_k(\Omega_{\text{test}}, \Omega_{\text{k}}) = \sqrt{(\Omega_{\text{test}} - \Omega_{\text{k}})^T C^{-1} (\Omega_{\text{test}} - \Omega_{\text{k}})} \qquad (\text{II}.30)$$

Where C is the covariance between the variables involved.

Eq (II.30) can be reduced to obtain another formula of mahalanobis distance which is given by:

$$\varepsilon_k(\Omega_{\text{test}}, \Omega_{\text{k}}) = -\sum_{i=1}^{M} (\Omega_{test})_i (\Omega_k)_i z_i \quad k = 1, \dots, M \qquad (\text{II}.31)$$

$$z_i = \frac{1}{{\lambda_i}^{1/2}} \qquad (\text{II}.32)$$

Where λ_i= eigenvalues of the ith eigenvector.

5. L1 + Mahalanobis distance:

$$\boldsymbol{\varepsilon_k(\Omega_{\text{test}}, \Omega_{\text{k}}) = \sum_{i=1}^{M} |(\Omega_{test})_i - (\Omega_k)_i|\, z_i \quad k = 1, \dots, M} \tag{II.33}$$

6. L2 + Mahalanobis distance:

$$\boldsymbol{\varepsilon_k(\Omega_{\text{test}}, \Omega_{\text{k}}) = \sum_{i=1}^{M} ((\Omega_{test})_i - (\Omega_k)_i)^2\, z_i \qquad k = 1, \dots, M} \tag{II.34}$$

7. Angle + Mahalanobis distance:

$$\boldsymbol{\varepsilon_k(\Omega_{\text{test}}, \Omega_{\text{k}}) = -\frac{\sum_{i=1}^{M} (\Omega_{test})_i (\Omega_k)_i z_i}{\left[\sum_{i=1}^{M} ((\Omega_{test})_i)^2 \sum_{i=1}^{k} ((\Omega_k)_i)^2\right]^{1/2}} \qquad k = 1, \dots, M} \tag{II.35}$$

Step 5: Classification of the input face.

Classification is performed by comparing the feature vectors of the face database members with the feature vector of the input face image. This comparison is based on the distance between the two members to be smaller than a user defined threshold θ.

- If $min\{\varepsilon_k\} \geq \theta (k = 1, \dots M)$ it is classified as unknown face.
- If $min\{\varepsilon_k\} < \theta$ it is classified as known face.

II.5.2.Drawbacks of PCA approach and variants:

Penev and Sirovich **[78]** discussed the problem of the dimensionality of the “face space” when eigenfaces are used for representation. Wiskott et al. **[79]** pointed out that PCA could not capture even the simplest invariance unless this information is explicitly provided in the training data. They proposed a technique known as elastic bunch graph matching to overcome the weaknesses of PCA. Extensions of the PCA include the Nonlinear PCA **[80]**. Bartlett et al. **[81]** and Draper et al. **[32]** proposed using ICA for face representation. Yang **[82]** used Kernel PCA for face feature extraction and recognition. PCA represents image intensity as a vector, thus the size of the vector could be very large. This large size of vector creates problem to the PCA implementation when estimating the eigenvectors of the covariance matrix of the sample data. To avoid such drawback, Yang et al. **[83]** proposed the two-dimensional PCA (2DPCA), (or IMPCA **[84])** which works directly with the 2-D matrix of the image intensity.

In **[85]**, the authors proposed to transform the transpose of the face images into image matrices, while in **[86]** DiaPCA proposed to transform the original face images into diagonal face images by rotating each row one pixel to its right.

Inspired by the idea of 2D process, MatPCA **[87]** was proposed by matrixizing 1D input into 2D matrices and then applying the 2D PCA. Usually, compared with PCA, 2D PCA methods need more coefficients for image representation. To solve this problem, several alternatives were proposed. For instance, the Bilateral-projection-based 2DPCA (B2DPCA) **[88]** reduces the redundancies among both rows and columns of the face images by projecting them to the left- and right multiplying projection matrices. Similarly, Bidirectional PCA (BD-PCA) **[89]** utilizes the two projection matrices. Both the PCA and 2DPCA rely on a single projection subspace. The subspace dimension **d** significantly affects the recognition accuracy of these methods. If **d** is small, the images could lose valuable discrimination information when projected onto the subspace. A large value of **d** could make the projected images overfitted to the sample data and reduce the recognition accuracy. The overfitting problem could be solved by using the random subspace (RS) technique as demonstrated in **[90]**. Nguyen proposed a method that combines the 2DPCA and RS technique in face recognition (RS-2DPCA) **[91]**. Shan et al. proposed other method called Unified Principal Component Analysis (UPCA) **[92]**. Jiang proposed an asymmetric principal component analysis (APCA) to remove the unreliable dimensions more effectively than the conventional PCA **[93]**.

II.6.Fisher Linear Discriminant (FLD)

The Fisherface method is based on the linear discriminant analysis (LDA, also known as FLD) and is used to find the optimal set of projection vectors which maximizes the determinant of the between-class scatter matrix (S_b) and at the same time minimizes the determinant of the within class scatter matrix (S_w) **[94]**. Fisher's Linear Discriminant is a "classical" technique in pattern recognition, first developed by Robert Fisher in 1936 for taxonomic classification. Depending upon the features being used, it has been applied in different ways in computer vision and even in face recognition.

Fisher discriminant group images of the same class and separates images of different classes. Images are projected from N^2-dimensional space to C dimensional space (where C is the number of classes of images). For example, consider two sets of points colored red and blue, in 2-dimensional space (Figure II.5 (a)) that are projected onto a single line. Depending on the direction of the line, the points can either be mixed together (Figure II.5 (b)) or separated Figure II.5 (c)). Fisher discriminant finds the line that best separates the points. In terms of face recognition this means grouping images of the same class and separate images of different classes **[58]**.

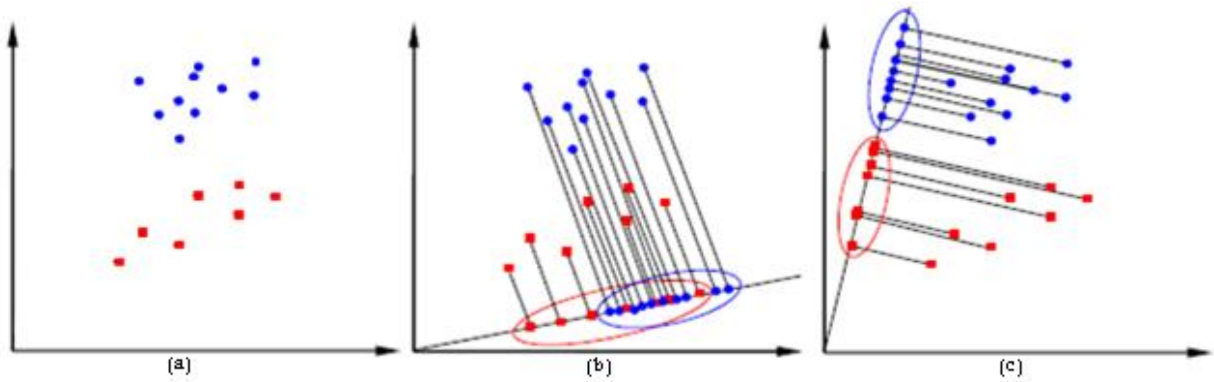

Figure II.5: Point projection **(a)** Points in two-dimensional space **(b)** Points mixed when projected onto a line. **(c)** Points separated when projected onto another line.

By applying the FLD method, we find the projection directions that on one hand maximize the distance between the face images of different classes and on the other hand minimize the distance between the face images of the same class. In another words, maximizing the between-class scatter matrix $\boldsymbol{S_b}$ while minimizing the within-class scatter matrix $\boldsymbol{S_W}$ in the projective subspace. Figure II.6 shows good and bad class separation.

Figure II.6: Class separation **(a)** Good class separation **(b)** Bad class separation.

The Eigenface method is based on linearly projecting the image space to a low dimensional feature space. However, the Eigenface method, which uses principal components analysis (PCA) for dimensionality reduction, yields projection directions that maximize the total scatter across all classes, i.e., across all images of all faces i.e.

$$\boldsymbol{W} = \mathbf{arg}\,\boldsymbol{max}|\boldsymbol{W}^{\boldsymbol{T}}\boldsymbol{S}_{\boldsymbol{T}}\boldsymbol{W}| \quad (\mathbf{II.36})$$

In choosing the projection which maximizes the total scatter, PCA retains unwanted variations due to lighting and facial expression. As stated by Moses et al., **“the variations between the images of the same face due to illumination and viewing direction are almost always larger than image variations due to change in face identity”**. Thus, while the PCA projections are optimal for reconstruction from a low dimensional basis, they may not be optimal from a discrimination standpoint **[94]**.

The Fisher’s Linear Discriminant (FLD) overcomes the limitations of the Eigenfaces method by applying a new criterion. This criterion tries to maximize the ratio of between-class scatter to that of within-class scatter.

$$\mathrm{J}_{\boldsymbol{FLD}}(\boldsymbol{W}_{\boldsymbol{opt}}) = \boldsymbol{argmax}\frac{|\boldsymbol{W}^{\boldsymbol{T}}\boldsymbol{S}_{\boldsymbol{b}}\boldsymbol{W}|}{|\boldsymbol{W}^{\boldsymbol{T}}\boldsymbol{S}_{\boldsymbol{W}}\boldsymbol{W}|} \quad (\mathbf{II.37})$$

Where $\boldsymbol{S}_{\boldsymbol{b}}$ is the between-class scatter matrix and $\boldsymbol{S}_{\boldsymbol{W}}$ is the within-class scatter matrix **[58]**.

- **The within-class scatter matrix:**

The within-class scatter matrix $\boldsymbol{S}_{\boldsymbol{W}}$, also called **intra-personal**, represents variations in appearance of the same individual due to different lighting and face expression and it represents how face images are distributed closely within classes,

- **The between-class scatter matrix:**

The between-class scatter matrix $\boldsymbol{S}_{\boldsymbol{b}}$, also called the **extra-personal**, represents variations in appearance due to a difference in identity and it describes how classes are separated from each other.

II.6.1.The "small sample size problem" (SSS) problem:

The face recognition problem, one is confronted with the difficulty that the within-class scatter matrix $\boldsymbol{S_w} \in \boldsymbol{R^{nxn}}$ is always singular. This problem is known as the "small sample size problem" or (SSS) problem. It stems from the fact that the rank of $\boldsymbol{S_w}$ is at most M - c, and, in general, the number of images in the learning set M is much smaller than the number of pixels in each image n. This implies that the traditional FLD algorithm fails to use **[94]**.

Recently several variants of LDA **[58, 95, 96, 97, 98, 99, 100, 101, 102, 103]** have been introduced, mainly to solve the small sample size (SSS) problem **[104]**. In the Fisherface method, PCA is applied first as a pre-processing step aiming to reduce the dimensionality prior to performing FLD. In this method the final optimal projection vector matrix becomes

$$\boldsymbol{W_{opt} = W_{PCA}W_{FLD}} \qquad \textbf{(II.38)}$$

Where

$$\boldsymbol{W_{PCA} = \mathbf{arg}\, max|W^T S_T W|} \qquad \textbf{(II.39)}$$

$$\boldsymbol{W_{FLD} = argmax\frac{|W^T {W_{PCA}}^T S_b W_{PCA} W|}{|W^T {W_{PCA}}^T\, S_W W_{PCA} W|}} \qquad \textbf{(II.40)}$$

II.6.2. Face Recognition using FLD (Fisherfaces method):

PCA is a classical technique for signal representation, but fisher's linear discrimanant (FLD) is a classical technique for pattern recognition **[105]**. The basic steps in Fisherfaces method are as follows **[106]**:

Step1: We need a training set composed of a relatively large group of subjects with diverse facial characteristics. The database should contain several examples of face images for each subject in the training set and at least one example in the test set. These examples should represent different frontal views of subjects with minor variations in view angle. They should also include different facial expressions, different lighting and background conditions, and examples with and without glasses.

Step 2: For each image starting with the two-dimensional N XN array of intensity values $I(x, y)$, we construct the lexicographic vector expansion $\Gamma \in R^{NXN}$. This vector corresponds to the initial representation of the face. Thus the set of all faces in the feature space is treated as a high-dimensional vector space.

Step 3: Define all instances of the same person's face as being in one class and the faces of different subjects as being in different classes for all subjects in the training set, also having labeled all instances in the training set and having defined all the classes.

Class 1

$$\Gamma_1{}^1 = \begin{bmatrix} \gamma_{11} \\ \gamma_{12} \\ \vdots \\ \gamma_{1N} \\ \gamma_{21} \\ \vdots \\ \gamma_{2N} \\ \gamma_{N1} \\ \gamma_{N2} \\ \vdots \\ \gamma_{NN} \end{bmatrix}_{N^2X1} \quad \ldots \quad \Gamma_{n_1}{}^1 = \begin{bmatrix} \gamma_{11} \\ \gamma_{12} \\ \vdots \\ \gamma_{1N} \\ \gamma_{21} \\ \vdots \\ \gamma_{2N} \\ \gamma_{N1} \\ \gamma_{N2} \\ \vdots \\ \gamma_{NN} \end{bmatrix}_{N^2X1}$$

Class 2

$$\Gamma_1{}^2 = \begin{bmatrix} \gamma_{11} \\ \gamma_{12} \\ \vdots \\ \gamma_{1N} \\ \gamma_{21} \\ \vdots \\ \gamma_{2N} \\ \gamma_{N1} \\ \gamma_{N2} \\ \vdots \\ \gamma_{NN} \end{bmatrix}_{N^2X1} \quad \ldots \quad \Gamma_{n_2}{}^2 = \begin{bmatrix} \gamma_{11} \\ \gamma_{12} \\ \vdots \\ \gamma_{1N} \\ \gamma_{21} \\ \vdots \\ \gamma_{2N} \\ \gamma_{N1} \\ \gamma_{N2} \\ \vdots \\ \gamma_{NN} \end{bmatrix}_{N^2X1}$$

Class 3

$$\Gamma_1{}^3 = \begin{bmatrix} \gamma_{11} \\ \gamma_{12} \\ \vdots \\ \gamma_{1N} \\ \gamma_{21} \\ \vdots \\ \gamma_{2N} \\ \gamma_{N1} \\ \gamma_{N2} \\ \vdots \\ \gamma_{NN} \end{bmatrix}_{N^2X1} \quad \ldots \quad \Gamma_{n_3}{}^3 = \begin{bmatrix} \gamma_{11} \\ \gamma_{12} \\ \vdots \\ \gamma_{1N} \\ \gamma_{21} \\ \vdots \\ \gamma_{2N} \\ \gamma_{N1} \\ \gamma_{N2} \\ \vdots \\ \gamma_{NN} \end{bmatrix}_{N^2X1}$$

…

Class c

$$\Gamma_1{}^c = \begin{bmatrix} \gamma_{11} \\ \gamma_{12} \\ \vdots \\ \gamma_{1N} \\ \gamma_{21} \\ \vdots \\ \gamma_{2N} \\ \gamma_{N1} \\ \gamma_{N2} \\ \vdots \\ \gamma_{NN} \end{bmatrix}_{N^2X1} \quad \ldots \quad \Gamma_{n_c}{}^c = \begin{bmatrix} \gamma_{11} \\ \gamma_{12} \\ \vdots \\ \gamma_{1N} \\ \gamma_{21} \\ \vdots \\ \gamma_{2N} \\ \gamma_{N1} \\ \gamma_{N2} \\ \vdots \\ \gamma_{NN} \end{bmatrix}_{N^2X1}$$

$n_1, n_2, \ldots, n_c$ are the number of samples in class 1,2,…,c respectively.

Step 4: In order to overcome the problem of a singular $\boldsymbol{S_w}$, we use PCA first to reduce the dimension of the feature space to M - c, and then applying the standard FLD to reduce the dimension to c - 1.

Class 1

$$\boldsymbol{\Omega_{PCA}}_1^1 = \begin{bmatrix} W_{11}^1 \\ W_{12}^1 \\ \vdots \\ W_{1(M-c)}^1 \end{bmatrix} \dots \boldsymbol{\Omega_{PCA}}_{n_1}^1 = \begin{bmatrix} W_{n_1 1}^1 \\ W_{n_1 2}^1 \\ \vdots \\ W_{n_1(M-c)}^1 \end{bmatrix}$$

...

Class c

$$\boldsymbol{\Omega_{PCA}}_1^c = \begin{bmatrix} W_{11}^c \\ W_{12}^c \\ \vdots \\ W_{1(M-c)}^c \end{bmatrix} \dots \boldsymbol{\Omega_{PCA}}_{n_c}^c = \begin{bmatrix} W_{n_c 1}^c \\ W_{n_c 2}^c \\ \vdots \\ W_{n_c(M-c)}^c \end{bmatrix}$$

Step 5: Calculate the mean of each class μ_j.

$$\boldsymbol{\mu_j = \frac{1}{n_j}\sum_{i=1}^{n_j} \Omega_{PCA}{}_i^j \qquad j = 1, \dots, c} \qquad \textbf{(II.41)}$$

$$\boldsymbol{\mu_1} = \frac{1}{n_1}\begin{bmatrix} W_{11}^1 & + & \dots & W_{n_1 1}^1 \\ W_{12}^1 & + & \cdots & W_{n_1 2}^1 \\ \vdots & & \ddots & \vdots \\ W_{1(M-c)}^1 & + & \cdots & W_{n_1(M-c)}^1 \end{bmatrix} \dots \boldsymbol{\mu_c} = \frac{1}{n_c}\begin{bmatrix} W_{11}^c & + & \dots & W_{n_c 1}^c \\ W_{12}^c & + & \cdots & W_{n_c 2}^c \\ \vdots & & \ddots & \vdots \\ W_{1(M-c)}^c & + & \cdots & W_{n_c(M-c)}^1 \end{bmatrix} \qquad \textbf{(II.42)}$$

Where

μ_j is $(M-c)X1$ column vector.

n_j is the number of samples in class j.

$\Omega_{PCA}{}_i^j$ is the i^th PCA feature vector of class j.

Ω_{PCA} is $(M-c)XM$ matrix M is the total number of images.

Step 5: Calculate the mean of all classesμ.

$$\boldsymbol{\mu = \frac{1}{M}\sum_{j=1}^{c} \Omega_{PCA}{}_i^j \qquad i = 1, \dots, n_j} \qquad \textbf{(II.43)}$$

Where

μ is $(M-c)X1$ column vector.

M is the total number of images.

Step 6: Subtract the mean of each class from the PCA projected images.

$$\boldsymbol{\Phi}_i^j = \boldsymbol{\Omega}_{PCA_i^j} - \boldsymbol{\mu}_j \qquad i = 1, \dots, n_j \qquad j = 1, \dots, c \tag{II.44}$$

Class 1

$$\boldsymbol{\Phi}_1^1 = \boldsymbol{\Omega}_{PCA_1^1} - \boldsymbol{\mu}_1 = \begin{bmatrix} W_{11}^1 - \mu_{11} \\ W_{12}^1 - \mu_{12} \\ \vdots \\ W_{1(M-c)}^1 - \mu_{1(M-c)} \end{bmatrix} \dots \boldsymbol{\Phi}_{n_1}^1 = \boldsymbol{\Omega}_{PCA_{n_1}^1} - \boldsymbol{\mu}_1 = \begin{bmatrix} W_{n_1 1}^1 - \mu_{11} \\ W_{n_1 2}^1 - \mu_{12} \\ \vdots \\ W_{n_1(M-c)}^1 - \mu_{1(M-c)} \end{bmatrix}$$

⋮

Class c

$$\boldsymbol{\Phi}_1^c = \boldsymbol{\Omega}_{PCA_1^c} - \boldsymbol{\mu}_c = \begin{bmatrix} W_{11}^1 - \mu_{11} \\ W_{12}^1 - \mu_{12} \\ \vdots \\ W_{1(M-c)}^1 - \mu_{1(M-c)} \end{bmatrix} \dots \boldsymbol{\Phi}_{n_c}^1 = \boldsymbol{\Omega}_{PCA_{n_c}^c} - \boldsymbol{\mu}_c = \begin{bmatrix} W_{n_c 1}^c - \mu_{c1} \\ W_{n_c 2}^c - \mu_{c2} \\ \vdots \\ W_{n_c(M-c)}^c - \mu_{c(M-c)} \end{bmatrix}$$

Where

$\boldsymbol{\Phi}_i^j$ are $(M-c)X1$ column vectors.

Step 7: Build scatter matrices for each class $S_1, S_2 \dots S_c$.

$$\boldsymbol{S}_j = \sum_{i=1}^{n_j} (\boldsymbol{\Phi}_i^j)\,(\boldsymbol{\Phi}_i^j)^T \qquad j = 1, \dots, c \tag{II.45}$$

$$\boldsymbol{S}_j = \sum_{i=1}^{n_j} (\boldsymbol{\Omega}_{PCA_i^j} - \boldsymbol{\mu}_j)\,(\boldsymbol{\Omega}_{PCA_i^j} - \boldsymbol{\mu}_j)^T \qquad j = 1, \dots, c \tag{II.46}$$

Where

S is $(M-c)X(M-c)$ matrix.

Step 8: Calculate within-class scatter matrix S_w.

The within-class scatter matrix $\boldsymbol{S_w}$ shows the average scatter (i of the sample vectors ($\boldsymbol{\Omega_{PCA}}$) of different classes c_i around their respective mean vectors $\boldsymbol{\mu_j}$, given as follows :

$$\boldsymbol{S_w = \sum_{j=1}^{c}\sum_{i=1}^{n_j}(\Omega_{PCA}{}_i^j - \mu_j)\,(\Omega_{PCA}{}_i^j - \mu_j)^T} \qquad \textbf{(II.47)}$$

$$\boldsymbol{S_w = \sum_{j=1}^{c} S_j = S_1 + S_2 +, \dots, S_c} \qquad \textbf{(II.48)}$$

$\boldsymbol{S_w}$ is $(M-c)X(M-c)$ matrix.

Where:

$\boldsymbol{\Omega_{PCA}{}_i^j}$ is the i^{th} PCA feature vector of class j.

$\boldsymbol{\mu_j}$ is the mean of class j.

c is the number of classes.

$\boldsymbol{n_j}$ is the number of samples in class j.

$\boldsymbol{\mu}$ represents the mean of all classes.

Step 9: Calculate between-class scatter matrix S_b.

The between-class scatter matrix S_b represents the scatter of the conditional mean vectors ($\boldsymbol{\mu_j}$) around the overall mean vector $\boldsymbol{\mu}$, which is given by:

$$\boldsymbol{S_b = \sum_{j=1}^{C} n_j(\mu_j - \mu)(\mu_j - \mu)^T} \qquad \textbf{(II.49)}$$

Where

$\mathrm{S_b}$ is $(\mathrm{M}-\mathrm{c})\mathrm{X}(\mathrm{M}-\mathrm{c})$ matrix.

Step 10: Calculate the eigenvectors of the projection matrix.

The optimal projection $\boldsymbol{W_{opt}}$ is chosen as the matrix with orthonormal columns which maximizes the ratio of the determinant of the between-class scatter matrix of the projected samples to the determinant of the within-class scatter matrix of the projected samples, i.e.,

$$\boldsymbol{W_{opt} = argmax\frac{|W^T S_b W|}{|W^T S_W W|}}$$

This ratio is maximized when the column vectors of the projection matrix W are the eigenvectors of $\boldsymbol{S_W}^{-1}\boldsymbol{S_b}$ i.e.

$$\boldsymbol{W = eig(S_W^{-1}S_b)} \qquad (\mathbf{II.50})$$

Columns of W are eigenvectors satisfying

$$\boldsymbol{S_b W_i = \lambda_i S_w W_i} \qquad \boldsymbol{i = 1, 2, \dots, m} \qquad (\mathbf{II.51})$$

Where m=c-1

✓ The generalized eigenvalues are the roots of the characteristic polynomial:

$$\boldsymbol{|S_b - \lambda_i S_w| = 0} \qquad (\mathbf{II.52})$$

✓ The generalized eigenvectors $\boldsymbol{W_i}$ are obtained by solving directly:

$$\boldsymbol{(S_b - \lambda_i S_w) W_i = 0} \qquad (\mathbf{II.53})$$

These eigenvectors of $\boldsymbol{S_W}^{-1}\boldsymbol{S_b}$ are also referred to as the Fisherfaces.

$$\boldsymbol{W_{FLDi}}^{\boldsymbol{T}} = [\boldsymbol{W_{i1}\, W_{\,i2} \dots W_{\,i(c-1)}}] \qquad \boldsymbol{for\ i = 1, 2, \dots M - c} \qquad (\mathbf{II.54})$$

Step 11: Project faces onto the Fisher Linear Discriminant space.

$$\boldsymbol{\Omega_{FLD} = W_{FLD}}^{\boldsymbol{T}}\, \boldsymbol{\Omega_{PCA}} \qquad (\mathbf{II.55})$$

$\boldsymbol{\Omega_{FLD}}$ is the fisher projection matrix and it is $(c-1)XM$.

$\boldsymbol{\Omega_{PCA}}$ is the PCA projection matrix $(M-c)XM$.

$\boldsymbol{W_{FLD}}$ is the Fisherfaces matrix and it is $(M-c)X(c-1)$.

Step 12: Classification of the test image.

The test image is first projected onto PCA subspace for dimensionality reduction and then projected on FLD subspace for feature extraction.

✓ **Projection of the test image onto PCA subspace:**

To project the test image onto PCA subspace, follow the same steps as in Eigenfaces method.

$$\boldsymbol{W_k = U_k^T \Phi_{\mathrm{test}} = U_k^T(\Gamma_{test} - \Psi)} \qquad \boldsymbol{for\ k = 1 \dots M - c} \qquad (\mathbf{II.56})$$

$$\boldsymbol{(\Omega_{PCA})_{test}}^{\boldsymbol{T}} = [\boldsymbol{W_1\, W_{\,2} \dots W_{\,M-c}}] \qquad (\mathbf{II.57})$$

$\boldsymbol{\Gamma_{\mathrm{test}}}$ is the concatenated vector of the test image.

$\boldsymbol{\Psi}$ is the mean image of the original set.

$\boldsymbol{U_k^T}$ are the eigenvectors of the covariance matrix.

$\boldsymbol{(\Omega_{PCA})_{test}}$ is the PCA feature vector of the test image.

- ✓ **Projection of the test image onto FLD subspace:**

$(\boldsymbol{\Omega_{FLD}})_{test} = \boldsymbol{W_{FLD}}^{\boldsymbol{T}}\ (\boldsymbol{\Omega_{PCA}})_{test}$

$(\boldsymbol{\Omega_{FLD}})_{test}$ is the FLD feature vector of the test image.

The test image is identified using a similarity measure. The face which has the minimum distance with the test face image is labeled with the identity of that image. The minimum distance can be calculated using the Euclidian distance method as given earlier in Eigenfaces method.

II.7. Singular Value Decomposition:

Most conventional techniques of image analysis treat images as elements of a vector space. Lately, there has been a steady growth of literature which regards images as matrices, e.g. **[83**, **107**, **108]**. As compared to a vectorial method, the matrix-based representation helps to better exploit the spatial relationships between image pixels. SVD is one of the methods which regard an image as a matrix.

Singular value decomposition (SVD) **[109]** plays the central role in reducing high dimensional data into lower dimensional data which is also called principal component analysis (PCA) **[65]** in statistics. It often occurs that in the reduced space, coherent patterns can be detected more clearly. Such unsupervised dimension reduction is used in very broad areas such as image processing **[69]** and information retrieval **[20]**.

Many successful methods have been proposed using holistic features of the faces and one popular category is based on singular value decomposition (SVD) for face recognition **[110**, **111**, **112**, **113**, **114]**.

II.7.1.Process of Singular Value Decomposition

If $\boldsymbol{A} \in \boldsymbol{R}^{m\times n}$, then there exist orthogonal matrices U and V, Such that

$$\boldsymbol{A} = \boldsymbol{U}{\textstyle\sum}_{\boldsymbol{A}}\boldsymbol{V}^{\boldsymbol{T}} \qquad (\boldsymbol{II.58})$$

See figure II.7 for illustration.

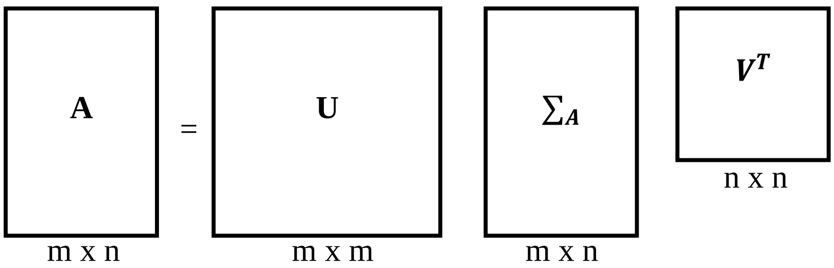

Figure II.7: Illustration of factoring A to USV^T.

Where

Matrix U is an $m \times m$ orthogonal matrix.

$$\boldsymbol{U} = [\boldsymbol{u_1}, \boldsymbol{u_2}, \dots, \boldsymbol{u_r}, \boldsymbol{u_{r+1}}, \dots, \boldsymbol{u_m}] \qquad (\boldsymbol{II.59})$$

Column vectors u_i , for $i = 1, 2, \dots, m$ form an orthonormal set:

$$\boldsymbol{u_i^T u_j} = \delta_{ij} = \begin{cases} 1 \; if \; i = j \\ 0 \; if \; i \neq j \end{cases} \qquad (\boldsymbol{II.60})$$

And matrix V is an $n \times n$ orthogonal matrix.

$$\boldsymbol{V} = [\boldsymbol{v_1}, \boldsymbol{v_2}, \dots, \boldsymbol{v_r}, \boldsymbol{v_{r+1}}, \dots, \boldsymbol{v_n}] \qquad (\boldsymbol{II.61})$$

Column vectors v_i , for $i = 1, 2, \dots, m$ form an orthonormal set:

$$\boldsymbol{v_i^T v_j} = \delta_{ij} = \begin{cases} 1 \; if \; i = j \\ 0 \; if \; i \neq j \end{cases} \qquad (\boldsymbol{II.62})$$

Here, $\sum_{\boldsymbol{A}}$ is an $m \times n$ diagonal matrix with singular values (SV) on the diagonal. The matrix $\sum_{\boldsymbol{A}}$ can be shown in following

$$\sum\nolimits_{A} = \begin{bmatrix} \boldsymbol{\sigma_1} & \mathbf{0} & \cdots & \mathbf{0} & \mathbf{0} & \cdots & \mathbf{0} \\ \mathbf{0} & \boldsymbol{\sigma_2} & \cdots & \mathbf{0} & \mathbf{0} & \cdots & \mathbf{0} \\ \vdots & \vdots & \ddots & \vdots & \vdots & \ddots & \vdots \\ \mathbf{0} & \mathbf{0} & \cdots & \boldsymbol{\sigma_r} & \mathbf{0} & \cdots & \mathbf{0} \\ \mathbf{0} & \mathbf{0} & \ddots & \mathbf{0} & \boldsymbol{\sigma_{r+1}} & \cdots & \mathbf{0} \\ \vdots & \vdots & \cdots & \vdots & \vdots & \ddots & \vdots \\ \mathbf{0} & \mathbf{0} & \cdots & \mathbf{0} & \mathbf{0} & \cdots & \boldsymbol{\sigma_p} \\ \mathbf{0} & \mathbf{0} & \cdots & \mathbf{0} & \mathbf{0} & \cdots & \mathbf{0} \end{bmatrix} \qquad (\boldsymbol{II.63})$$

$$\sum\nolimits_{A} = \boldsymbol{diag}(\boldsymbol{\sigma_1}, \boldsymbol{\sigma_2}, \dots, \boldsymbol{\sigma_r}, \boldsymbol{\sigma_{r+1}}, \dots, \boldsymbol{\sigma_p}), \qquad \boldsymbol{p} = \boldsymbol{min}(\boldsymbol{m}, \boldsymbol{n}) \qquad (\boldsymbol{II.64})$$

$$\boldsymbol{\sigma_1} \geq \boldsymbol{\sigma_2} \geq \cdots \geq \boldsymbol{\sigma_p} \geq \mathbf{0} \qquad (\boldsymbol{II.67})$$

Where $\boldsymbol{\sigma_i}$, $i = 1,2,\dots,p$, are the singular values of A and are the diagonal element of $\sum_{\boldsymbol{A}}$. The singular values are the square roots of the eigenvalues λ_i of AA^H or A^HA, that is $\sigma_i = \sqrt{\lambda_i}$. The superscript on A^H stands for *Hermitian transpose* and denotes the complex conjugate transpose of a complex matrix. If the matrix is real, then A^T denotes the same matrix. Equation (II.58) called singular value decomposition of matrix A. The columns in **U** and **V** are called left-hand and right-hand singular vectors for **A**, respectively.

II.7.2.Properties of the singular values:

The properties of the singular values are described in details as follows **[27]**:

→ **The stability of Singular value.**

Theorem 1:

Assume $A, B \in R^{m\times n}$, and their singular values are $\sigma_1 \geq, \sigma_2, \dots, \geq \sigma_p$ and $\tau_1 \geq, \tau_2, \dots, \geq \tau_p$ respectively, then $|\sigma_i - \tau_i| \leq \|A - B\|_2$

The stability of Singular value indicates that when there is a disturbance at A, the change of its singular values is not more than the $\|\cdot\|_2$ -norm of the disturbance matrix.

→ **Proportion invariance of singular value.**

Theorem 2:

Suppose a matrix $A \in R^{m\times n}$ and singular values of A and **α**A are denoted by $\sigma_1 \geq, \sigma_2, \dots, \geq \sigma_p$ and $\sigma_1{}^* \geq, \sigma_2{}^*, \dots, \geq \sigma_p{}^*$ respectively then$|\alpha|\left(\sigma_1 \geq, \sigma_2, \dots, \geq \sigma_p\right) = \left(\sigma_1{}^* \geq, \sigma_2{}^*, \dots, \geq \sigma_p{}^*\right)$.

→ **The rotation invariant property**.

Theorem 3:

If P is a unitary matrix, then the singular values of PA are the same as those of A. Rotation invariance of singular value indicates singular value invariance of matrix when the matrix is multiplied by unitary matrix. The above properties of SVD are very desirable in face recognition, especially when images are taken under different noise and viewpoint conditions.

II.7.3. SVD-Based Face Recognition:

In face recognition, singular valued decomposition (SVD) method had functioned as a new way for extracting algebraic features from an image. Among the properties which made SVD approach favorable in defining the face recognition process is defined as follows: the SVD of a face image has good stability in which it defined that whenever a small disturbance is added to a face image, a large variance of its singular values (SVs) will not occur. Singular values represent algebraic properties of an image. Hence, SV features possess algebraic and geometric invariance.

The block diagram of SVD-based face recognition is illustrated in figure II.8.

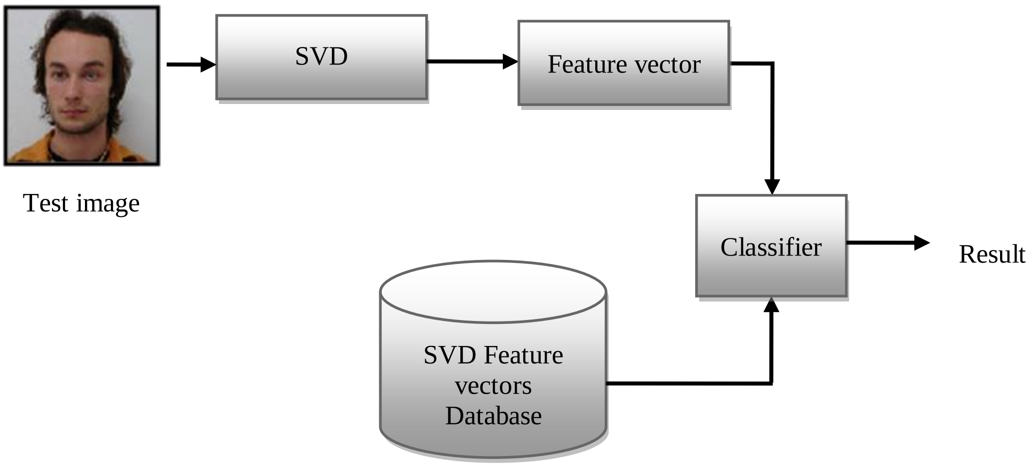

Figure II.8: Block diagram for face recognition using SVD.

Steps involved in SVD-based face recognition are:

Step1: Training set of M face images (A_i; i = 1… M) is first acquired.

Step2: SVD is an efficient algebraic feature extraction method which regards an image as a matrix. Conventional SVD based face recognition method uses the singular values as the feature vectors. Singular values represent important attributes of a matrix. As images are regarded as matrices, singular values can serve as image features in image similarity evaluation.

Suppose $\boldsymbol{A}_i$ is matrix of a face image. After $\boldsymbol{A}_i$ is decomposed by equation (II.58), the new feature vector $\boldsymbol{Y}_i^{SVD} \in \boldsymbol{R}^P$ is formed by arranging singular values:

$$\boldsymbol{Y}_i^{SVD} = [\boldsymbol{\sigma}_1, \boldsymbol{\sigma}_2, \boldsymbol{\sigma}_3, \dots, \boldsymbol{\sigma}_P\ ]^T \qquad (\boldsymbol{II.68})$$

Step3: A test face image is also decomposed by equation (II.58) and its feature vector $\boldsymbol{Y}_{test}^{SVD} \in \boldsymbol{R}^P$ is formed by arranging singular values:

$$\boldsymbol{Y}_{test}^{SVD} = [\boldsymbol{\sigma}_1, \boldsymbol{\sigma}_2, \boldsymbol{\sigma}_3, \dots, \boldsymbol{\sigma}_P\ ]^T \qquad (\boldsymbol{II.69})$$

Step 4: Compute the Euclidean distance between feature vector of the test face image and feature vectors training face images.

$$\boldsymbol{d}_i = \left\|\boldsymbol{Y}_{test}^{SVD} - \boldsymbol{Y}_i^{SVD}\right\| \qquad \textbf{for i = 1 \dots M} \qquad (\boldsymbol{II.70})$$

Step 5: The face which has the minimum distance with the test face image is labeled with the identity of that image. When the minimum d_i is less than some predefined threshold $\boldsymbol{\theta}$ the face image is classified as "known", otherwise the face is classified as “unknown face”.

II.8.Discrete Cosine Transform (DCT)

The Discrete Cosine Transform (DCT) is a popular technique in imaging and video compression, which was first applied in image compression **[115]** in 1974 by Ahmed *et al.*, transforming signals in the spatial representation into a frequency representation. The family of DCTs has been described by Wang and Hunt (1985). The set consists of 8 versions of DCT, where each transform is identified as even or odd and of type I, II, III, and IV. All present digital signal and image processing applications involve only even types of the DCT **[116]**. DCT-II was the one first suggested by Ahmed et al., and it is the one of concern in this project. The DCT was reported to be the second best transformation after PCA in **[117]** with an energy compaction that closely approximates that of PCA. Although PCA is the optimal transform in an energy packing sense, most practical transform coding systems still apply the DCT. It offers numerous advantages over PCA including producing good quality images at suitable compression ratios and the ability to perform in real time situations due to its computational efficiency. Face recognition algorithms incorporating DCT can be found in **[38**, **51**, **118**, **119**, **120**, **121]**.

II.7.1. DCT Theory:

The Discrete Cosine Transform (DCT) is an invertible linear transform that can express a finite sequence of data points in terms of a sum of cosine functions oscillating at different frequencies. The original signal is converted to the frequency domain by applying the direct DCT transform and it is possible to convert back the transformed signal to the original domain by applying the inverse DCT transform.

The Discrete Cosine Transform is one of many transforms that takes its input and transforms it into a linear combination of weighted basis functions. These basis functions are commonly in the form of frequency components **[116]**. The DCT is derived from the Discrete Fourier Transform where the sine component of DFT is zero. One dimensional discrete cosine transform is useful in processing one-dimensional signals such as speech waveforms. For analysis of two-dimensional (2D) signals such as images, a 2D version of the DCT is required.

The formal definition for the DCT of one-dimensional sequence of length N is given by the following formula:

$$C(u) = \alpha(u)\sum_{x=0}^{N-1} I(x)cos\left[\frac{\pi(2x+1)u}{2N}\right] \quad u = 0, 1, \dots, N-1 \qquad (II.71)$$

The inverse transformation is defined as

$$I(x) = \sum_{u=0}^{N-1} \alpha(u)C(u)cos\left[\frac{\pi(2x+1)u}{2N}\right] \quad x = 0, 1, \dots, N-1 \qquad (II.72)$$

$$\alpha(u) = \begin{cases} \sqrt{\frac{1}{N}} & for\ u = 0 \\ \sqrt{\frac{2}{N}} & for\ u = 1 \dots . N-1 \end{cases} \qquad (II.73)$$

As can be seen from (II.71) the substitution of u = 0 yields $C(0) = \alpha(0)\sum_{x=0}^{N-1} I(x)$, which is the mean of the sample. By convention, this value is called the DC coefficient of the transform and the others are referred to as AC coefficients. For every value u = 0, 1... N −1, transform coefficients correspond to a certain waveform. The first waveform renders a constant value, whereas all other waveforms (u=1, 2... N −1) produce a cosine function at increasing frequencies. The output of the transform for each u is the convolution of the input signal with the corresponding waveform. Figure II.9 shows plots of waveforms mentioned previously.

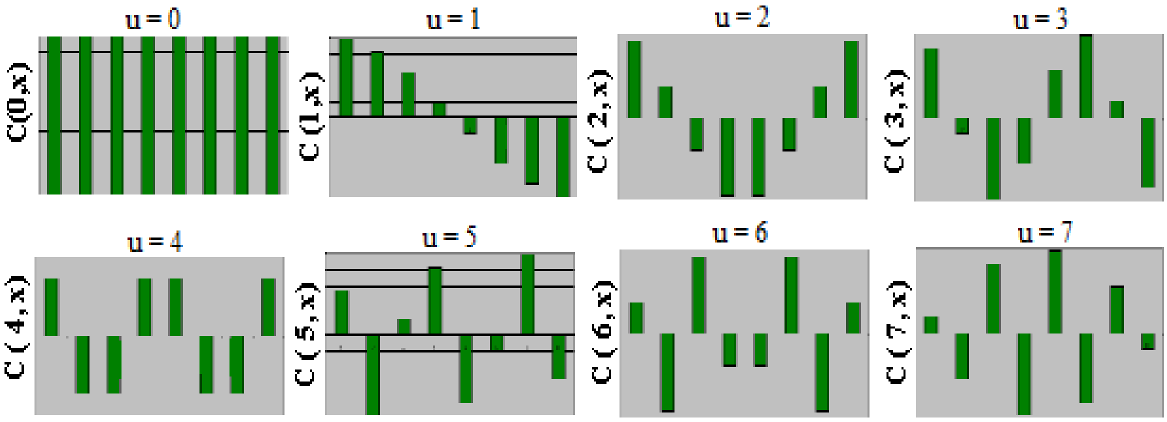

Figure II.9: 1D basis functions for *N=8*.

The two-dimensional DCT for a sample of size $N \times N$ is defined as follows:

$$\boldsymbol{C(u,v)=\alpha(u)\alpha(v)\sum_{x=0}^{N-1}\sum_{y=0}^{N-1}I(x,y)cos\left[\frac{\pi(2y+1)v}{2N}\right]cos\left[\frac{\pi(2x+1)u}{2N}\right]} \quad (\mathbf{II.74})$$

For $u, v = 1,2, \ldots, N-1$

The inverse of two-dimensional DCT for a sample of size $N \times N$:

$$\boldsymbol{I(x,y)=\sum_{u=0}^{N-1}\sum_{v=0}^{N-1}\alpha(u)\alpha(v)C(u,v)cos\left[\frac{\pi(2y+1)v}{2N}\right]cos\left[\frac{\pi(2x+1)u}{2N}\right]} \quad (\mathbf{II.75})$$

For $x, y = 0, 1, 2, \ldots, N - 1$

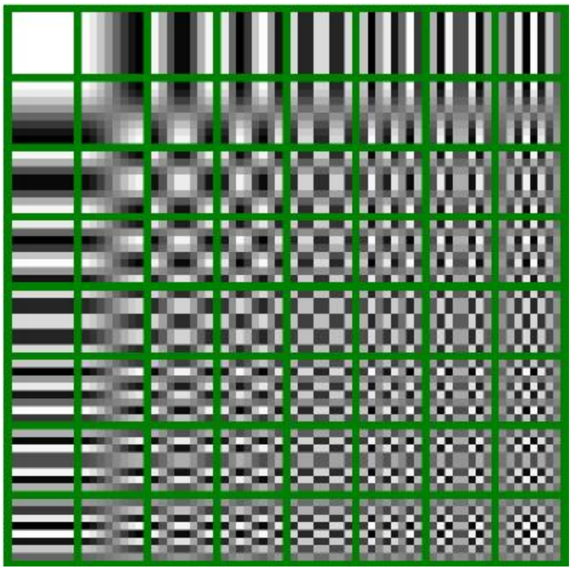

Figure II.10: 2D basis functions for N = 8.

II.8.2. Properties of DCT:

DCT has good properties which make it particularly useful in the image processing area. These properties are: decorrelation, energy compaction, separability, symmetry, and orthogonality **[122]**.

a. Decorrelation

The principle advantage of image transformation is the removal of redundancy between neighboring pixels. This leads to uncorrelated transform coefficients which can be encoded independently.

b. Energy Compaction

Efficacy of a transformation scheme can be directly gauged by its ability to pack input data into as few coefficients as possible. This allows the quantizer to discard coefficients with relatively small amplitudes without introducing visual distortion in the reconstructed image. DCT exhibits excellent energy compaction for highly correlated images.

c. Separability

The DCT transform in equation (II.4) can be expressed as,

$$\boldsymbol{C(u,v) = \alpha(u)\alpha(v)\sum_{x=0}^{N_p-1} cos\left[\frac{(2x+1)u\Pi}{2N}\right]\sum_{y=0}^{N_p-1} I(x,y)cos\left[\frac{(2y+1)v\Pi}{2N}\right]} \qquad \textbf{(II.76)}$$

This property known as separability, has the principle advantage that $C\ (u,v)$ can be computed in two steps by successive 1-D operations on rows and columns of an image. This idea is graphically illustrated in figure II.11.

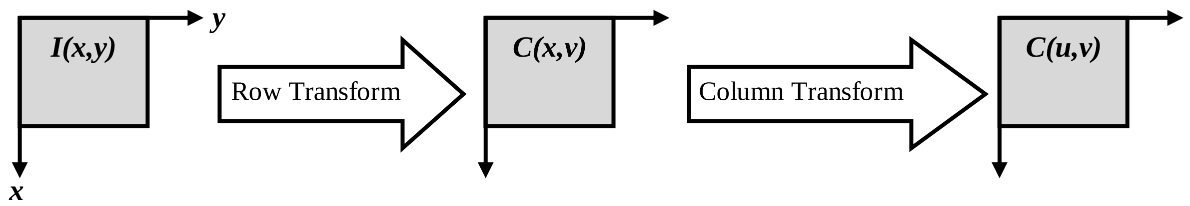

Figure II.11: Computation of 2-D DCT using separability property.

d. Symmetry

Another look at the row and column operations in equation II.76 reveals that these operations are functionally identical. Such a transformation is called a symmetric transformation. A separable and symmetric transform can be expressed in the form

$$\boldsymbol{T\ =\ AIA} \qquad \textbf{(II.77)}$$

Where *A* is an *N*×*N* symmetric transformation matrix with entries *a* (*i*, *j*) which is given by

$$\boldsymbol{a(i,j) = \alpha(j)\sum_{x=0}^{N-1} cos\left[\frac{\Pi(2j+1)i}{2N}\right]} \qquad \textbf{(II.78)}$$

And *I* is the *N*×*N* image matrix. This is an extremely useful property since it implies that the transformation matrix can be pre-computed offline and then applied to the image thereby providing orders of magnitude improvement in computation efficiency.

e. Orthogonality

The inverse transformation of equation (II.77) is $I\ =\ A^{-1}TA^{-1}$. DCT basis functions are orthogonal Thus, the inverse transformation matrix of *A* is equal to its transpose i.e. $A^{-1}\ =\ A^{T}$ in addition to its decorrelation characteristics, and this property renders some reduction in the pre-computation complexity. It guarantees the independency between two components, that is, the effect of modifying one component will not affect other components.

II.8.3. Face recognition using DCT:

Face recognition using DCT is divided into two stages training and classification. Figure II.12 shows the block diagram of DCT-based face recognition.

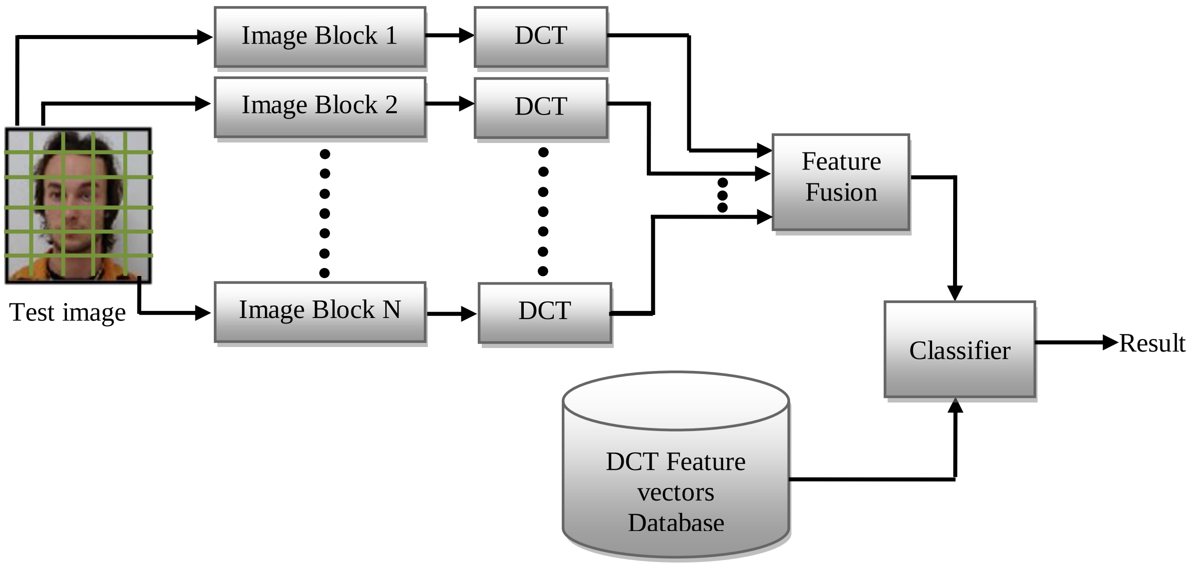

Figure II.12: Block diagram for face recognition using DCT

A. Training stage

The DCT transform is used for facial features extraction. Face images having high correlation and redundant information cause computational burden in terms of processing speed and memory utilization. Therefore, the 2D blocked-DCT segments an image non-overlapping blocks and applies the DCT to each block, which results in low frequency and high frequency subbands. Most of the visually significant signal energy lies at low-frequency sub-band which contains the most important visual parts of the image. These coefficients can be used as a type of signature that is useful for face recognition **[123**, **124**, **125]**.

The given face image is analyzed on block by block basis. Given an image block I (x, y), where $\mathrm{x}, \mathrm{y} = 0,1, \ldots, \mathrm{N}-1$, we decompose it in terms of orthogonal 2D DCT basis functions. The result is a $\mathrm{N} \times \mathrm{N}$ matrix $\mathrm{C}\,(\mathrm{u}, \mathrm{v})$ containing DCT coefficients. The DCT equations are given by formula (II.74). The DCT coefficients with large magnitude are mainly located in the upper-left corner of the DCT matrix. Accordingly, we scan the DCT coefficient matrix in a zig-zag manner starting from the upper-left corner (reflecting the amount of information stored) and subsequently convert it to a one-dimensional (1-D) vector **[120**, **126**, **127**, **128]** as given in figure II.13. For block located at (b, a) the DCT feature vector is composed of:

$$\boldsymbol{x} = \left[\boldsymbol{C}_{\boldsymbol{0}}^{(\boldsymbol{a},\boldsymbol{b})} \boldsymbol{C}_{\boldsymbol{1}}^{(\boldsymbol{a},\boldsymbol{b})} \ldots \ldots \ldots \ldots \ldots \ldots \ldots .. \boldsymbol{C}_{\boldsymbol{M-1}}^{(\boldsymbol{a},\boldsymbol{b})}\right]^{\boldsymbol{T}} \quad \textbf{(II.79)}$$

Where $\boldsymbol{C}_{\boldsymbol{n}}^{(\boldsymbol{a},\boldsymbol{b})}$ denotes the n^{th} DCT coefficient and M is the number of retained coefficients.

To obtain the final feature vector, the DCT coefficients obtained from each block are concatenated which is used by the classifier.

The first element, value of C (0, 0) is the average of all the samples in the input image and is referred to as Direct Current (DC) component. The remaining elements in C (u, v) each indicate the amplitude corresponding to the frequency component of I(x, y), and are defined as Alternate Current (AC) coefficients. It is well-known that the DC coefficient is only dependent to the brightness of the image. Consequently, it becomes DC-free (i.e., zero mean) and invariant against uniform brightness change by simply removing the DC coefficient **[126, 129]**.

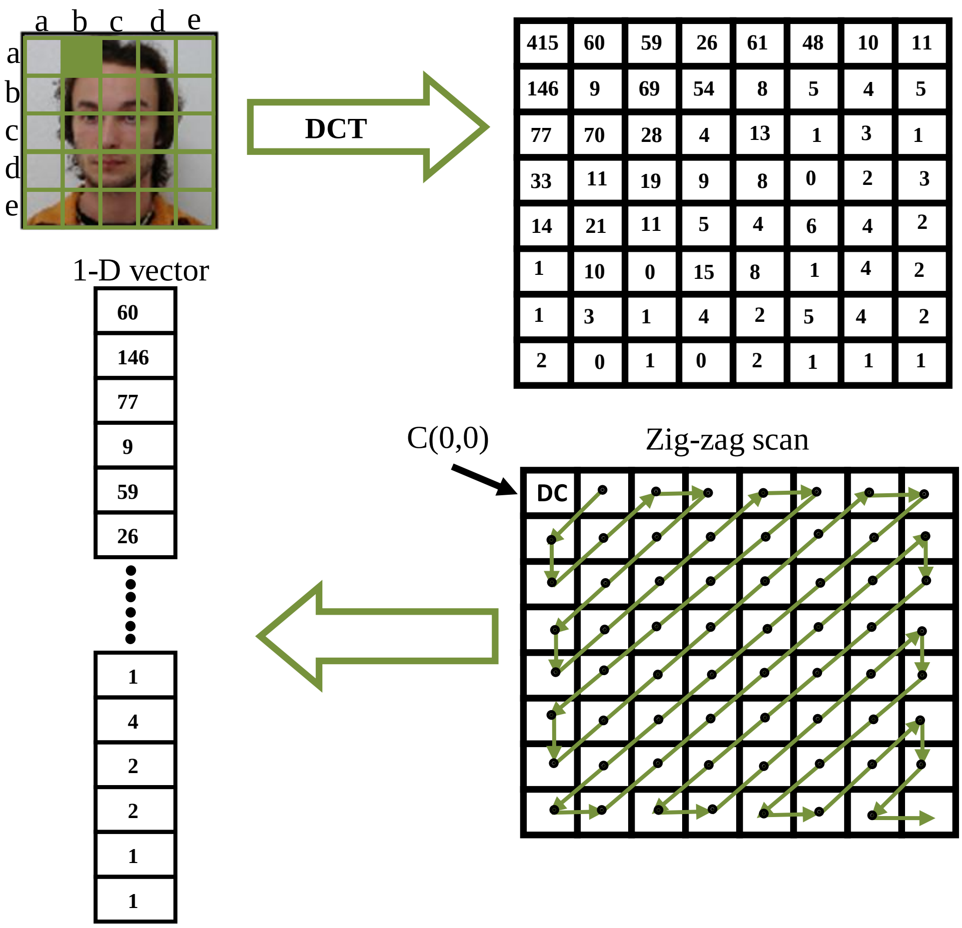

Figure II.13: Scheme of converting 2D DCT coefficients to 1-D vector

B. Classification Stage

The test face image is decomposed using DCT to form its feature vector following the same steps done with the training set. Then, its distances to all stored feature vectors are calculated. The face which has the minimum distance with the test face image is labeled with the identity of that image.

II.9. Wavelet transformation:

In recent years, wavelet transformation is being increasingly used in signal processing, image processing, computer vision and pattern recognition etc. Nastar et al. studied the relations between face and its spectrum. He found that facial expression and few occlusions only affect intensity manifold locally. If we represent by a frequency, it will only affect high frequency part. It is called high frequency phenomenon. We will have better effect if we represent human face by low frequency images and filter high frequency using wavelet.

Wavelet transformation is a method of representing signals across space and frequency. The signal is divided across several layers of division in space and frequency and then analyzed. The goal is to determine which space/frequency bands contain the most information about an image's unique features, both the parts that define an image as a particular type (fingerprint, face, etc.) and those parts which aid in classification between different images of the same type.

Wavelet analysis decomposes (sounds and images) into component waves of varying durations, called wavelets. These wavelets are localized vibrations of a sound signal, or localized variations of detail in an image. The heart of wavelet analysis is multiresolution analysis. Multiresolution analysis is the decomposition of a signal (such as an image) into subsignals (subimages) of different size resolution levels **[130]**.

The wavelet transform decomposes signals over dilated and translated wavelets. A wavelet is a function $\psi \in \mathbf{L^2}(\mathrm{R})$ with a zero average **[7]**:

$$\int_{-\infty}^{+\infty} \boldsymbol{\psi(t)dt = 0} \qquad (\boldsymbol{II.80})$$

The wavelet transform of an image *I(x,y)* is a linear transformation of this image onto a set of its inner products with basis functions $\psi_{u,s}(x,y)$ called wavelets These wavelets are generated from dilation and translation of a mother wavelet $\psi(x,y)$ as follows:

$$\boldsymbol{\psi_{u,s}(t) = \frac{1}{\sqrt{u_x u_y}}\, \psi\left(\frac{x - s_x}{u_x}, \frac{y - s_y}{u_y}\right) \quad u, s \in R, u \neq 0} \qquad (\boldsymbol{II.81})$$

Where $u = (u_x, u_y)^T$ *and* $s = (s_x, s_y)^T$ are the scaling, and the translation parameters respectively in *x-y* axes.

II.9.1.Discrete wavelet decomposition (DWT):

Discrete wavelet transform (DWT) is a well-known signal analysis tool, is widely used in feature extraction, compression and denoising applications. Discrete wavelet transform has been used in various studies in face recognition **[131**, **132**, **133**, **134**, **135**, **136]**.

2-D wavelet decomposition is carried out by applying a 1-D transform to the rows of the original image data and the columns of the row-transformed data respectively as shown in figure II.14 (a). The original image of resolution NxN is first filtered along the rows and downsampled by 2 yielding two NxN/2 images that have high and low frequency contents, respectively. After this decomposition, the wavelet transform is applied to the columns of these NxN/2 resolution images. In the last stage of the decomposition, we have four N/2xN/2 resolution subband images as shown in Figure II.14 (b). This decomposition can be repeated for n-levels as shown in figure II.14(c). Figure II.15 is 2-D wavelet decomposition of a face image. First, we decompose the original face images (as illustrated in figure II.15 (a)) into four sub-images via one level wavelet decomposition as shown in figure II.15 (b). Then, we decompose sub-image LL again, and we obtained 2-level decomposition image of original image as shown in figure II.15 (c). We can decompose sub-image LLL again, and we obtain 3-level decomposition image of original image as shown in figure II.15 (d). Following the process, we can make multiplayer wavelet decomposition. Sub-image LL denotes low frequency component of original face image and it is smoothing similar image of original image. In sub-image LH, sharp changes in the horizontal direction, i.e., vertical edges. However, in the sub-image HL, sharp changes in the vertical direction, i.e., horizontal edges. In the subimage HH, sharp changes in non-horizontal, non-vertical directions, i.e., inclined edges.

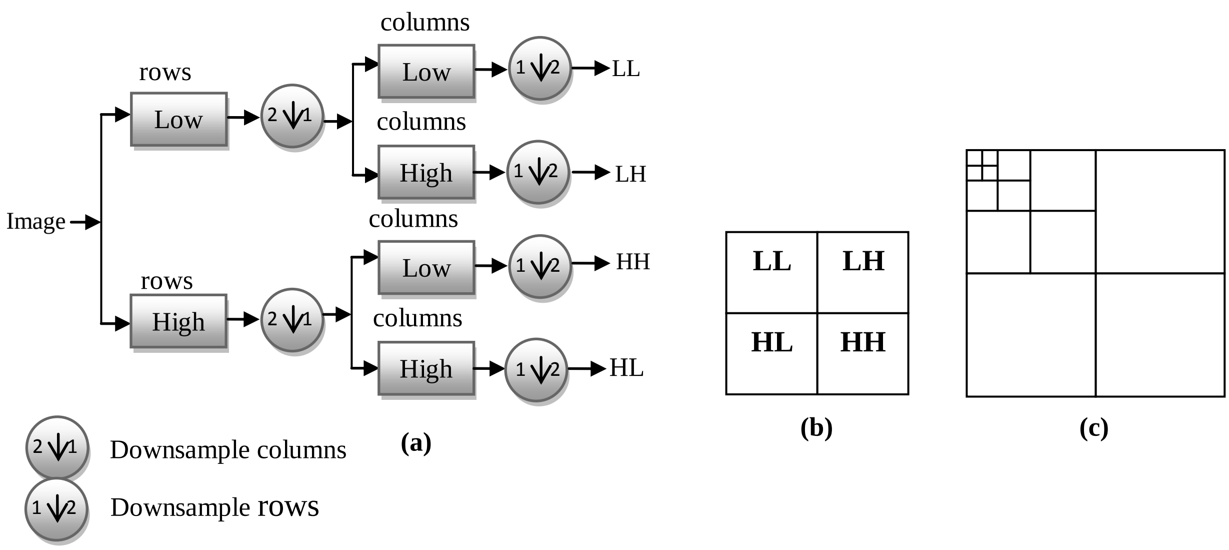

Figure II.14 (a) 2-D wavelet decomposition **(b)** four sub-images after one-level wavelet decomposition **(c)** n-level wavelet decomposition.

The term L and H refer to whether the processing filter is lowpass or highpass.

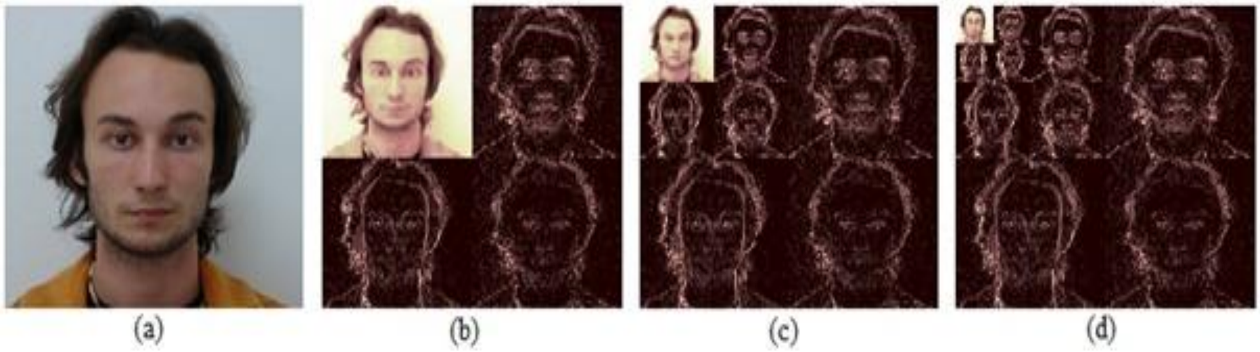

Figure II.15: Wavelet Decomposition at different level **(a)** original image, Wavelet Decomposition **(b)** at levels 1 **(c)** at levels 2 **(d)** at level 3.

II.9.2.Wavelet Packet Decomposition (WPD):

In the wavelet decomposition, only LL is further decomposed. Conversely, the wavelet packet decomposition all LL, LH, HL and HH are further decomposed **[137]** as shown in figure II.16 (c) figure II.16 (a) illustrates the wavelet packet decomposition at level 1 of the original image is given in figure II.15 (a). However, the wavelet packet decomposition at level 2 is given in figure II.16 (b).

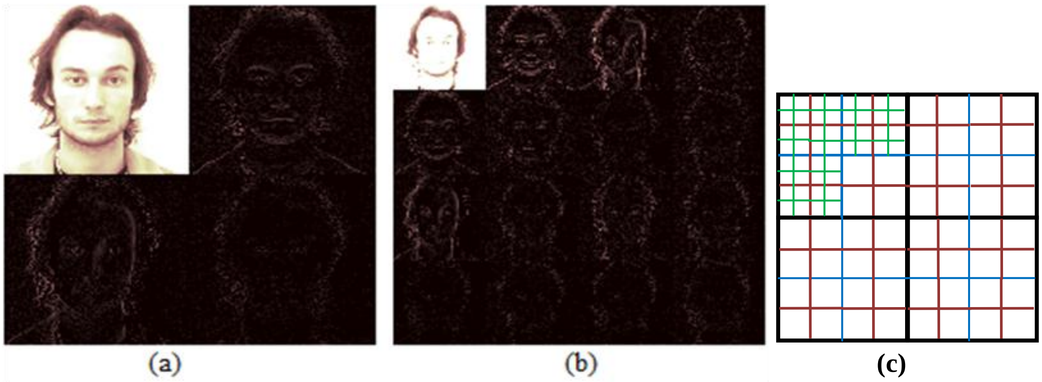

Figure II.16: Wavelet Packet Decomposition **(a)** at levels 1 **(b)** at level 2 **(c)** n-level wavelet packet decomposition.

II.9.3. Face recognition using DWT:

Face recognition system based on DWT consists of two processes, training and recognition processes. In the training process; we adopt db4 wavelet to decompose images of training set. After appropriate wavelet decomposition, we obtain the sub-image LL which is low dimension image. And we can obtain the wavelet feature vector. In recognition process, for an unknown image, we find wavelet feature vector from its sub-image LL after appropriate wavelet decomposition. According to the Nearest Neighbor Classifier, we can recognize the unknown face image.

II.9.4. Face recognition using PCA and DWT (DWT–PCA):

Li and Liu **[138]** used wavelet transformation prior to PCA in their work and reported a considerable performance improvement. Zhang *et al.* **[135]** applied Daubechies D8 wavelet transform to original face images, kept only the LL subband and used it as an input into the kernel associative memory neural network. Ekenel and Sankur **[131]** made a multiresolution face recognition system using Daubechies 4 wavelet and PCA and ICA for classification. The steps involved in the used system are:
1. For images training set, wavelet decomposition was performed using appropriate level to reduce the size of the original image and only the lowband wavelet was taken as the approximation image. 2. Next, PCA was performed on this approximation image to obtain its eigenfaces and were then stored in the database as training images. 3. Eigenfaces of the testing and database images were compared to find the best match.

II.9.4. Face recognition using PCA and WPD (WPD–PCA):

Face recognition using PCA and WPD is achieved by decomposing initial image into *n* parts using the Wavelet Packet Decomposition. Then, PCA is applied on each subband. The results from the various wavelet channels are fused to achieve possibly higher correct recognition rates. We investigated two schemes, namely, feature vectors fusion, and decision fusion.

→ **Decision fusion**

In decision fusion, face classification is run separately in each subband by computing the distances between the feature vector of test face and feature vectors of the individuals in the database. The final decision is made through these confidence values by using maximum rule and mean rule (Figure II.17).

→ **Feature fusion**

In feature fusion, PCA is performed on each subband (approximations and details), and then the extracted feature vectors are concatenated to construct a new feature vector to be used for classification (Figure II.18).

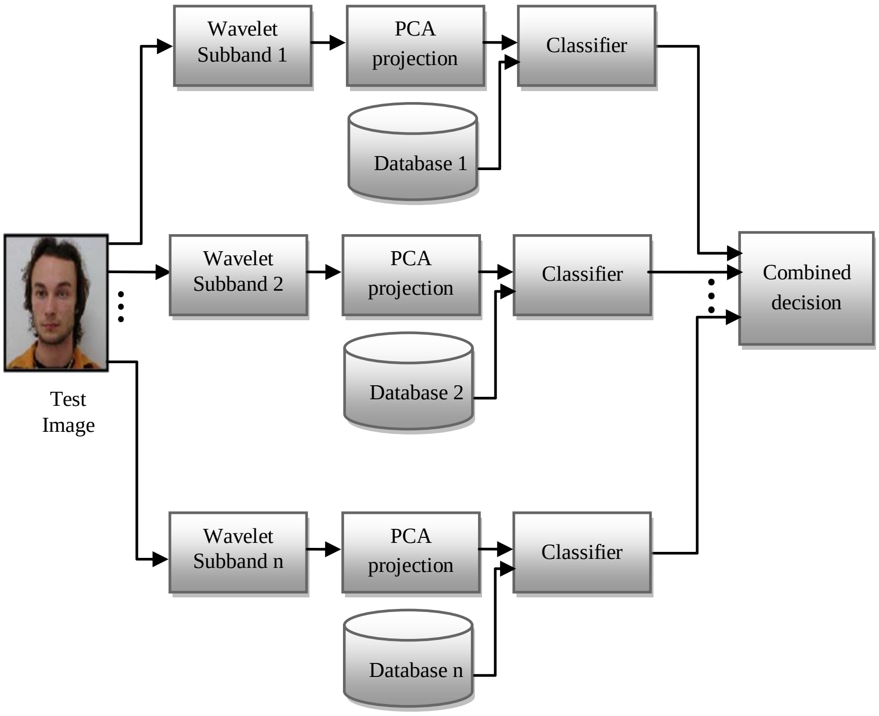

Figure II.17: Block diagram of decision fusion scheme for WPD-PCA method.

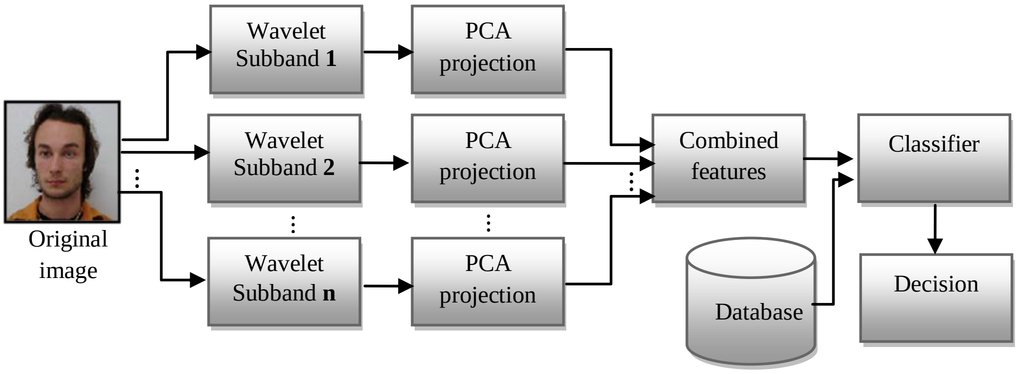

Figure II.18: Block diagram of feature fusion scheme for WPD-PCA method.

II.10. Proposed method based on PCA and PWD using YCbCr color space (YCbCr-PCA-PWD):

Much research on face recognition has focused on using grey-scale images. With the increasing availability of color images, it makes sense to develop approaches for integrating color information into the recognition process. Since the grey-scale approach is sensitive to lighting variations, we have chosen an approach which takes into consideration the intensity information as well as the chromatic information such as the YCbCr color space.

→ YCbCr Color space:

YCbCr is a family of color spaces used as a part of the color image pipeline in video and digital photography systems. It is a way of encoding RGB information. The RGB color space has been widely used for processing and storing digital image data. This model describes each color as a weighted combination of three base components Red, Green and Blue. However, high correlation between components and mixing luminance with chromaticity makes it very sensitive to changes in imaging conditions such as lighting **[139]**. Unlike the RGB space, YCbCr separates luminance from chrominances using a linear transform consisting of a weighted sum of the three components **[159, 10]**. The Y value represents the luminance or brightness component while the Cr and Cb values also known as the color difference signals represent the chrominance component of the image **[140]**.

The Y, Cb, and Cr component can be obtained as follow:

$$\begin{aligned} Y &= 16 + 0.2567882\,\mathbf{R} + 0.5041294\,\mathbf{G} + 0.0979059\,\mathbf{B} \\ Cb &= 128 - 0.148223\,\mathbf{R} - 0.2909928\,\mathbf{G} + 0.4392157\,\mathbf{B} \\ Cr &= 128 + 0.439216\,\mathbf{R} - 0.3677884\,\mathbf{G} - 0.0714274\mathbf{B} \end{aligned} \quad \text{(II.82)}$$

Where

Y is luminance, Cb is blue chromaticity, and Cr is red chromaticity.

The separate components of the YCbCr representation of the face are depicted in figure II.19. The person is recognizable form the Y image, but the Cr and Cb components are less recognizable.

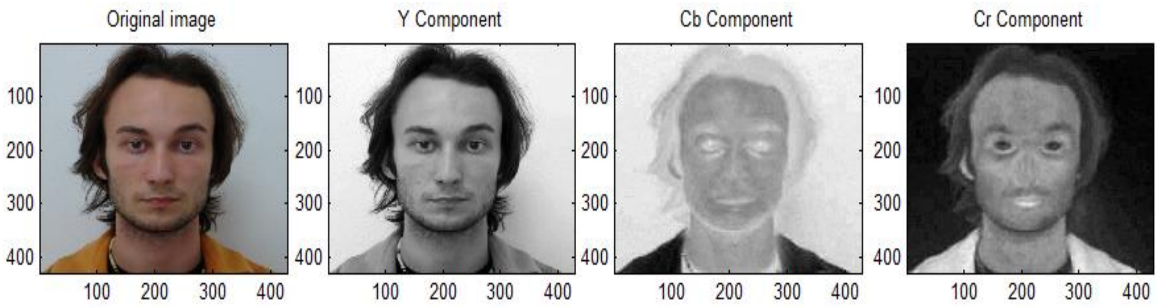

Figure II.19: Different views of a face

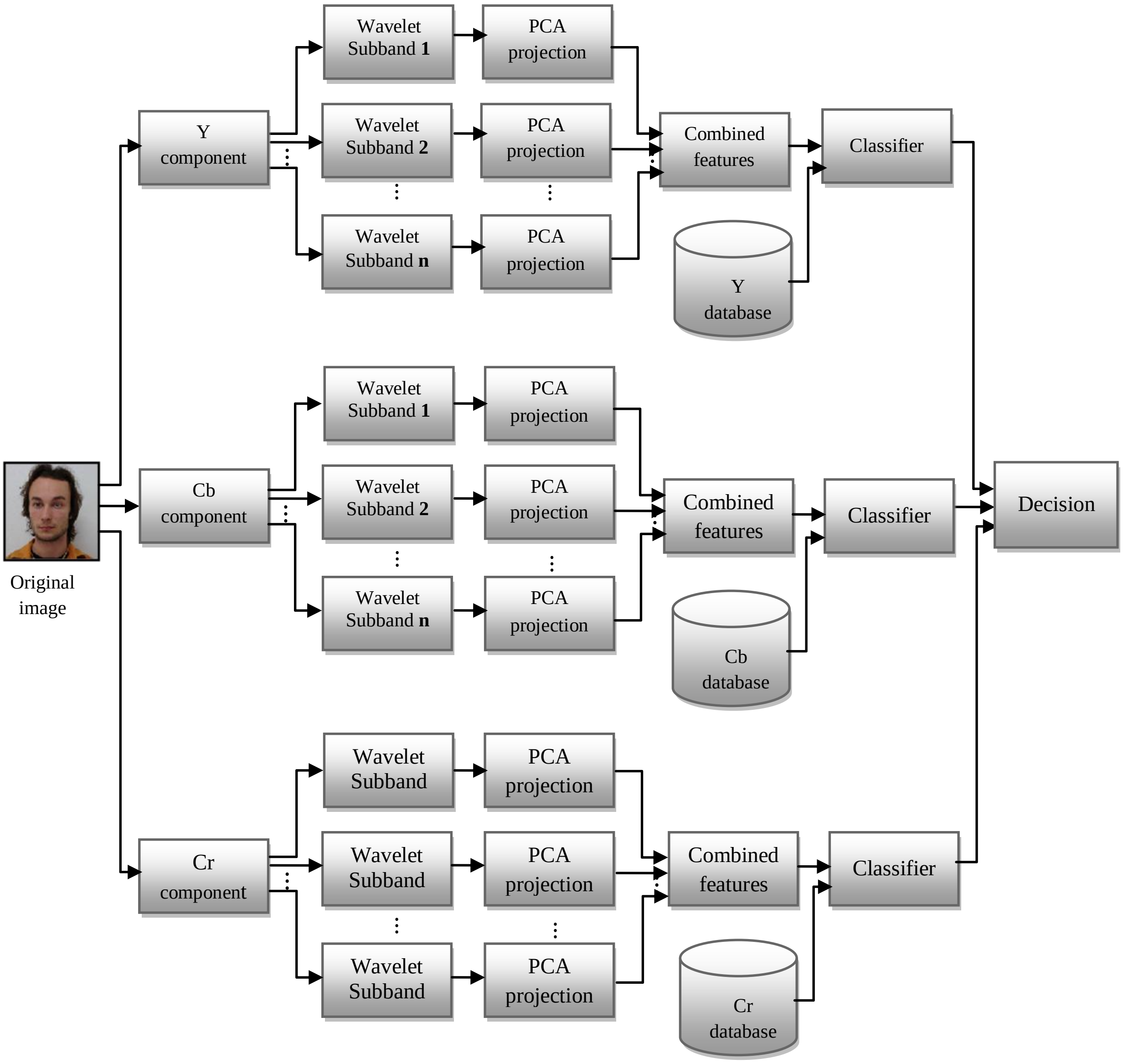

Figure II.20: Block diagram of the proposed method.

Steps followed in this method are:

Step1: Convert each face image into Y, Cb, and Cr components.

Step2: Decompose Y, Cb, Cr components obtained from the original images into k parts using the Wavelet Packet Decomposition. In our method, we have used the wavelet packet decomposition at level two. At the second level of decomposition, we obtain one image of approximation (low-resolution image) and 15 images of details. Therefore, the face image is described by 16 wavelet coefficient matrices, which represent quite a huge amount of information (equal to the size of the input image). Each of the 16 coefficient matrices contains information about the texture of the face.

Step3: Perform PCA for k-times on the Y, Cb, and Cr subbands (approximations and details). After the training, we get k eigenspaces and k feature vectors for each of Y, Cb, and Cr subbands.

Step4: The k feature vectors obtained from k eigenspaces are merged into one vector. The features are selected corresponding to the largest eigenvalues of the merged and sorted eigenvalues vector.

Step5: In the classification phase, the test image is projected onto the Y-eigenspace, Cb-eigenspace, and Cr-eigenspase after being decomposed into k part using the Wavelet Packet Decomposition. Then, compute the euclidean distance between the test image and all the training images in Y-subspace, Cb-subspace, and Cr-subspace. The euclidean distance is computed between the merged feature vectors. In the decision level, we compute the mean of the euclidian distances obtained from Y, Cb, and Cr subspaces. The face that has best match with the test image is which has the minimum distance.

II.11. Fusion Methods:

The pronounced need for establishing identity in a reliable manner leads to an active research in the field of biometrics. It is now evident that a single biometric is not sufficient to meet the variety of requirements including matching performance imposed by several large-scale authentication systems. Multibiometric systems seek to remove some of the drawbacks encountered by unibiometric systems by consolidating the evidence presented by multiple biometric traits/sources. These systems can significantly improve the recognition performance of the biometric system, besides improving population coverage, deterring spoof attacks, and reducing the failure-to-enroll rate. Although the storage requirements, processing time and the computational demands of a multibiometric system are much higher than a unibiometric system, the above mentioned advantages present a compelling case for deploying multibiometric systems in large-scale authentication systems. Biometric fusion or multibiometric system is the use of multiple types of biometric data, or methods of processing, to improve the performance of biometric systems **[141]**.

II.11.1. Fusion scenarios:

Depending on the number of traits, sensors, and the used feature sets, different scenarios are possible in a multibiometric system **(**see figure II.21) **[142**, **143**, **144**, **145**, **146]**.

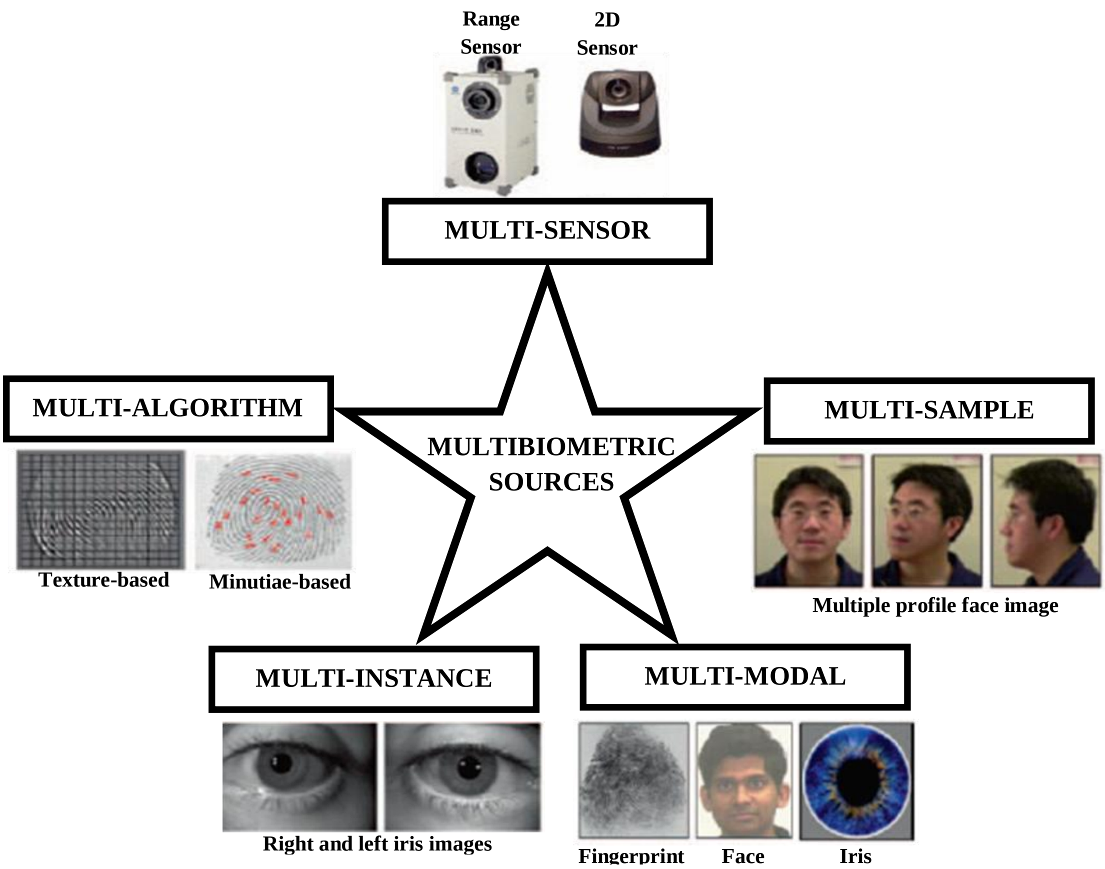

Figure II.21: The various sources of information in a multibiometric system.

II.11.1.1.Multi-sensor systems:

Multi-sensor systems employ multiple sensors to capture a single biometric trait of an individual. Chang et al. **[147]** acquire both 2D and 3D images of the face and combine them at the data level as well as the match score level to improve the performance of the face recognition system. Kumar et al. **[148]** describe a hand based verification system that combines the geometric features of the hand with palmprints at the feature and match score levels. An infrared sensor may be used in conjunction with a visible-light sensor to acquire the subsurface information of a person's face **[149**, **150**, **151**, **152]**. A multispectral camera may be used to acquire images of the iris, face, or finger **[153]**, or optical and capacitive sensors may be used to image the fingerprint of a subject **[154]**.

II.11.1.2.Multi-algorithm systems:

In some cases, invoking multiple feature extraction and/or matching algorithms on the same biometric data can result in improved matching performance.

Multi-algorithm systems consolidate the output of multiple feature extraction algorithms or that of multiple matchers operating on the same feature set. Ross et al. **[155]** combine the matching score of a minutiae-based fingerprint matcher with that of a texture-based matcher to improve matching performance. Lu et al. extract three different types of feature sets from the face image of a subject (using PCA, LDA and ICA) and integrate the output of the corresponding classifiers at the match score level **[156]**. In **[157]**, they combine visual and infrared images for face recognition, and in **[158]**, they fuse the audio and visual features for speaker identification.

II.11.1.3.Multi-instance systems:

These systems use multiple instances of the same body trait and have also been referred to as multi-unit systems in the literature. For example, the left and right index fingers, or the left and right irises of an individual, may be used to verify an individual's identity **[159]**.

II.11.1.4.Multi-sample systems:

A single sensor may be used to acquire multiple samples of the same biometric trait in order to account for the variations that can occur in the trait or to obtain a more complete representation of the underlying trait **[160]**. A face system, for example, may capture (and store) the frontal profile of a person's face along with the left and right profiles in order to account for variations in the facial pose. Similarly, a fingerprint system equipped with a small size sensor may acquire multiple dab prints of an individual's finger in order to obtain images of various regions of the fingerprint. A mosaicing scheme may then be used to stitch the multiple impressions and create a composite image. Uludag et al. **[161]** discuss two such schemes in the context of fingerprint recognition. Examples of Multi-sample for face recognition are given in **[162**, **163]**.

II.11.1.5.Multimodal systems:

Multimodal systems establish identity based on the evidence of multiple biometric traits. For example, some of the earliest multimodal biometric systems have utilized face and voice features to establish the identity of an individual **[164**, **165]**. Also, face and gait **[166]**, Face and speech **[167]**, palm and finger **[168]**, ear and face **[169]**, face and palmprint **[170]** have been used.

II.11.1.6. Hybrid systems:

Chang et al. use the term hybrid to describe systems that integrate a subset of the five scenarios discussed above. For example, Brunelli et al. **[171]** discuss an arrangement in which two speaker recognition algorithms are combined with three face recognition algorithms at the match score and rank levels via a HyperBF network. Thus, the system is multi-algorithmic as well as multimodal in its design. Hybrid systems attempt to extract as much information as possible from the various biometric modalities such as multi unit and multi sample **[172]**.

II.11.2. Levels of Fusion:

Based on the type of information available in a certain module, different levels of fusion may be defined. Sanderson and Paliwal categorize the various levels of fusion into two broad categories: pre-classification or fusion before matching and post-classification or fusion after matching. Pre-classification schemes include fusion at the sensor (or raw data) and the feature levels while post-classification schemes include fusion at the match score, rank and decision levels.

II.11.2.1. Sensor-level fusion:

Sensor-level fusion refers to the consolidation of (a) raw data obtained by using multiple sensors or (b) multiple snapshots of a biometric using a single sensor **[173**, **174]**. Another example of sensor level fusion is the mosaicing of multiple fingerprint impressions to form a more complete fingerprint image **[175**, **176**, **177**, **178**, **179]**.

II.11.2.2. Feature-level fusion:

In feature-level fusion, the feature sets originating from multiple biometric algorithms are consolidated into a single feature set by the application of appropriate feature normalization, transformation, and reduction schemes **[180]**. When the feature sets are homogeneous (e.g., multiple fingerprint impressions of a user's finger), a single resultant feature set can be calculated as a weighted average of the individual feature sets (e.g., mosaicing of fingerprint minutiae **[173]**). When the feature sets are non-homogeneous (e.g., feature sets of different biometric modalities like face and hand geometry), we can concatenate them to form a single feature set. Examples of feature level fusion schemes proposed in the literature can be found in Gan and Liang **[181]** (face and iris), Kumar et al. **[182]** (hand geometry and palmprint) and Ross and Govindarajan **[183]** (face and hand geometry).

II.11.2.3. Score-level fusion:

In score-level fusion the match scores output by multiple biometric matchers are combined to generate a new match score (a scalar) that can be subsequently used by the verification or identification modules for rendering an identity decision **[184]**. Fusion at this level is the most commonly discussed approach in the biometric literature primarily due to the ease of accessing and processing match scores (compared to the raw biometric data or the feature set extracted from the data). Fusion methods at this level can be broadly classified into three categories **[185]**: density-based schemes **[186**, **141]**, transformation-based schemes **[187]**, and classifier-based schemes **[188]**.

II.11.2.4. Rank-level fusion:

This type of fusion is relevant in identification systems where each classifier associates a rank with every enrolled identity (a higher rank indicating a good match). Thus, fusion entails consolidating the multiple ranks associated with an identity and determining a new rank that would aid in establishing the final decision.

II.11.2.5. Decision-level fusion:

Decision-level fusion and score-level fusion methods are most popular in the field of multimodal biometrics **[145**, **181]**. When each matcher outputs its own class label (i.e., accept or reject in a verification system, or the identity of a user in an identification system), a single class label can be obtained by employing techniques like majority voting, behavior knowledge space, etc. Methods proposed in the literature for decision-level fusion include "AND" and "OR" rules **[189]**, majority voting **[190]**, weighted majority voting, Bayesian decision fusion **[191]**, the Dempster–Shafer theory of evidence **[191]**, and behavior knowledge space **[192]**.

II.11.3. Fusion rules:

In the fusion approach, the individual matching scores are combined to generate a single scalar score, which is then used to make the final decision. The matching scores are the outputs of the classifiers measuring the similarities of the testing samples to the claimed class. The classifier combination can be implemented at two levels, feature level and decision level. We use the decision level combination that is more appropriate when the component classifiers use different types of features **[194]**. Let S_1, S_2,…,S_m be the matching scores generated from different classifier, where m is the number of feature vectors or classifiers. A few of the well-known fusion techniques are the mean, minimum, maximum and product rule **[193**, **195]**.

→ **Mean or Sum Rule**

$$\boldsymbol{S^j = (S_1 + S_2 + \cdots + S_m)/m} \qquad (\boldsymbol{II.82})$$

→ **Min Rule**

$$\boldsymbol{S^j = min(S_1, S_2, \dots, S_m)} \qquad (\boldsymbol{II.83})$$

→ **Max Rule**

$$\boldsymbol{S^j = max(S_1, S_2, \dots, S_m)} \qquad (\mathbf{II.84})$$

→ **Product Rule**

$$\boldsymbol{S^j = product(S_1, S_2, \dots, S_m)} \qquad (\mathbf{II.85})$$

II.11.4.Face recognition using fusion:

Given different types of feature vectors $\boldsymbol{Y_i^{PCA}}, \boldsymbol{Y_i^{FLD}}, \boldsymbol{Y_i^{SVD}}, \boldsymbol{Y_i^{DCT}}, and\ \boldsymbol{Y_i^{DWT}}$, the task is how to form the final distance measure. Four strategies are used averaging, multiplying, minimum and maximum. The possible combinations are given in the table II.1 below when we use only two and three types of features vectors.

Feature vectors	Methods using two types of feature vectors	Methods using three types of feature vectors
PCA FLD SVD DCT DWT	PCA+FLD	PCA+FLD+SVD
	PCA+SVD	PCA+FLD+DCT
	PCA+DCT	PCA+FLD+DWT
	PCA+DWT	PCA+SVD+DCT
	FLD+SVD	PCA+SVD+DWT
	FLD+DCT	PCA+DCT+DWT
	FLD+DWT	FLD+SVD+DCT
	SVD+DCT	FLD+SVD+DWT
	SVD+DWT	FLD+DCT+DWT
	DCT+DWT	SVD+DCT+DWT

Table II.1: Possible combination in fusion methods.

Process of fusion using two types and three types of feature vectors and the block diagram of face recognition using fusion are given in figure II.22 and figure II.23 respectively.

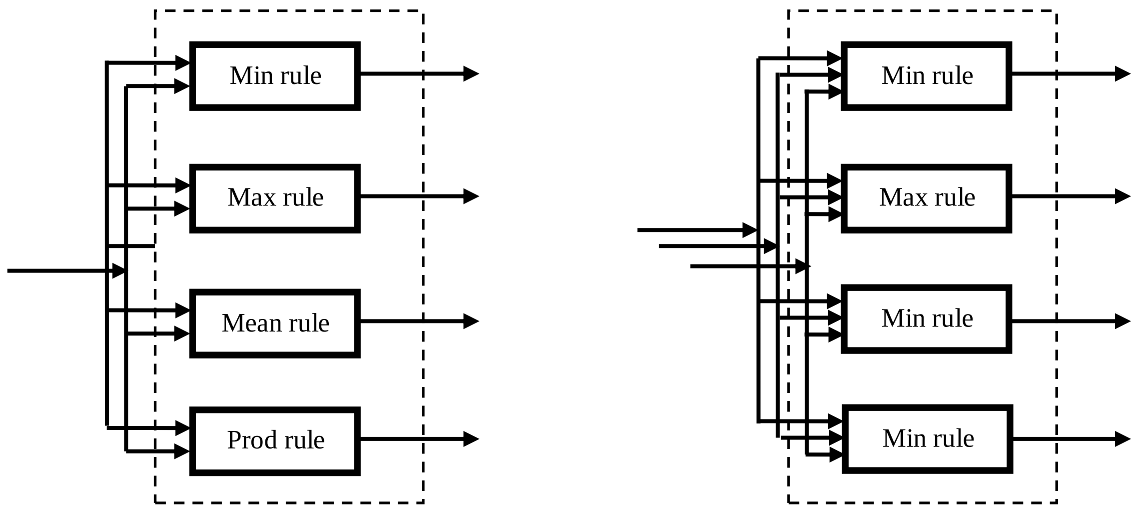

Figure II.22: Process of fusion using two types and three types of feature vectors.

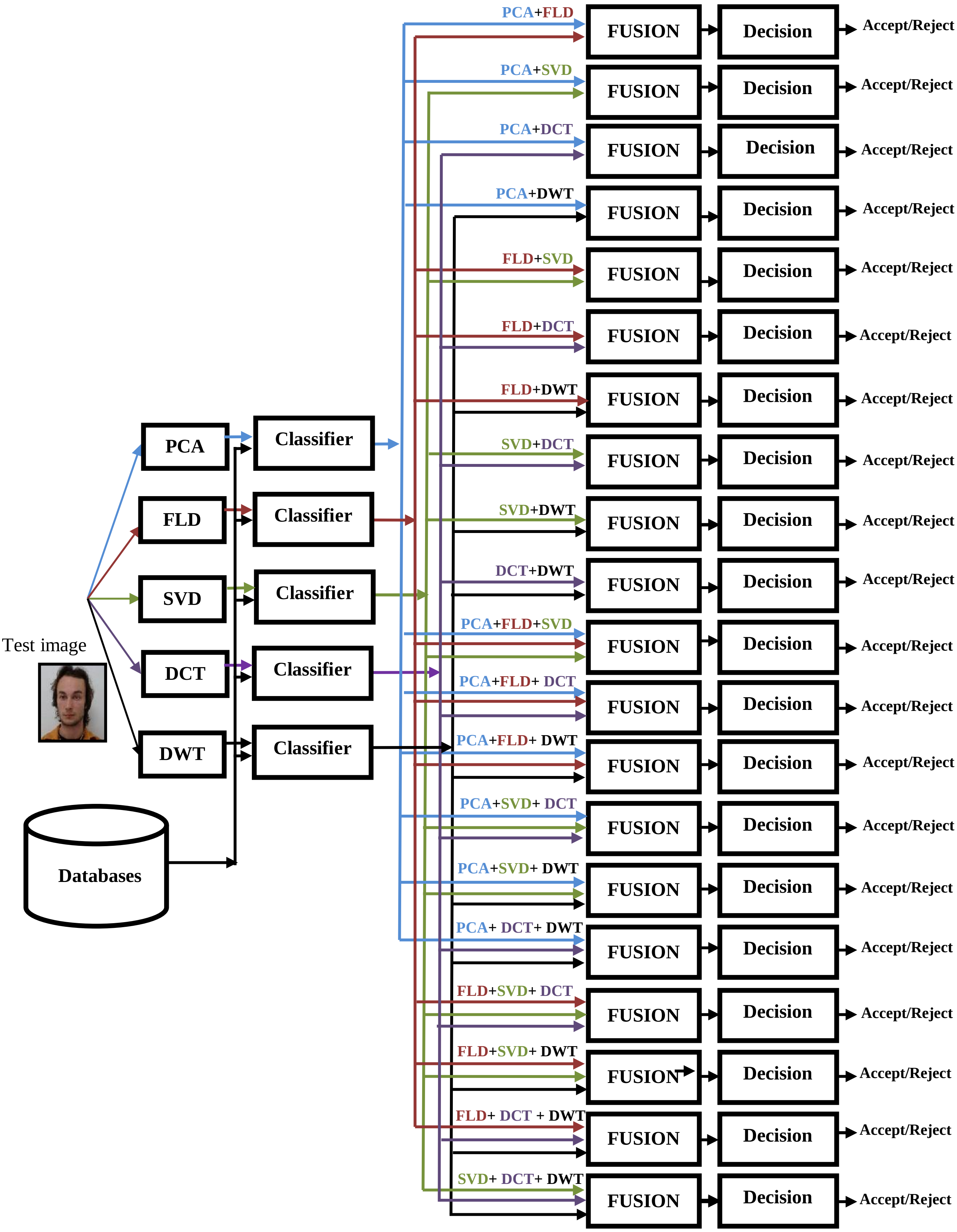

Figure II.23: Block diagram of face recognition using fusion method.

The process of testing is:

1) Choose one of the method proposed in table II.1.

2) Input a query face image $\boldsymbol{x}_i$, extract different types of feature vectors depending on the method chosen.

3) Compute the distances of the query face image to all the training images:

$$\begin{gathered}\boldsymbol{d}_{\boldsymbol{i}}^{Type\ 1} = (\boldsymbol{d}_{\boldsymbol{i1}}^{Type\ 1}, \boldsymbol{d}_{\boldsymbol{i2}}^{Type\ 1}, \dots, \boldsymbol{d}_{\boldsymbol{iM}}^{Type\ 1}) \\ \vdots \\ \boldsymbol{d}_{\boldsymbol{i}}^{Type\ N} = (\boldsymbol{d}_{\boldsymbol{i1}}^{Type\ N}, \boldsymbol{d}_{\boldsymbol{i2}}^{Type\ N}, \dots, \boldsymbol{d}_{\boldsymbol{iM}}^{Type\ N})\end{gathered} \qquad (\boldsymbol{II.86})$$

Where: M is the number of training images.

N is the number of features vectors

If the Type 1,…, Type N feature vectors of training images $\boldsymbol{x}_j$ are $\boldsymbol{Y}_{\boldsymbol{j}}^{\boldsymbol{Type\,1}}, \dots, \boldsymbol{Y}_{\boldsymbol{j}}^{\boldsymbol{Type\,N}}$ respectively. Then,

$$\begin{gathered}\boldsymbol{d}_{\boldsymbol{ij}}^{Type\ 1} = \left\| \boldsymbol{Y}_{\boldsymbol{i}}^{Type\ 1} - \boldsymbol{Y}_{\boldsymbol{j}}^{Type\ 1} \right\| \\ \vdots \\ \boldsymbol{d}_{\boldsymbol{ij}}^{Type\ N} = \left\| \boldsymbol{Y}_{\boldsymbol{i}}^{Type\ N} - \boldsymbol{Y}_{\boldsymbol{j}}^{Type\ N} \right\|\end{gathered} \qquad (\boldsymbol{II.87})$$

4) Calculate the final distances which contain information of different types of feature vectors using different fusion rules such as:

1. The minimum rule:

$$\begin{aligned} d_i &= (d_{i1}, d_{i2}, \dots, d_{iM}) \\ &= \left(min\left(d_{i1}^{Type\ 1}, \dots, d_{i1}^{Type\ N}\right), min\left(d_{i2}^{Type\ 1}, \dots, d_{i2}^{Type\ N}\right), \dots, min\left(d_{iM}^{Type\ 1}, \dots, d_{iM}^{Type\ N}\right) \right) \end{aligned} \qquad (\boldsymbol{II.88})$$

$$\text{i.e.}\ d_{ij} = min\left(\boldsymbol{d}_{\boldsymbol{ij}}^{Type\ 1}, \dots, d_{ij}^{Type\ N}\right) \qquad (\boldsymbol{II.89})$$

2. The maximum rule:

$$\begin{aligned} d_i &= (d_{i1}, d_{i2}, \dots, d_{iM}) \\ &= \left(max\left(d_{i1}^{Type\ 1}, \dots, d_{i1}^{Type\ N}\right), max\left(d_{i2}^{Type\ 1}, \dots, d_{i2}^{Type\ N}\right), \dots, max\left(d_{iM}^{Type\ 1}, \dots, d_{iM}^{Type\ N}\right) \right) \end{aligned} \qquad (\boldsymbol{II.90})$$

$$\text{i.e.}\ d_{ij} = max\left(\boldsymbol{d}_{\boldsymbol{ij}}^{Type\ 1}, \dots, d_{ij}^{Type\ N}\right) \qquad (\boldsymbol{II.91})$$

3. **Mean rule**:

$$d_i = (d_{i1}, d_{i2}, \dots, d_{iM})$$
$$= \left(\frac{d_{i1}^{Type\ 1} + \cdots + d_{i1}^{Type\ N}}{N}, \frac{d_{i2}^{Type\ 1} + \cdots + d_{i2}^{Type\ N}}{N}, \dots, \frac{d_{iM}^{Type\ 1} + \cdots + d_{iM}^{Type\ N}}{N}\right) \qquad (\boldsymbol{II.92})$$

$$\text{i.e. } d_{ij} = \frac{d_{ij}^{Type\ 1} + \cdots + d_{ij}^{Type\ N}}{N} \qquad (\boldsymbol{II.93})$$

4. **The Product rule**:

$$d_i = (d_{i1}, d_{i2}, \dots, d_{iM})$$
$$= \left(prod\left(d_{i1}^{Type\ 1}, \dots, d_{i1}^{Type\ N}\right), prod\left(d_{i2}^{Type\ 1}, \dots, d_{i2}^{Type\ N}\right), \dots, prod\left(d_{iM}^{Type\ 1}, \dots, d_{iM}^{Type\ N}\right)\right) \qquad (\boldsymbol{II.94})$$

$$\text{i.e. } d_{ij} = product\left(d_{ij}^{Type\ 1}, \dots, d_{ij}^{Type\ N}\right) \qquad (\boldsymbol{II.95})$$

4) Based on the distances$(\boldsymbol{d_{i1}}, \boldsymbol{d_{i2}}, \dots, \boldsymbol{d_{iM}})$, the nearest neighbor classifier is employed to accomplish the task of classification. Categorize the face image $\boldsymbol{x}_i$ into class label *k*, where *k* is determined by

$$\boldsymbol{d_{ik}} = \min_{\boldsymbol{1 \le j \le M}} \{\boldsymbol{d_{ij}}\} \qquad \boldsymbol{1 \le k \le c} \qquad (\boldsymbol{II.96})$$

The goal of fusion is to get a higher accuracy than each individual classifier or feature vectors. The premise of fusion is that different classifiers or features can overcome the drawbacks of each other.

II.12.Conclusion:

In this chapter, the role of face in modern life has been presented, and the properties and tasks associated to face recognition systems have been introduced. Many methods of face recognition have been proposed. Basically, they can be divided into three categories: Global-Appearance-based methods, local appearance-based methods and hybrid methods. The most successful and well-studied techniques are the appearance-based methods. So, in this thesis some of them are discussed namely: PCA, FLD, SVD, and DWT or WPD. The local appearance-based methods can be divided into two groups: The ones that require the use of specific regions and the ones that simply partition the input face image into blocks without considering any specific regions. For the latter type we have implemented the Discrete Cosine Transform (DCT) method.

Since the grey-scale approach is sensitive to lighting variations we have chosen an approach which takes into consideration the intensity information as well as the chromatic information. Method has been proposed by combining principal component, wavelet packet decomposition and YCbCr color space.

It is now evident that a single biometric (unibiometric) is not sufficient to meet the variety of requirements including matching performance imposed by several large-scale authentication systems. Multibiometric systems seek to overcome some of the drawbacks encountered by unibiometric systems by consolidating the evidence presented by multiple biometric traits/sources or methods of processing. Based on the nature of these sources, a multibiometric system can be classified into one of the following six categories: multi-sensor, multi-algorithm, multi instance, multi-sample, multimodal and hybrid. In this thesis we have utilized multi-algorithm systems that consolidate the output of multiple feature extraction algorithms. We have used fusion of two types and three types of feature vectors at score levels using four fusion rules i.e. minimum, maximum, mean, and product. In the next chapter, we will discuss the experimental results of the methods described in this chapter.

Chapitre III

Experimantal results and discussion

III.1.Introduction:

To evaluate the efficiency of the methods discussed in the previous chapter, we have used three face database, ORL database, Yale database, and FEI database. These databases are presented with depiction of some sample images in the first section. In the second section, the experiments carried out on the databases are presented and discussed. The accuracy of each algorithm has been identified and a comparison was performed between them in terms of recognition rates or Equal Error Rate (EER) or the Receiver Operating Curves (ROC). All of our experiments have been carried out through the use of a laptop with dual CPU T2330 1.4 GHz and 2GB memory and the MATLAB as developing software tool.

III.2.Face databases:

III.2.1.The ORL database:

The ORL database (**http://www.cl.cam.ac.uk/research/dtg/attarchive/facedatabase.html**) consists of 40 distinct persons. There are 10 images per person. The images are taken at different times and contain various facial expressions (open/closed eyes, smiling/not smiling) and facial details (glasses or no glasses). The size of the images is 92 X 112 pixels with 256 gray levels. Figure III.1 depicts some sample images in the ORL database. None of the 10 samples are identical to each other; so there was no overlap between the training and test sets. Besides, the original images are used in training and testing without pre-processing.

(a)

(b)

Figure III.1: Example images of ORL database **(a)**: Training images **(b)**: Testing images.

III.2.2.The Yale database:

The Yale face database (**http://cvc.yale.edu/projects/yalefaces/yalefaces.html**) contains 165 grayscale images of 15 individuals. There are 11 images per subject, and these images demonstrate variations in lighting condition (center-light, left-light, right-light) and facial expression (happy, normal, sad, sleepy, surprised, and winking) and facial details (glasses/no glasses). All face images were cropped into 100 X 100 from original frames based on the location of the two eyes. Figure III.2 shows the presentations of one individual. There was no overlap between the training and test sets. Besides, the original images are used in training and testing without pre-processing.

(a)

(b)

(c)

Figure III.2: Examples of one subject in the Yale Face Database under: (a) facial details (glasses/no glasses) (b) Different lighting conditions (c) Different facial expression.

III.2.3.The FEI database:

The FEI face database is a Brazilian face database that contains a set of face images taken between June 2005 and March 2006 at the Artificial Intelligence Laboratory of FEI in São Bernardo do Campo, São Paulo, Brazil. There are 14 images for each of 200 individuals, a total of 2800 images. All images are colorful and taken against a white homogenous background in an upright frontal position with profile rotation of up to about 180 degrees. Scale might vary about 10% and the original size of each image is 640x480 pixels. All faces are mainly represented by students and staff at FEI, between 19 and 40 years old with distinct appearance, hairstyle, and adorns. The number of male and female subjects is exactly the same and equal to 100. Figure III.3 shows some examples of image variations from the FEI face database. This database is available at http://www.fei.edu.br/~cet/facedatabase.html

Figure III.3: Some examples of image variations from the FEI face database.

III.3.Experiments results and discussion:

III.3.1.Experiments on Yale database:

These experiments are carried out on the Yale face database with a special emphasis on testing the effects of various changes in face images, such as variations of facial expressions, illumination and facial details.

→ **PCA under facial details:**

To evaluate the effect of facial details (glasses, and no glasses) on the system performance of PCA (eigenfaces) we have used the Yale face database. The face images of different facial details from Yale face database were used in the experiments (Figure III.3 (a)). The faces in neutral expression were used as single models of the subjects. Totally, there were 15 models (representing 15 individuals) and 30 test images. The experimental results were summarized in table III.1. Facial details using glasses do not affect the recognition rate in Eigenfaces using L2 and Mah ; while with L1+Mah caused the recognition rate to drop by 33.3% as compared to no glasses, the L1, COS, L2+Mah, COS+Mah caused only a 6.67 % drop of the rate.

	Recognition rate (%)	
Facial Details / Similarity Measure	No glasses	glasses
L1	93.33	86.67
L2	100	100
COS	100	93.33
Mah	100	100
L1+Mah	80	46.67
L2+Mah	100	93.33
C0S+Mah	100	93.33

Table III.1: Result of face recognition under facial details.

→ PCA under varying lighting conditions:

To evaluate the effects of different illumination (left light, center light, and right light) on the system performances we have used Yale face database. The face images of different illumination from Yale face database were used in the experiments (Figure III.3 (b)). The faces in neutral expression were used as single models of the subjects. Totally, there were 15 models (representing 15 individuals) and 45 test images. The experimental results were summarized in table III.2. We have found that the recognition rates with left light on were always higher than that with right light on using different distance measure except when using L1+Mah. This could be due to the fact that the illumination on faces from the right light was slightly stronger than that from the left light. The recognition rates with center light are always higher than that with right light on and left light on.

	Recognition rate (%)		
Different Illumination / Similarity Measure	Left light	Center light	Right light
L1	33.33	33.33	20.00
L2	33.33	46.67	26.67
COS	33.33	40.00	26.67
Mah	26.67	46.67	20.00
L1+Mah	6.67	20.00	13.33
L2+Mah	26.67	46.67	26.67
C0S+Mah	33.33	46.67	26.67

Table III.2: Result of face recognition under varying lighting conditions.

→ PCA under Facial Expression Changes

To evaluate the effects of different facial expressions (happy, sleepy, sad, surprised, and winking) on the system performances we have used Yale face database. The face images of different facial expressions from Yale face database were used in the experiments (Figure III.3 (c)). The faces in neutral expression were used as single models of the subjects. Totally, there were 15 models (representing 15 individuals) and 75 test images. The experimental results on faces with happy, sleepy, sad, surprised, and winking expressions were summarized in table III.3. The happy expression in eigenfaces using COS, Mah, and COS+Mah attain a recognition rate of 100%, whereas in eigenfaces using L1+Mah gives the lowest rate of 60%. The sad expression attains the highest recognition rate of 100% using Mah distance and the lowest recognition of 40% using L1+Mah distance.

In sleepy expression, the best recognition rate of 100% is given by L1, L2, COS, and L2+Mah distances. In surprised and winking expressions the lowest recognition rate of 40% and 60% respectively is given by L1+Mah distance.

Facial Expression / Similarity Measure	Recognition rate (%)				
	Happy	Sad	Sleepy	Surprised	Winking
L1	93.33	93.33	100	86.67	93.33
L2	93.33	93.33	100	73.33	93.33
COS	100	93.33	100	86.67	93.33
Mah	100	100	93.33	80.00	86.67
L1+Mah	60.00	40.00	60.00	40.00	60.00
L2+Mah	93.33	93.33	100	80.00	93.33
C0S+Mah	100	93.33	93.33	93.33	93.33

Table III.3: Result of face recognition under facial expression changes.

III.3.2.Experiments on ORL database:

In this set of experiments, we have compared nine methods namely PCA using (L1, L2, COS, Mah, L2+Mah, and COS+Mah distances), DWT, SVD, and DCT methods. All experiments were performed using the ORL database with 5 training images (figure III.3 (a)) and 5 test images per person (figure III.3 (b)) for a total of 200 training images and 200 test images. The experimental results are summarized in table III.4. We have found that the DWT method gives the best recognition rate of 93% compared with other methods. PCA using COS gives the best rate of 92% compared with PCA using L1, L2, Mah, L2+Mah, and COS+Mah methods.

	Methods								
	PCA						DCT	SVD	DWT
	L1	L2	COS	Mah	L2 +Mah	COS +Mah			
Recognition rate (%)	86	90.5	92	85.5	91.5	91	71.5	64	93

Table III.4: Result of face recognition using different methods.

III.3.3.Experiments on FEI database:

For this set of experiments, part 1 of FEI database was divided on two parts. First part represented authorized persons and has 10 persons, from which 5 random images were used for training (total 50 images), other 5 for testing (total 50 images). Second part represented unauthorized persons. It has 10 persons and 5 images per person (total 50 images) only for testing purposes. Thus system has 50 images for training, and 100 for testing (50 authorized and 50 unauthorized). In order to measure performance of the verification system we have used following factors:

- ✓ The false acceptance rate, or FAR, is the measure of the likelihood that the biometric security system will incorrectly accept an access attempt by an unauthorized user.

- ✓ The false rejection rate, or FRR, is the measure of the likelihood that the biometric security system will incorrectly reject an access attempt by an authorized user. The values of FAR and FRR are computed using:

$$\boldsymbol{FAR = \frac{n_{ac}}{n_u} \quad FRR = \frac{n_{re}}{n_a}}$$

Where

n_a is the number of access attempts by an authorized user,

n_u is the number of access attempts by an unauthorized user,

n_{ac} is the number of acceptances for unauthorized users , and

n_{re} is the number of rejections for unauthorized users.

- ✓ The Receiver Operating Curve (ROC) plots FAR versus FRR .The closer the ROC curve lies to the x and y axes, the lower the verification error and thus the more reliable the system.

- ✓ The Equal Error Rate (EER) is defined as the point where the value of FAR equals the value of FRR in the ROC-curve. The EER is a quick way to compare the accuracy of devices with different ROC curves. In general, the device with the lowest EER is most accurate.

III.3.3.1. PCA and FLD (PCA-LDA) methods:

Various groups have reported various performance results for PCA and FLD algorithms and no straightforward conclusion can be easily drawn. Beveridge et al **[196]** claim that in their tests using different distance measures LDA performed uniformly worse than PCA, but they do not give any explanation as to why it is so. Martinez and Kak **[61]** state that PCA is better for some tasks; PCA might outperform LDA when the number of samples per class is small or when the training data nonuniformly sample the underlying distribution. Belhumeur et al **[94]** and Navarrete **[197]** claim that LDA outperforms PCA on all tasks in their tests (for more than two samples per class in training phase). Zhao et al **[198]** report improved performance for combined PCA and LDA approach over the pure LDA.

Research group	Database	Algorithms tested	Best result
Zhao	FERET&USC	LDA, PCA+LDA	PCA+LDA
Beveridge	FERET	PCA, PCA+LDA	PCA
Belhemur	Harvard & Yale	Correlation, linear subspace, PCA, LDA	LDA
Navarrete	FERET & Yale	PCA, LDA, EP	LDA
Martinez	AR	PCA, LDA	PCA for some tasks

Table III.5. Results reported by different research groups.

In this experiment we compare PCA and FLD methods. The comparison is performed between them in terms of Equal Error Rate (EER). We have used three, five, and six samples per class. We have plotted the FAR vs FRR graphs and ROC curves for different number of samples per class. From the figures we can see that the system performance increases as the number of samples per class increases. We have found also that PCA outperforms FLD in the three cases.

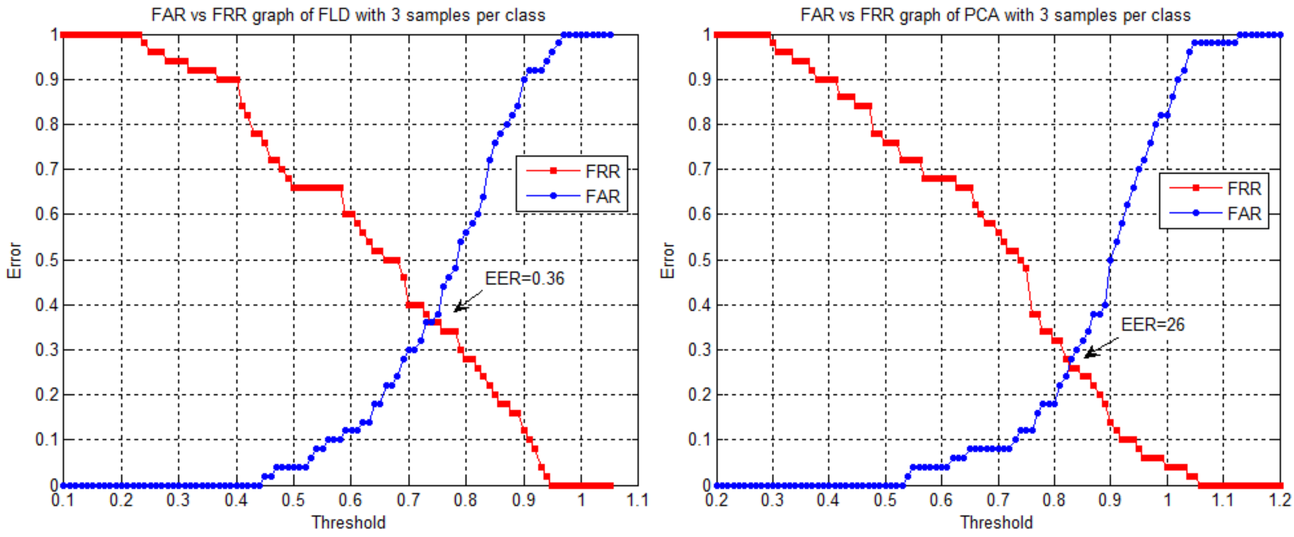

Figure III.4: FAR vs FRR graphs of FLD and PCA with three samples per class.

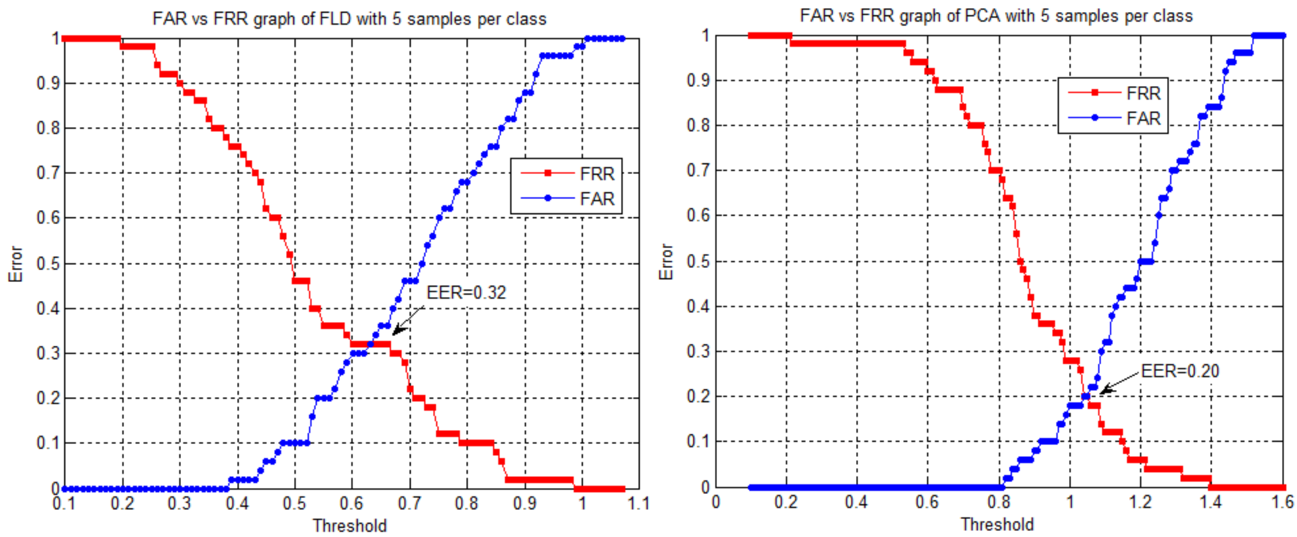

Figure III.5: FAR vs FRR graphs of FLD and PCA with five samples per class.

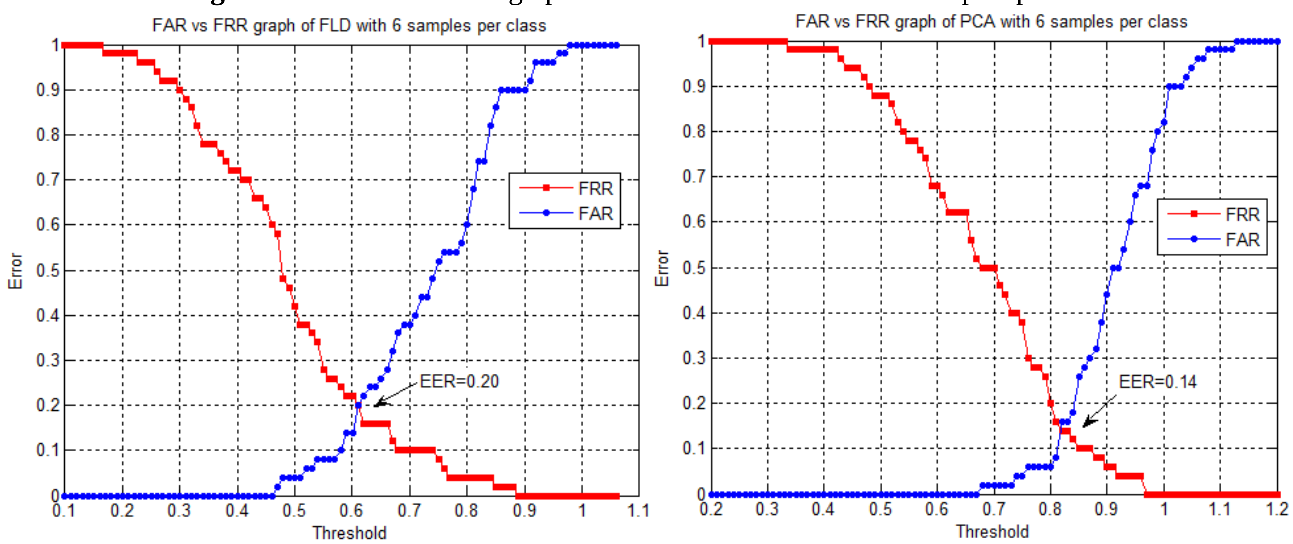

Figure III.6: FAR vs FRR graphs of FLD and PCA with six samples per class.

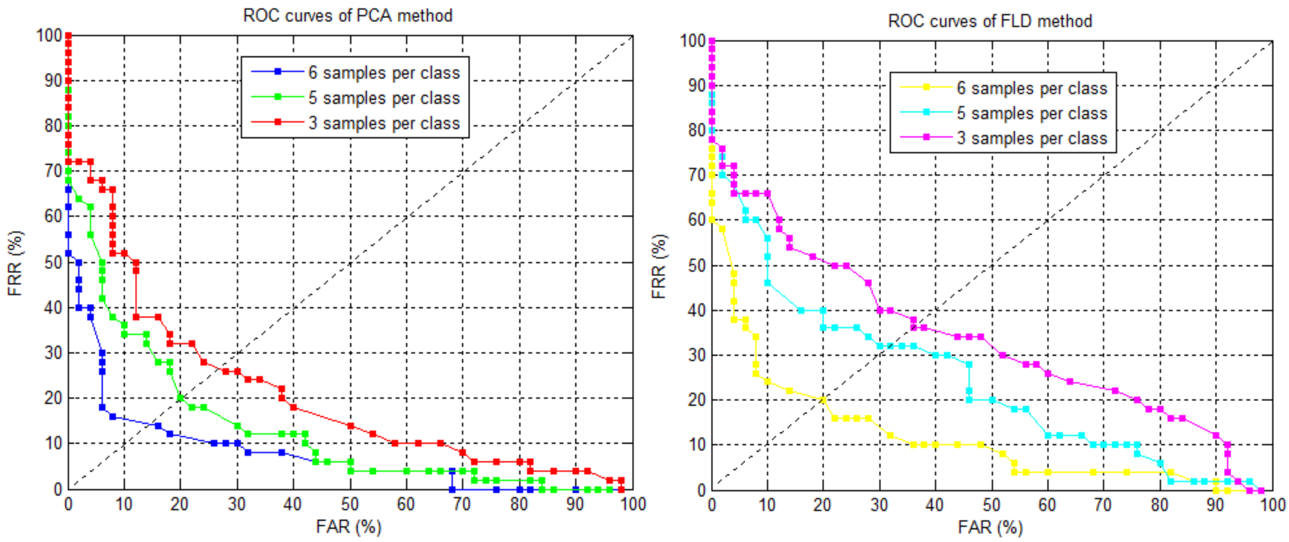

Figure III.7: ROC curves of FLD and PCA with three, five and six samples per class.

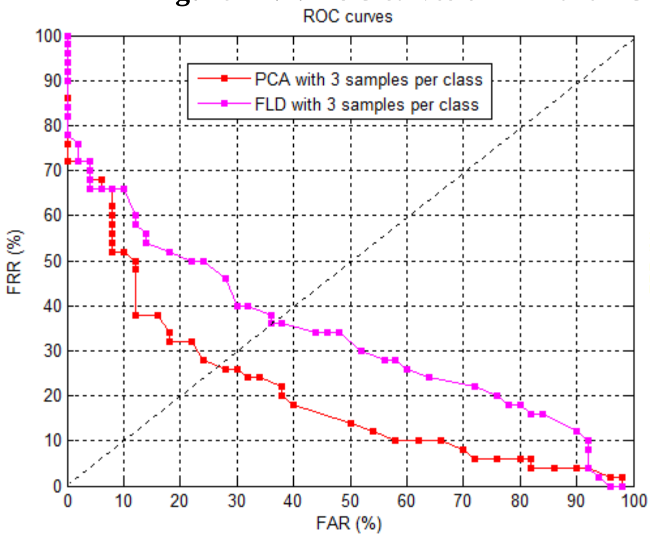

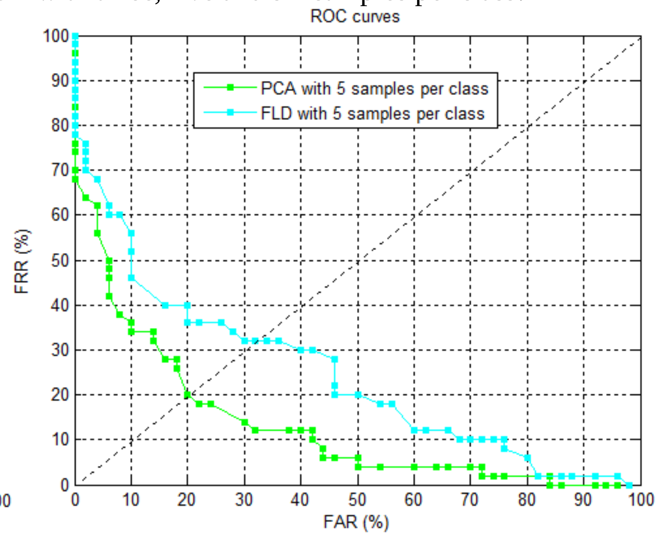

(a) **(b)**

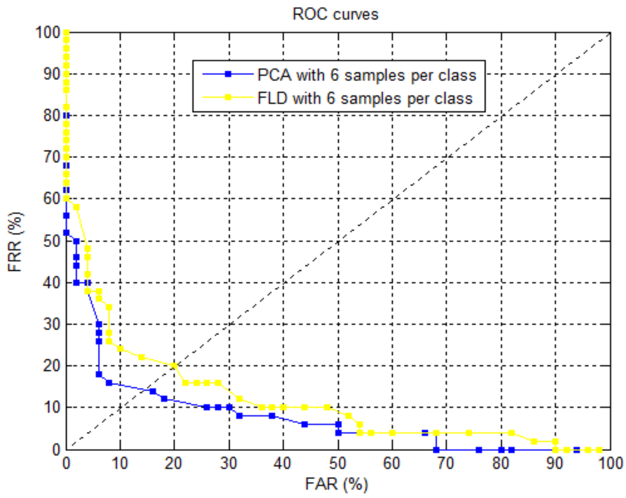

(c)

Figure III.8: ROC curves of FLD and PCA with **(a)** 3samples per class **(b)** 5 samples per class **(c)** 6 samples per class

III.3.3.2.FLD (PCA-LDA) and DWT-LDA methods:

Many methods have been introduced to solve the small sample size (SSS) problem. In the Fisherface method, PCA is applied first as a pre-processing step aiming to reduce the dimensionality prior to performing LDA. We have another approach that uses the discrete wavelet decomposition (DWT) before performing LDA (DWT-LDA). In this experiment we will compare the two methods. The comparison was performed between them in terms of Equal Error Rate (EER). The FAR vs FRR graphs and ROC curves are given in figures III.9 and II.10 respectively. The DWT-LDA performs better than FLD since it has the lowest EER of 19%.

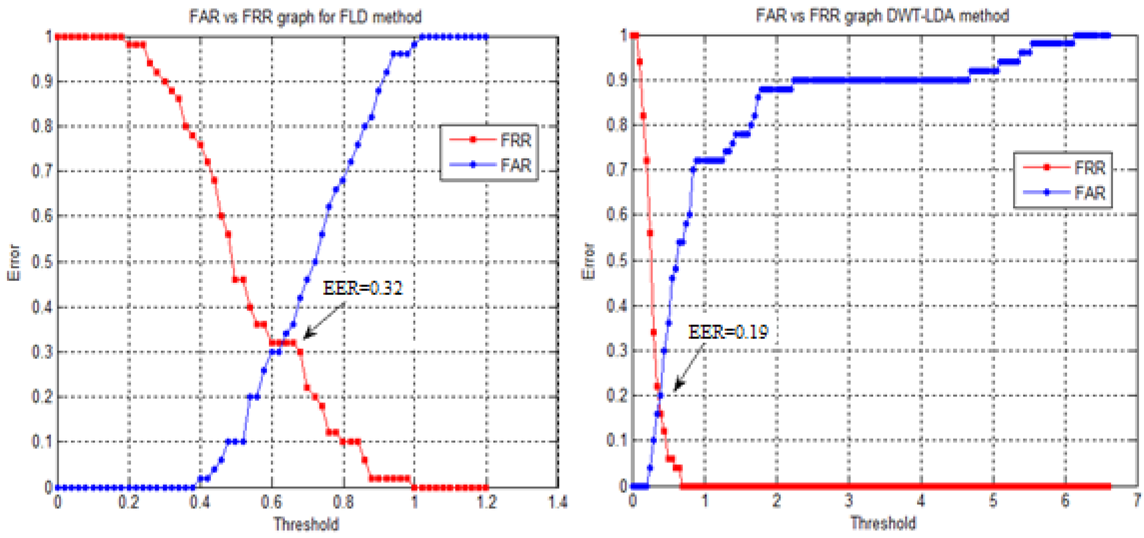

(a) (b)

Figures III.9: FAR vs FRR graphs of **(a)** FLD (PCA-LDA) method **(b)** DWT-LDA method.

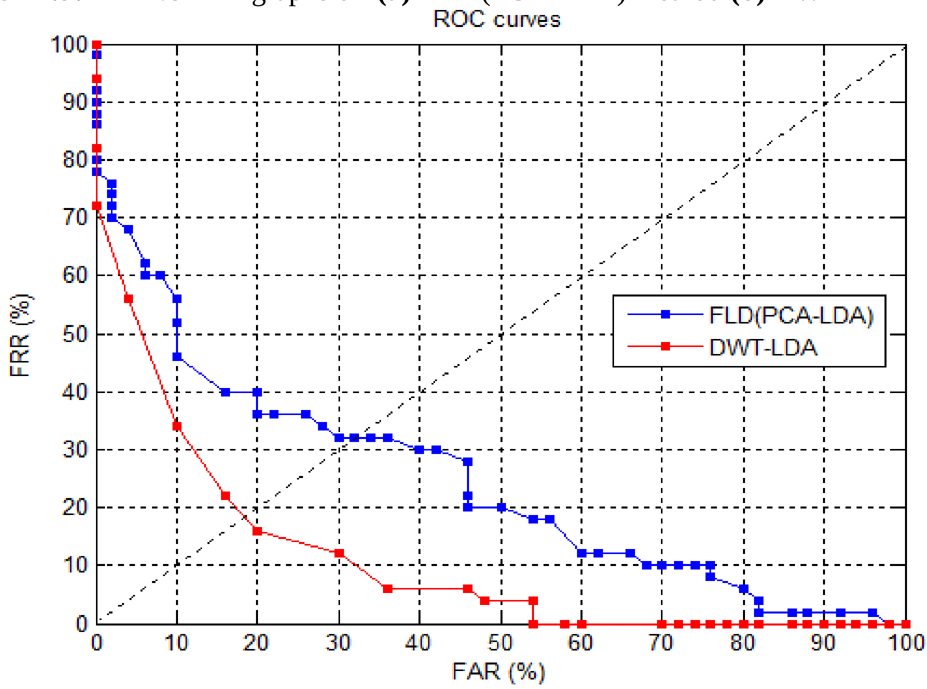

Figure III.10: ROC curves of FLD (PCA-LDA) and DWT-LDA methods.

III.3.3.3. SVD and DWT-SVD methods:

To show the effect of applying DWT before SVD, we have compared between SVD and DWT-SVD. The comparison was performed between them in terms of Equal Error Rate (EER). The FAR vs FRR graphs and ROC curves are given in figure III.11 and figure III.12 respectively. The EER rate is reduced by 2%, so the wavelet decomposition has improved the system performance.

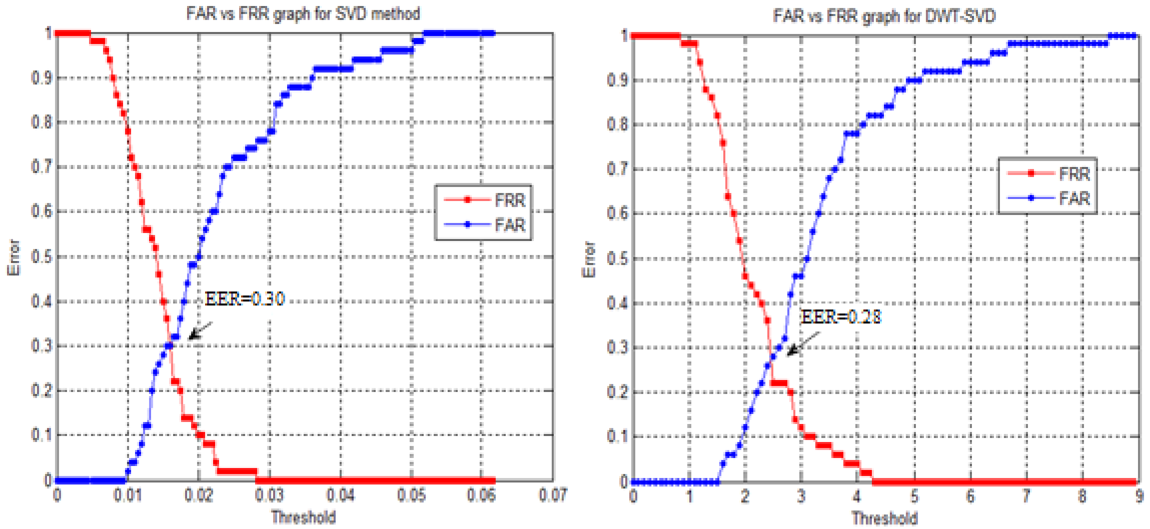

(a) **(b)**

Figure III.11: FAR vs FRR graphs of **(a)** SVD method **(b)** DWT-SVD method.

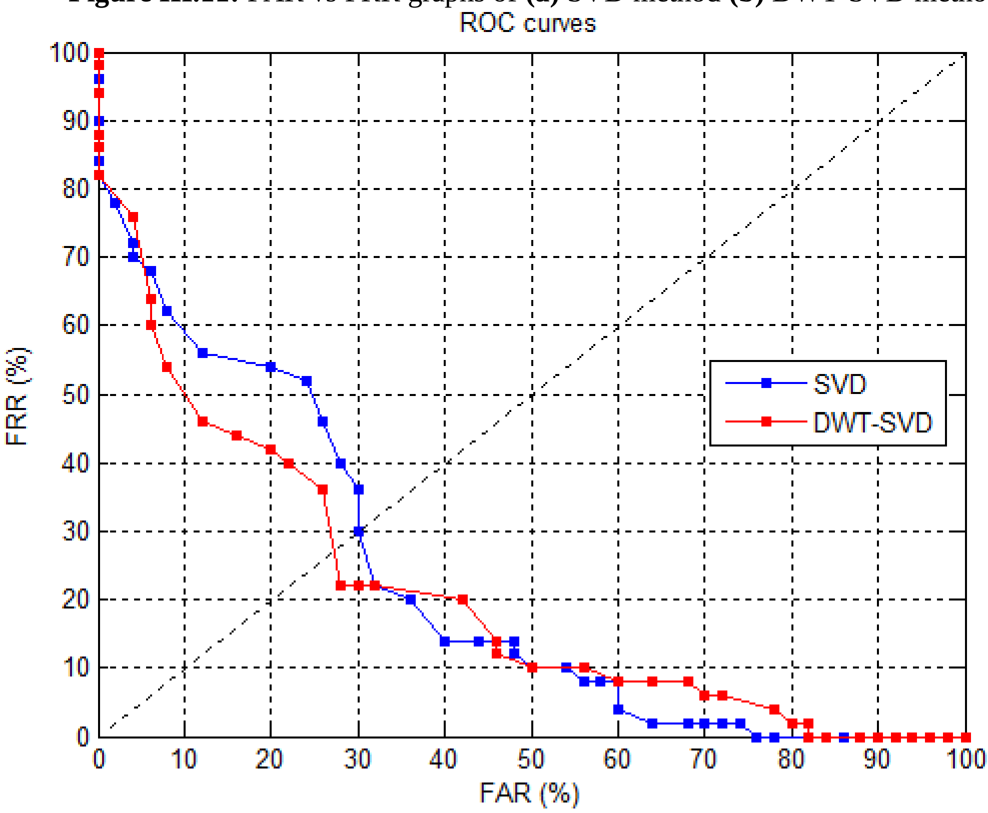

Figure III.12: ROC curves of SVD and DWT-SVD methods.

III.3.3.4. WPD-PCA and PCA methods:

In WPD-PCA, the fusion is done at feature level and at decision level. In decision level, two rules have been used: maximum and mean rules. In this experiment, we have compared these methods with PCA method. The FAR vs FRR graphs and ROC curves are given in figure III.13 and figure III.14 respectively. WPD-PCA method using Maximum decision fusion gives the best result since it has the lowest EER of 14%.

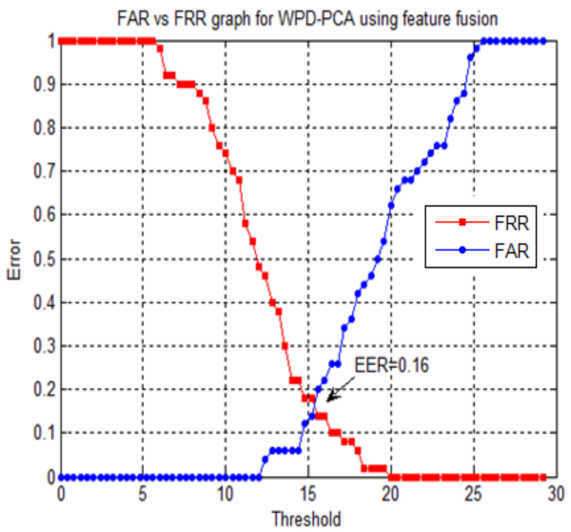

(a)

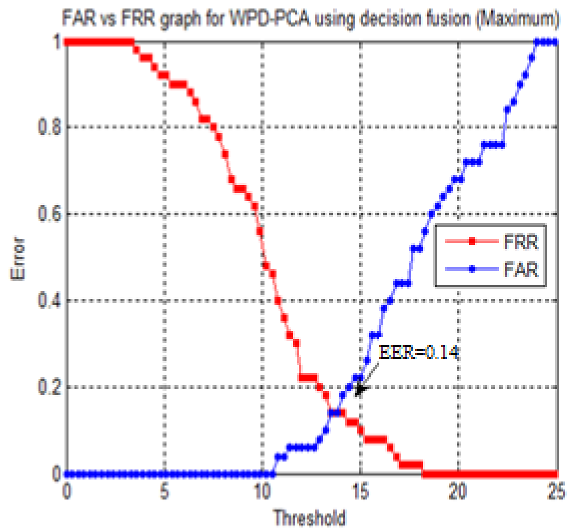

(b)

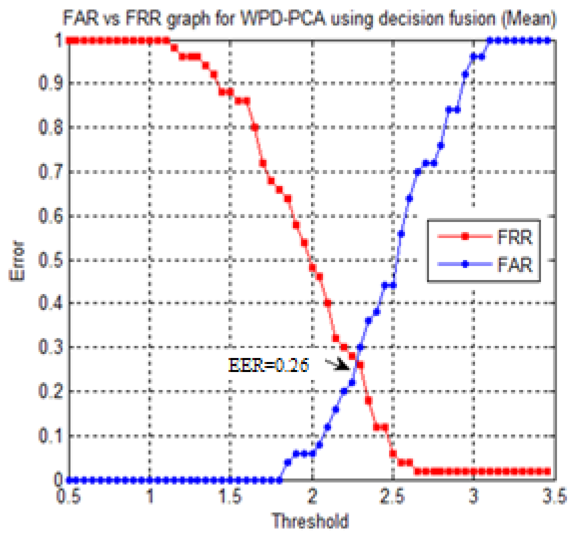

(c)

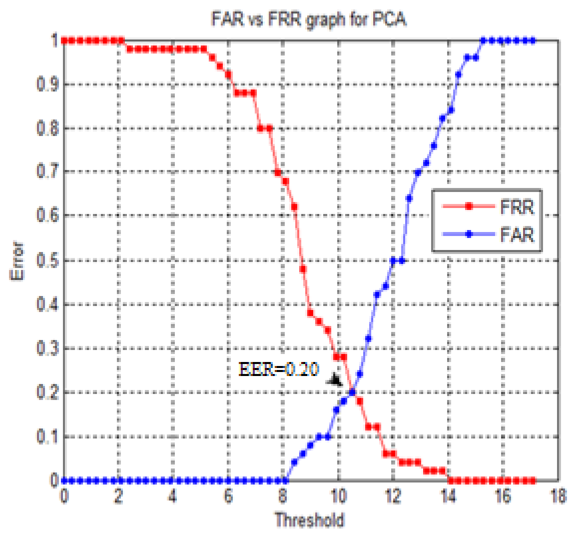

(d)

Figure III.13: FAR vs FRR graph of **(a)** WPD-PCA method using feature fusion **(b)** WPD-PCA method using Max decision fusion **(c)** WPD-PCA method using Mean decision fusion **(d)** PCA method

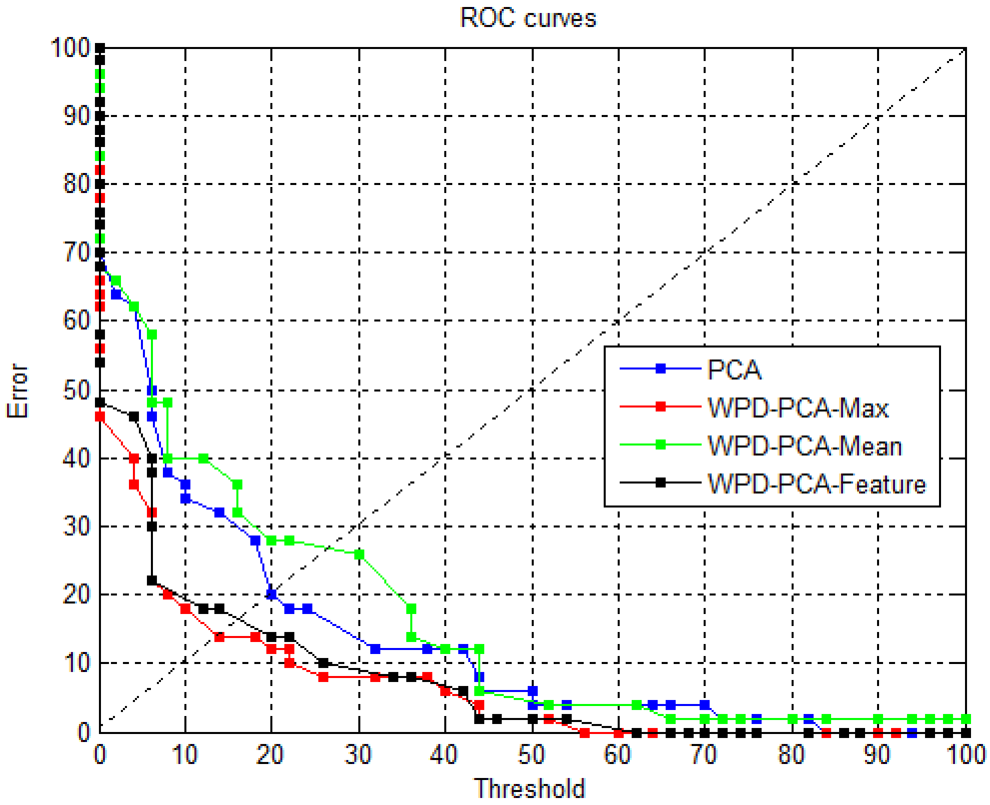

Figure III.14: ROC curves of WPD-PCA and PCA methods.

III.3.3.5. YCbCr-WPD-PCA method:

To identify the accuracy of our algorithm, a comparison was performed with other methods in terms of recognition rates and Equal Error Rate (EER).

Experiment 1

In this experiment, we have selected from FEI face database 20 images from part 1. The images with extensions (-01, -03, -05, -07, -09, -12, -13, and -14) are selected for testing and the remaining images are used in the training. In this Experiment, we have compared between PCA, DWT, DWT-PCA and YCbCr-WPD-PCA methods in terms of the recognition rates for one sample, three and six samples per class in the training set. The results of the tests are summarized in table III.6. We have seen that the recognition rates increase as we increase the numbers of samples per class. Our method (YCbCr-WPD-PCA) outperforms other methods; since it reaches recognition rates of 82.50%, 86.87%, and 93.12% with one sample, three and six samples per class respectively.

Method	Number of images per class	Number of misclassified /rejected images	Recognition rate (%)
PCA	1	52	67.50
	3	30	81.25
	6	/	/
DWT	1	43	73.31
	3	24	85.00
	6	17	89.37
DWT-PCA	1	64	60.00
	3	40	71.87
	6	31	80.62
YCbCr-WPD-PCA	1	28	82.50
	3	21	86.87
	6	11	93.12

Table III.6: Result of the test.

→ Experiment 2

In this Experiment, we compare five methods (PCA, DWT, DWT-PCA, WPD-PCA using feature fusion, and WPD-PCA using decision fusion) with the proposed method. We plot the FAR versus FRR graphs and the ROC curves for the different methods which are given in figure II.15 and figure II.16 respectively. From the figures we can see that YCbCr-WPD-PCA method, achieved an equal error rate of 10%; this is the lowest EER. So, our method gives significant performance compared to other methods.

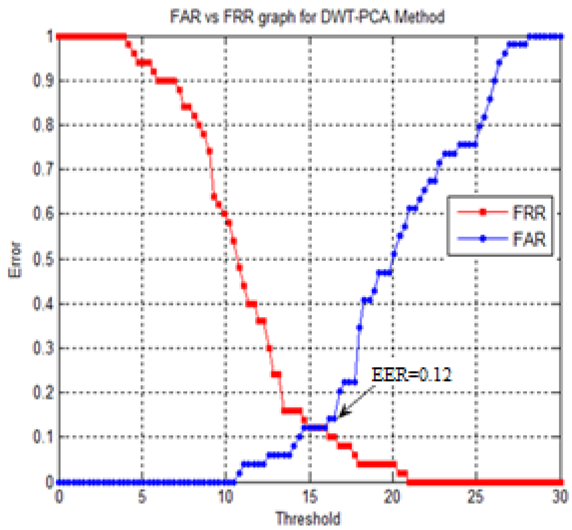

(a)

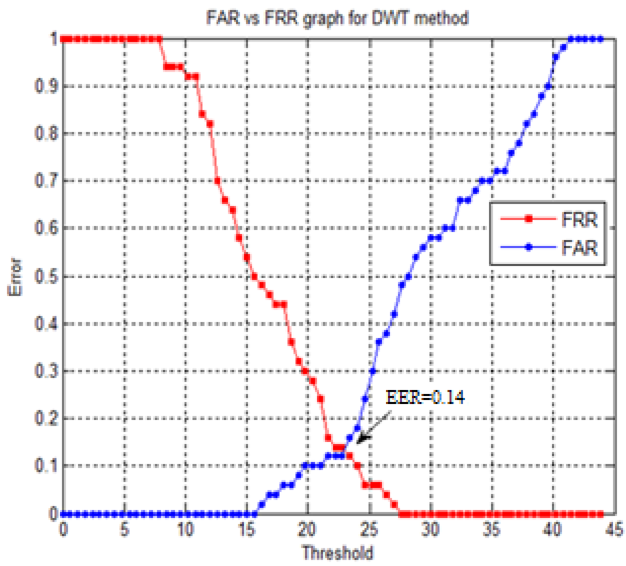

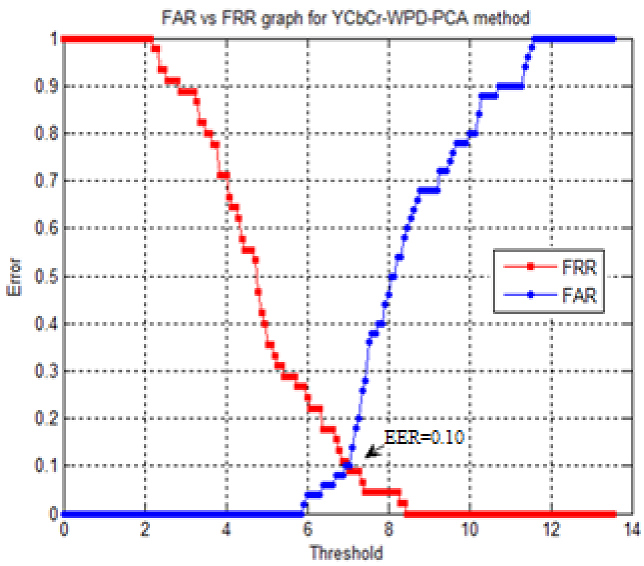

(b) **(c)**

Figure III.15: FAR vs FRR graph of **(a)** YCbCr-WPD-PCA method **(b)** DWT-PCA method **(c)**DWT method.

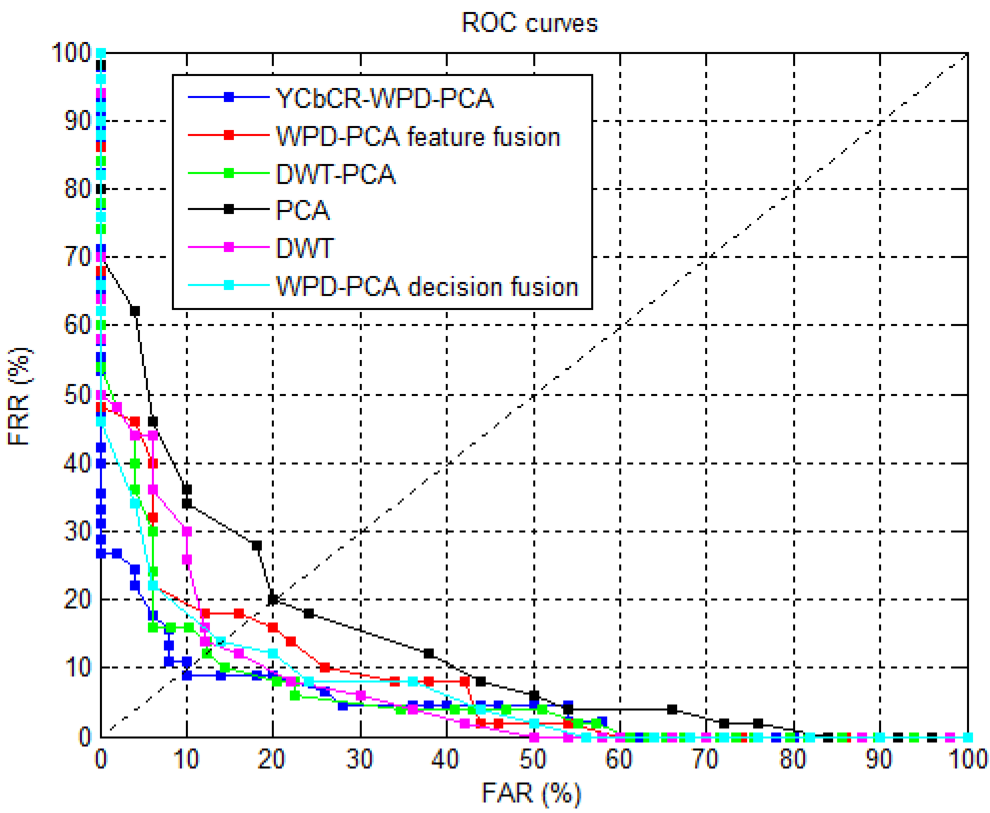

Figure III.16: ROC curves of PCA, DWT, DWT-PCA, WPD-PCA using decision fusion and feature fusion, and YCbCr-WPD-PCA methods.

III.3.3.6. Fusion methods:

In this experiment, we have compared each method separately using minimum, maximum, mean, and product rules. The comparison was performed between them in terms of Equal Error Rate (EER). The FAR vs FRR graphs and ROC curves are given bellow. We have 10 methods for each method we have 4 fusion rules have been utilized. So, the totals of 40 methods have been compared.

→ PCA+FLD

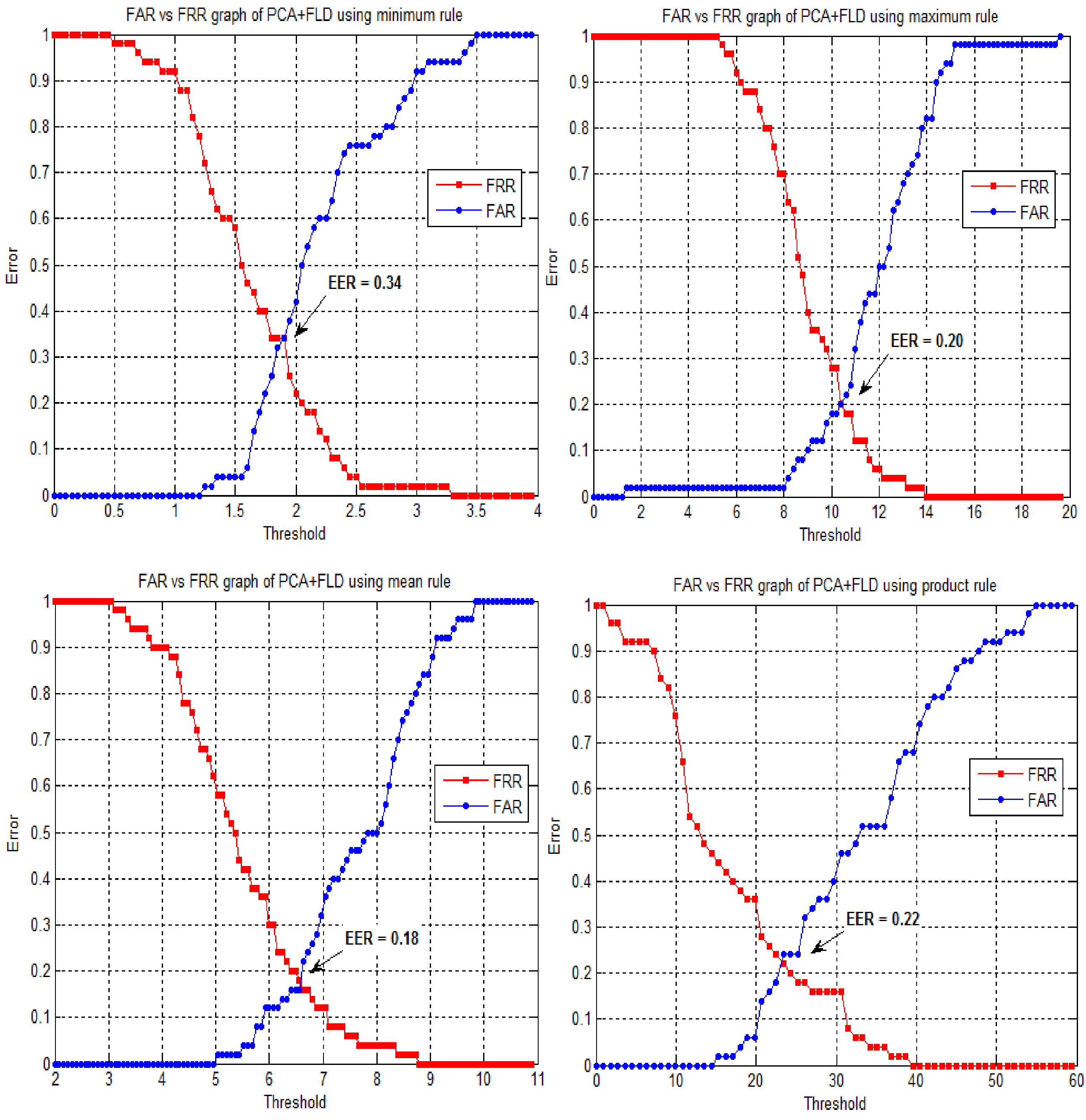

Figure III.17: FAR vs FRR graphs of PCA+FLD method using different fusion rules.

PCA+FLD associated with mean rule gives the best result, since it has the lowest EER of 18%.

→ PCA+SVD

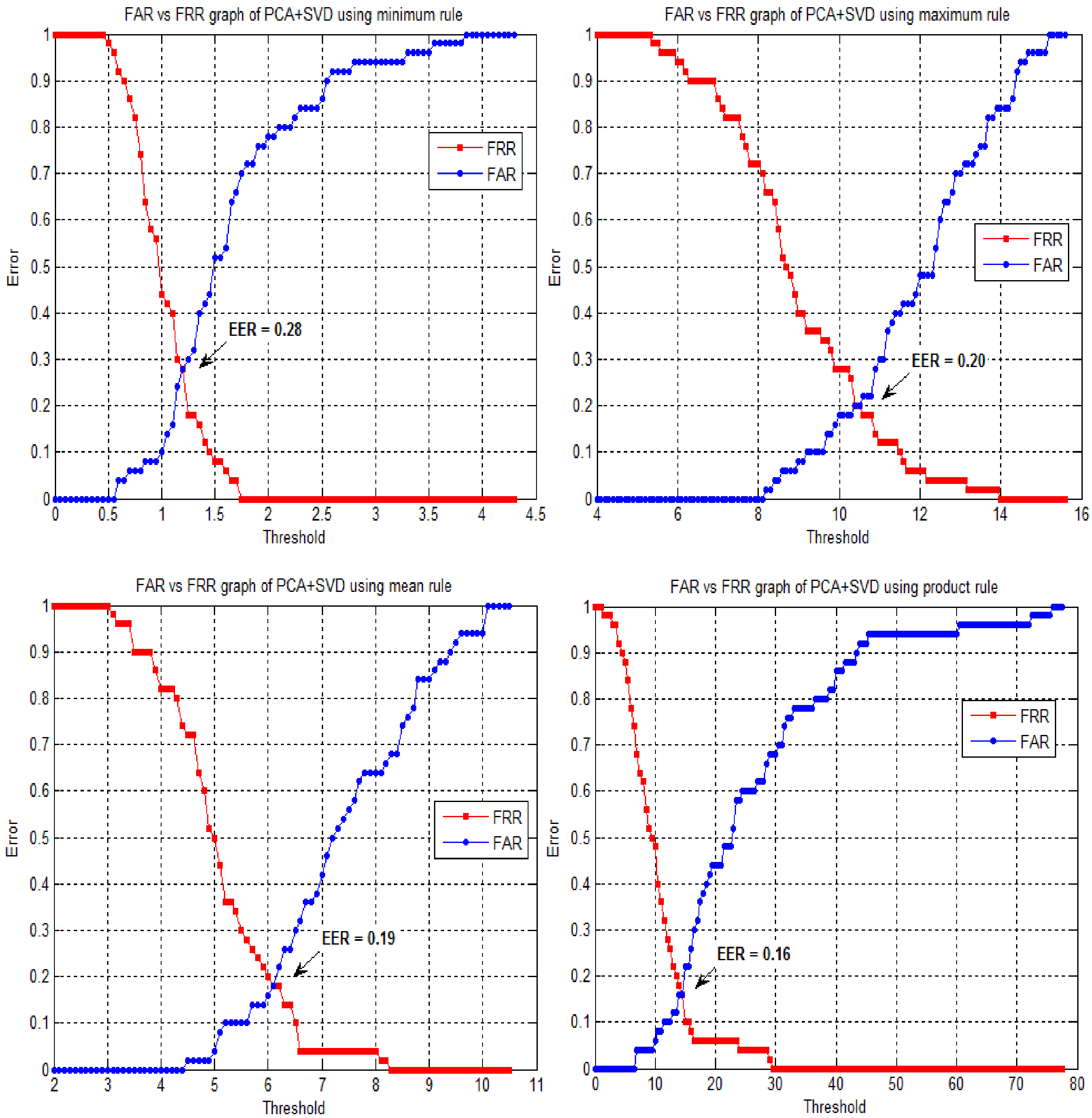

Figure III.18: FAR vs FRR graphs of PCA+SVD method using different fusion rules.

PCA+SVD associated with product rule gives the best result, since it has the lowest EER of 16%.

→ PCA+DCT

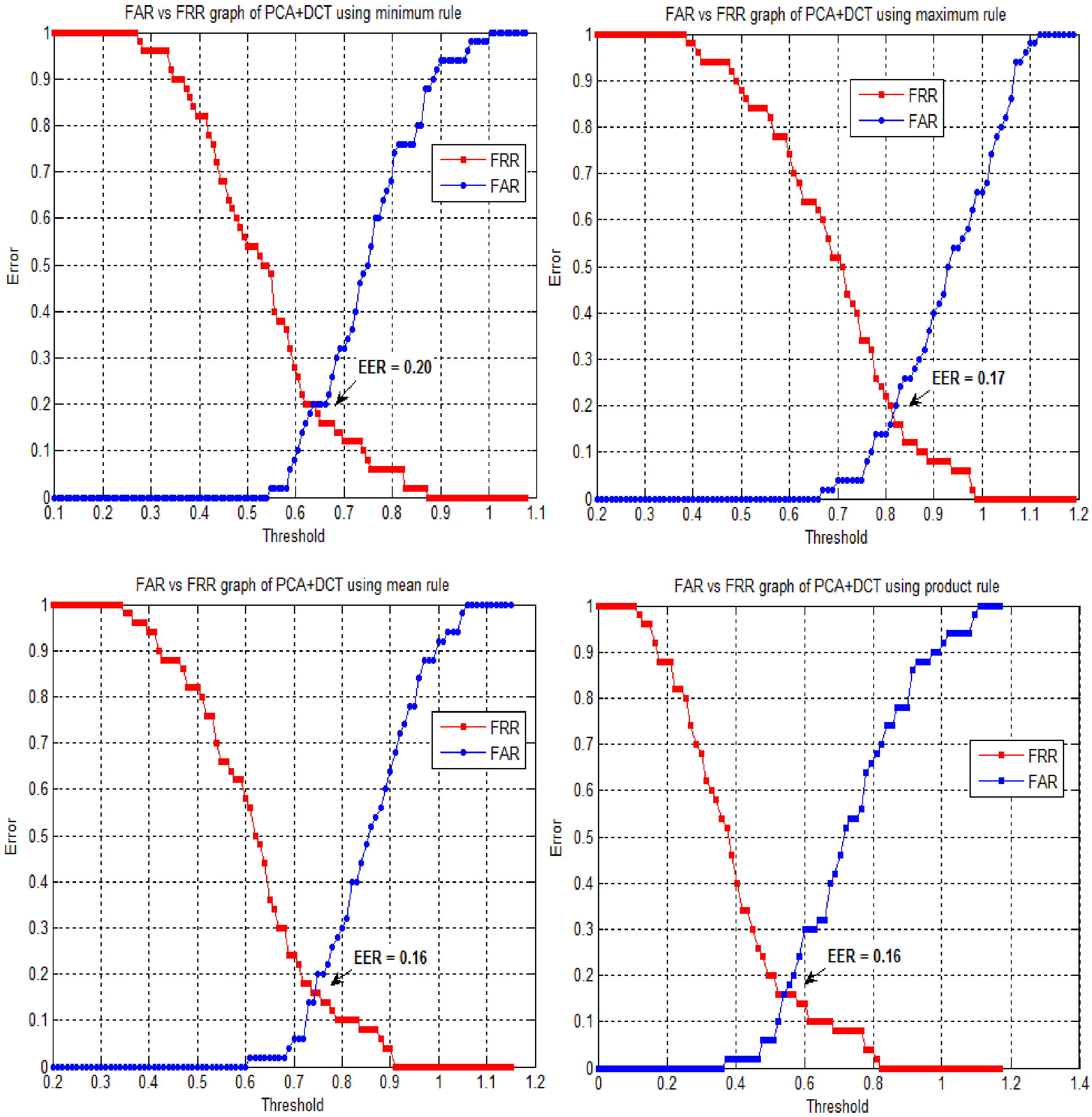

Figure III.19: FAR vs FRR graphs of PCA+DCT method using different fusion rules.

PCA+DCT through the use of mean and product rules give the best result with EER of 16%.

→ PCA+DWT

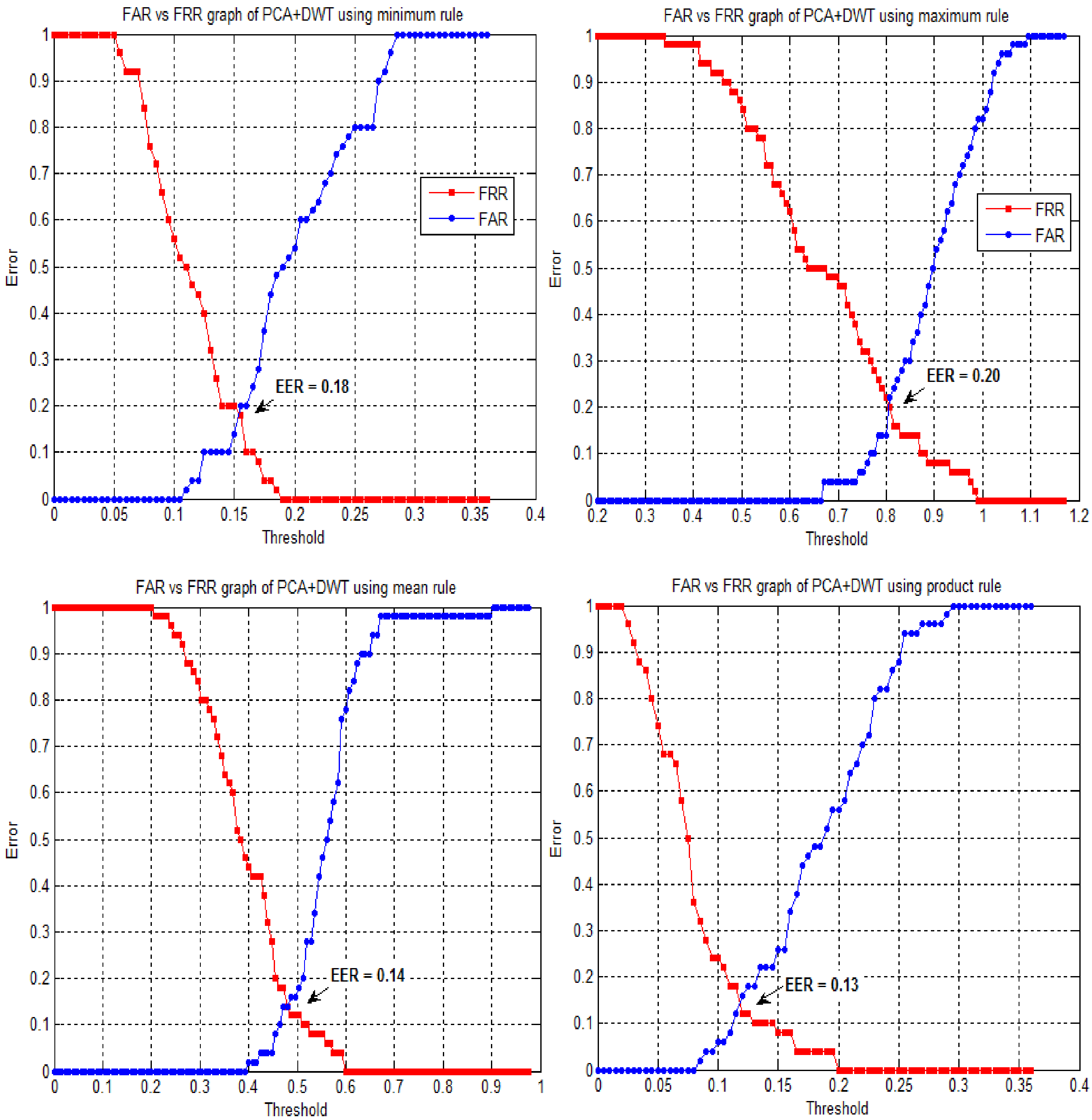

Figure III.20: FAR vs FRR graphs of PCA+DWT method using different fusion rules.

PCA+DWT associated with product rule gives the best result, since it has the lowest EER of 13%.

→ **FLD+SVD**

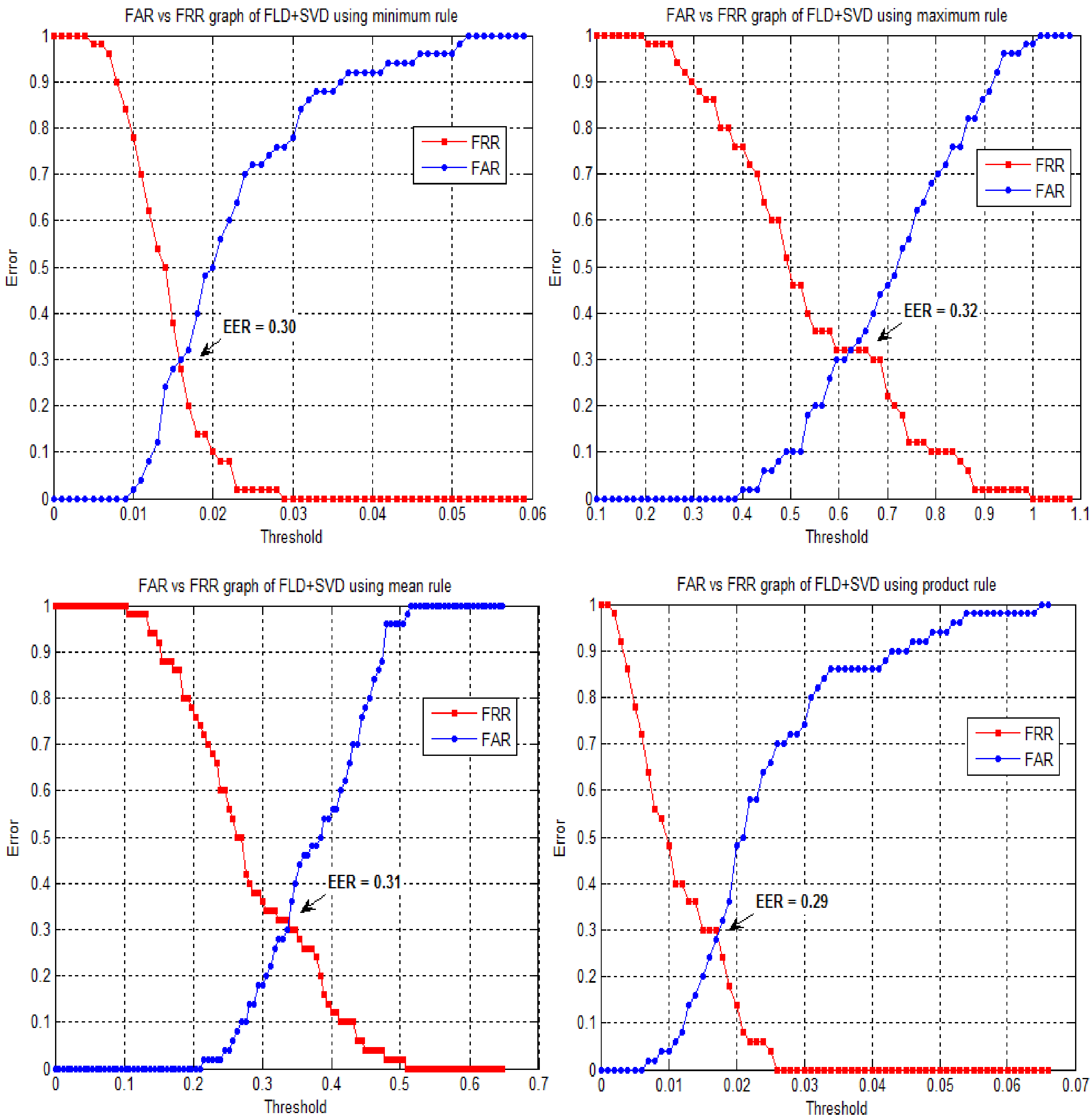

Figure III.21: FAR vs FRR graphs of FLD+SVD method using different fusion rules.

FLD+SVD associated with product rule gives the best result, since it has the lowest EER of 29%.

→ FLD+DCT

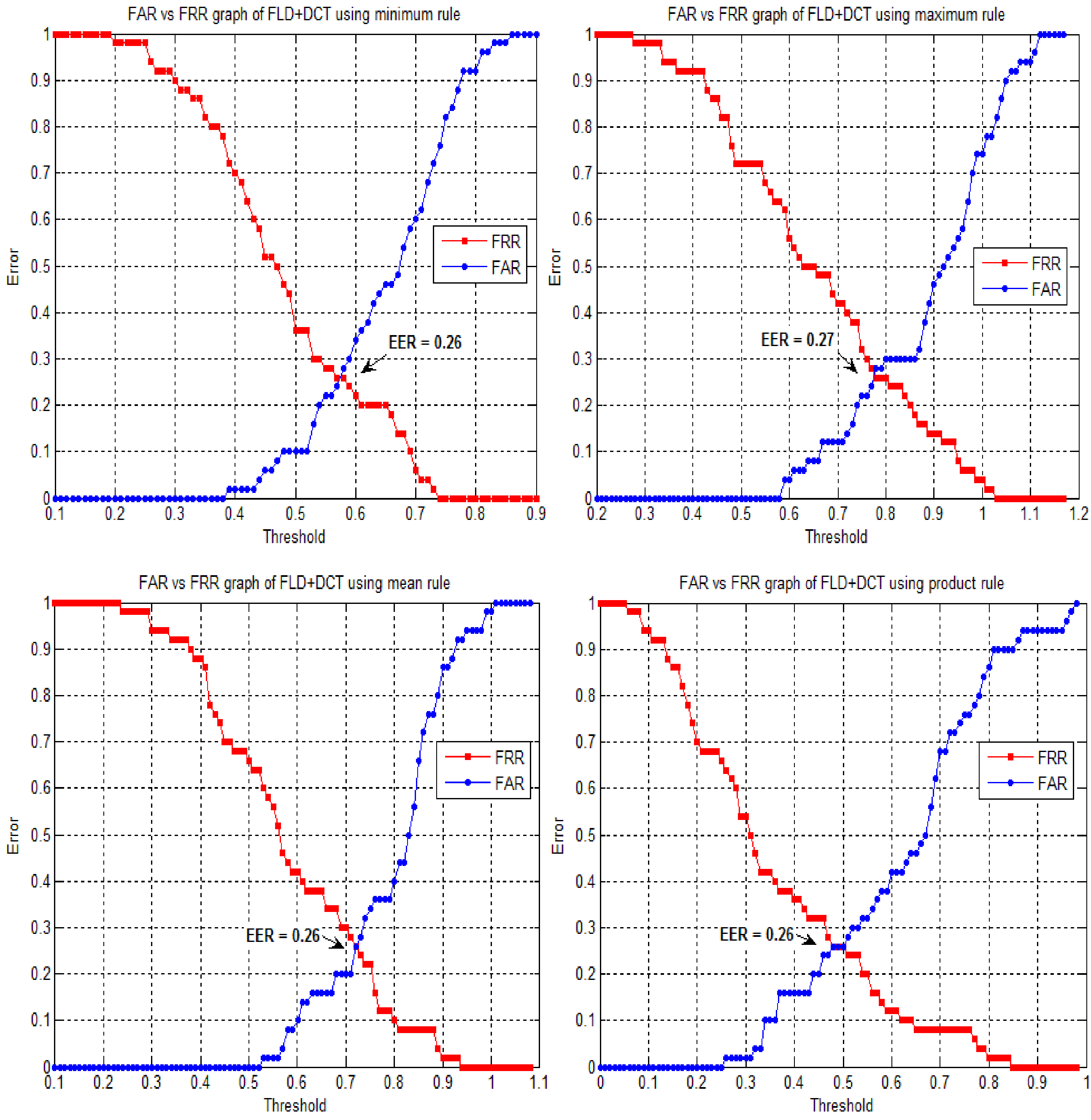

Figure III.22: FAR vs FRR graphs of FLD+DCT method using different fusion rules.

FLD+DCT through the use of product, mean and minimum rules give the same result with EER of 26%.

→ FLD+DWT

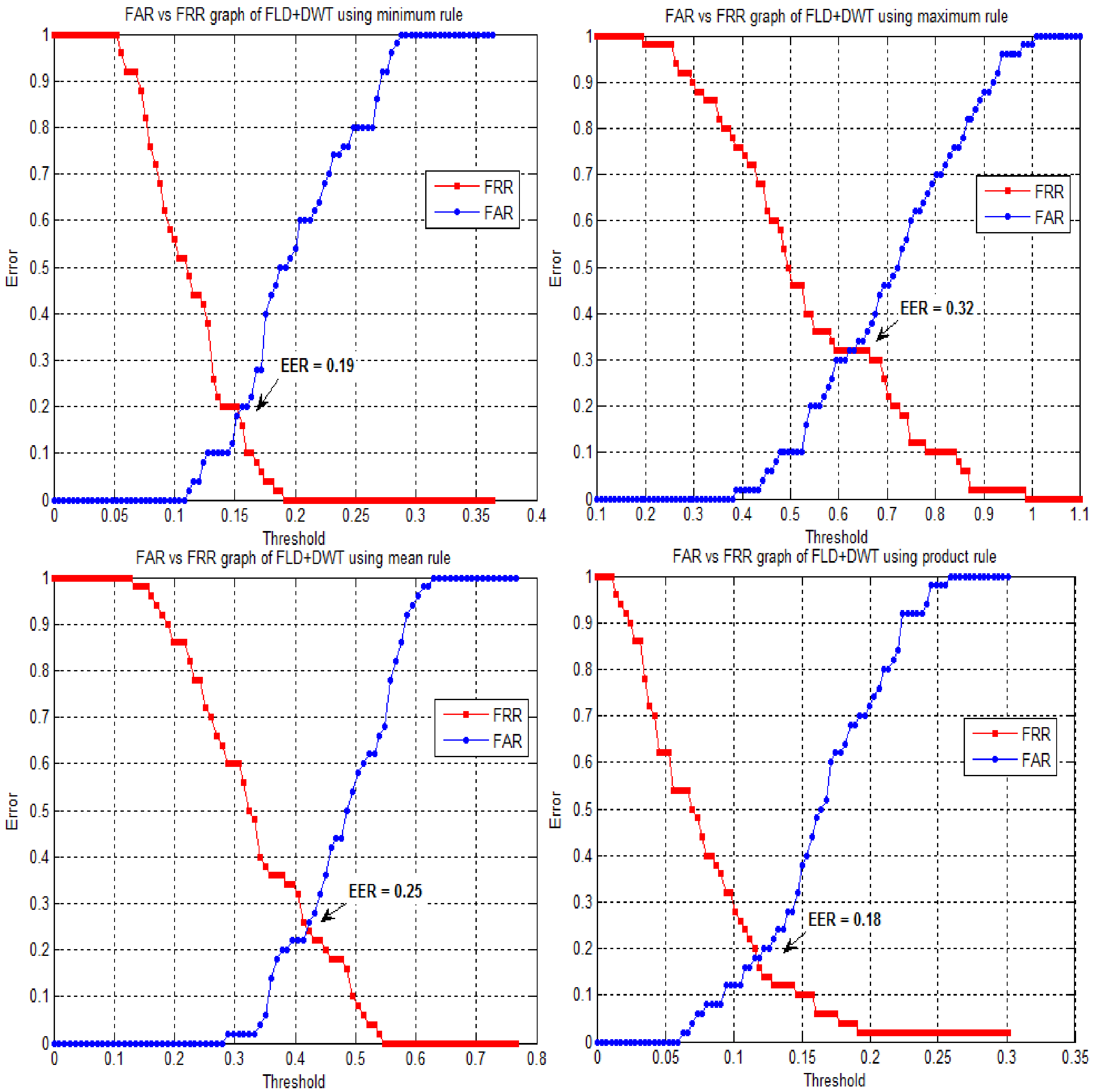

Figure III.23: FAR vs FRR graphs of FLD+DWT method using different fusion rules.

FLD+DWT associated with product rule give the best result with EER of 18%.

→ SVD+DCT

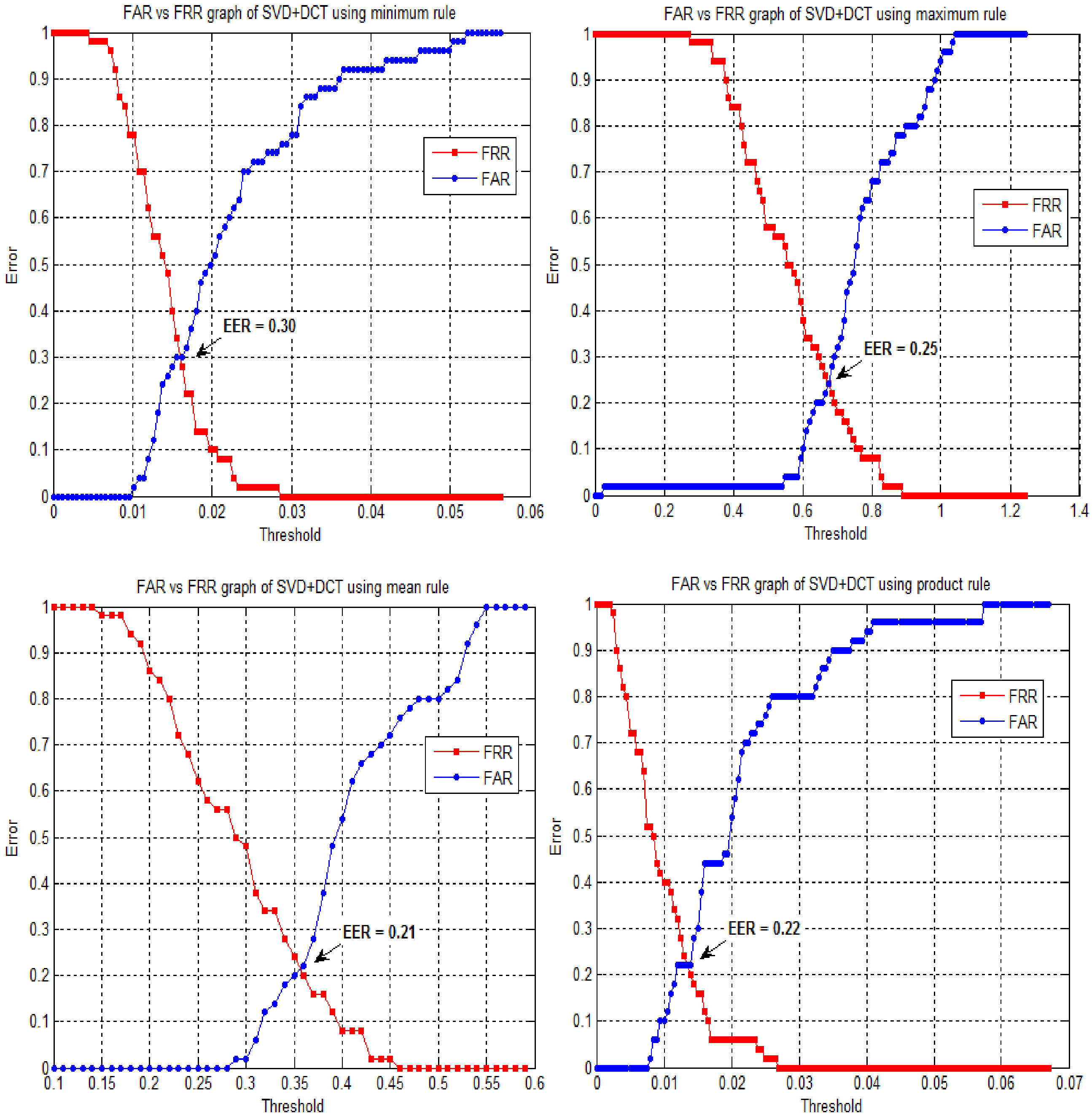

Figure III.24: FAR vs FRR graphs of SVD+DCT method using different fusion rules.

SVD+DCT associated with mean rule gives the best result with EER of 21%.

→ SVD+DWT

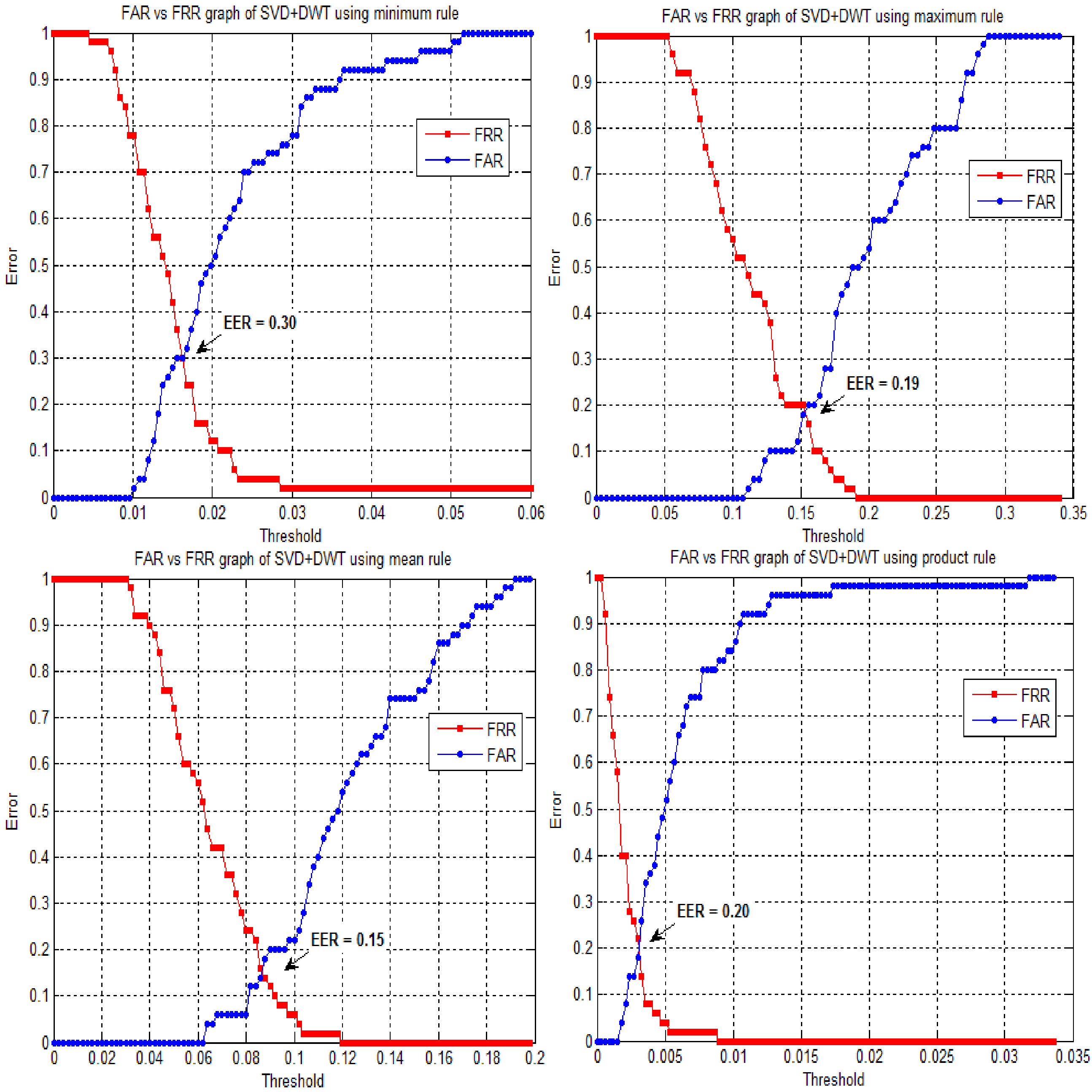

Figure III.25: FAR vs FRR graphs of SVD+DWT method using different fusion rules.

SVD+DWT associated with mean rule gives the best result with EER of 15%.

→ DCT+DWT

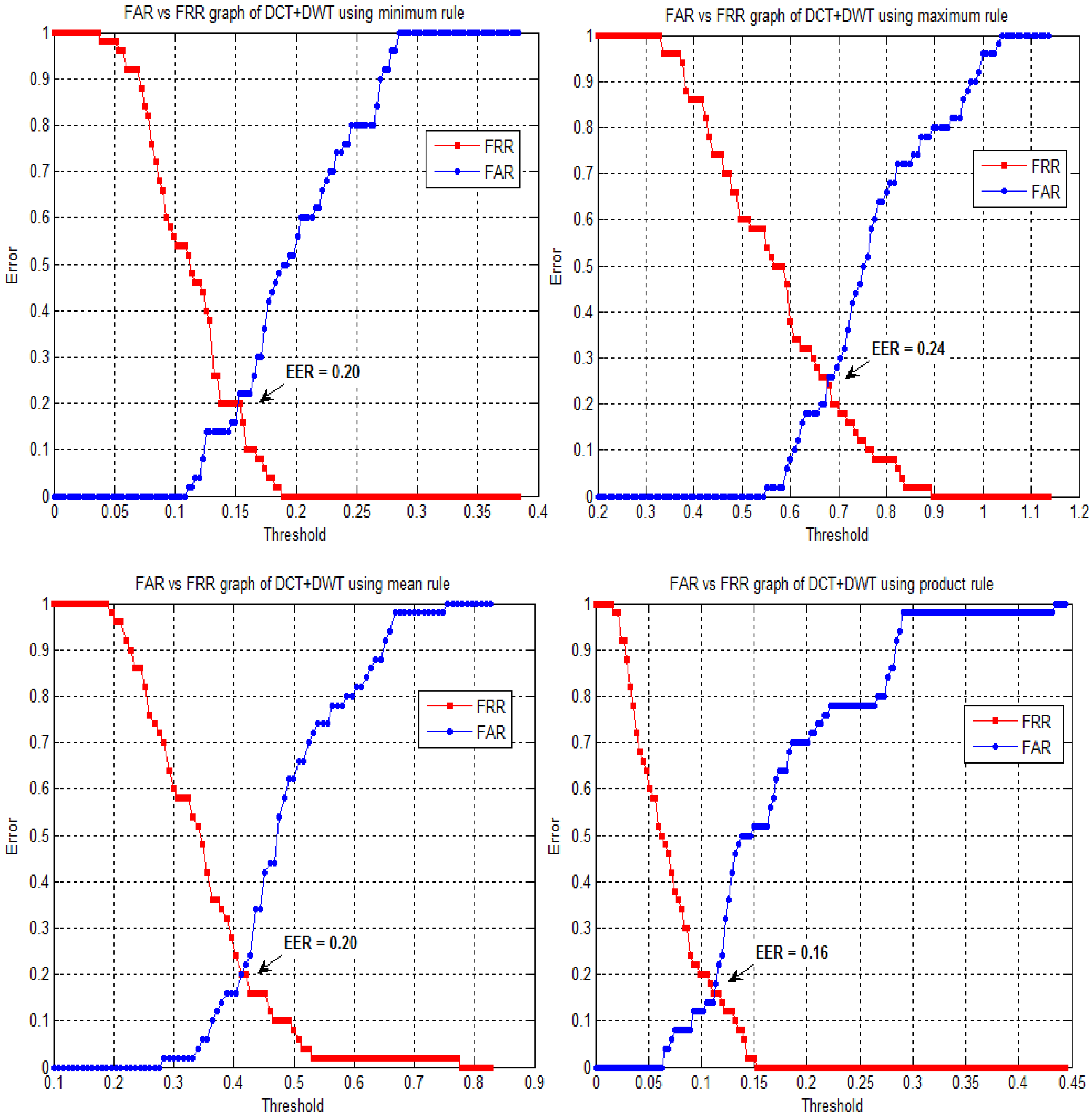

Figure III.26: FAR vs FRR graphs of DCT+DWT method using different fusion rules.

DCT+DWT associated with product rule gives the best result with EER of 16%.

The ROC curves of the all fusion methods are given bellow:

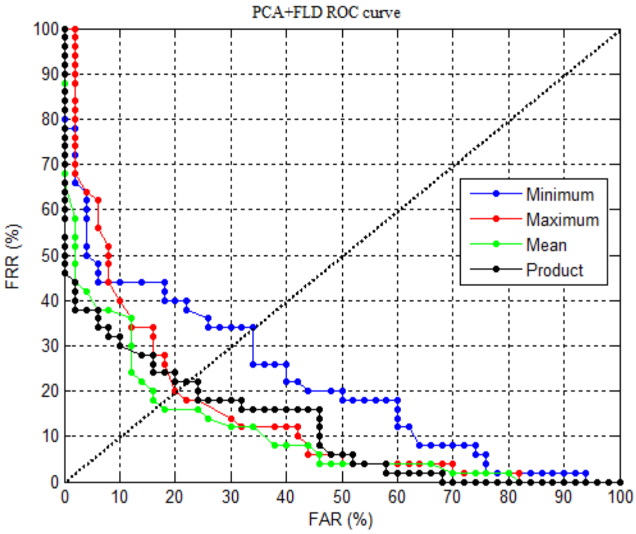

Figure III.27: ROC curves of PCA+FLD.

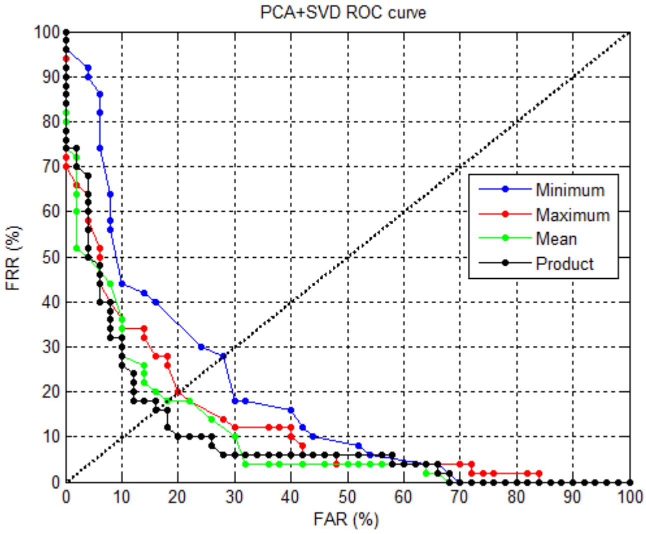

Figure III.28: ROC curves of PCA+SVD.

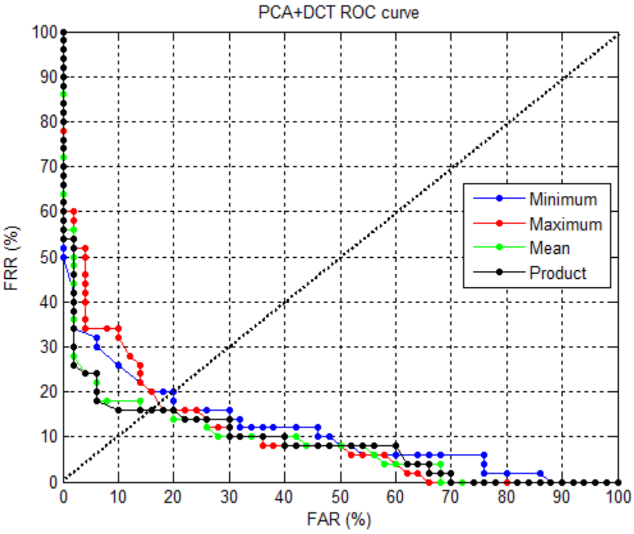

Figure III.29: ROC curves of PCA+DCT.

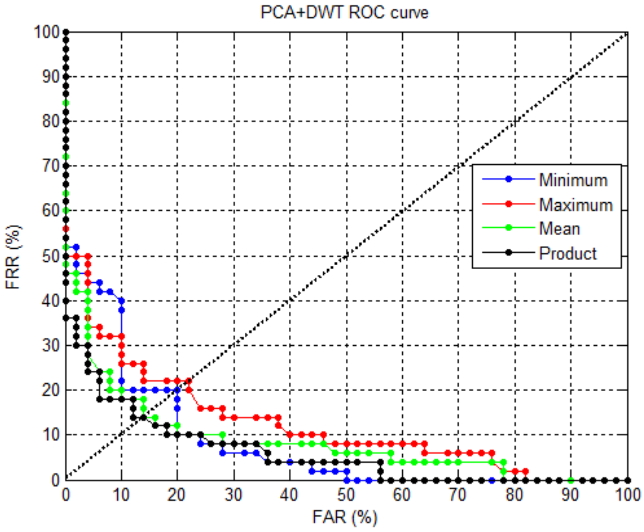

Figure III.30: ROC curves of PCA+DWT.

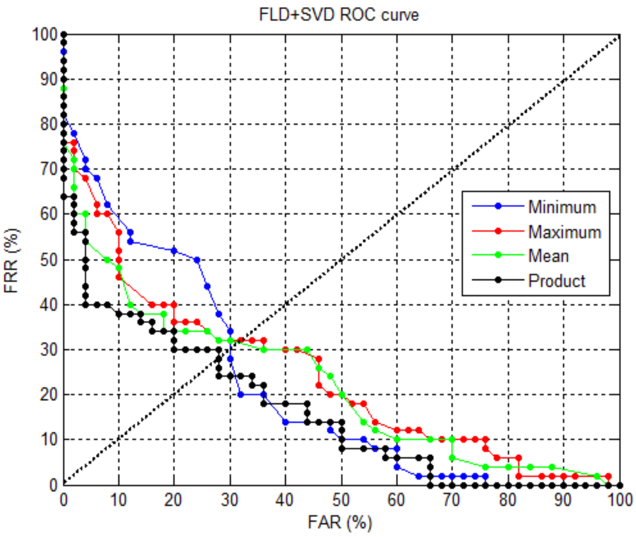

Figure III.31: ROC curves of FLD+SVD.

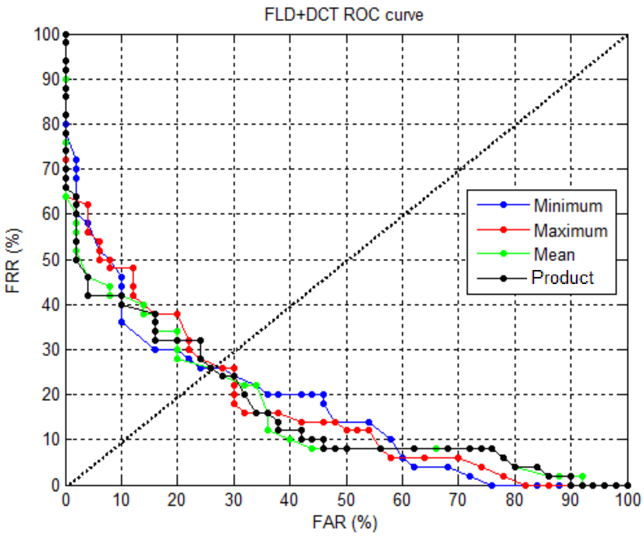

Figure III.32: ROC curves of FLD+DCT.

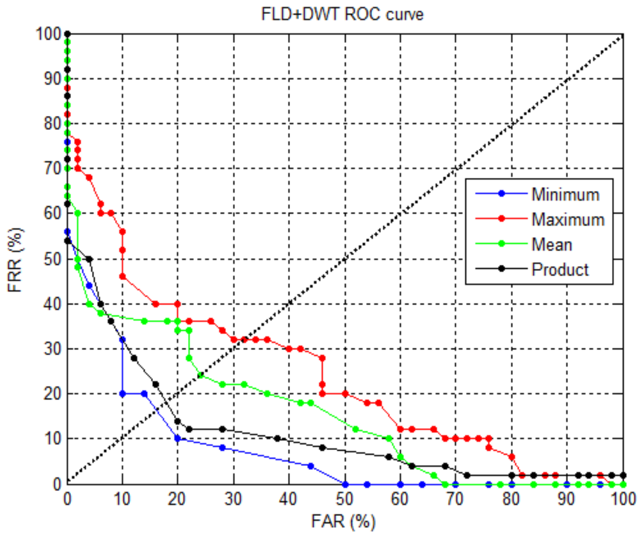

Figure III.33: ROC curves of FLD+DWT.

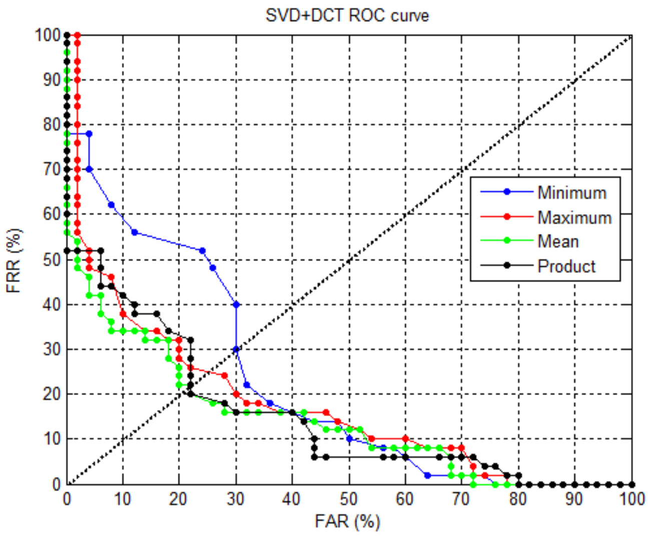

Figure III.34: ROC curves of SVD+DCT.

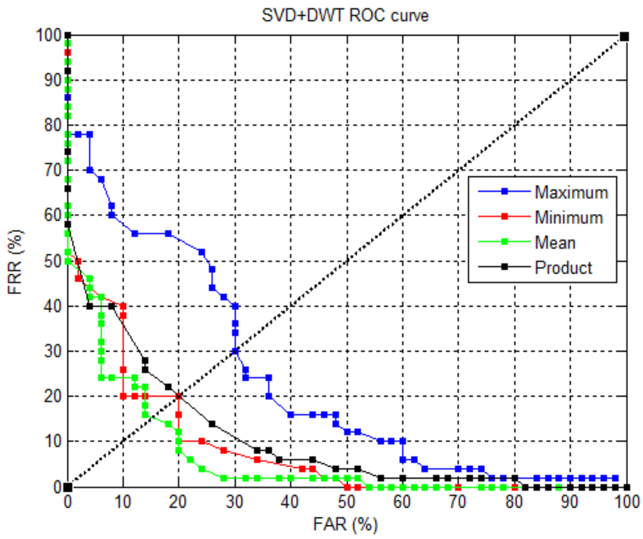

Figure III.35: ROC curves of SVD+DWT.

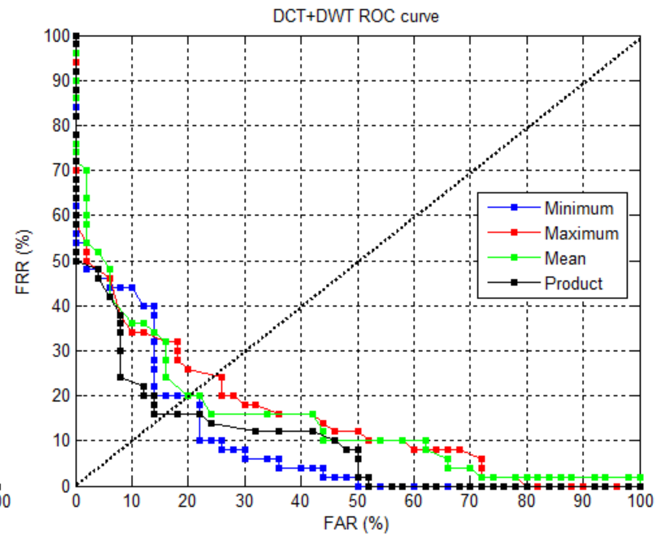

Figure III.36: ROC curves of DCT+DWT.

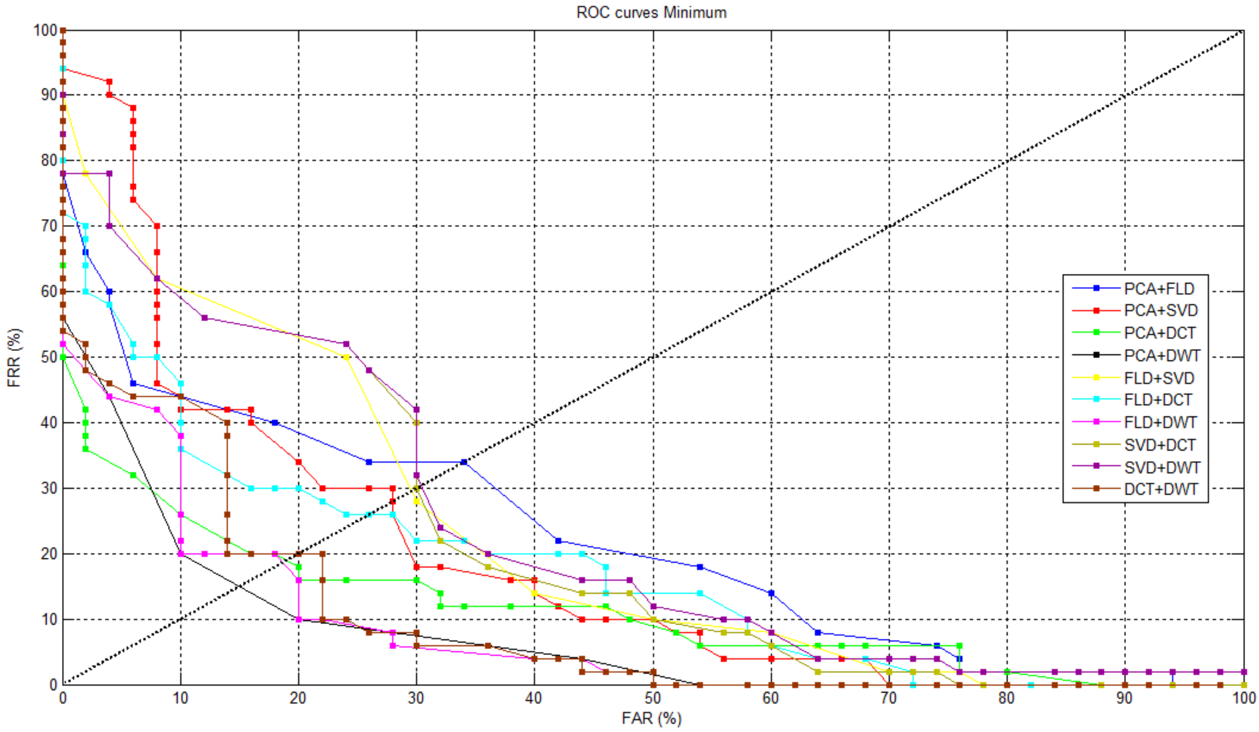

Figure III.37: ROC curves of the different fusion methods using Minimum rule.

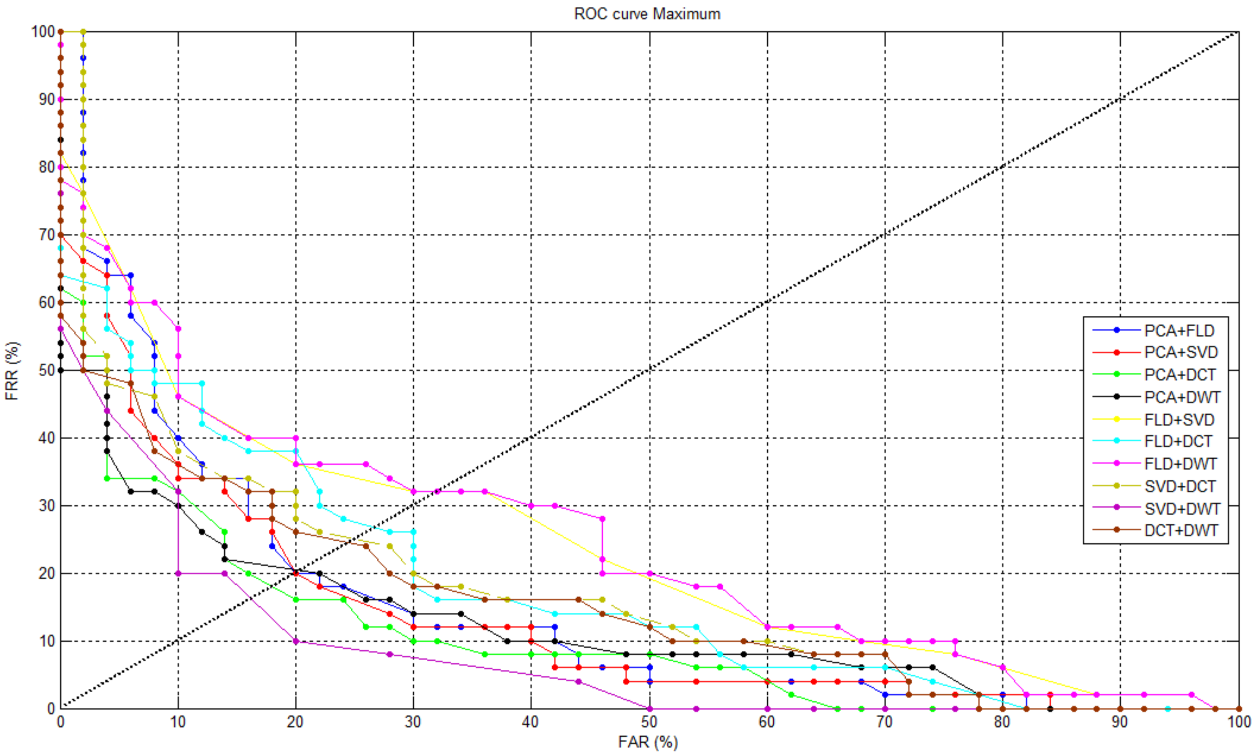

Figure III.38: ROC curves of the different fusion methods using Maximum rule.

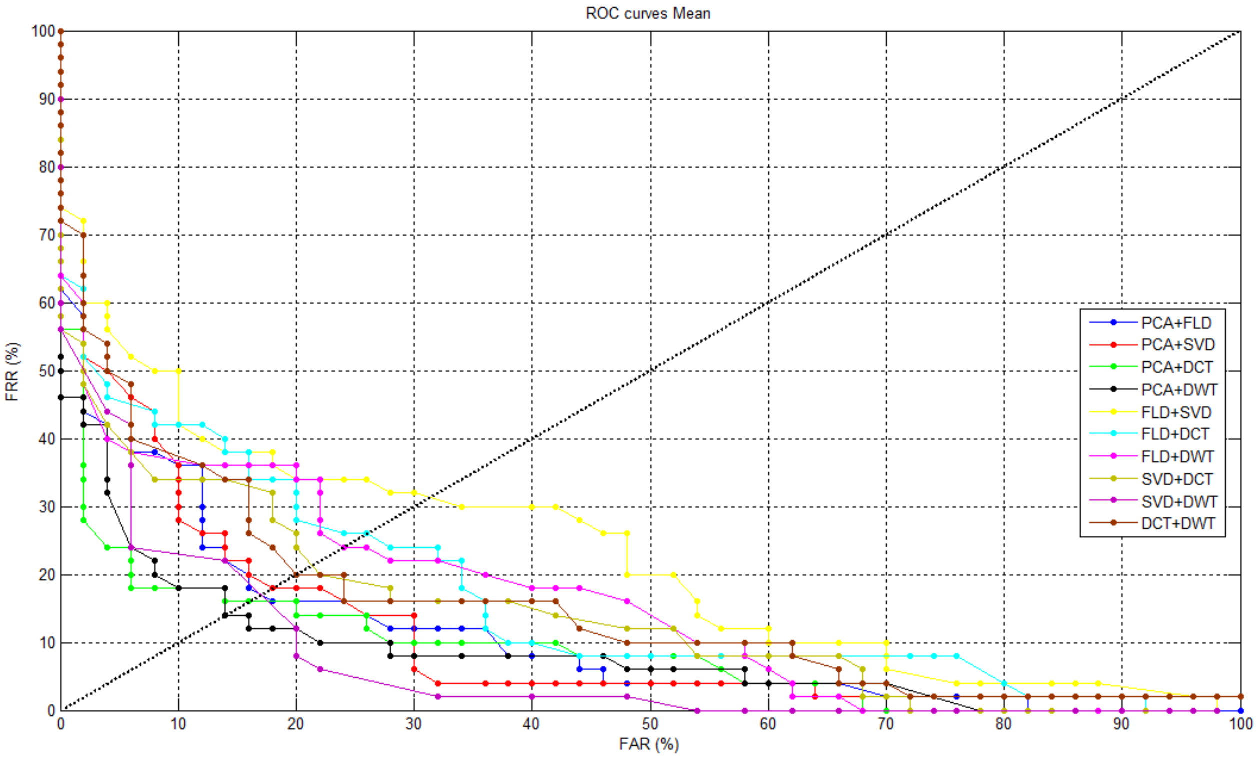

Figure III.39: ROC curves of the different fusion methods using Mean rule.

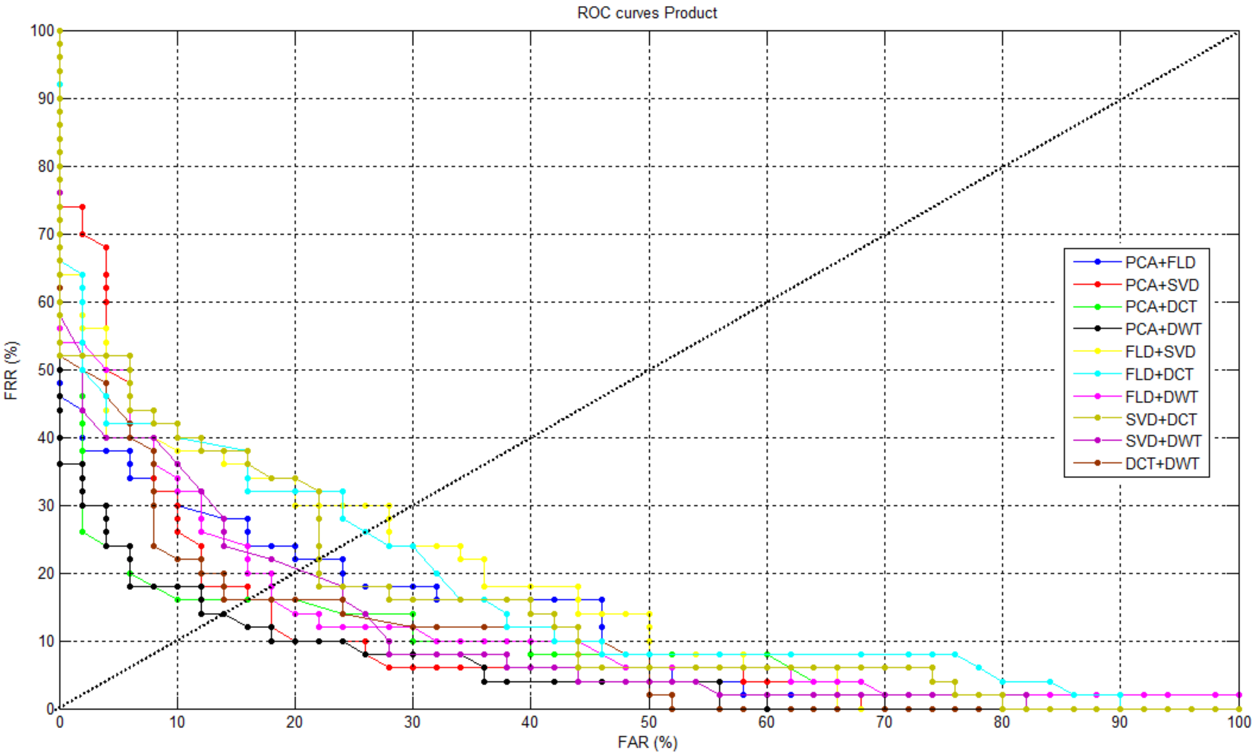

Figure III.40: ROC curves of the different fusion methods using Product rule.

The results are summarized in table III.7

Rule / Method	EER			
	Minimum	**Maximum**	**Mean**	**Product**
PCA+FLD	0.34	0.20	0.18	0.22
PCA+SVD	0.28	0.20	0.19	0.16
PCA+DCT	0.20	0.17	0.16	0.16
PCA+DWT	0.18	0.20	0.14	0.13
FLD+SVD	0.30	0.32	0.31	0.29
FLD+DCT	0.26	0.27	0.26	0.26
FLD+DWT	0.19	0.32	0.25	0.18
SVD+DCT	0.30	0.25	0.21	0.22
SVD+DWT	0.30	0.19	0.15	0.20
DCT+DWT	0.20	0.24	0.20	0.16

Table III.7: EER of fusion methods.

III.4.Conclusion:

In this chapter, several experiments are carried out using ORL, Yale, and FEI face databases. To evaluate the effect of different facial details (glasses, and no glasses), different facial expressions (happy, sleepy, sad, surprised, and winking), different illumination (left light, center light, and right light) on the system performance of PCA using (L1,L2, COS, Mah, L1+Mah,L2+Mah, COS+Mah) we have used the Yale face database.

The experiments are carried out on the ORL face database to compare nine methods namely PCA using (L1, L2, COS, Mah, L2+Mah, and COS+Mah distances), DWT, SVD, and DCT methods. We have found that the DWT method gives the best recognition rate of 93% compared with other methods. and PCA using COS gives the best rate of 92% compared with PCA using L1, L2, Mah, L2+Mah, and COS+Mah methods.

Many experiments are carried out on the FEI face database:
In the first experiment, we have compared between PCA and FLD (PCA-LDA) methods. In order to see the effect of the number of sample per class on the system performance, we have used three, five, and six samples per class. We have found that the system performance increases as the number of samples per class increases. We have found also that PCA outperforms FLD in the three cases.

In the second experiment, we have done a comparison between FLD (PCA-LDA) and DWT-LDA methods. We have found that DWT-LDA performs better than FLD (PCA-LDA) since it has the lowest EER of 19%.

In the third experiment, we have compared between SVD and DWT-SVD methods to show the effect of applying DWT before SVD. The comparison was performed between them in terms of EER. The EER rate is reduced by 2%, so the wavelet decomposition has improved the system performance.

In the fourth experiment, WPD-PCA and PCA methods were compared. In WPD-PCA, the fusion was done at feature level and at decision level; and at decision level two rules (maximum and mean rules) have been used. We have found that WPD-PCA method using maximum decision fusion gives the best result since it has the lowest EER of 14%.

In the fifth experiment, two set of experiments are carried on to identify the accuracy of our algorithm (YCbCr-WPD-PCA). In the first experiment, we tested the recognition rate of PCA, DWT, DWT-PCA and YCbCr-WPD-PCA for one sample, three and six samples per class in the training set. We have seen that the recognition rates increase as we increase the numbers of samples per class. Our method outperforms other methods; it reaches recognition rates of 82.50%, 86.87%, and 93.12% with one sample, three and six samples per class respectively. In the second experiment, we compare five methods (PCA, DWT, DWT-PCA, WPD-PCA using feature fusion, and WPD-PCA using decision fusion) with our proposed method in terms of Equal Error Rate (EER). YCbCr-WPD-PCA method, achieved an equal error rate of 10%; this is the lowest EER. So our method gives significant performance compared to other methods.

In The last experiment, we have compared each fusion method separately using minimum, maximum, mean, and product rules. We have found that PCA+FLD using mean rule, PCA+SVD using product rule, PCA+DWT using product rule PCA+DCT using mean and product rules, FLD+SVD using product rule, FLD+DCT using minimum, product and mean rules, FLD+DWT using product rule, SVD+DCT using mean rule, SVD+DWT using mean rule, and DCT+DWT using product rule give the best result since they reach the lowest EER of 18% , 16%, 13%; 16%, 29% 26% 18% 21% , 15%, and 16% respectively, so, PCA+DWT using product rule outperforms the other methods. From the table III.7 we have concluded that in minimum rule DCT+DWT method gave the best result with lowest EER of 18%, in maximum rule PCA+DCT method gave the lowest EER of 17% ,in mean rule PCA+DWT method gave the lowest EER of 14%, and in product rule PCA+DWT method gave the lowest EER of 13%.

In the next chapter, we will present an overview of graphical user interface developed.

Chapitre IV

Graphical User Interface (GUI)

IV.1.Introduction:

This chapter deals with the used software in our experiments that are carried out through the use of a laptop (dual CPU T2330 1.4 GHz and 2GB memory) and the MATLAB language as tool of development.

IV.2: Application:

Our application consists of many graphical interfaces. Each interface contains buttons and menus. The main interface is given in figure IV.1.

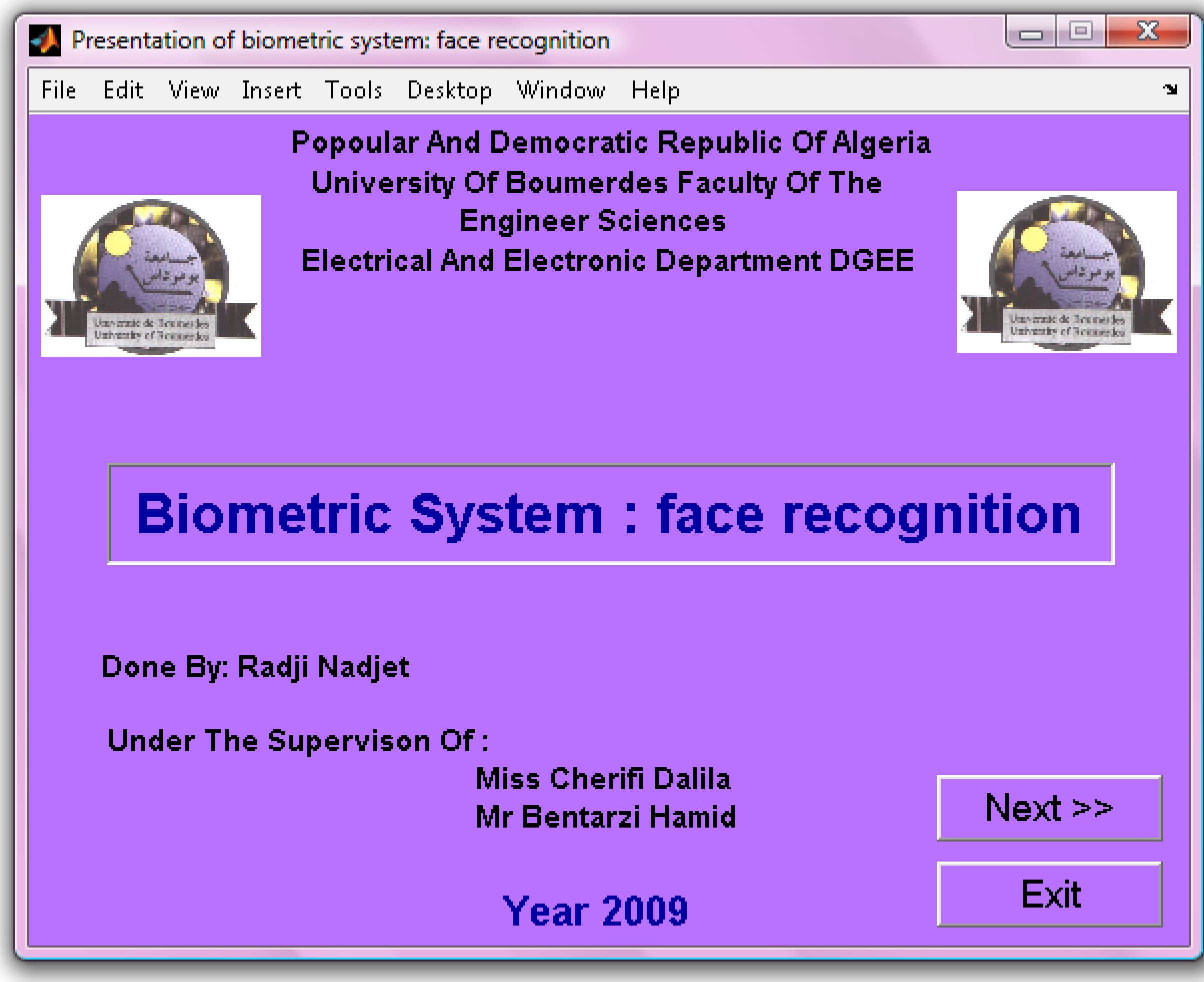

Figure IV.1: Main interface.

In order to go to the next interface, it is required to press the push button "**Next** >>". This interface (figure IV.2) contains the methods of face recognition. The methods are divided into three categories: simple methods, cascade methods, fusion methods, and proposed method. In the simple methods, we have five methods namely PCA, FLD, SVD, DCT and, DWT. In the cascade methods, we have four methods DWT-PCA, WPD-PCA, DWT-SVD, and finally DWT-FLD. To show the fusion methods or the proposed method interfaces, press the push buttons **"fused methods"** or "**YCbCr-WPD-PCA**" respectively.

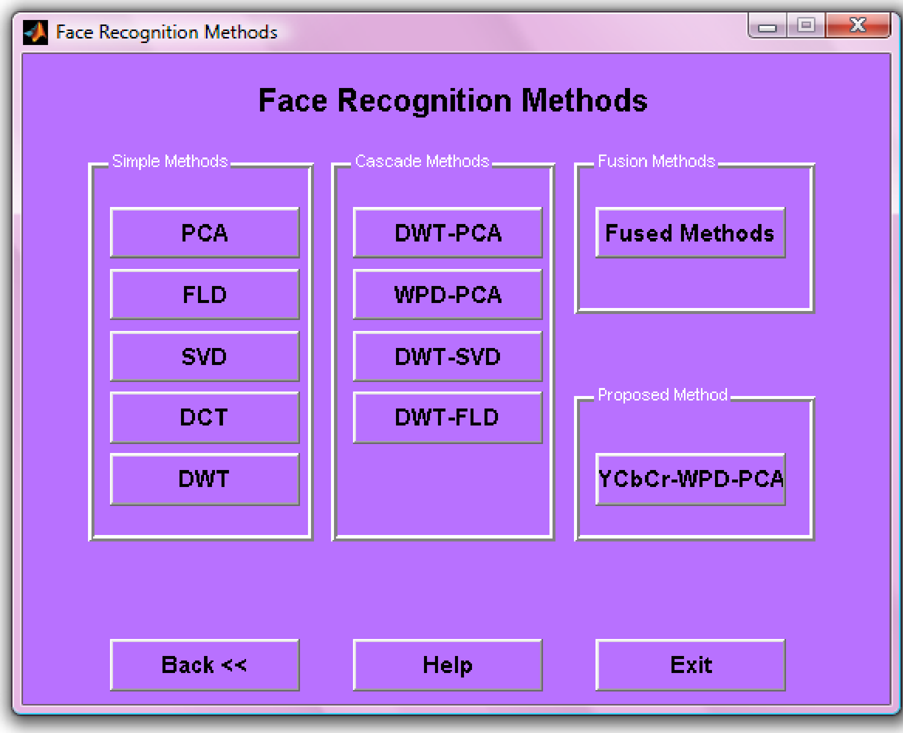

Figure IV.2: Face recognition methods interface.

IV.2.1.Face recognition using PCA:

After pressing the push button "**PCA**" the interface of figure IV.3 will appear.

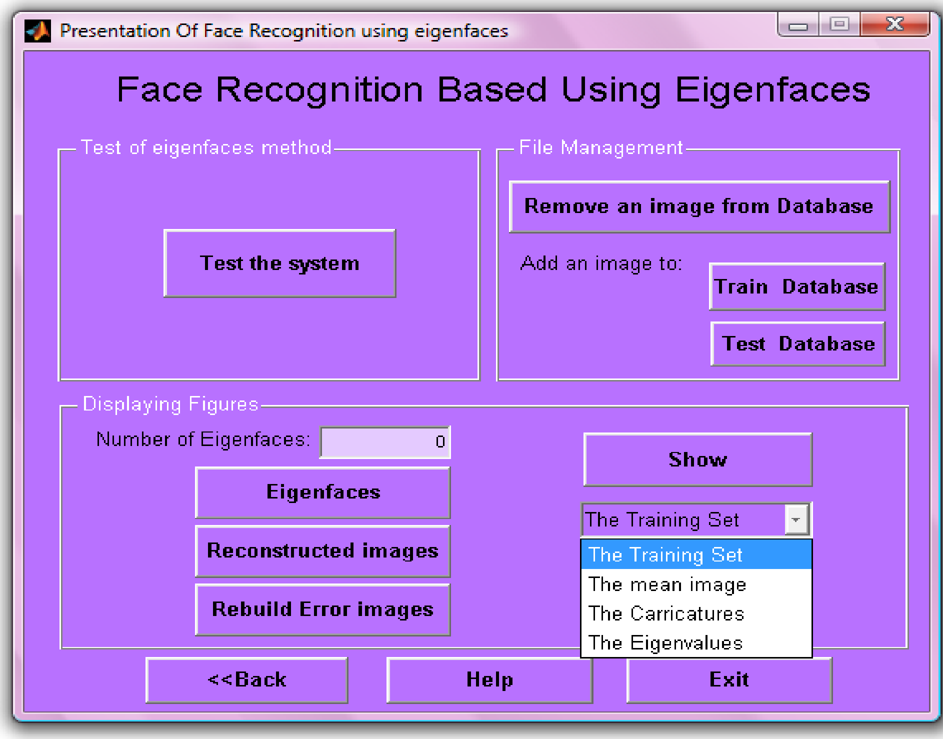

Figure IV.3: The main interface of face recognition using Eigenfaces.

To show the training set, the mean image, caricatures or eignvalues select from the popup menu one of the items and then press the push button "**show**". The results are given in figure IV.4, figure IV.5, figure IV.6, and figure IV.7 respectively.

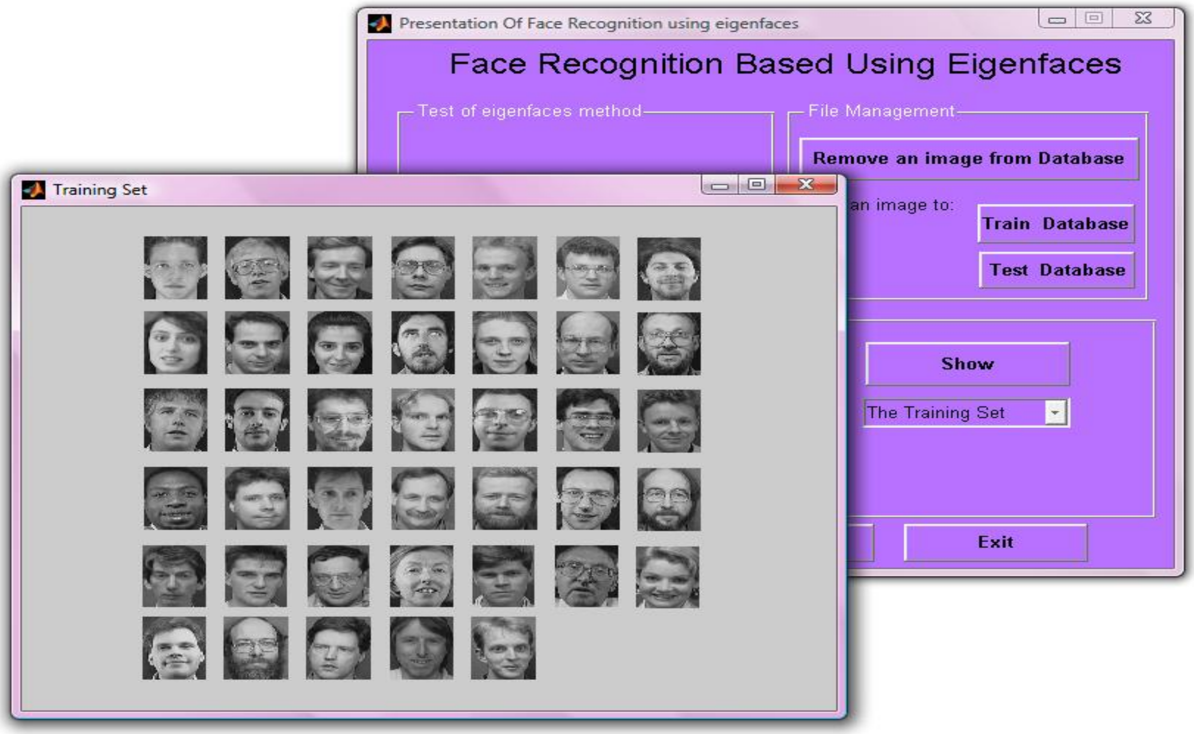

Figure IV.4: The training set.

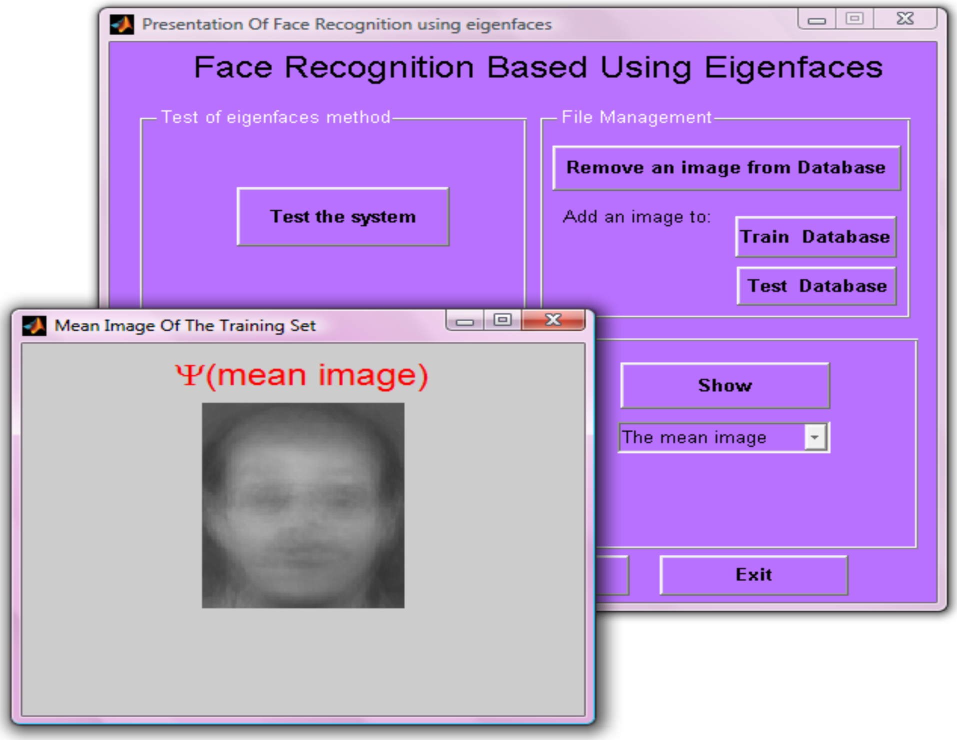

Figure IV.5: Mean image in PCA method.

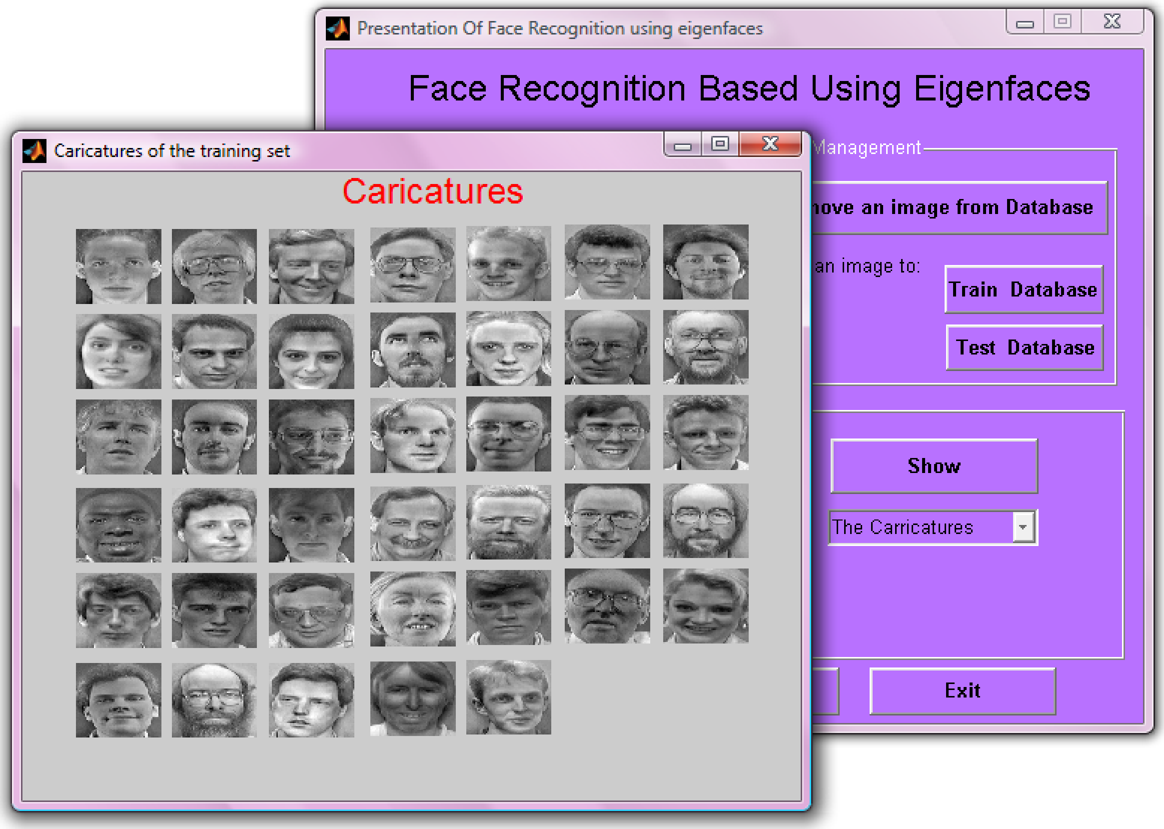

Figure IV.6: Caricatures in PCA method.

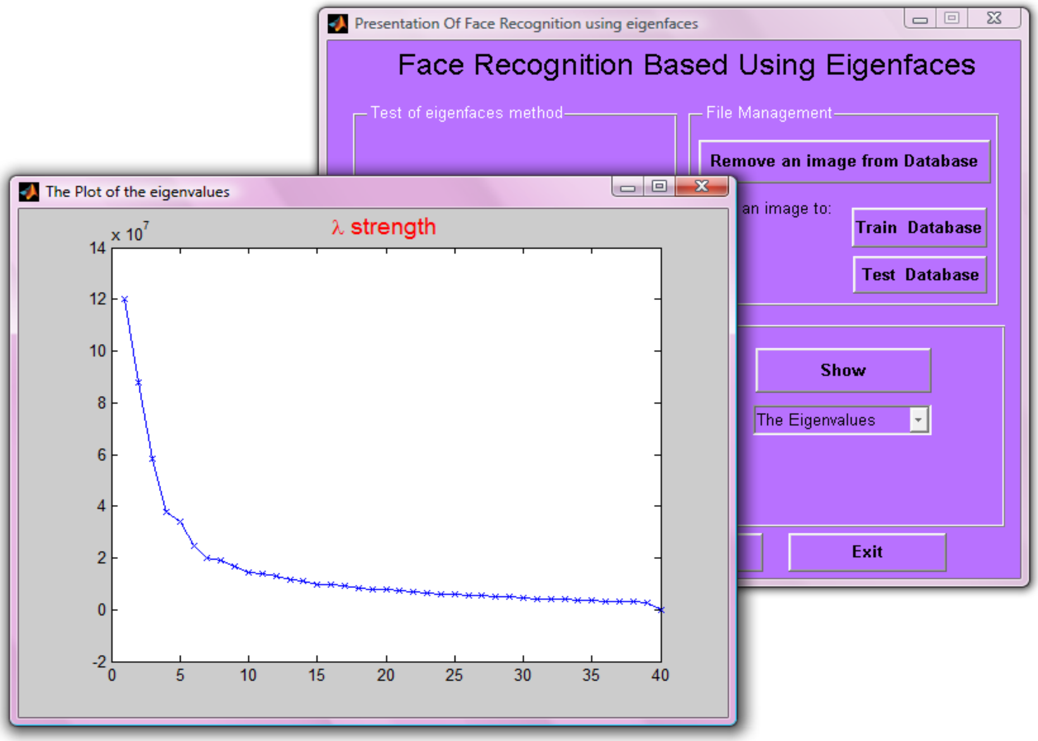

Figure IV.7: Eigenvalues in PCA method.

To show the effect of the number of eigenfaces selected for reconstructing the images, select the number of eigenfaces which must be a number between 1 to M where M is the total number of images and then press the push button "**Reconstructed images**". To show the rebuilt error and eigenfaces press the push button "**rebuilt error images**" and "**Eigenfaces**" respectively. We have seen that the rebuilt error decreases as the number of eigenfaces increases.

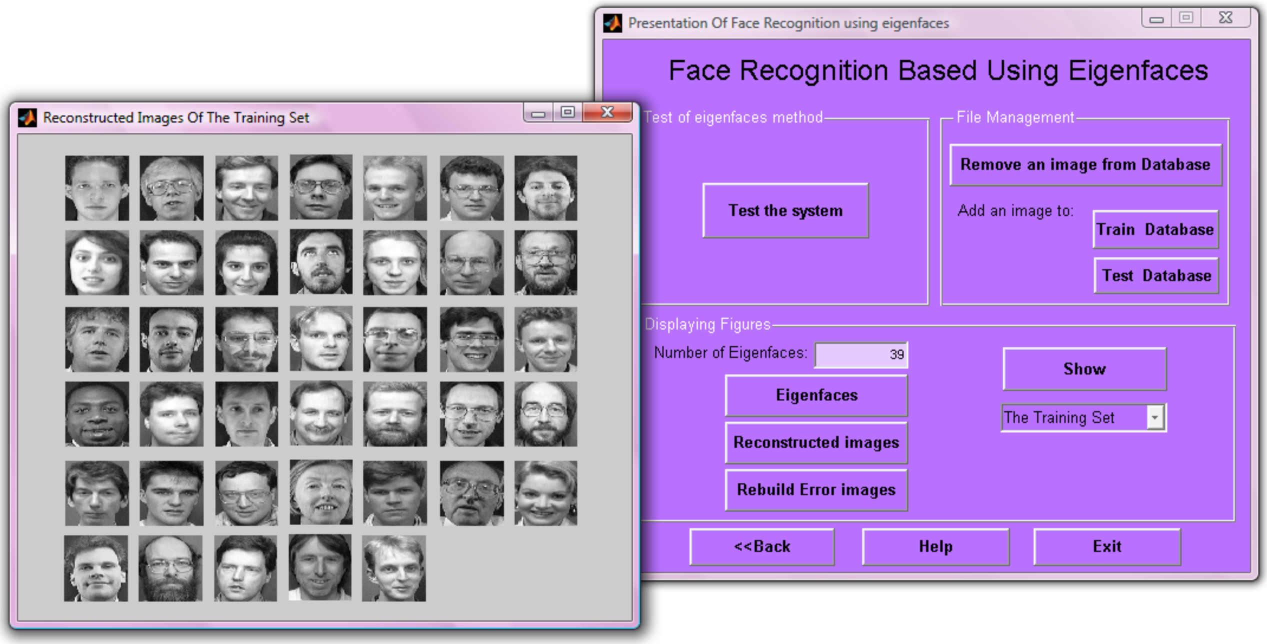

Figure IV.8: Reconstructed images with N=39.

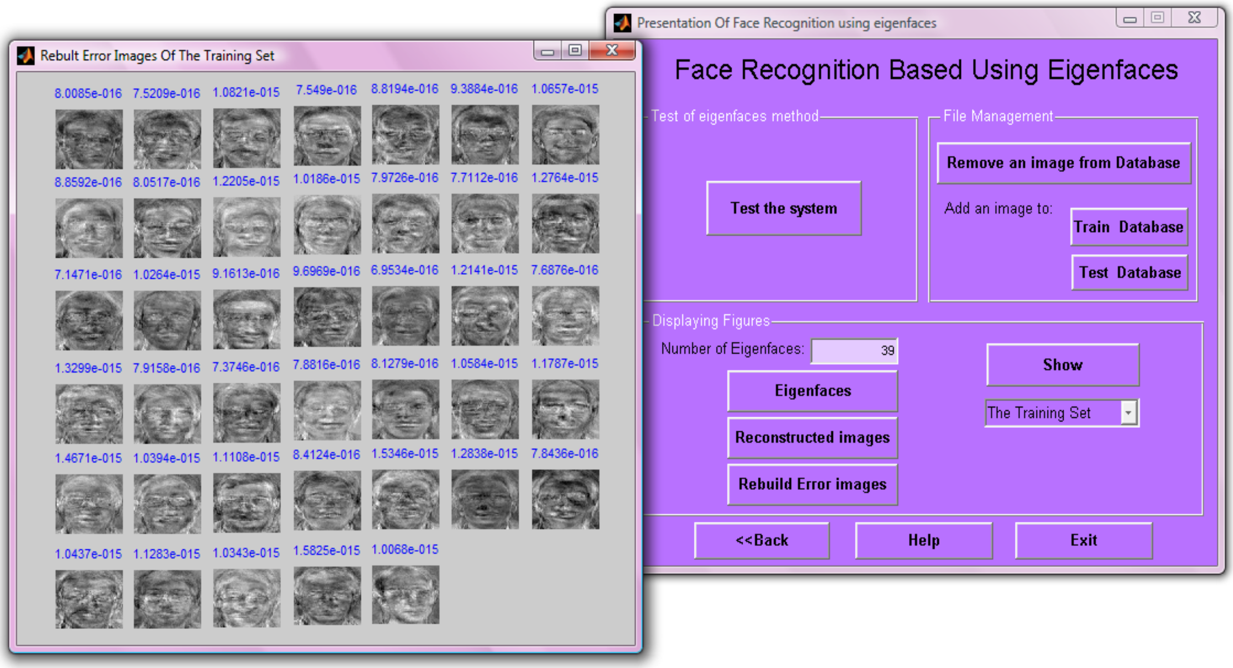

Figure IV.9: Rebuilt error images with N=39.

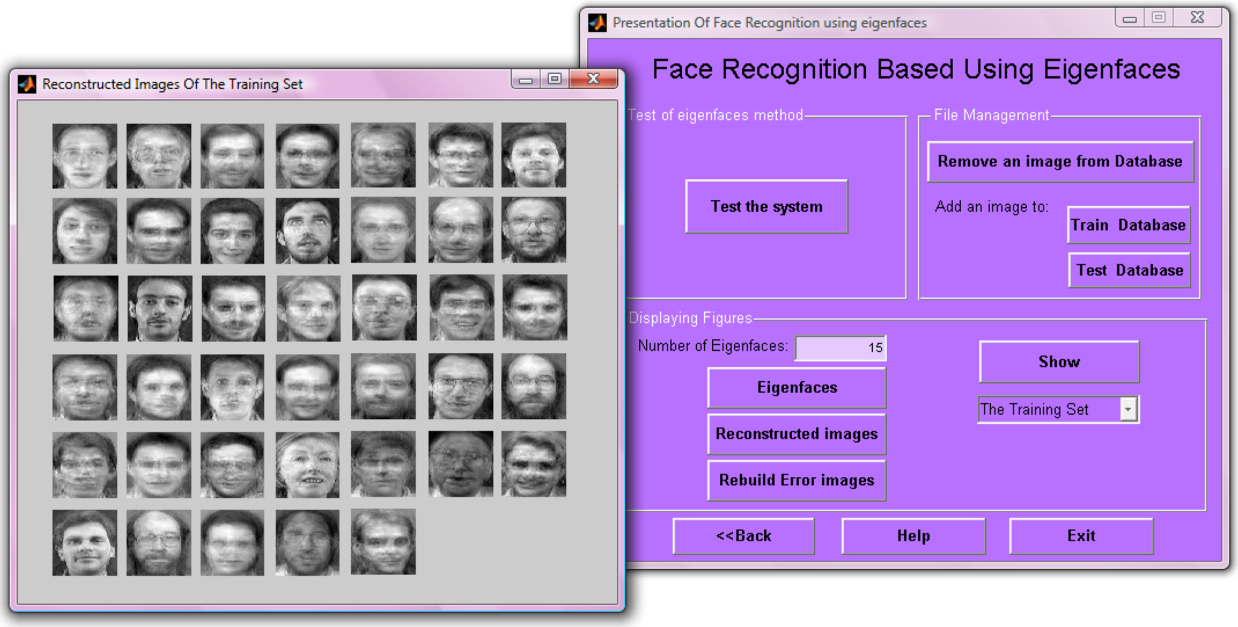

Figure IV.10: Reconstructed images with N=15.

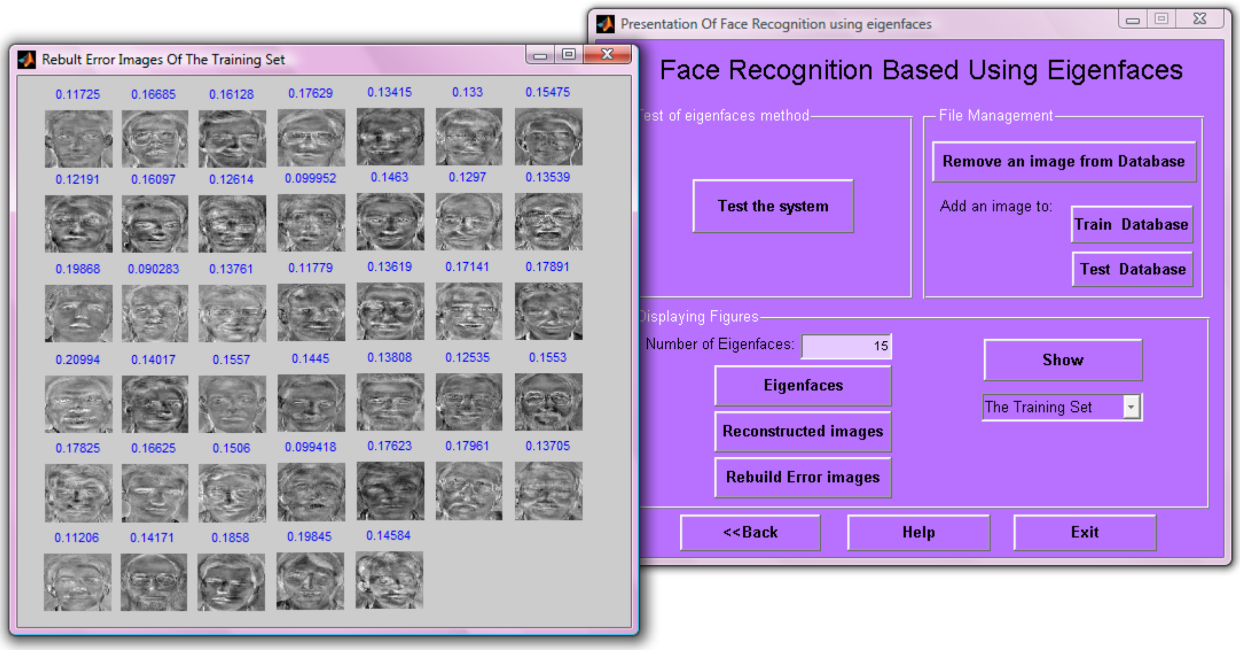

Figure IV.11: Rebuilt error images with N=15.

To test the system, press the push button "**Test the system**", it will appear a new window (figure IV.12). Seven similarity measures are used: city block, euclidean, mahalanobis, COS, L1+mahalanobis, L2+mahalanobis, and COS +mahalanobis; select one of them, then press the push button "**select**", it will appear a prompt window, select an image and then press the push button "**search**" to do the test. If you want to show the different similarity measures press the push button "**show**". The results are given in the figures bellow.

Figure IV.12: Test of PCA using different similarity measure Interface.

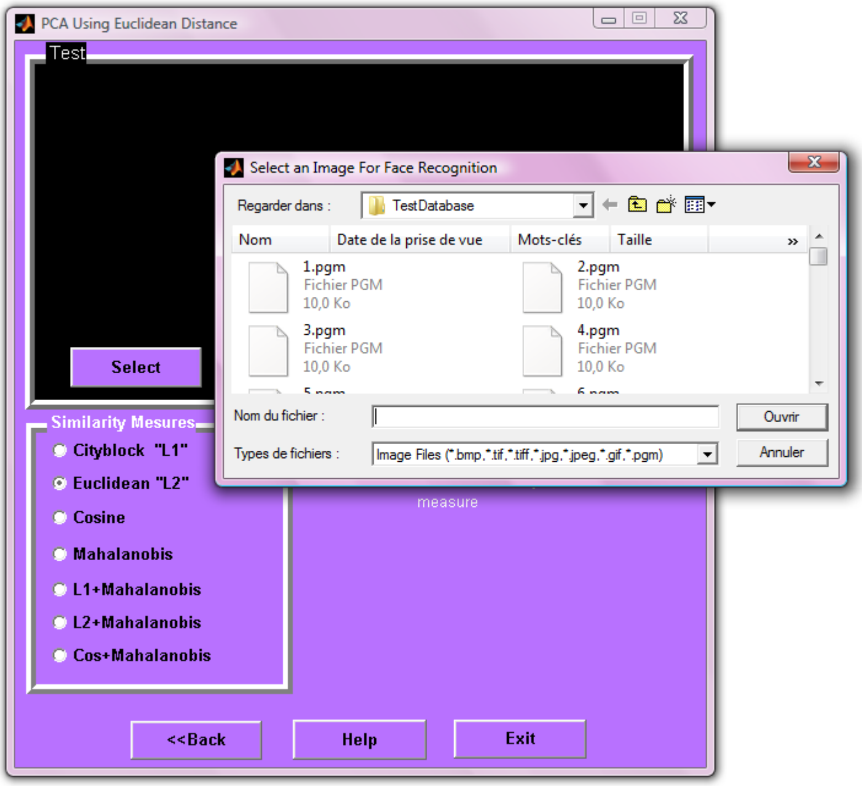

Figure IV.13: Select window.

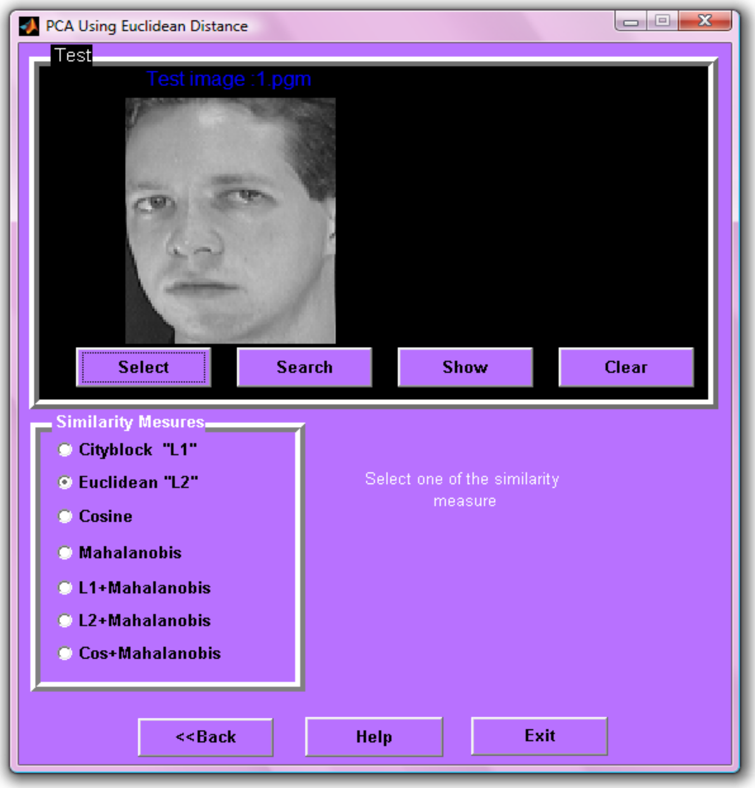

Figure IV.14: Selected image in PCA method.

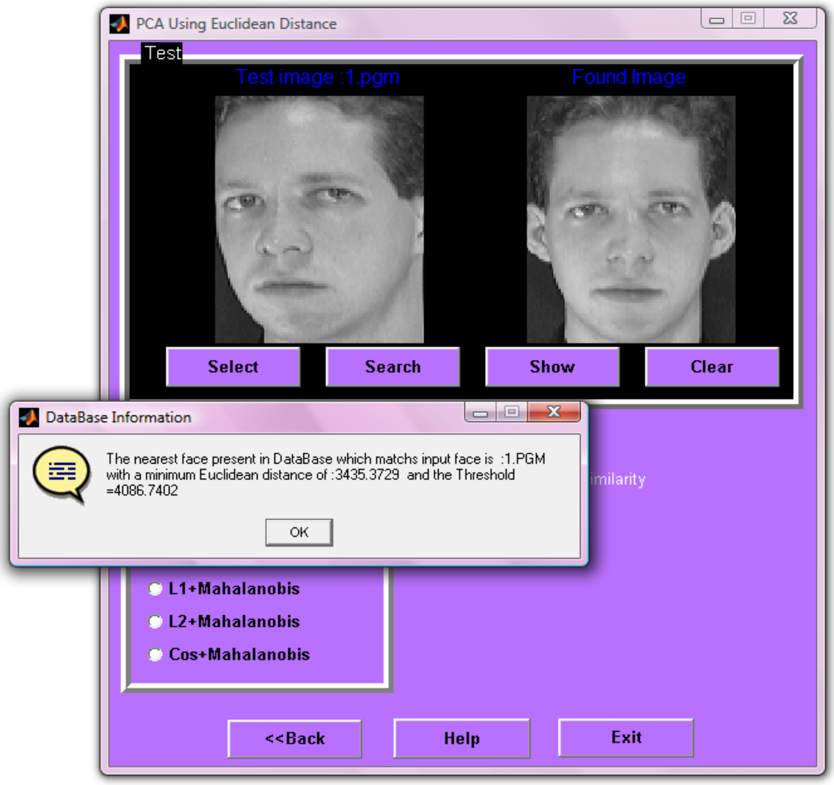

Figure IV.15: Result of test in PCA method.

Figure IV.16: Euclidean distance of the test image.

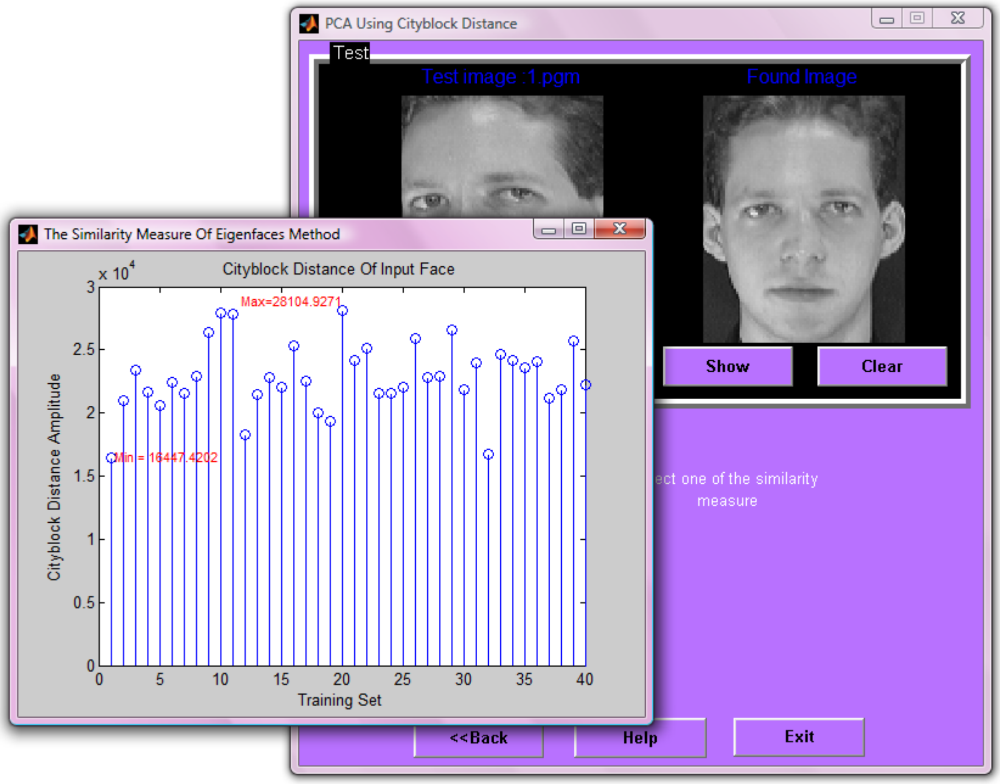

Figure IV.17: City block distance of the test image.

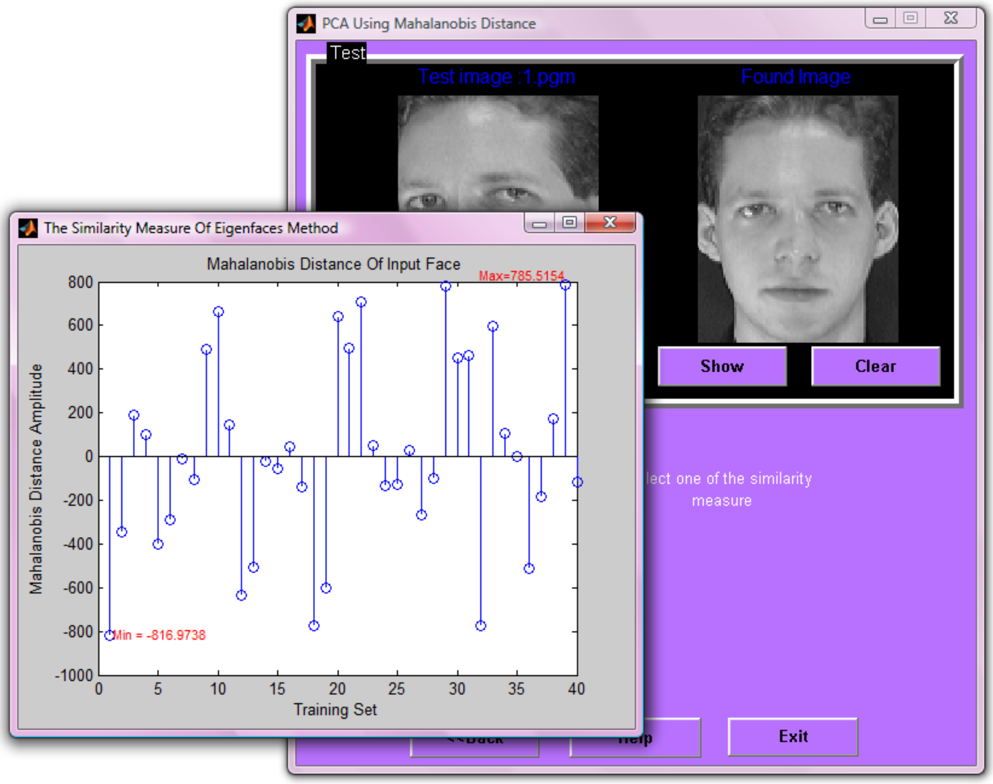

Figure IV.18: Mahalanobis distance of the test image.

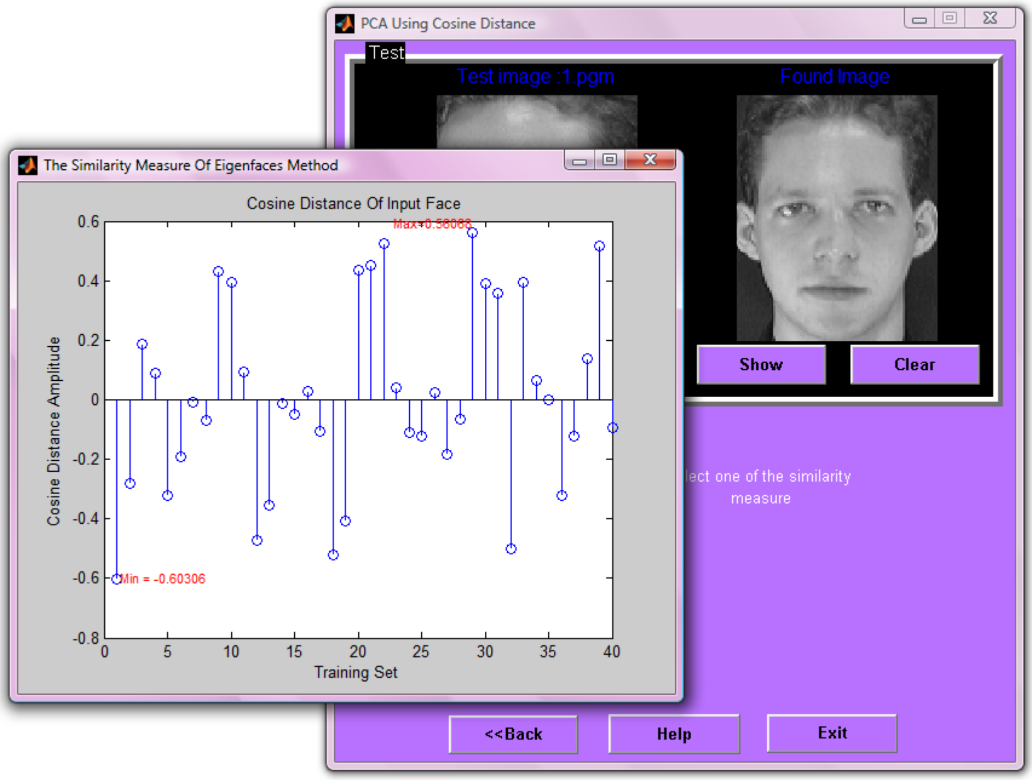

Figure IV.19: Cosine distance of test image.

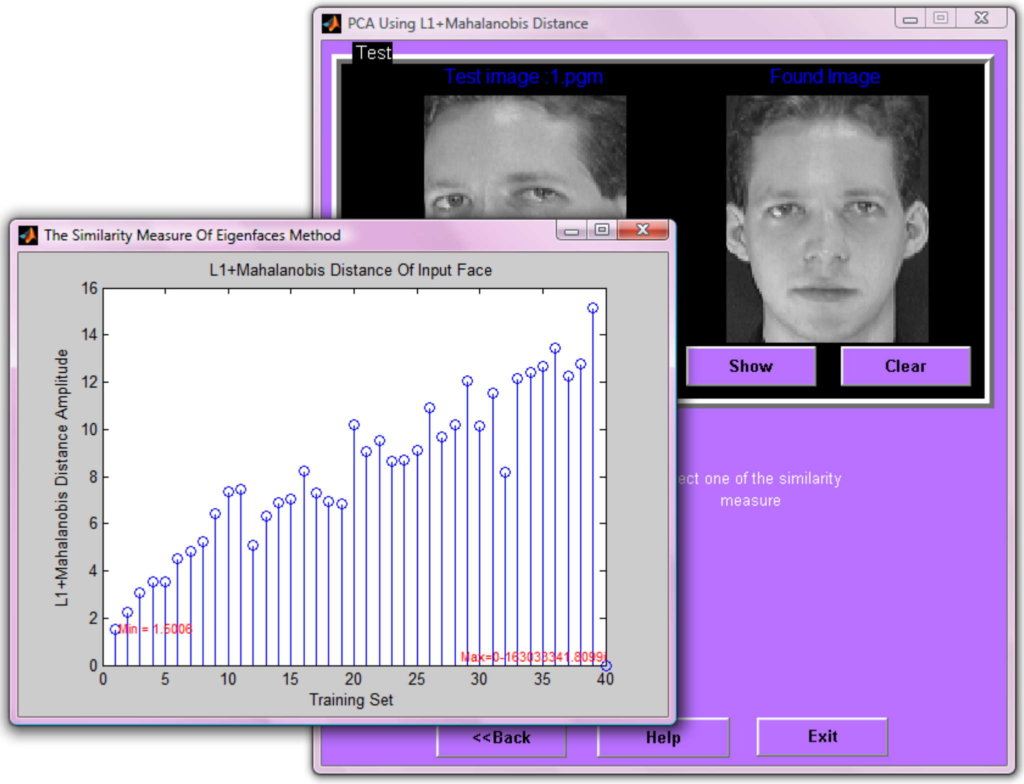

Figure IV.20: L1+mahalanobis distance of test image.

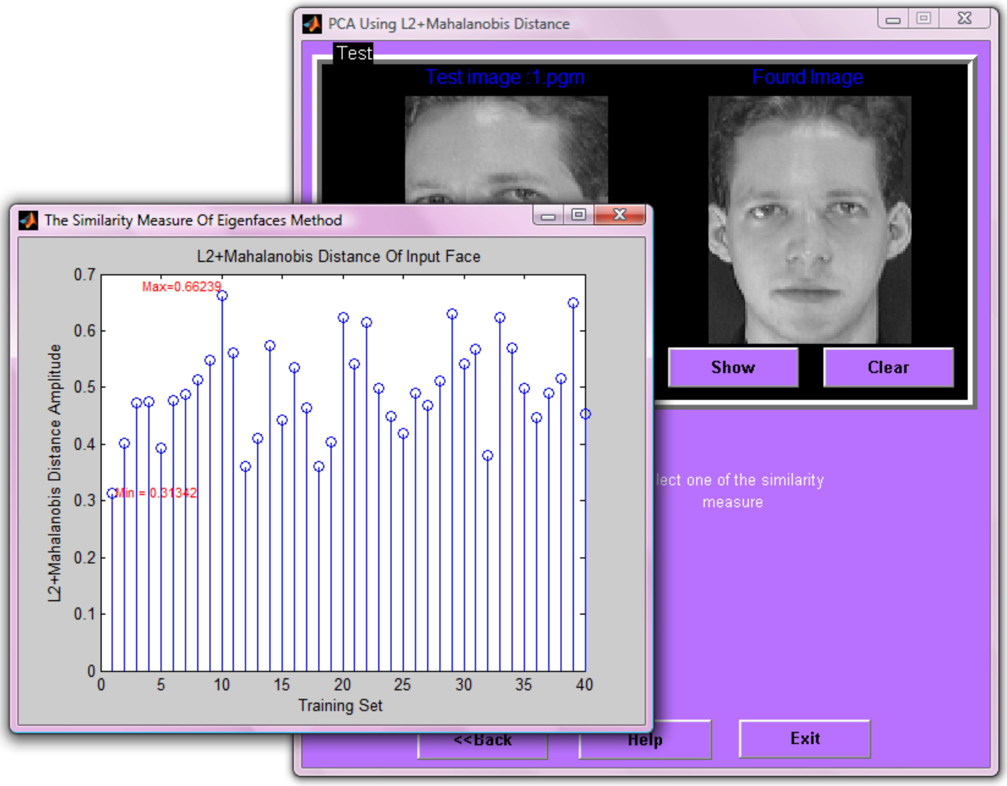

Figure IV.21: L2+mahalanobis distance of the test image.

Figure IV.22: Cos + mahalanobis distance of the test image.

To quit the system press the push button "**Exit**" it will appear a message box, for the confirmation to exit the application.

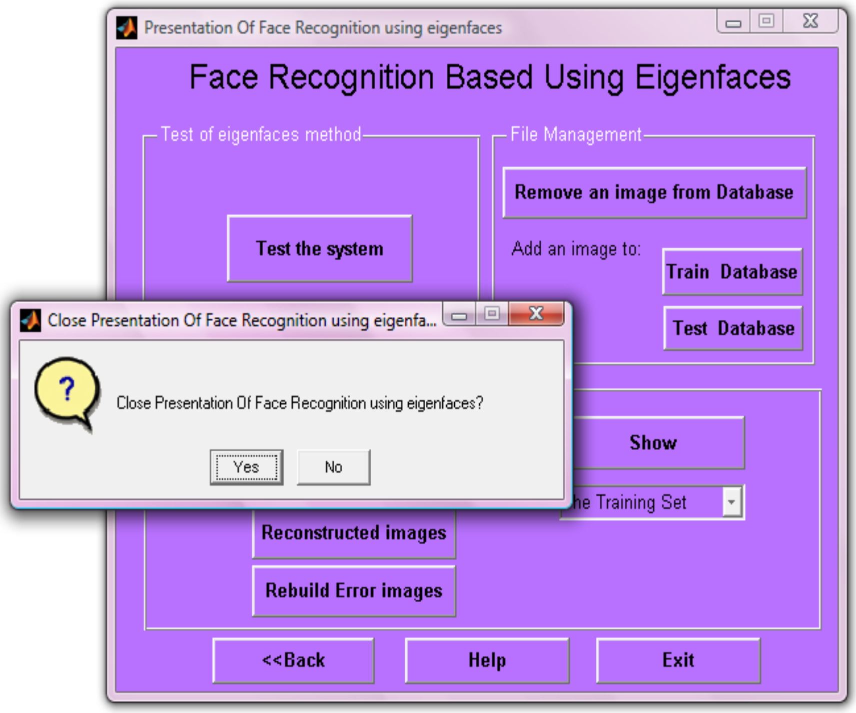

Figure IV.23: Exit window.

IV.2.2.Face recognition using FLD:

After pressing the push button "**FLD**" the interface (figure IV.24) will appear.

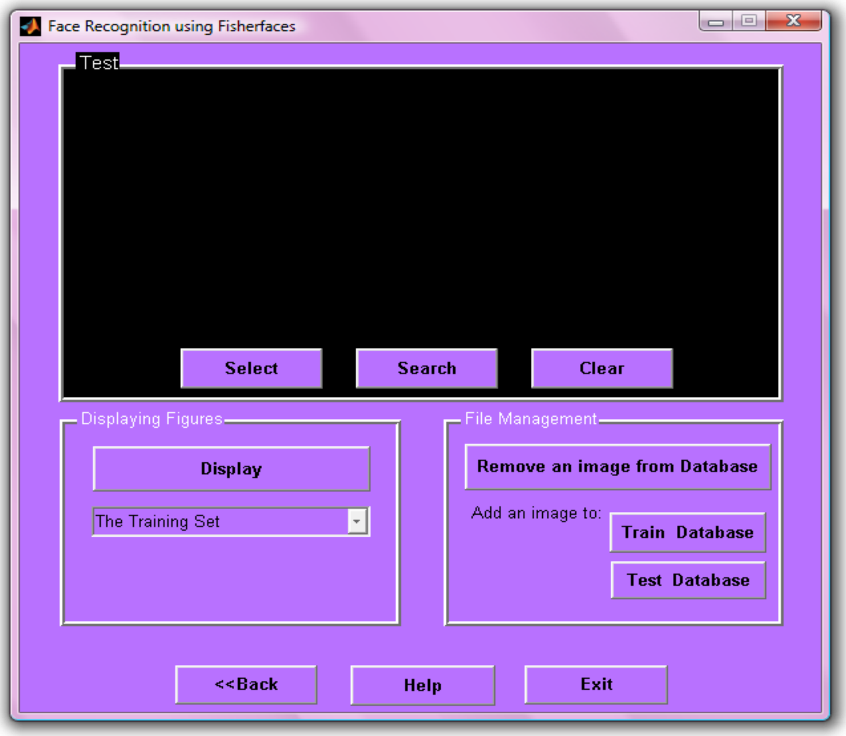

Figure IV.24: Face recognition using FLD interface.

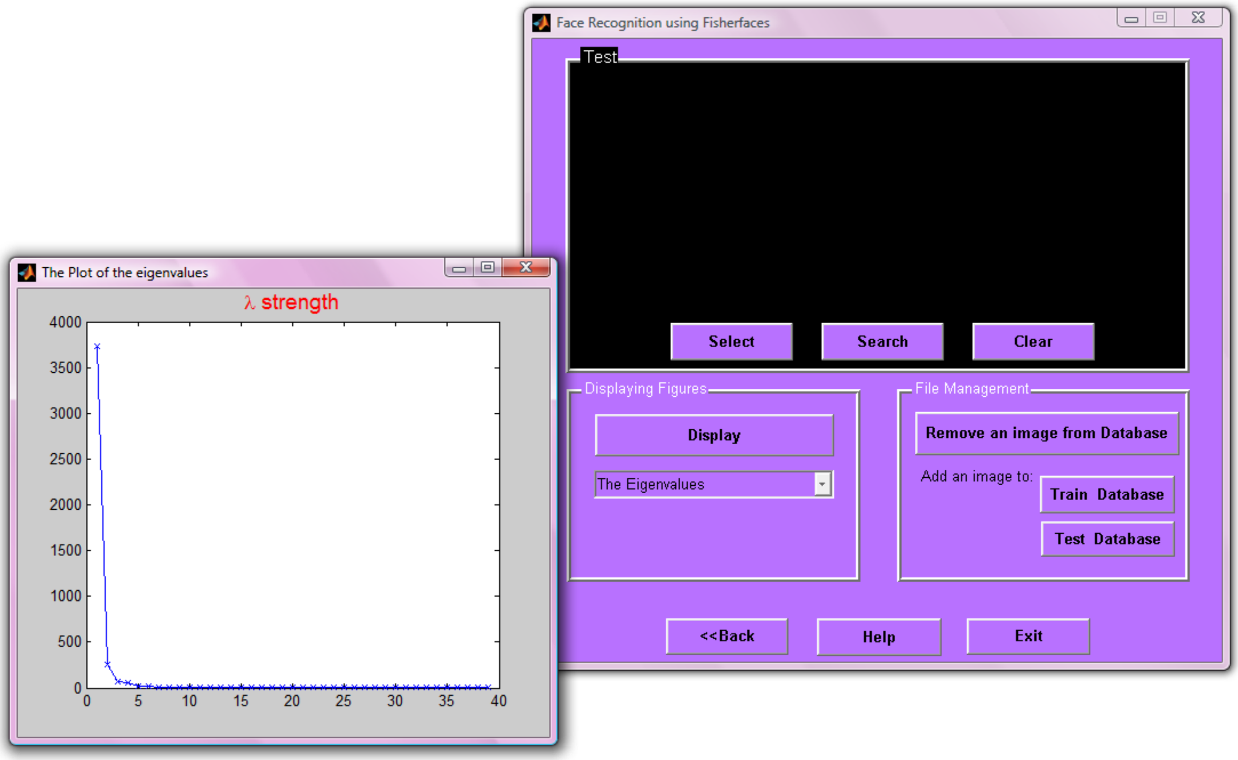

Figure IV.25: Eigenvalues in FLD method.

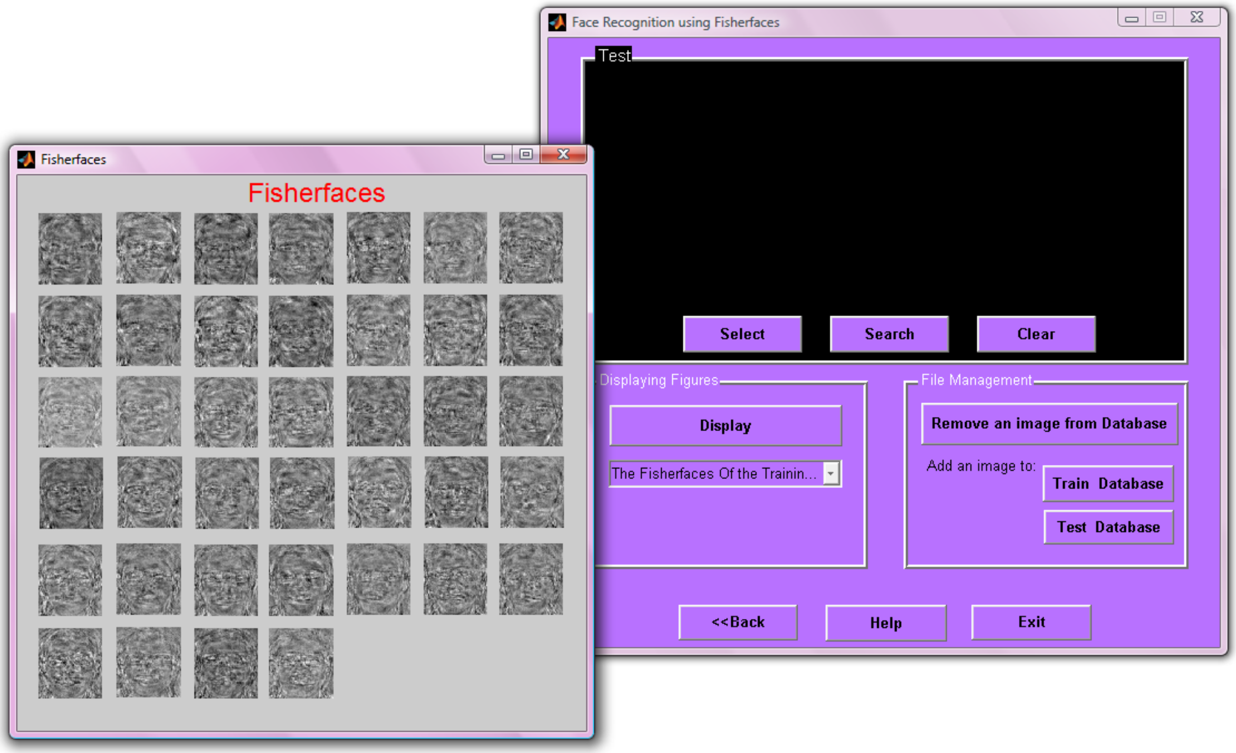

Figure IV.26: Fisherfaces.

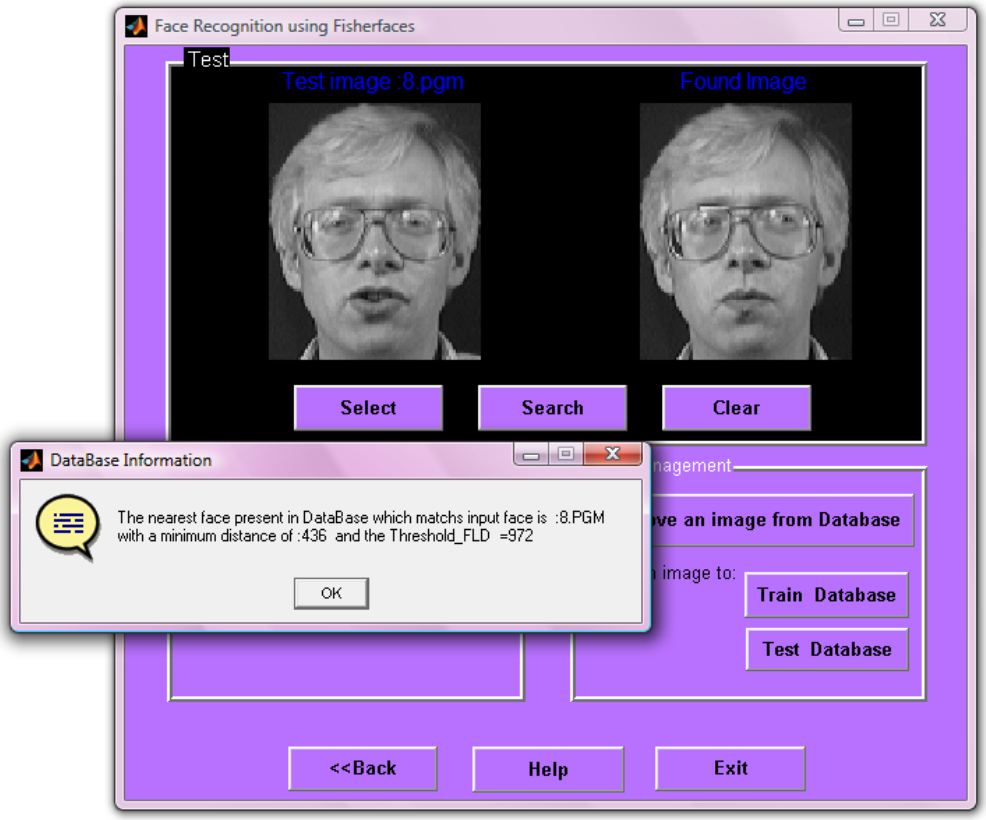

Figure IV.27: Result of the test in FLD method.

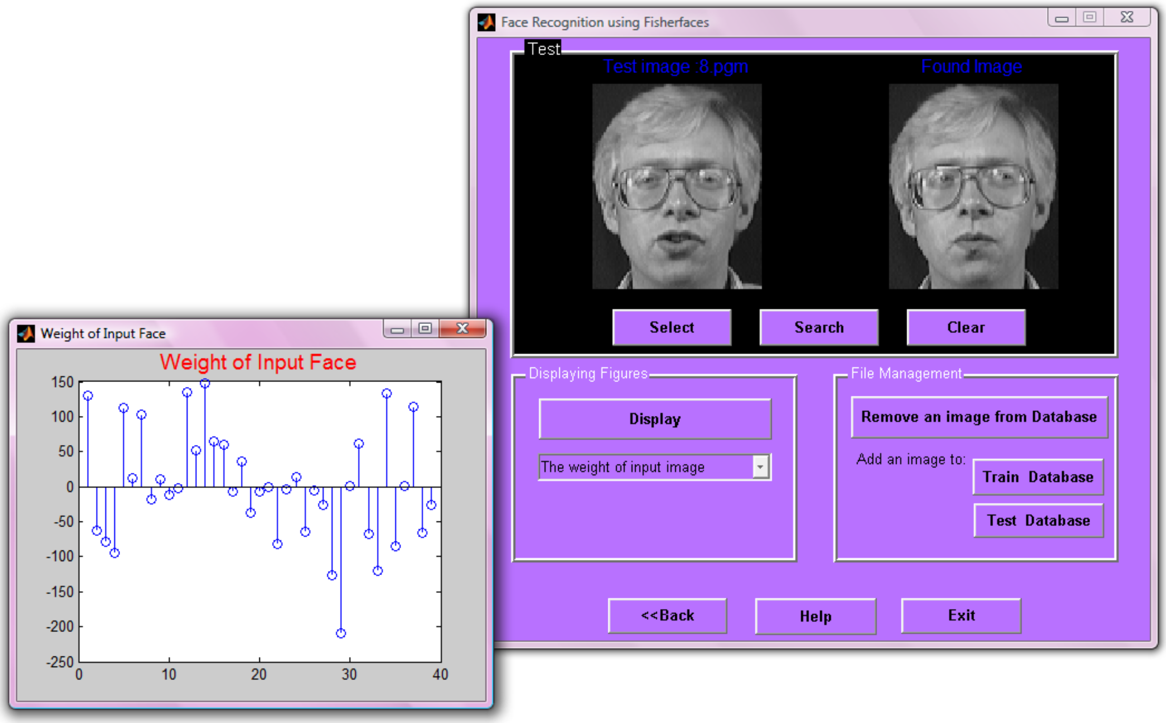

Figure IV.28: Weight of test image in FLD method.

IV.2.3.Face recognition using SVD interface:

After pressing the push button "**SVD**" the interface in figure (IV.29) will appear.

To do the test you follow the same steps as before. To see the euclidean distance and the SVD component press the push button "**show**".

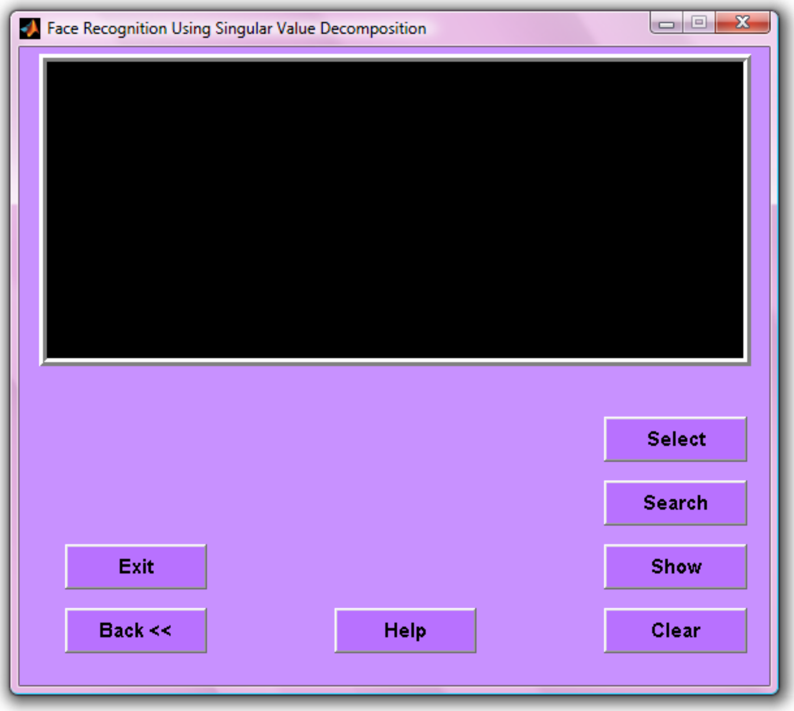

Figure IV.29: Face recognition using SVD interface.

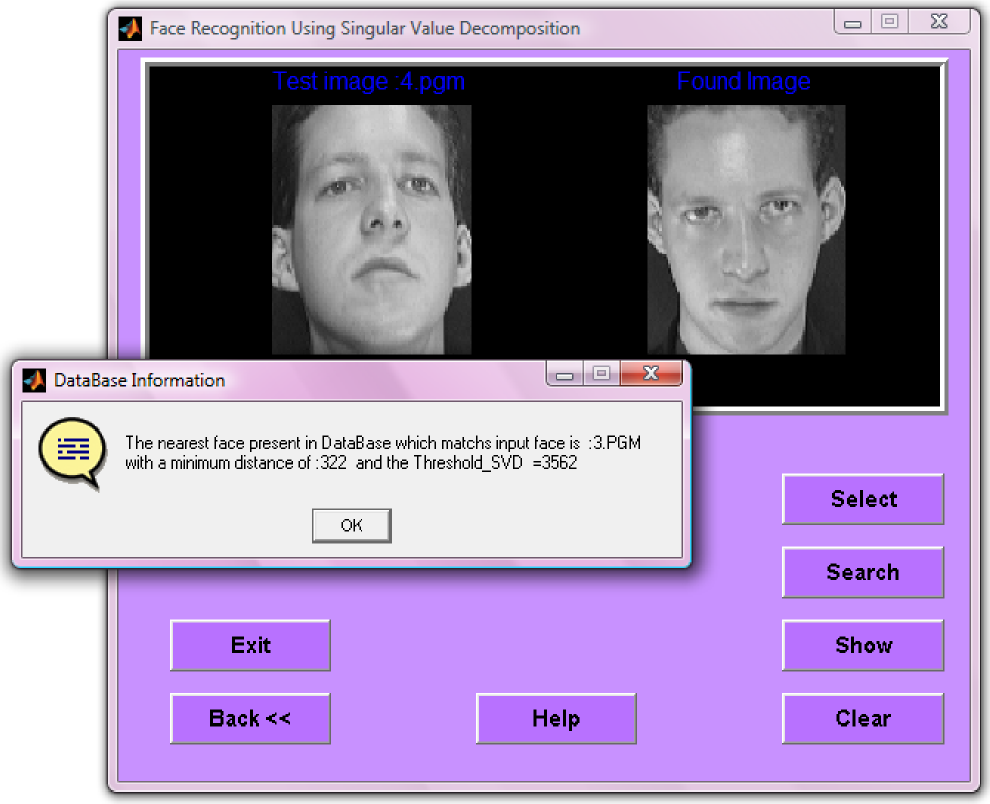

Figure IV.30: Result of the test in SVD method.

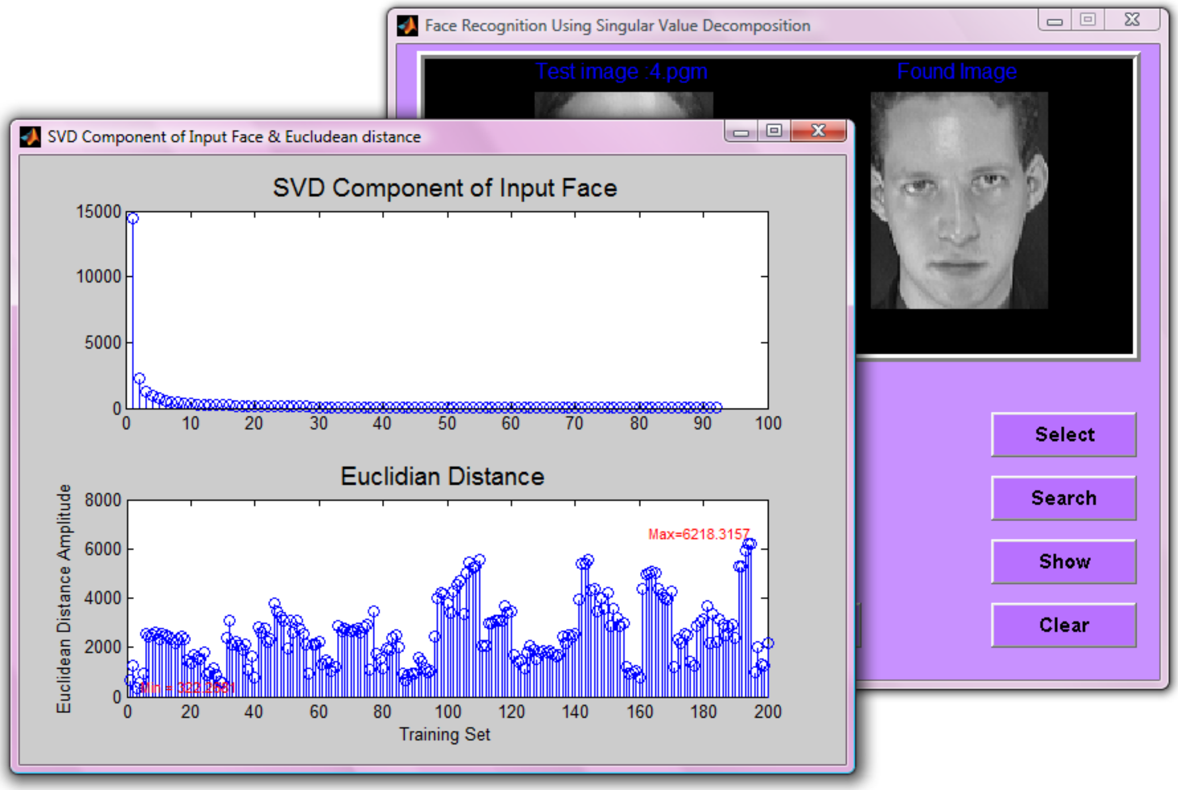

Figure IV.31: Euclidean distance and SVD component.

IV.2.4.Face recognition using DCT interface:

After pressing the push button "**DCT**" the interface in figure (IV.32) will appear. To do the test you follow the same steps as before. If you want to see the Euclidean distance and the DCT component press the push button "**show**". The results are given in the figures bellow.

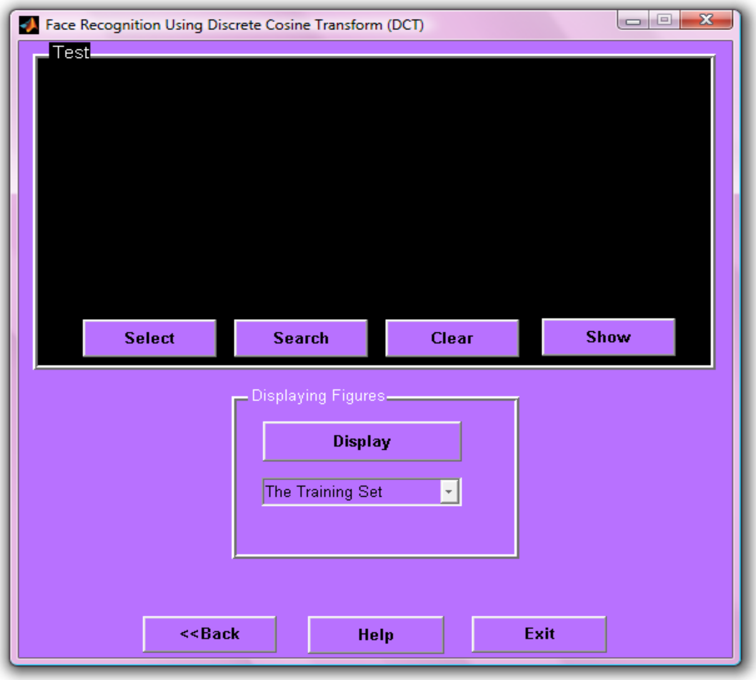

Figure IV.32: Face recognition using DCT interface.

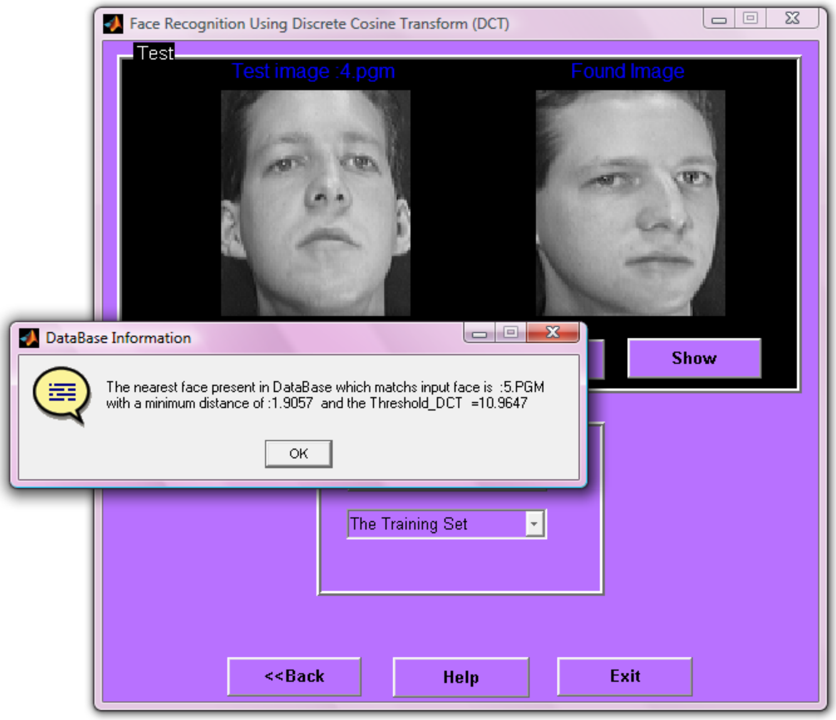

Figure IV.33: Result of the test in SVD method.

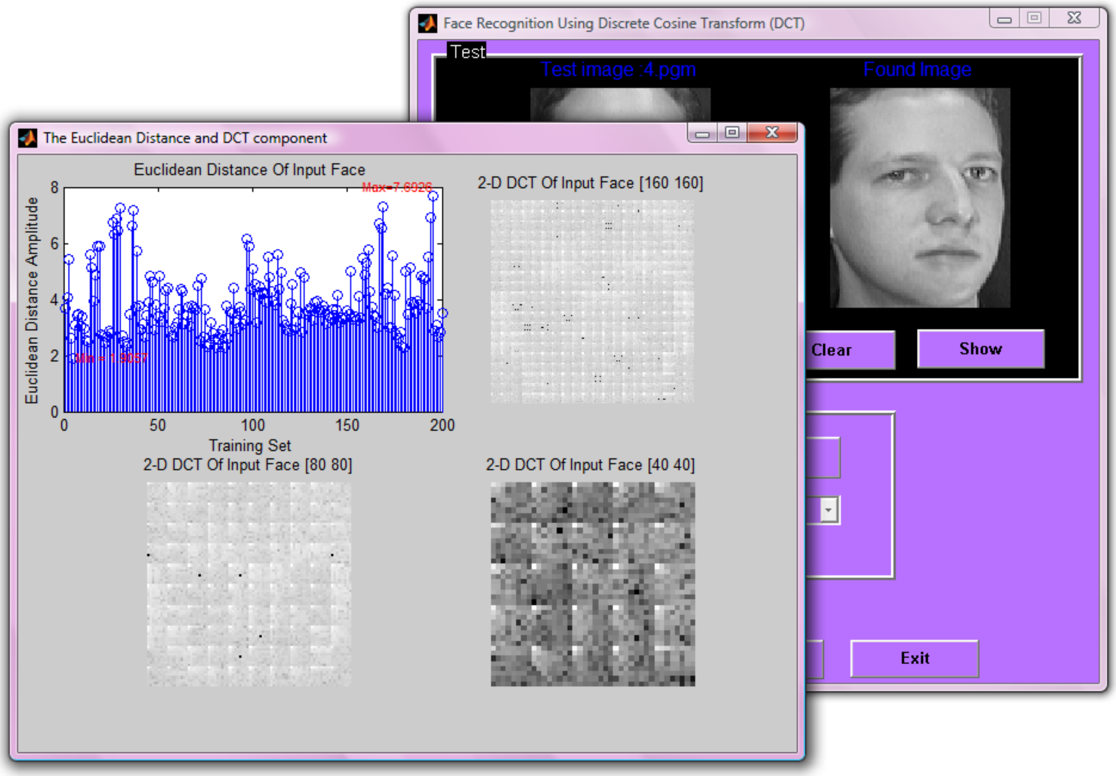

Figure IV.34: Euclidean distance and DCT component.

IV.2.5.Face recognition using DWT interface:

After pressing the push button "**DWT**" the interface bellow (figure IV.35) will appear.

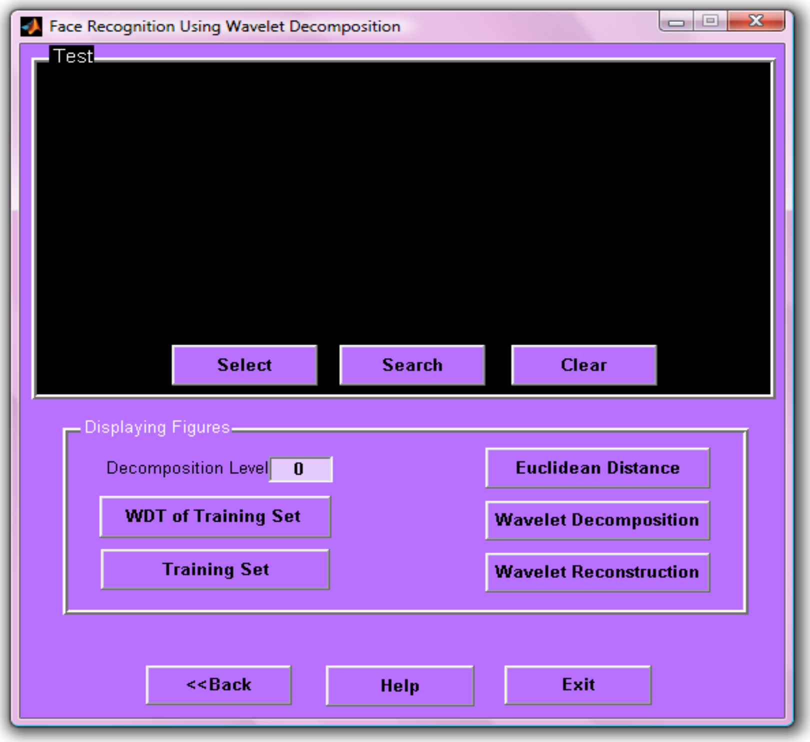

Figure IV.35: Face recognition using DWT interface.

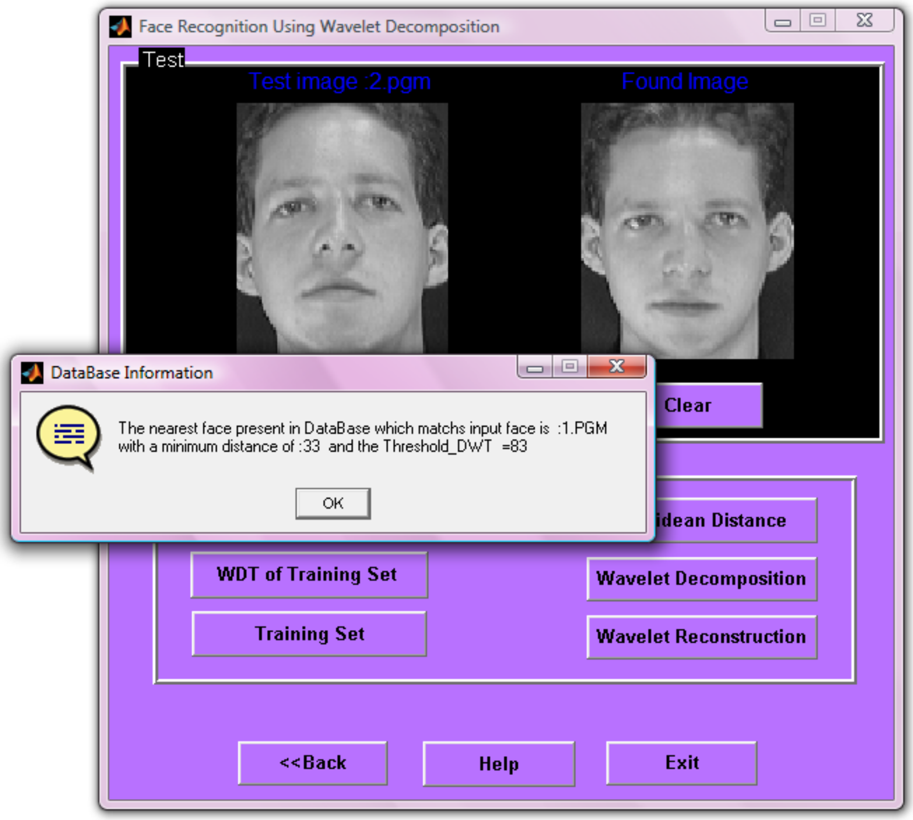

Figure IV.36: Result of the test in DWT method.

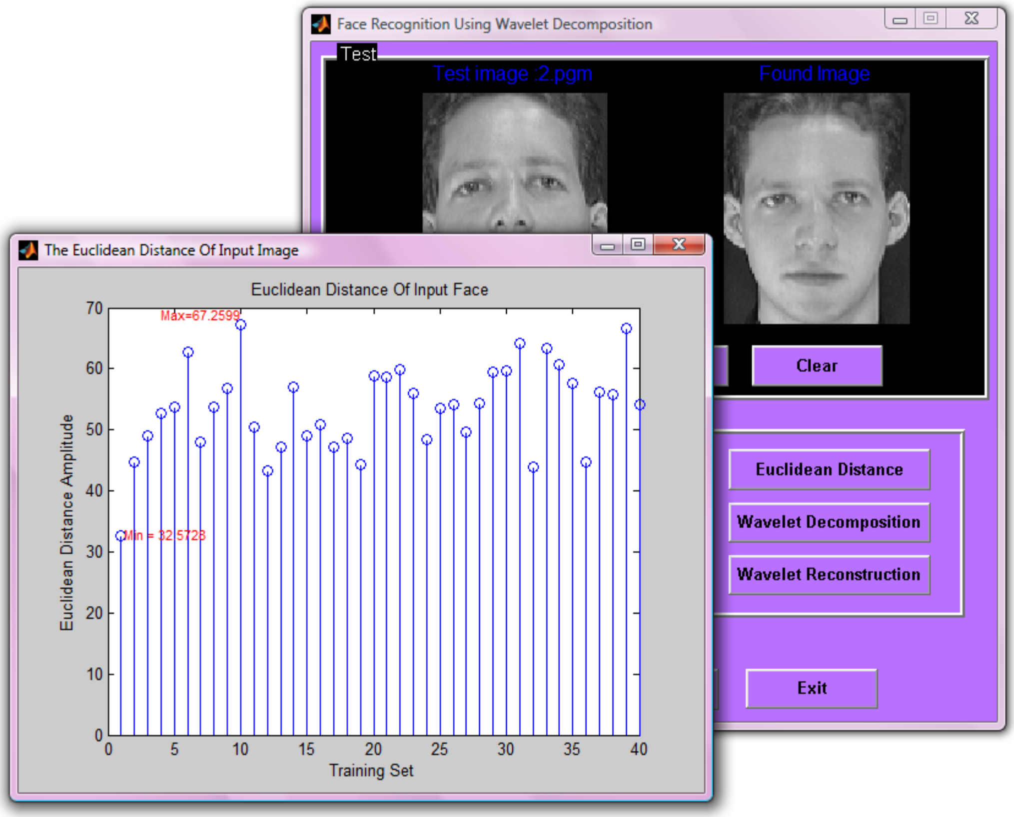

Figure IV.37: Euclidean distance of test image in DWT method.

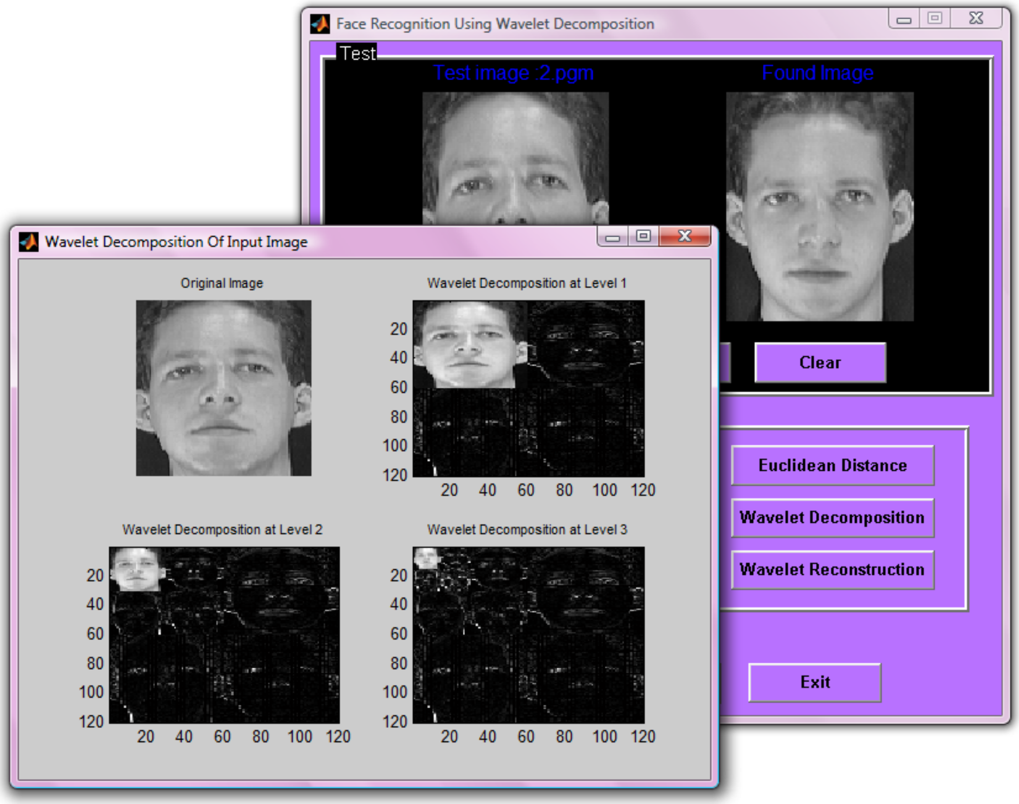

Figure IV.38: Wavelet decomposition of input image at level 1, 2 and 3 in DWT method.

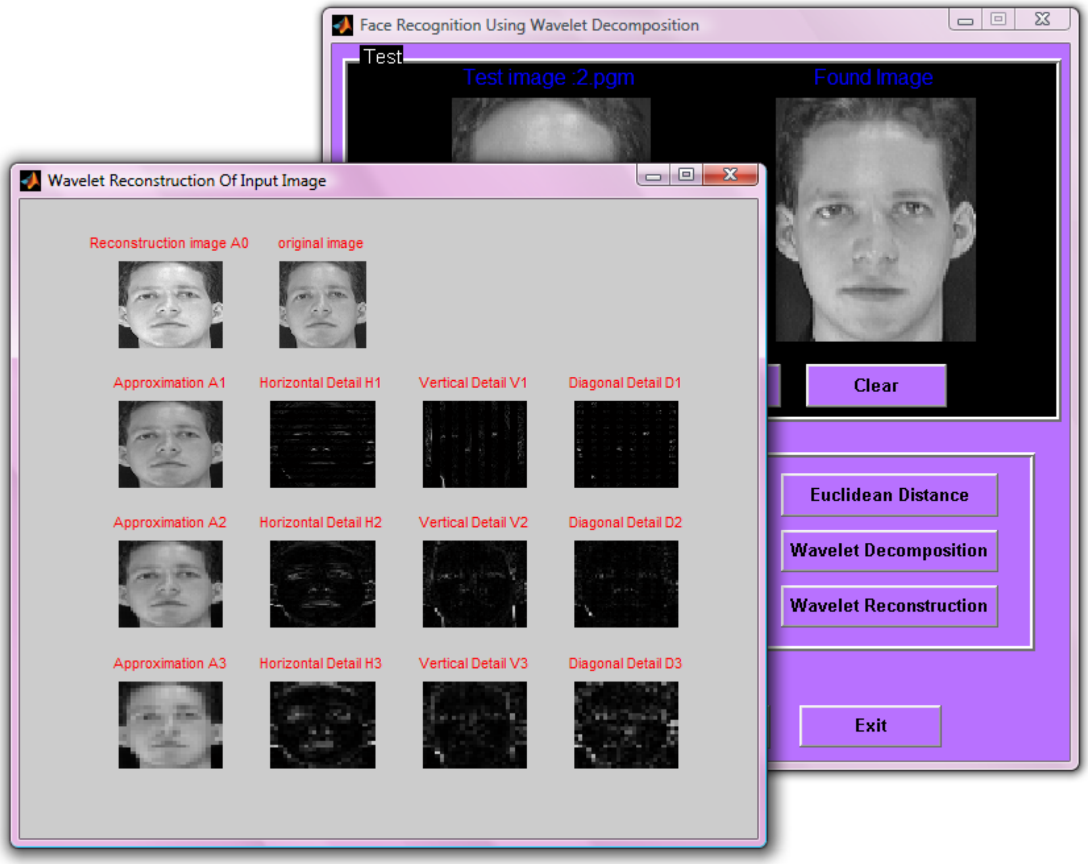

Figure IV.39: Wavelet reconstruction of input image in DWT method.

To show the wavelet decomposition of training set, select first the decomposition level and then press the push button "**WDT of training set**".

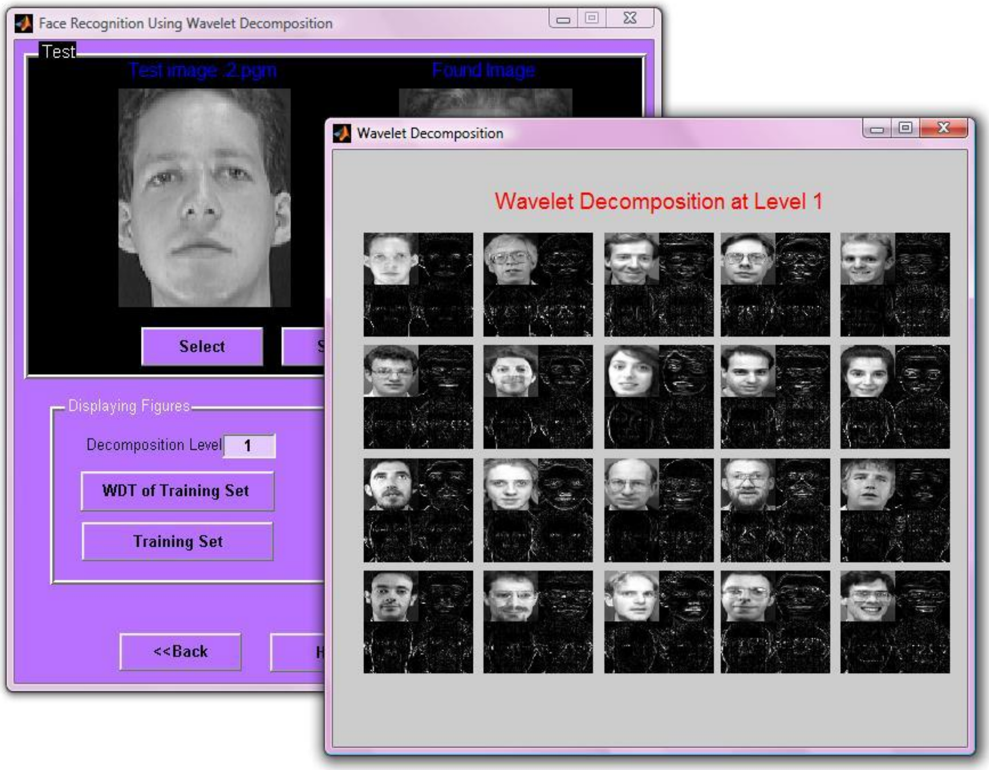

Figure IV.40: DWT at level 1.

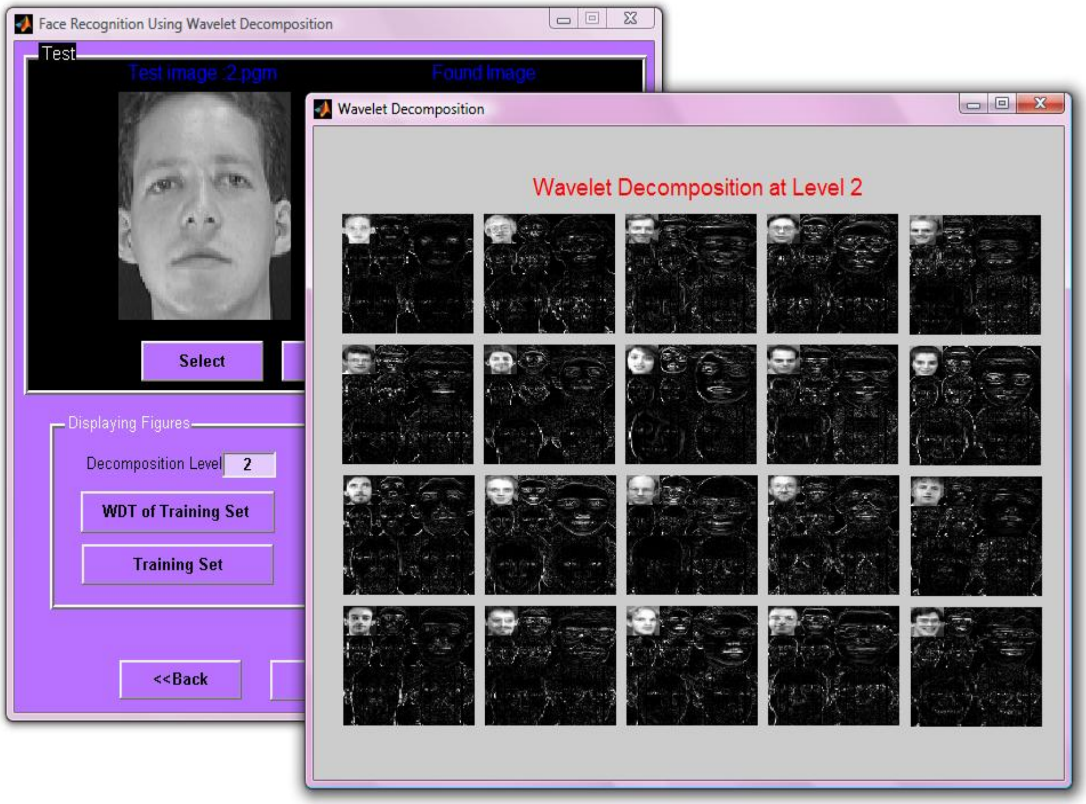

Figure IV.41: DWT at level 2.

IV.2.6.Face recognition using PWD and PCA interface:

After pressing the push button "PWD-PCA" the interface bellow will appear

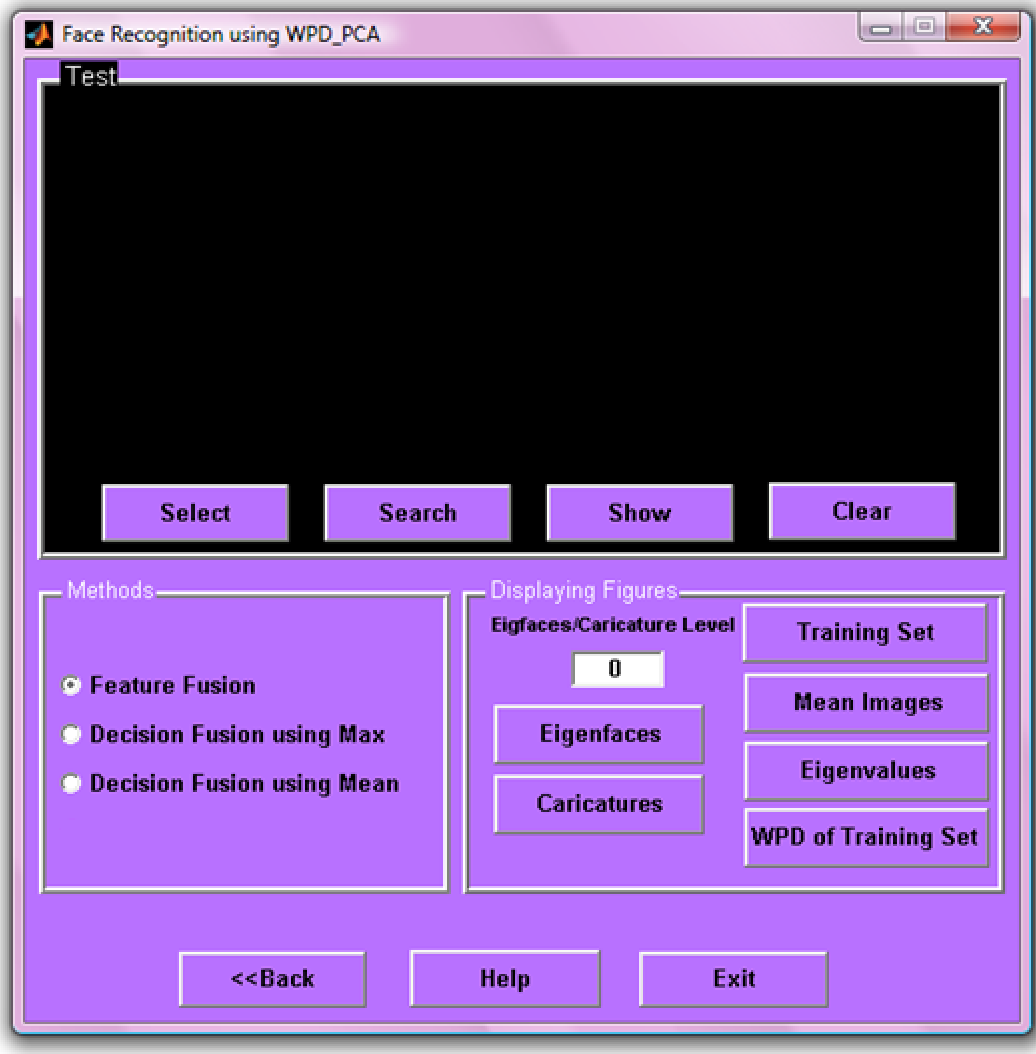

Figure IV.42: face recognition using PWD-PCA interface.

To test the system, select one of the methods proposed: "**Feature Fusion**", "**Decision Fusion using Max**", or "**Decision Fusion using Mean"**. By pressing the push button "**Select**", it will appear a prompt window. Then, you can select an image from the Test database. To see if the selected image belongs to the database or not press the push button "**Search**"; the selected image is compared against the images stored in the database and the system will return the image that minimize the euclidian distance. To show the euclidean distance and DWT at level 1and 2 press the push button "**Show**". The figures are given bellow.

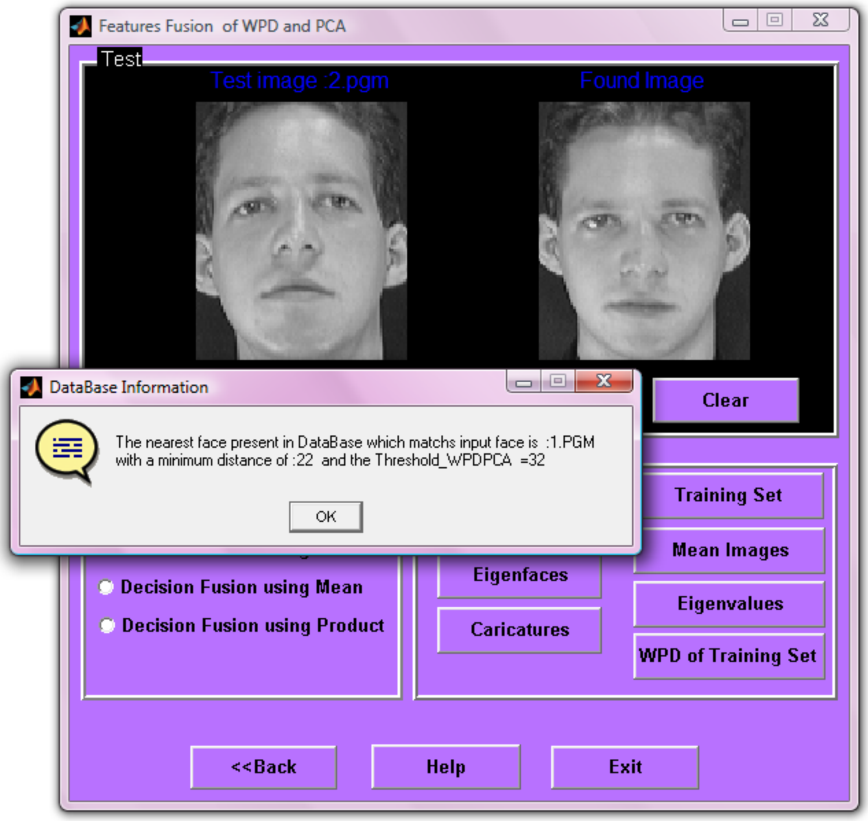

Figure IV.43: Result of the test of WPD-PCA method using features fusion.

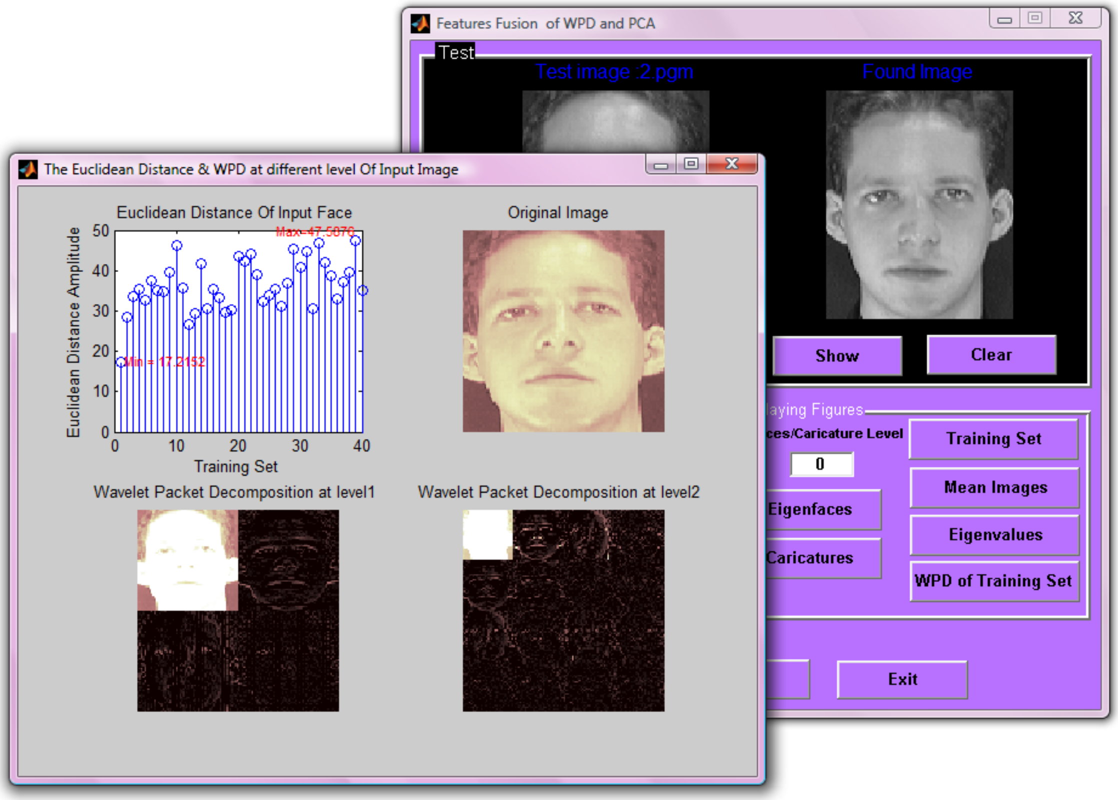

Figure IV.44: Euclidean distance and WPD of test image at level 1 and 2.

To show the mean images of the 16 subspaces press the push button "**Mean Images**".

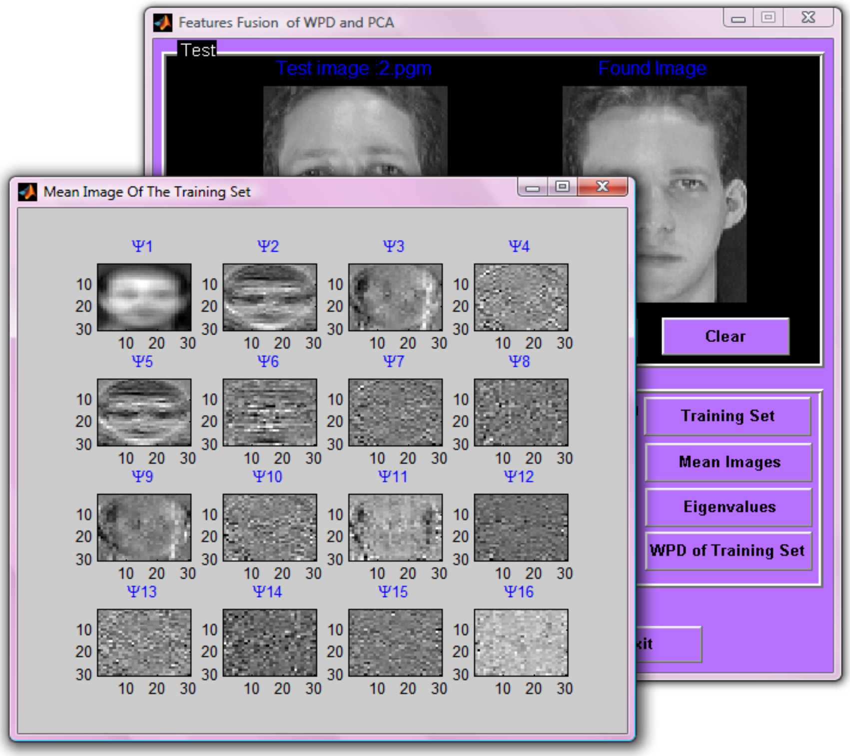

Figure IV.45: Mean images in PWD-PCA method.

To show the eigenvalues of the 16 subspaces press the push button "**Eigenvalues**".

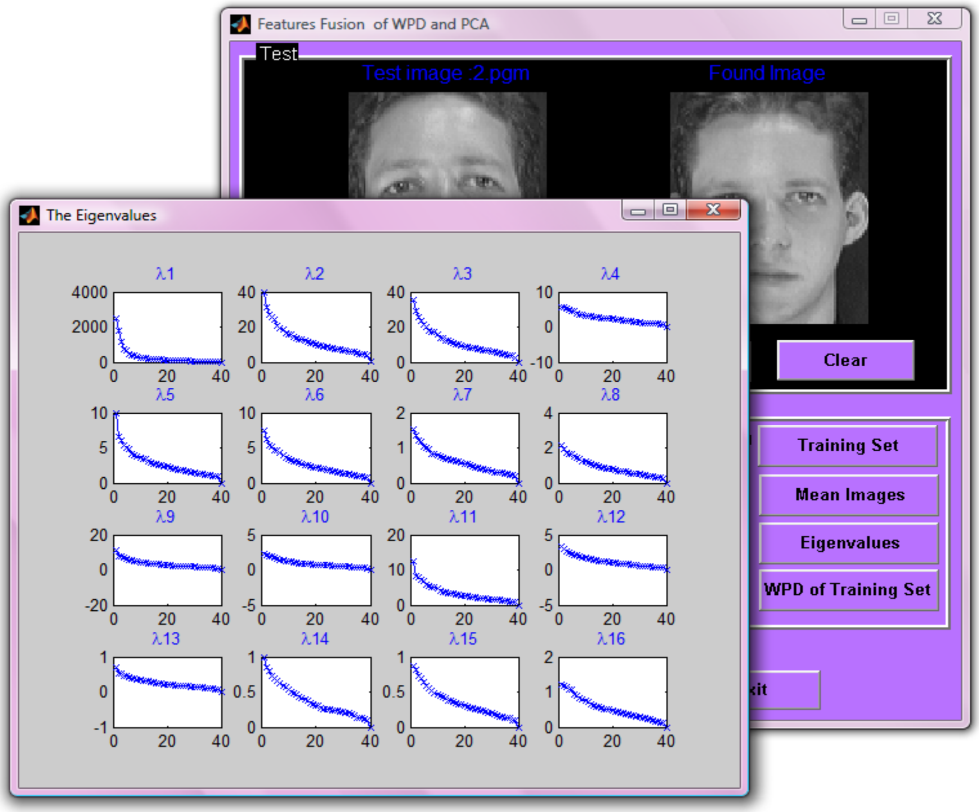

Figure IV.46: Eigenvalues in PWD-PCA method.

To show the wavelet packet decomposition of training set press the button "**WPD of training set**".

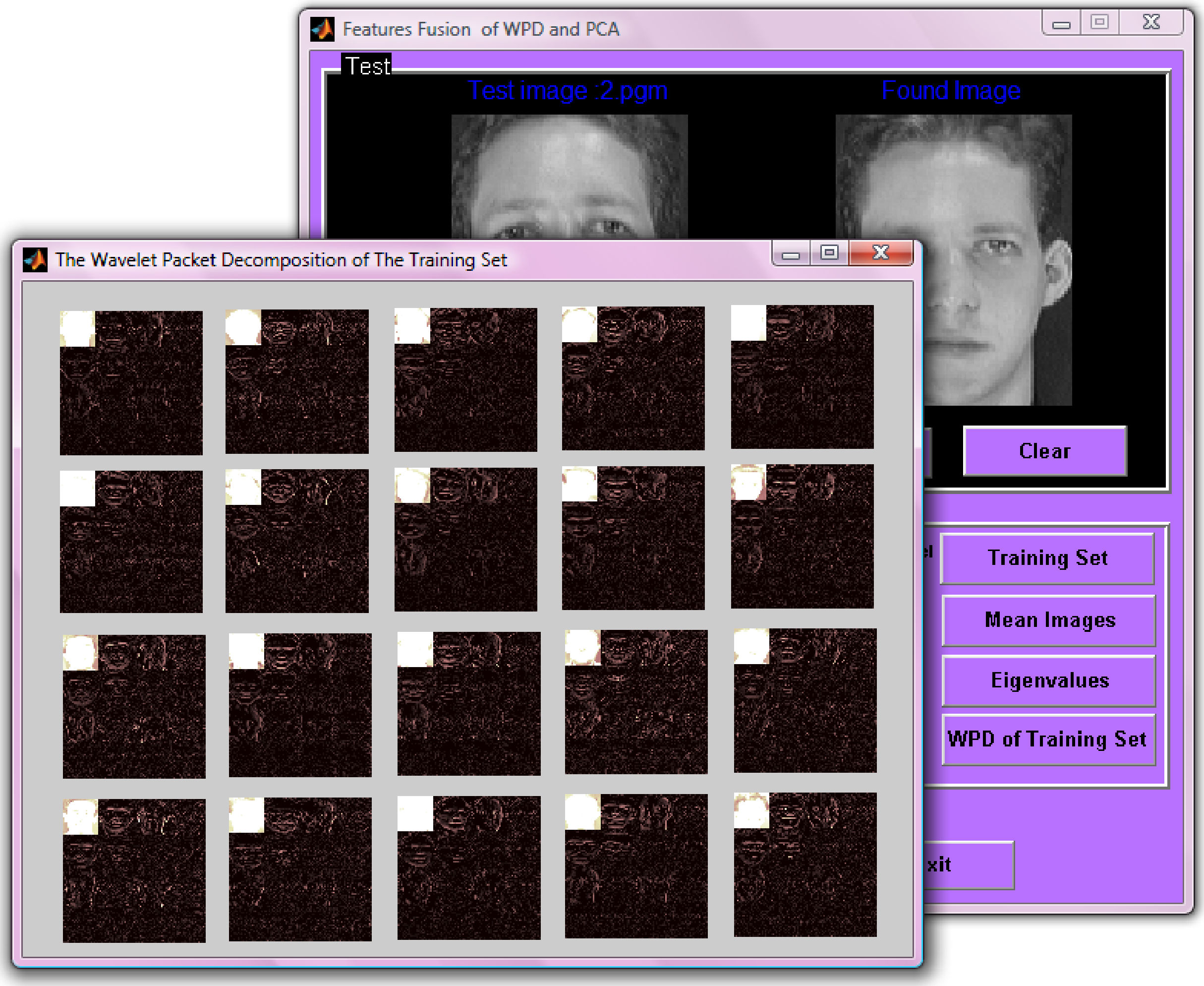

Figure IV.47: WPD at level 2 of training set.

IV.2.7.The proposed method (YCbCr-WPD-PCA) interface:

The interface of YCbCr-WPD-PCA method is given in figure IV.48. To test the system, press the push button "**Select**", it will appear a prompt window then select an image from the Testdatabase. To see if the selected image belongs to the database or not press the push button "**Search**". To show the euclidean distance of Y, Cb, and Cr subspaces press the push button "**Show**". To show the Y, Cb, and Cr, components of the training set press the push buttons, "**Y_component**", "**Cb_component**", and "**Cr_component**" respectively. To show the Mean images of Y, Cb, and Cr, subspaces press the push buttons "**Y_Mean images**", "**Cb_Mean images**", and "**Cr_Mean images**" respectively. To see the eigenvalues of Y, Cb, and Cr Cb subspaces press the push buttons "**Y_eigenvalues**", "**Cb_eigenvalues**", and "**Cb_eigenvalues**" respectively.

To show eigenfaces or caricatures of Y, Cr, and Cr subspaces select first the node which is a number between 1and 16 and then press the push button "Y or Cb or Cr _Eigenfaces" or "Y or Cb or Cr_Caricatures.

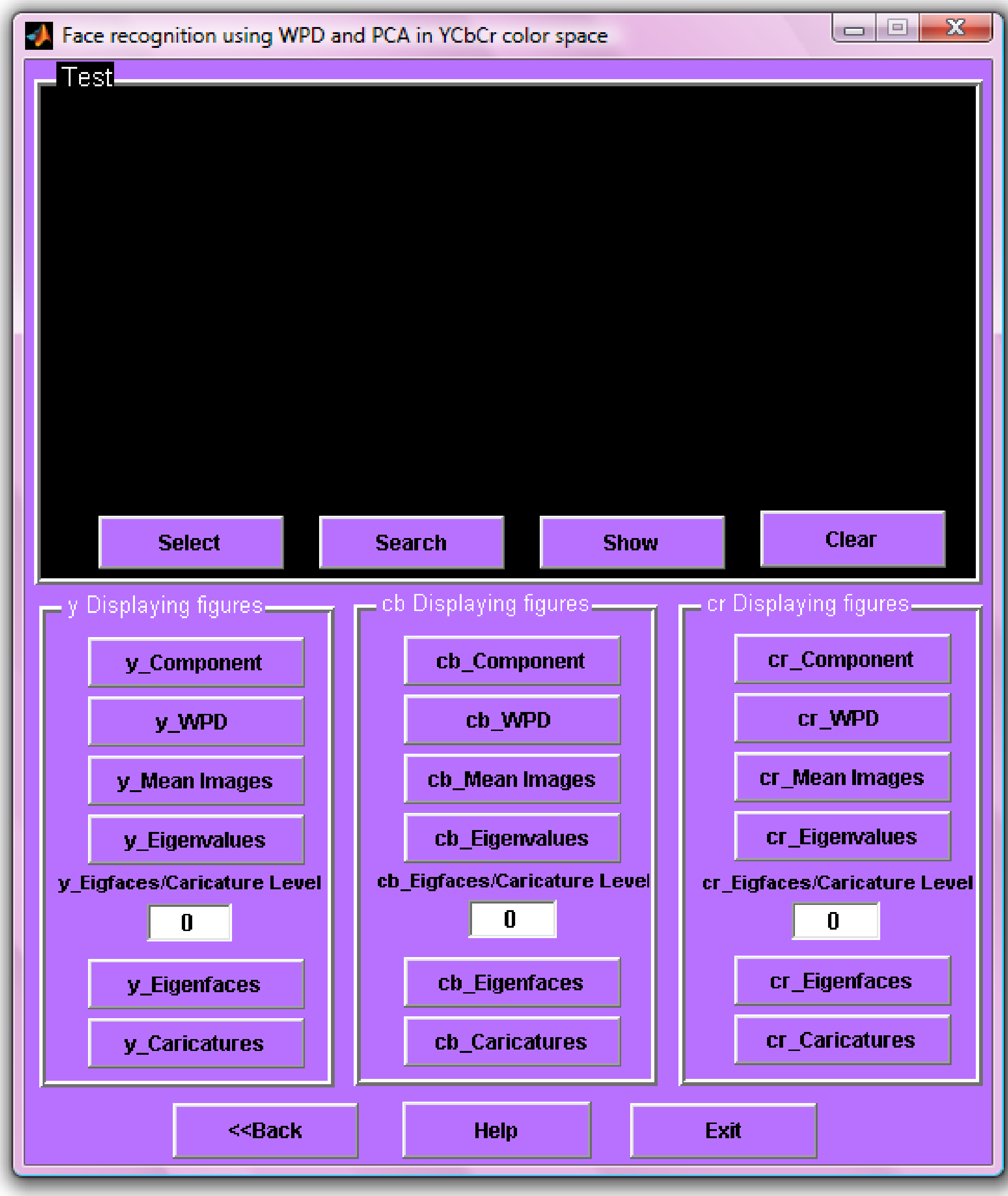

Figure IV.48: YCbCr-WPD-PCA method interface.

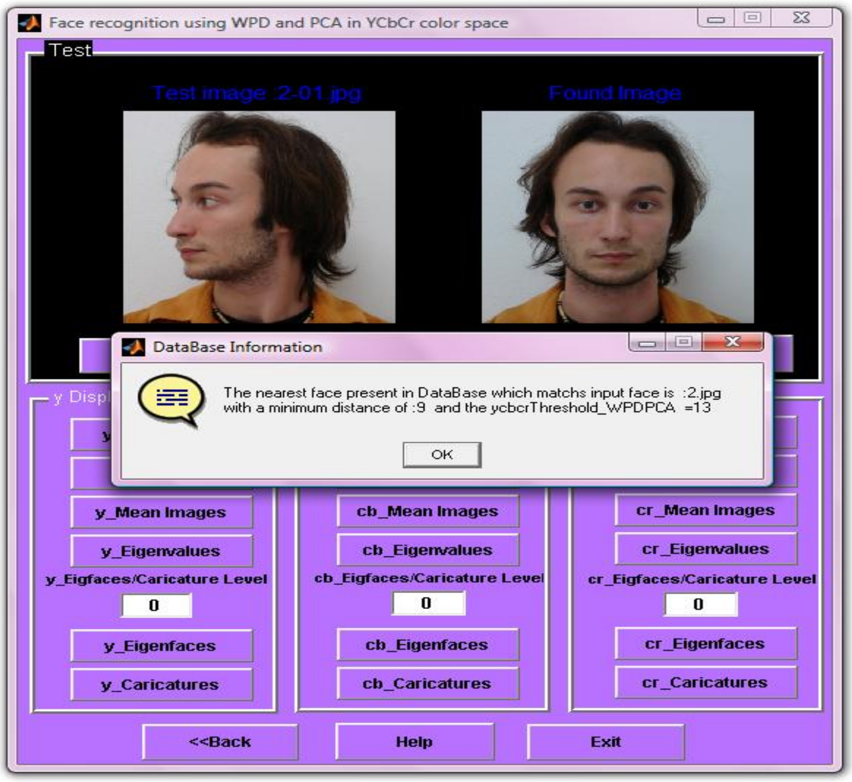

Figure IV.49: Result of the test of YCbCr-WPD-PCA method.

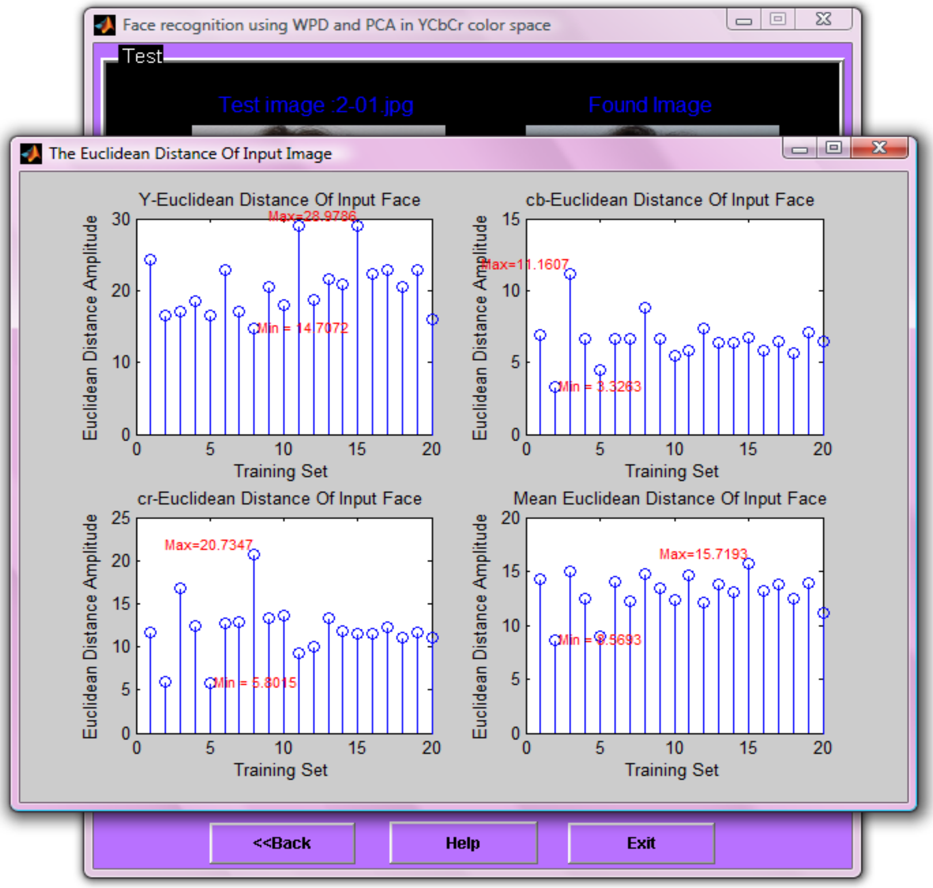

Figure IV.50: Euclidean distances of the input image in YCbCr-WPD-PCA method.

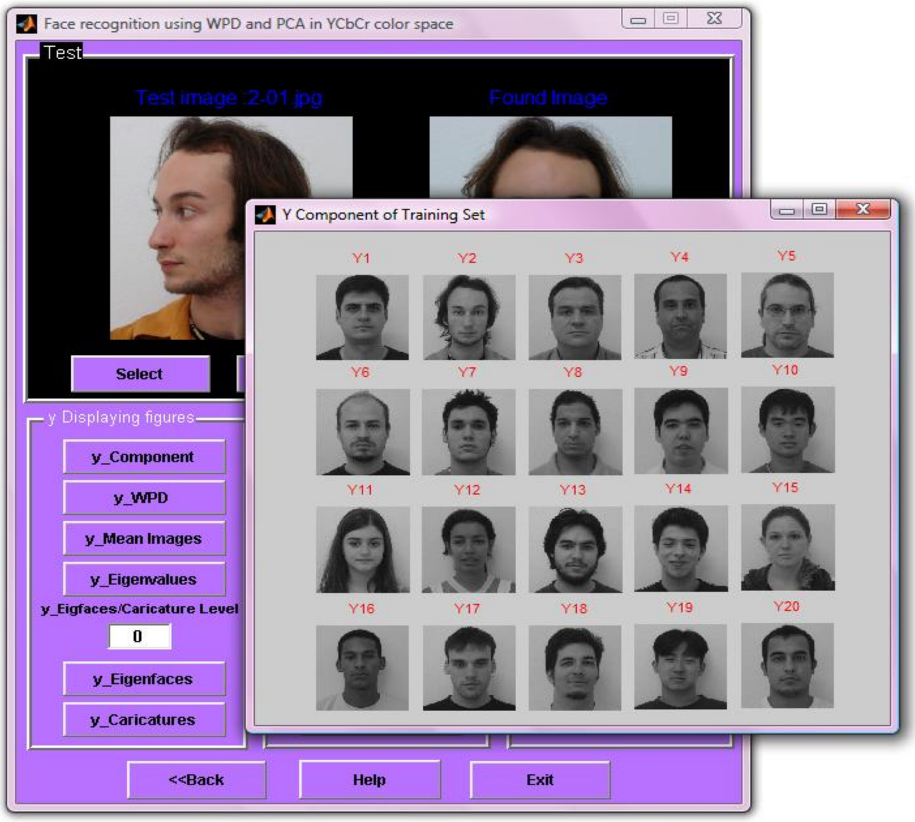

Figure IV.51: Y component of the training set.

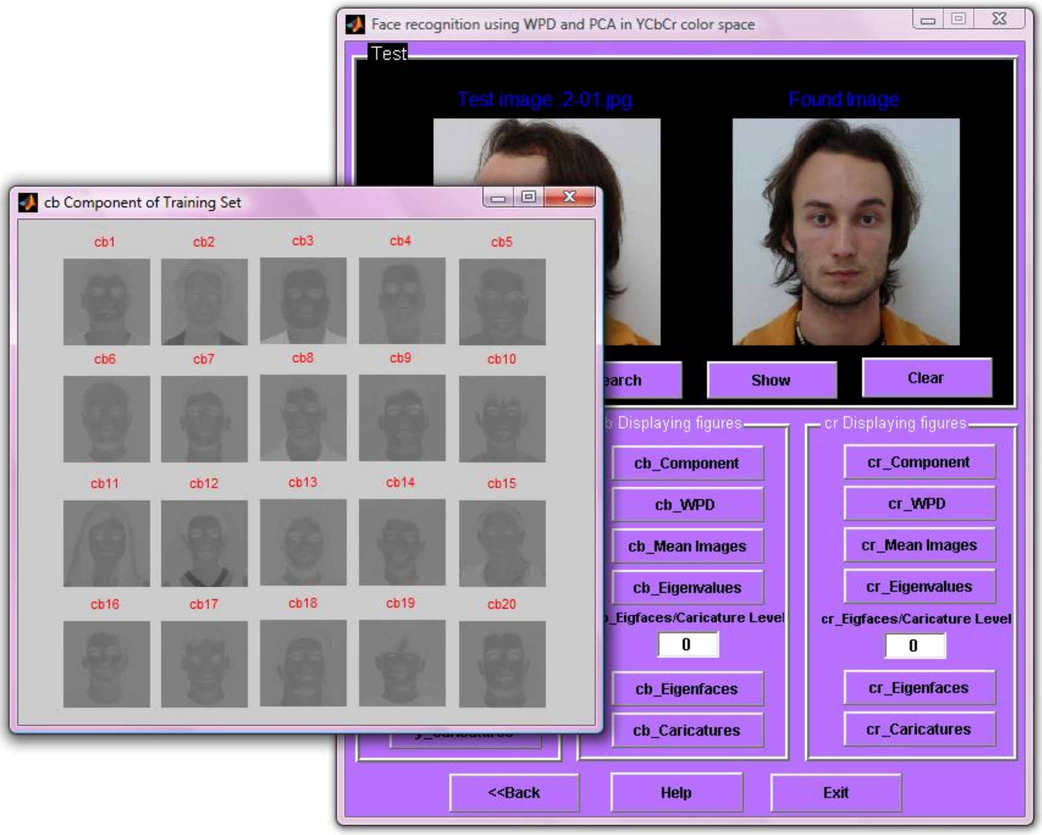

Figure IV.52: Cb component of the training set.

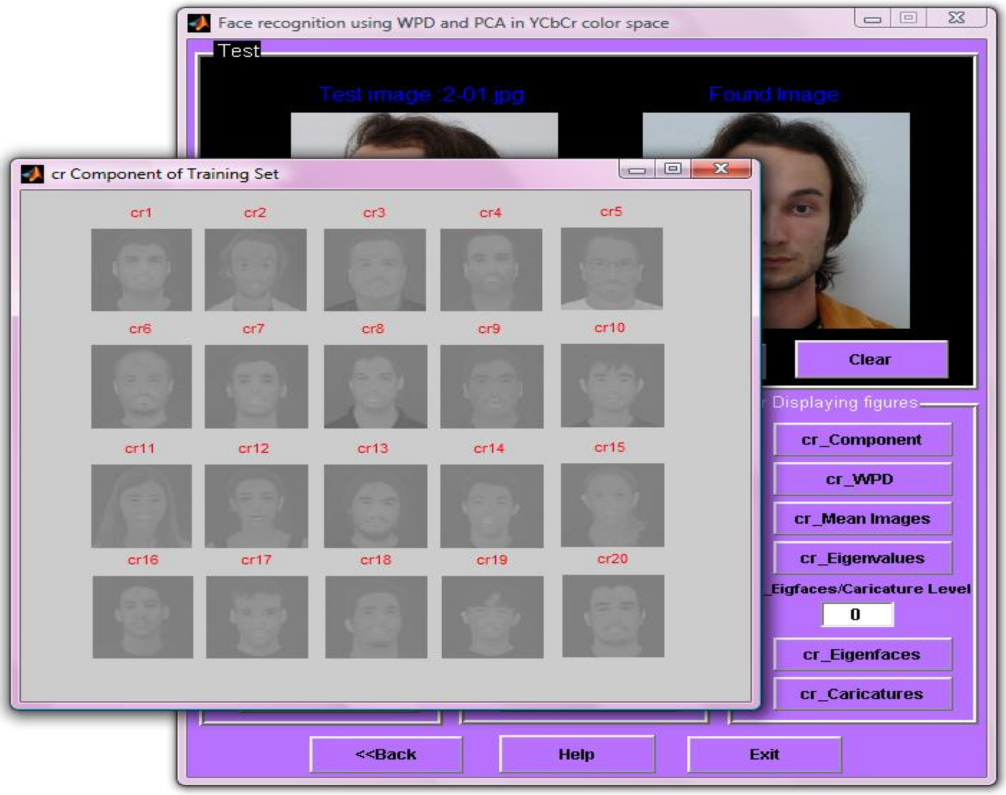

Figure IV.53: Cr component of the training set**.**

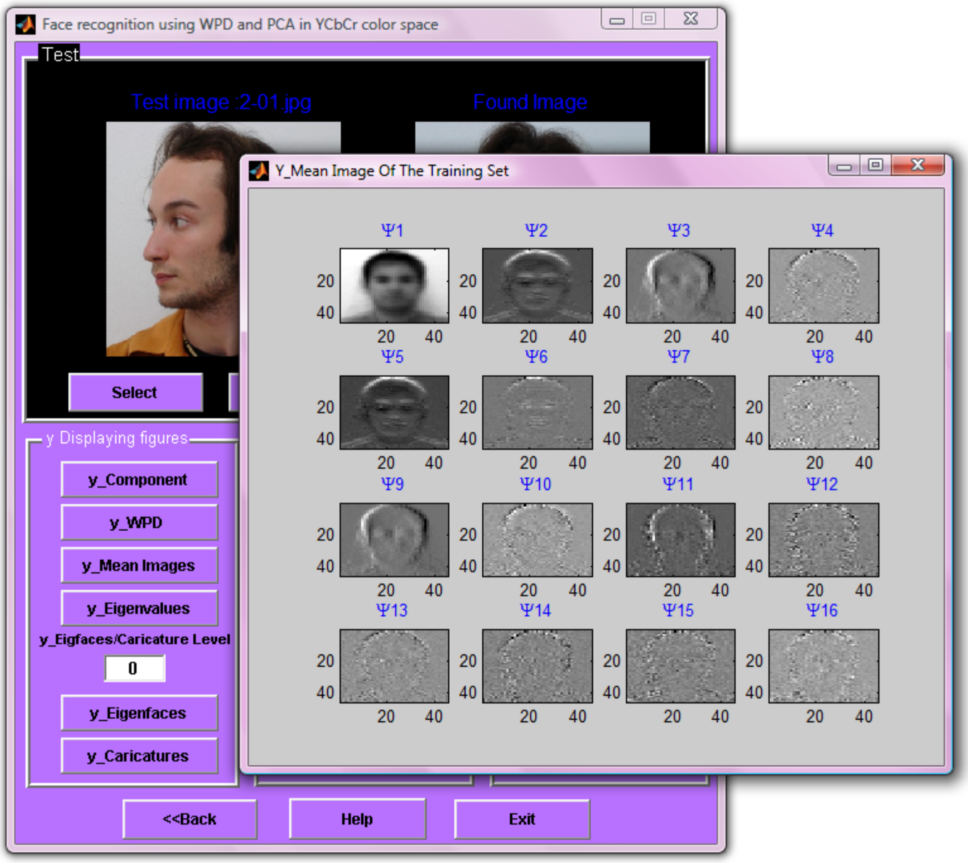

Figure IV.54: Mean images of Y subspace**.**

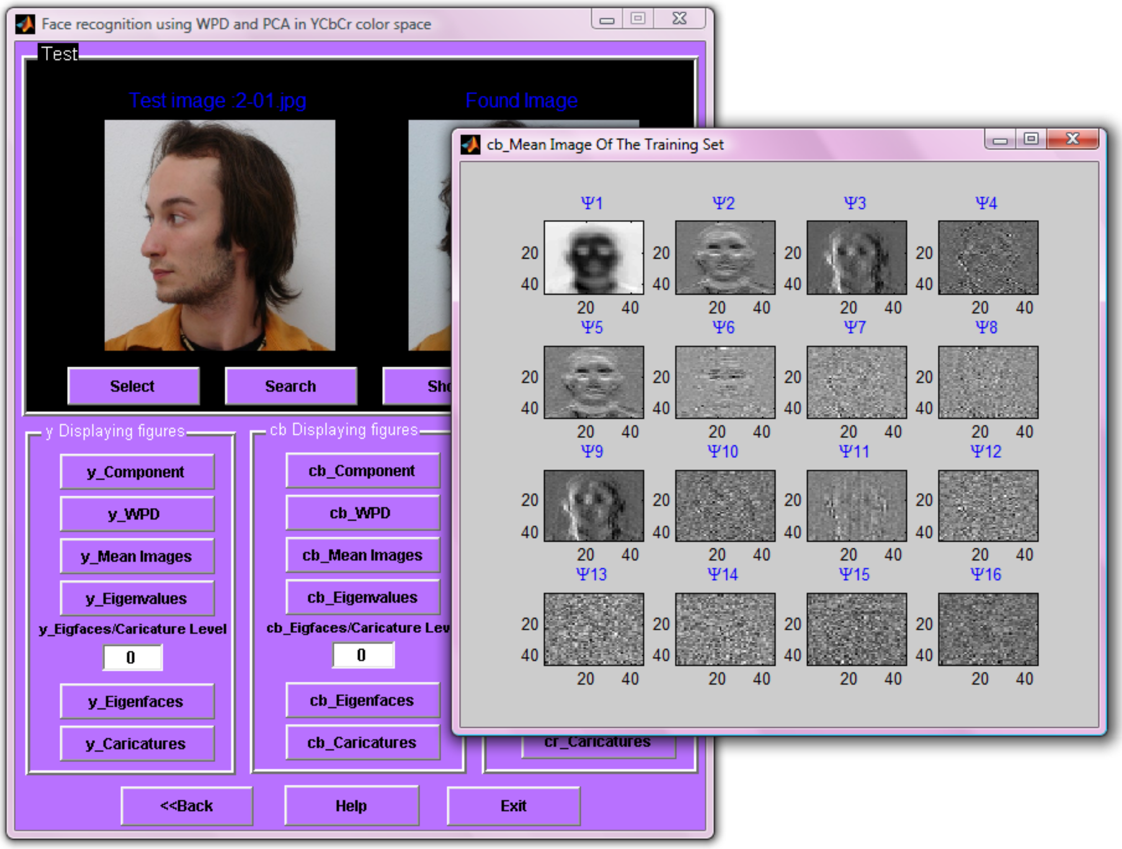

Figure IV.55: Mean images of Cb subspace.

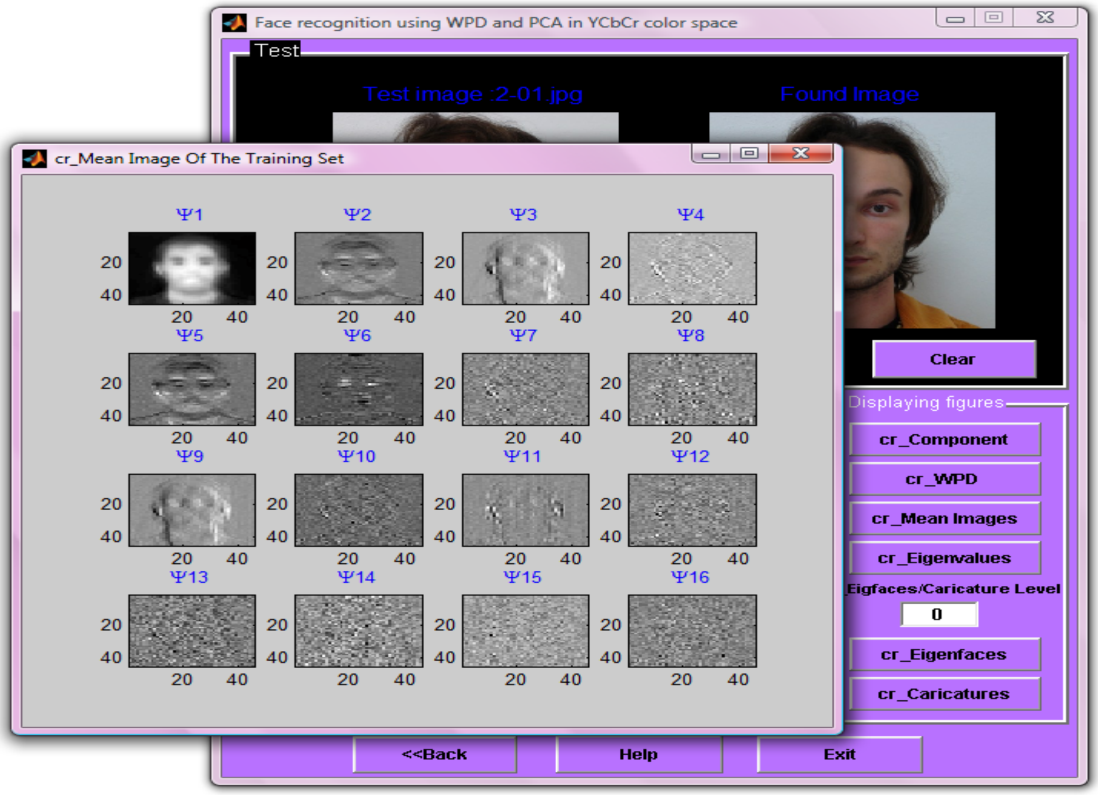

Figure IV.56: Mean images of Cr subspace.

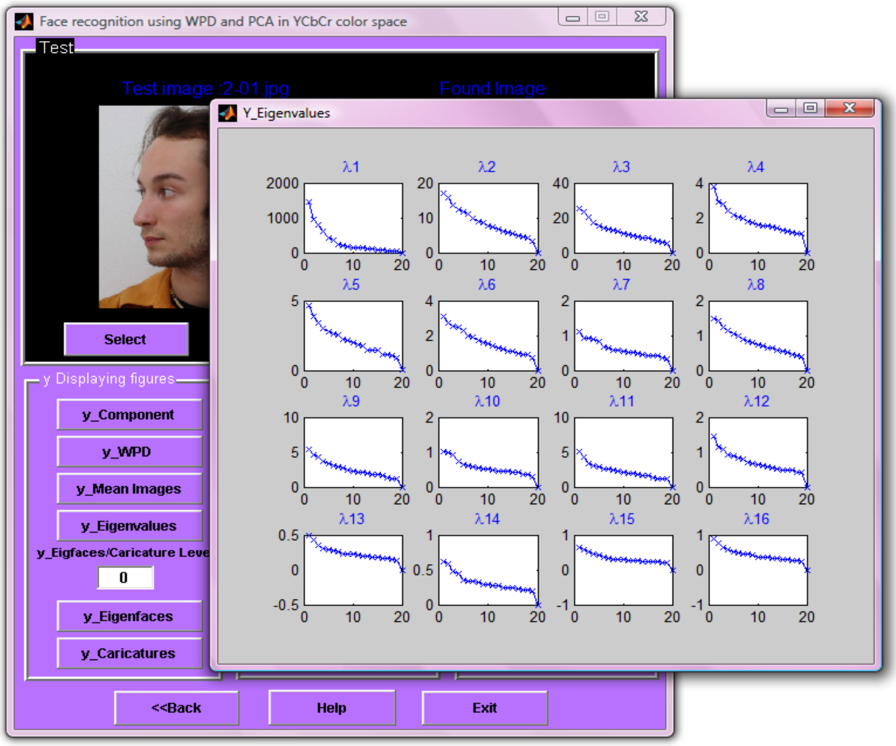

Figure IV.57: Eigenvalues of Y subspace.

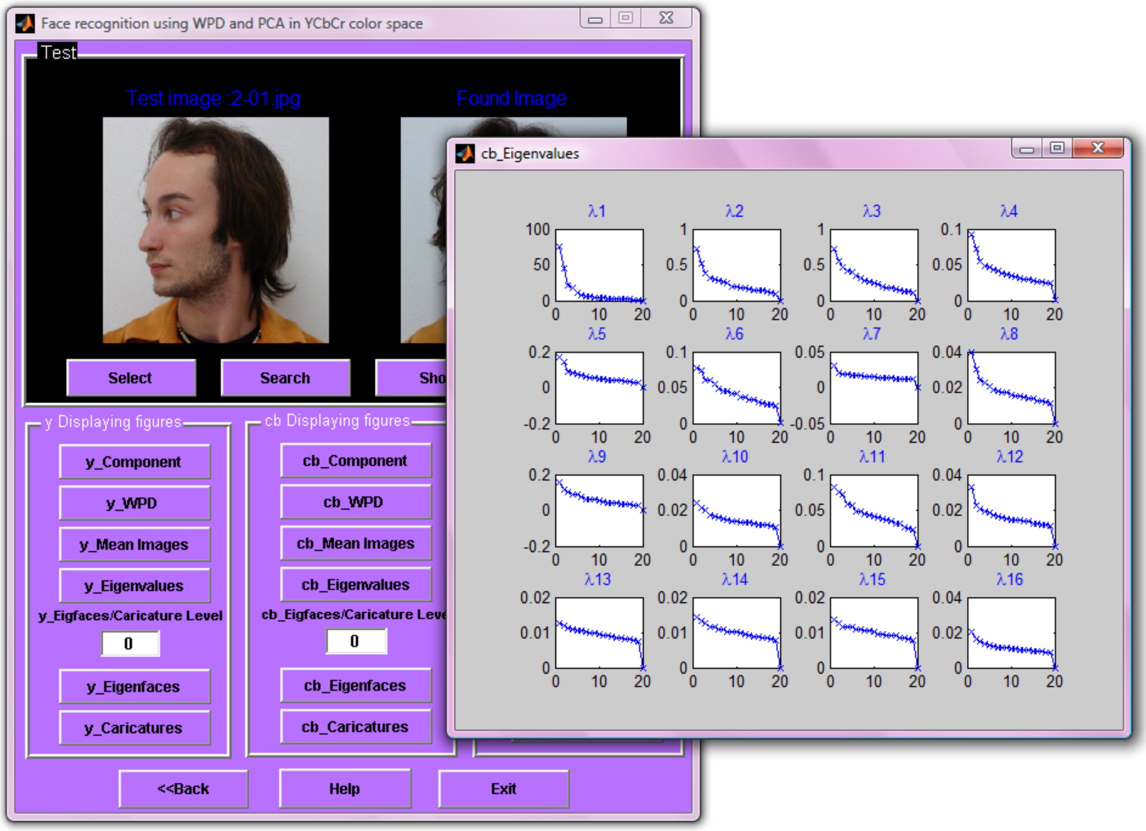

Figure IV.58: Eigenvalues of Cb subspace.

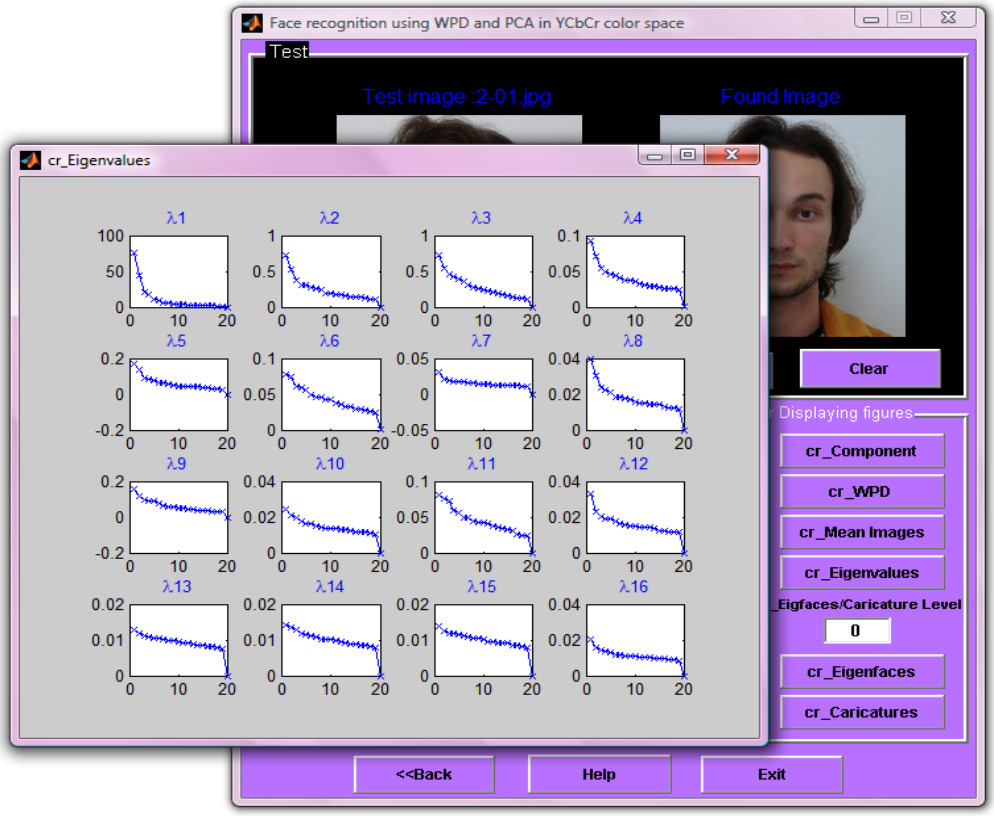

Figure IV.59: Eigenvalues of Cr subspace.

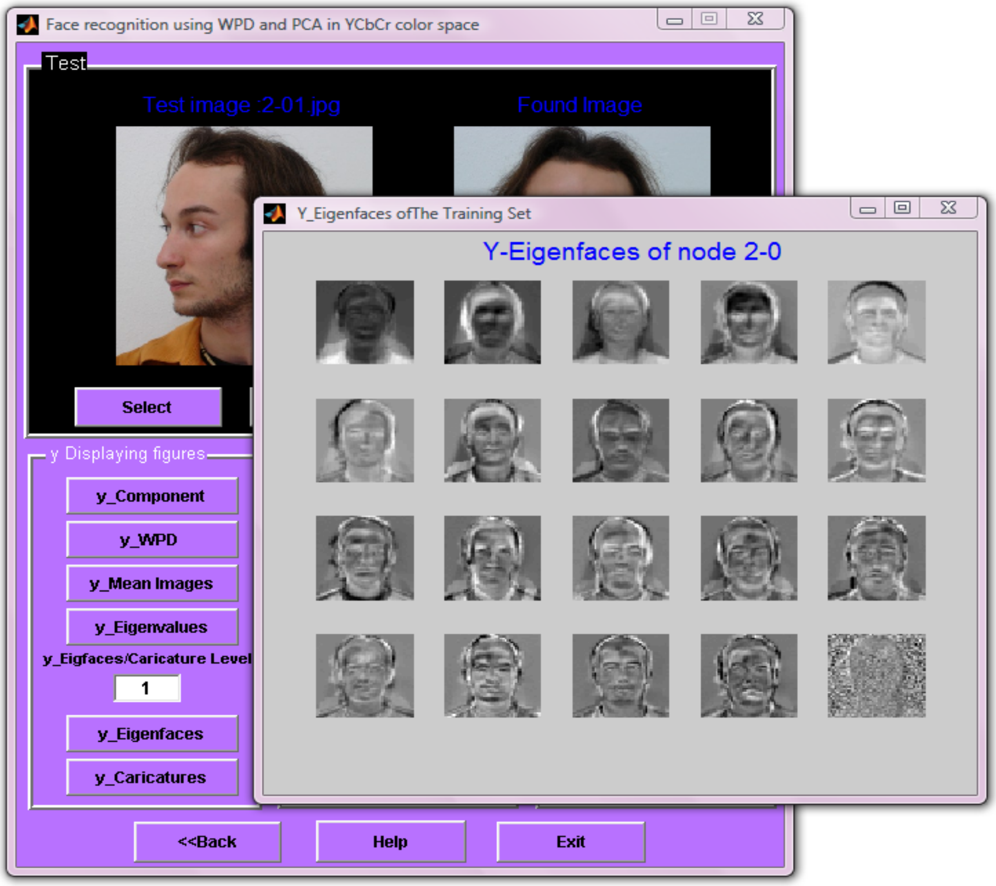

Figure IV.60: Eigenfaces of Y subspace of node 2_0.

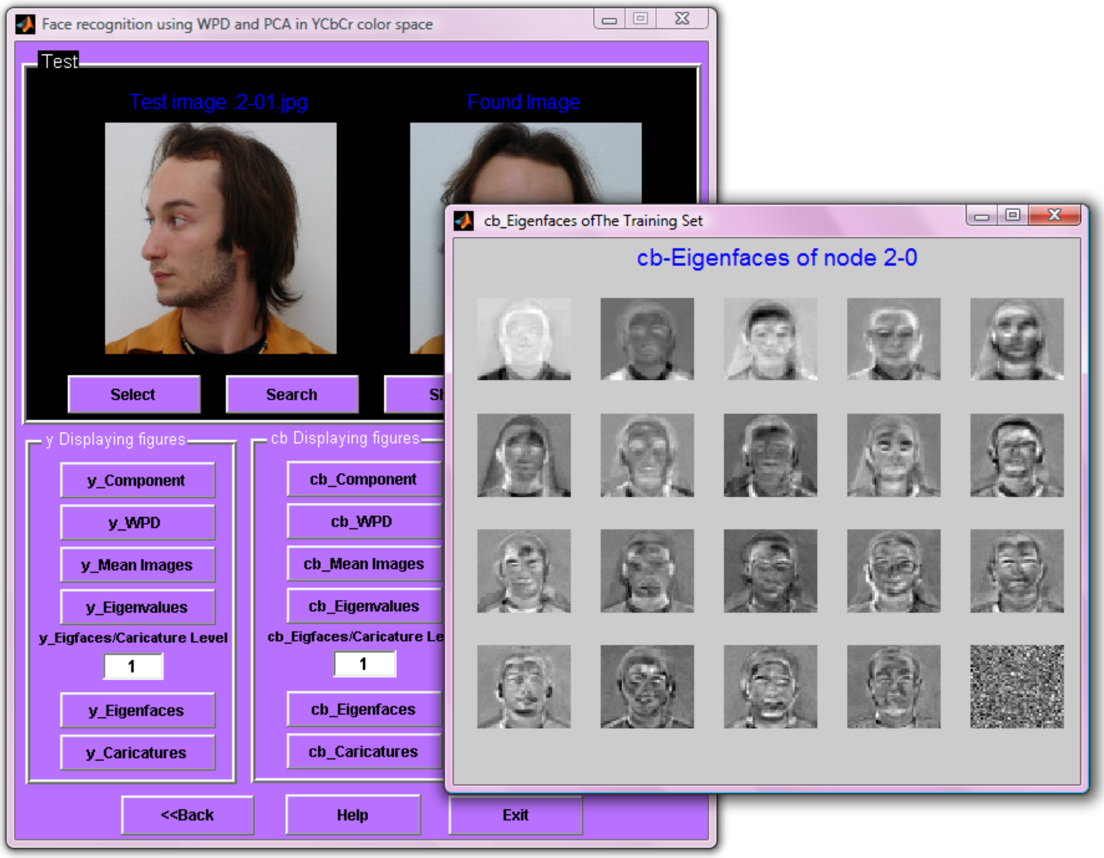

Figure IV.61: Eigenfaces of Cb subspace of node 2_0.

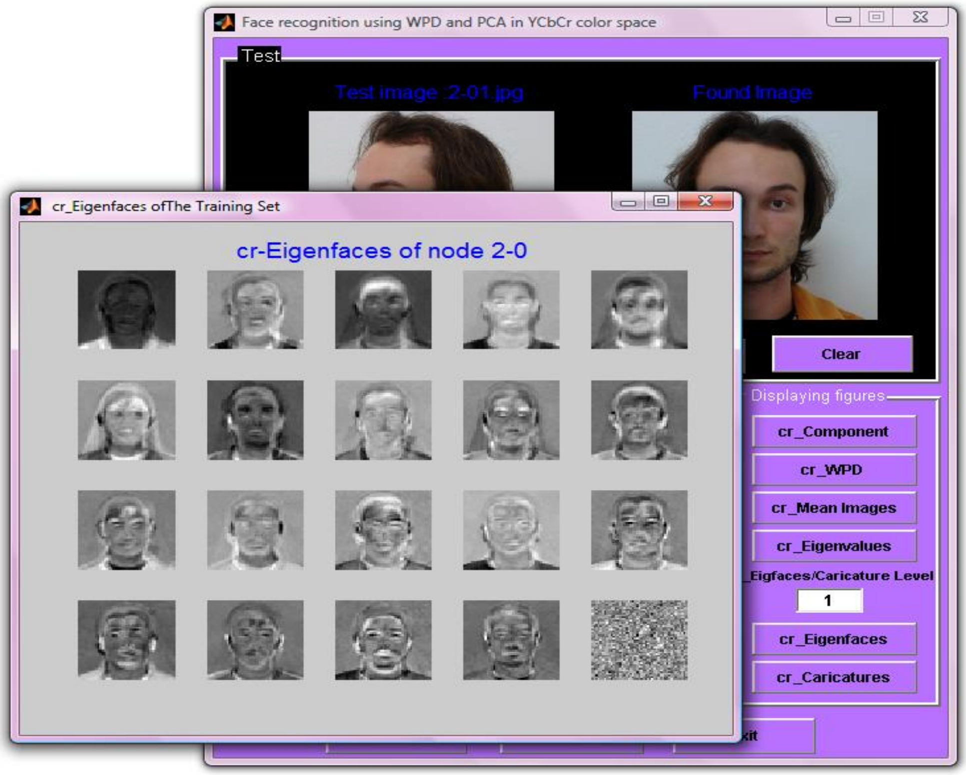

Figure IV.62: Eigenfaces of Cr subspace of node 2_0.

IV.2.8.Face recognition using fusion methods interface:

After pressing the push button "**DWT_SVD**" the interface in figure IV.63 will appear. To test the system; select one of the fusion methods: "PCA+FLD", "PCA+SVD", "PCA+DCT", "PCA+DWT", "FLD+SVD", "FLD+DCT", "FLD+DWT", "SVD+DCT", "SVD+DWT", "DCT+DWT", "PCA+FLD+SVD", "PCA+FLD+DCT", "PCA+FLD+DWT", "PCA+SVD+DCT", "PCA+SVD+DWT", "FLD+SVD+DCT", "FLD+SVD+DWT", "FLD+DCT+DWT", "SVD+DCT+DWT" and one of the fusion techniques : maximum, minimum, mean and product. Then, press the push button "**select**", it will appear a prompt window, select an image and then press the push button "**search**" to do the test. If you want to see the euclidean distance press the push button "**show**". The results are given in the figures bellow.

Figure IV.63: Face recognition using fusion interface.

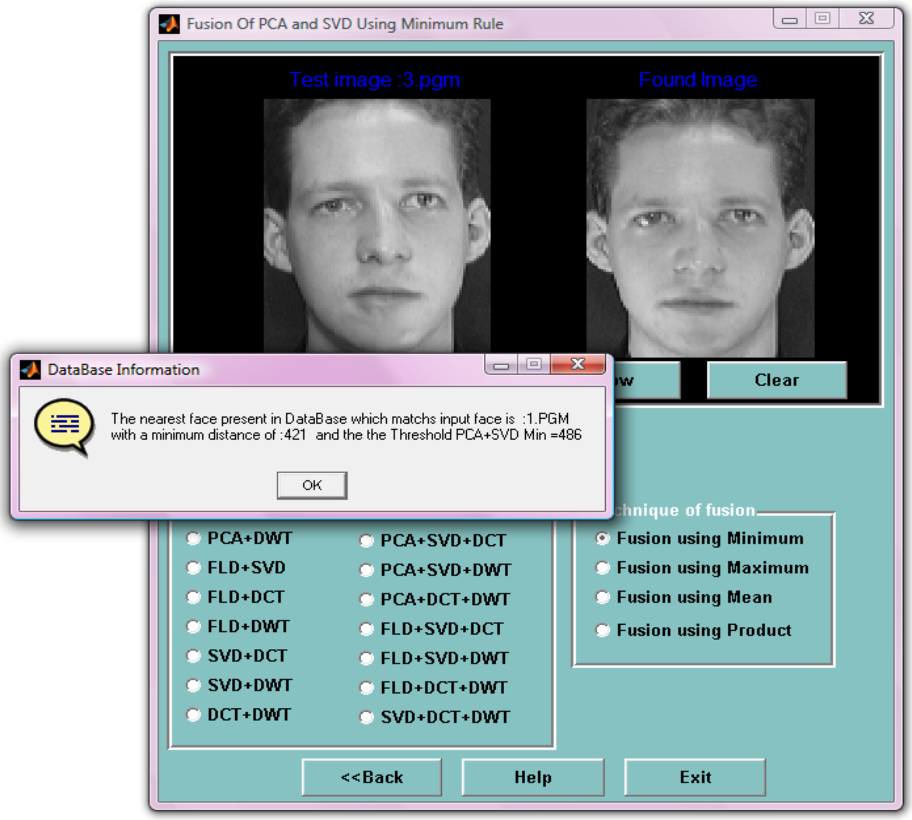

Figure IV.64: Result of the test of PCA+SVD using minimum.

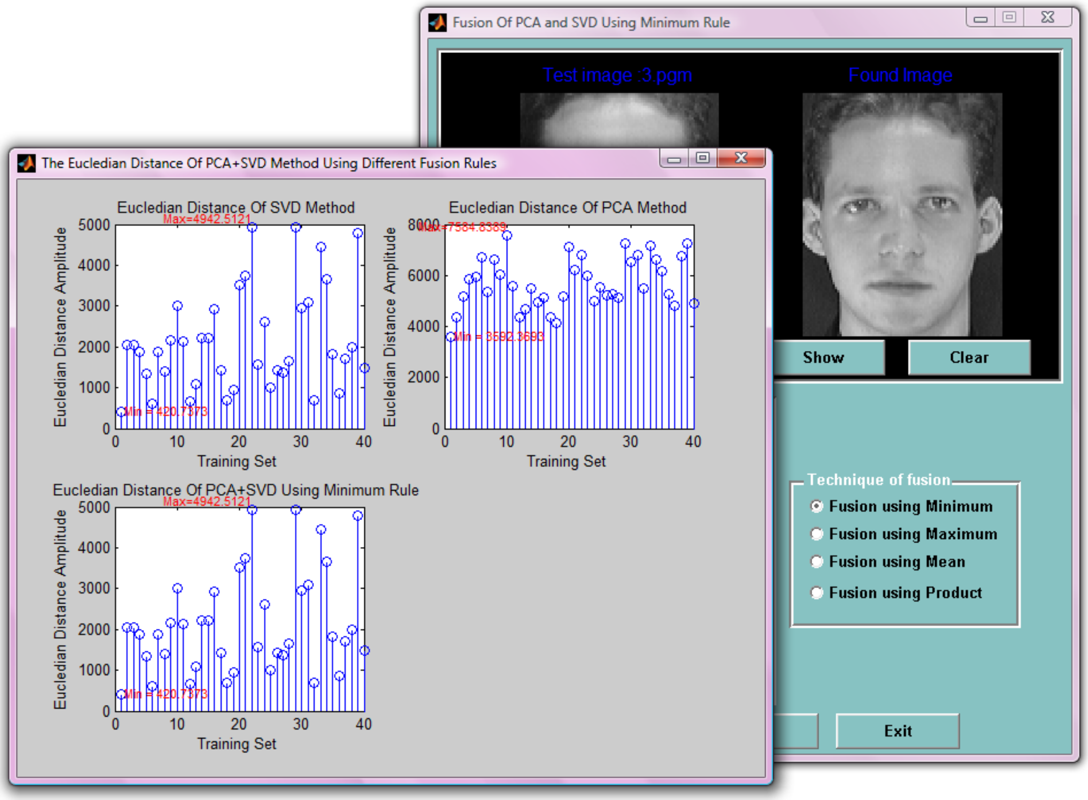

Figure IV.65: Euclidean distances of PCA+SVD using minimum.

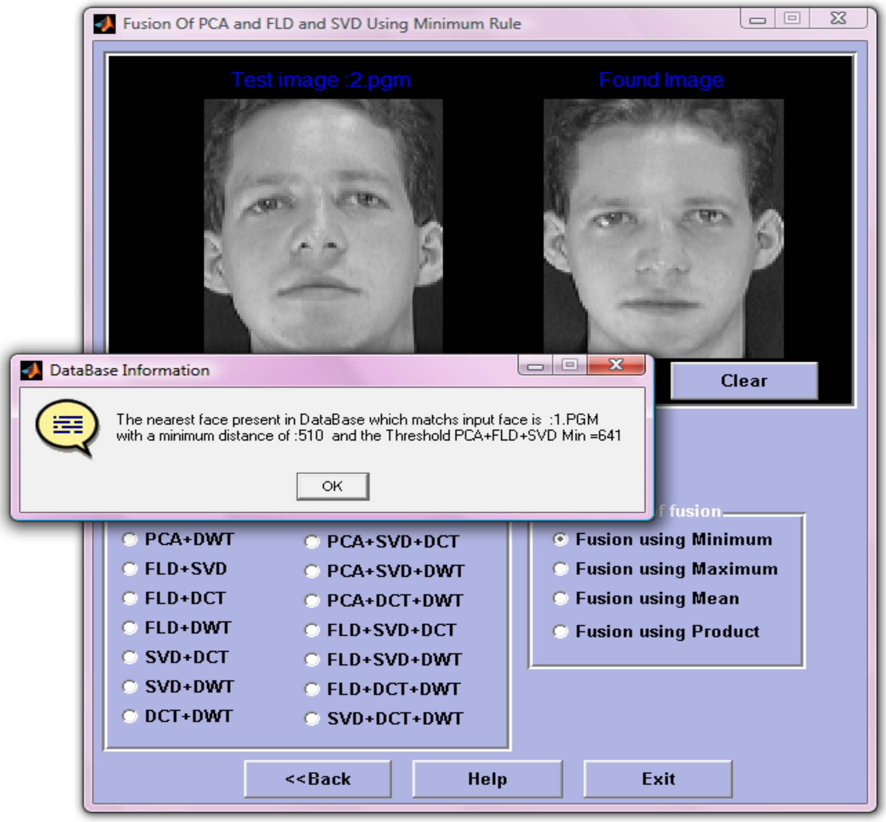

Figure IV.66: Result of the test of PCA+FLD+SVD using minimum.

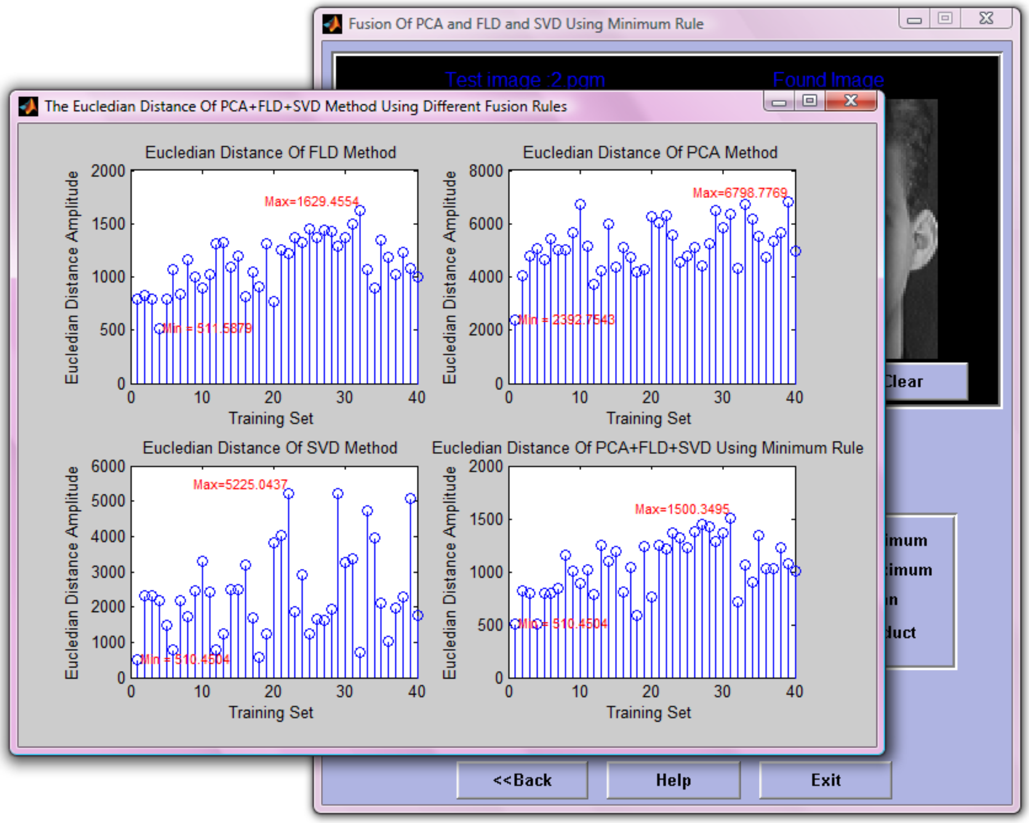

Figure IV.67: Euclidean distances of PCA+FLD+SVD using minimum.

To quit the system press the push button "**Exit**" it will appear a message boxe, for the confirmation to exit the application.

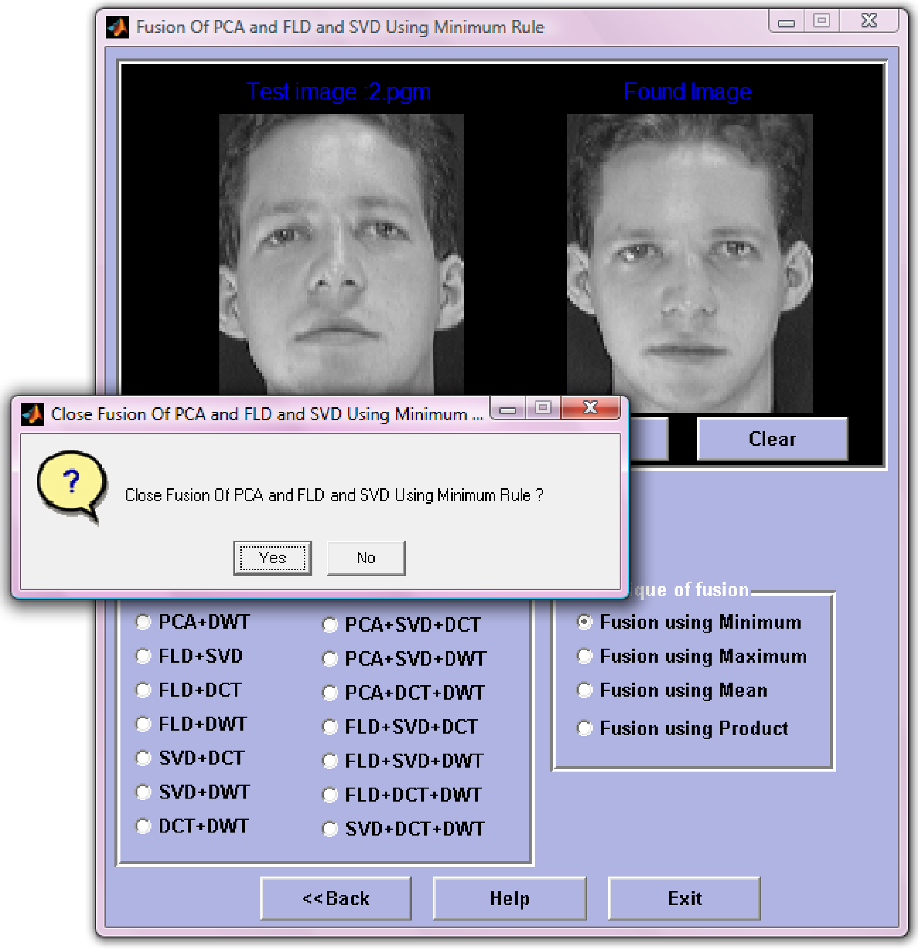

Figure IV.68: Exit window.

IV.3.Conclusion:

Details of the implemented face recognition methods were given in this chapter. The method are divided into three categories simple methods, cascade methods and fusion methods plus the proposed method which is face recognition using wavelet packet decomposition (WPD) and principle component analysis (PCA) in YCbCr color space YCbCr-WPD-PCA method.

Conclusion and perspectives

1. Conclusion:

Biometric systems are going to get more and more common in everyday applications due to the fact that new technologies are rapidly developing, they are widely used to overcome the traditional methods of authentication. Face recognition is a biometric method which has in recent years become more relevant and needed. Face recognition is difficult because there are lots of factors that distort the face images of a person such as illumination, pose, facial expression, camera distortion, and so on. Several face recognition algorithms were introduced. The new algorithms promised to have better recognition rate. The goal for researchers was to try to implement recognition algorithms that are more accurate in terms of face identification. In this thesis, we have implemented some of the popular face recognition methods which are PCA, FLD, SVD, DCT, and DWT. We have applied DWT and WPD as preprocessing step for PCA, also DWT for FLD and SVD to improve their performances. We have proposed a method that uses color information; we have chosen an approach takes into consideration the intensity information as well as the chromatic information. The proposed method combined between principal component analyses (PCA), wavelet packet decomposition (WPD), and YCbCr color space.

We have introduced as well as the multibiometric system since unibiometric systems fail in some cases. We have utilized multi-algorithm systems that consolidate the output of multiple feature extraction algorithms at score levels. We have used the fusion of two types and three types of feature vectors using four fusion rules minimum, maximum, mean, and product. All of our experiments are programmed in the MATLAB language. We have developed a graphical user interface (GUI) for testing the algorithms implemented. Experiments were carried out using three databases: ORL, Yale, and FEI face databases.

To evaluate the effect of different facial details (glasses, and no glasses), different facial expressions (happy, sleepy, sad, surprised, and winking), different illumination (left light, center light, and right light) on the system performance of PCA, seven similarity measures are used (L1, L2, COS, Mah, L1+Mah, L2+Mah, COS+Mah) and the experiments are carried out on the Yale face database.

We have compared nine methods using the ORL face database. The methods are PCA using (L1, L2, COS, Mah, L2+Mah, and COS+Mah distances), DWT, SVD, and DCT. We have found that the DWT method gives the best recognition rate of 93% compared with other methods. and PCA using COS gives the best rate of 92% compared with PCA using L1, L2, Mah, L2+Mah, and COS+Mah methods.

Conclusion and perspectives

Many experiments were carried out on the FEI face database:

- ✓ We have compared PCA and FLD methods for different sample per class (three, five, and six samples per class). We have found that the system performance increases as the number of samples per class increases. We have found also that PCA outperforms FLD in the three cases tested.
- ✓ To solve the small sample size (SSS) problem of LDA, we have applied PCA as a pre-processing step prior performing LDA. We have also used another approach that uses the discrete wavelet decomposition (DWT) before performing LDA (DWT-LDA). We have compared the two methods FLD (PCA-LDA) and DWT-LDA. We have found that DWT-LDA performs better than FLD (PCA-LDA) since it has the lowest EER of 19%.
- ✓ To see the effect of performing DWT before SVD we have compared between SVD and DWT-SVD methods. The EER rate is reduced by 2%; we have concluded that the wavelet decomposition has improved the system performance.
- ✓ We have compared between WPD-PCA using different fusion and PCA methods. In WPD-PCA, the fusion was done at feature level and at decision level. In the decision level two rules have been used maximum and mean rules. We have found that WPD-PCA method using maximum decision fusion gives the best result since it has the lowest EER of 14%.
- ✓ To identify the accuracy of our proposed algorithm (YCbCr-WPD-PCA). A comparison was performed with other methods (PCA, DWT, and DWT-PCA) using one sample, three and six samples per class in the training set in terms of recognition rates. We have found that the recognition rates increase as we increase the numbers of samples per class, and our method outperforms other methods; it reaches recognition rates of 82.50%, 86.87%, and 93.12% with one sample, three and six samples per class respectively. Another comparison was performed in terms of Equal Error Rate (EER) between our method and (PCA, DWT, DWT-PCA, WPD-PCA using feature fusion, and WPD-PCA using decision fusion). Our method achieved the lowest EER of 10%. So, our method gives significant performance compared to other methods.
- ✓ Each fusion method is compared separately using minimum, maximum, mean, and product rules. we found that PCA+FLD using mean rule, PCA+SVD using product rule, PCA+DWT using product rule PCA+DCT using mean and product rules, FLD+SVD using product rule, FLD+DCT using minimum, product and mean rules, FLD+DWT using product rule, SVD+DCT using mean rule, SVD+DWT using mean rule, and DCT+DWT using product rule give the best result since they have the lowest EER of 18% , 16%, 13%; 16%, 29% 26% 18%

21% , 15%, and 16% respectively, so, PCA+DWT using product rule outperforms the other methods.

2.Perspectives:

Some perspectives that may help extend the work in this thesis are:

- ✓ In this thesis we have chosen the face as biometrics, we propose to see other biometrics such as iris, retina, fingerprint etc.
- ✓ The current face recognition systems take the face images for testing from files of an existing photograph. We suggest implementing a system that identifies the persons automatically after capturing its image with the camera.
- ✓ In the systems implemented the recognition was done without detection of the face. We suggest adding the detection part to obtain a more robust system.
- ✓ The methods implemented in this study are for still images we can use video instead.
- ✓ In the proposed method, we have used the YCbCr color space. We suggest using other color spaces and doing a comparison between them in order to choose the best one. We have also used PCA as dimensionality reduction technique we can try other techniques such as SVD or FLD.
- ✓ In the multibiometric system, we have utilized multi-algorithm systems that consolidate the output of multiple feature extraction algorithms at score levels. The multibiometric system relies on the evidence presented by multiple sources of biometric information. There are six categories based on the nature of these sources: multi-sensor, multi-algorithm, multi instance, multi-sample, multimodal and hybrid. So, we can choose one of them instead of multi-algorithm systems that we have used. The fusion can be done at different levels based on the type of information available in a certain module. This includes fusion at the sensor, fusion at the feature levels, fusion at the match score, rank and decision levels. In this thesis we have used the fusion at decision level we suggest to integrate other fusion levels.
- ✓ Integrate face recognition to video surveillance. It is becoming more and more essential nowadays as society relies on video surveillance to improve security and safety.
- ✓ To improve the effectiveness of traditional face recognition systems working on 2D still images. We propose to use 3D face models since the availability of three dimensional (3D) data increased.

References

[1] Charles A. Shoniregun, S. Crosier. *Securing Biometrics Applications*. Springer Science+Business Media, LLC, 2008.

[2] Anil K. Jain, Patrick Flynn, Arun A. Ross. *Handbook of biometrics*. Springer Science+Business Media, LLC, 2008.

[3] S.S. Chikkerur. Online fingerprint verification system. *M.S. thesis, State Univ. of New York at Buffalo,* June 2005.

[4] Patrick Stadelmann. Features Extraction for Low-Power Face Verification. PhD thesis, 2008.

[5] Fingerprint recognition available at www.biometrics.gov/Documents/FingerprintRec.pdf,2006

[6] A. Ross, K. Nandakumar, and A. K. Jain. *Handbook of Multibiometrics*. 1st edition, Springer, New York, USA, 2006.

[7] P. Rosenzweig, A.Kochems, and A. Schwartz. Biometric Technologies: Security, Legal, and Policy Implications. *Legal memorandum*. No. 12. June 21, 2004

[8] K. Daimi and K. Snyder. Security Requirements for Multimodal Biometric Systems. conf/csreaSAM/DaimiS06, 2006

[9] B. Verma and M. Blumenstein. *Pattern Recognition Technologies and Applications: Recent Advances*. Information science reference. Hershey. New York. IGI Global, 2008.

[10] J. P. Campbell. Speaker recognition: a tutorial. *Proc. IEEE*, Vol. 85, No. 9, pp. 1437–1462, September 1997.

[11] Anil K. Jain, Arun Ross, Sharath Pankanti, Biometrics: A Tool for Information Security. *IEEE Transactions On Information Forensics And Security*, Vol. 1, No. 2, pp 125-143, June 2006.

[12] D. Maltoni, D. Maio, A. K. Jain, and S. Prabhakar, *Handbook of Fingerprint Recognition*. 2nd edition. Springer-Verlag London Limited, 2009.

[13] R. Bolle, Jonathan H. Connell, S. Pankanti, Nalini K. Ratha,Andrew W. Senior .*Guide to Biometrics*. Springer-Verlag New York,Inc, 2004

[14] John D. Woodward, John D. Woodward, Nicholas M. Orlans, Peter T. Higgins. Biometrics. The McGraw-Hill companies, 2003.

[15] S. Nanavati, M.Thieme, and R.Nanavati. *Biometrics Identity Verification in a Networked World*. A Wiley Tech Brief. John Wiley & Sons, Inc. 2002

[16] D. Petrovska-Delacrétaz, G. Chollet, and B. Dorizzi. *Guide to Biometric Reference Systems and Performance Evaluation*. Springer-Verlag London Limited, 2009.

[17] Jing Yan. Continuous authentication based on computer security. *Master's thesis,* Lulea, Sweden, May 2008.

[18] D. Kim and J. Sung. *Automated Face Analysis: Emerging Technologies and Research. Information Science Reference*. Hershey .New York. IGI Global, 2009.

[19] A. Eleyan and H. Demirel. PCA and LDA based Neural Networks for Human Face Recognition. Face Recognition, Book edited by: Kresimir Delac and Mislav Grgic, ISBN 978-3-902613-03-5, pp.558, I-Tech, Vienna, Austria, June 2007.

[20] M.W. Berry, S.T. Dumais, and Gavin W. O'Brien. Using linear algebra for intelligent information retrieval. *SIAM Review*, Vol. 37, pp. 573-595, 1995.

[21] Y. Pang, N. Yu, R. Zhang, J. Rong, and Z. Liu. Fusion Of SVD And LDA For Face Recognition. *IEEE*, pp. 1417- 1420, 2004

[22] Carmen Martínez and Olac Fuentes. Face Recognition Using Unlabeled Data. *Computación y Sistemas*. Vol. 7 No. 2 pp. 123 – 129, 2003.

[23] W. Zhao and R. Chellappa. *Face processing advanced modeling and methods*. Elsevier Inc, 2006

References

[24] W. Zhao, R. Chellappa, P. Phillips, and A. Rosenfeld, Face Recognition: A literature survey, *ACM Computing Surveys*, Vol. 35, No. 4, pp. 399-458, December 2003.

[25] A. S. Tolba, A.H. El-Baz, and A.A. El-Harby. Face Recognition: A Literature Review. *International Journal of Signal Processing*, Vol. 2, No. 2, pp 88-103, 2006.

[26] I. ATALAY. Face Recoginition Using Eigenfaces. *M.Sc Thesis, Istanbul Technical University Institute Of Science And Technology*, January 1996.

[27] J.-Y Gan and Y.-W. Zhang. A study of singular value decomposition of face image matrix. *In Proc. IEEE International Conference on Neural Networks and Signal Processing (ICNNSP'03*), Nanjing, China, pp. 14-17, December 2003.

[28] D. Masip, M. Bressan, J.Vitria. Feature Extraction Methods for Real-Time Face Detection and Classification. *EURASIP Journal on Applied Signal Processing*. vol. 2005, no. 13, pp. 2061-2071, 2005.

[29] S. Nagamalla and B. C. Dhara. A Novel Face Recognition Method using Facial Landmarks. *2009 Seventh International Conference on Advances in Pattern Recognition*, 2009.

[30] B. Heisele, P. Ho, J. Wu, and T. Poggio, Face recognition: component-based versus global approaches, Comput. Vision Image Understand. Vol. 91, No. 1-2, pp. 6–21, 2003.

[31] C. Kim, J. Oh, and C.H. Choi. Combined Subspace Method Using Global and Local Features for Face Recognition. *Proceedings of International Joint Conference on Neural Networks*, Montreal, Canada, July 31 - August 4 2005.

[32] B.A. Draper, K. Baek, M.S. Bartlett, and J.R. Beveridge. Recognizing Faces with PCA and ICA, Computer Vision and Image Understanding, Vol. 91, No. 1-2, pp. 115-137, 2003.

[33] Marian Stewart Bartlett, Javier R. Movellan, and Terrence J. Sejnowski, Face Recognition by Independent Component Analysis. *IEEE transactions on neural networks*, Vol. 13, No. 6, pp. 1450- 1463, November 2002.

[34] Francis R. Bach, Michael I. Jordan. Kernel Independent Component Analysis. *Journal of Machine Learning Research* Vol. 3, pp. 1-48. 2002

[35] Oja, E. and Hyvarinen, A. Independent component analysis: algorithms and applications. *Neural Networks,* Vol. 13, No. (4-5), pp. 411-430. 2000.

[36] Chengjun Liu and Harry Wechsler. Comparative Assessment of Independent Component Analysis (ICA) for Face Recognition. *Appears in the Second International Conference on Audio- and Video-based Biometric Person Authentication, AVBPA'99*, Washington D. C. USA, March 22-24 1999

[37] M. S. Bartlett, M. H. Lades, and T. J. Sejnowski, Independent component representations or face recognition. In *Human Vision and Electronic Imaging III*, Vol. 3299 of *Proceedings of SPIE*, pp. 528-539, San Jose, Calif, USA, January 1998.

[38] Hafed, Ziad M and Levine, Marin D. Face Recognition Using Discrete Cosine Transform. *International Journal of Computer Vision*, Vol. 43, No. 3, pp. 167-188, 2001.

[39] M. Rizon, M.H. Firdus, P. Saad, S. Yaacob, M.R. Mamat, A.Y.M. Shakkaf, A.R. Saad, Hdesa and M. Karthigayan. Face recognition using Eigenfaces and Neural Networks. *American Journal of Applied Sciences*, Vol. 2, pp. 1872-1875, 2006.

[40] Henry A. Rowley, Shumeet Baluja, and Takeo Kanade. Neural Network-Based Face Detection. *PAMI*, January 1998

[41] S. Ullman, M. Vidal-Naquet, E.Sali. Visual features of intermediate complexity and their use in classification. *Nature neuroscience*. Vol. 5, No. 7, pp. 682-687, July 2002.

References

[42] F. Jiao, W. Gao, X. Chen, G. Cui, and S. Shan. A Face Recognition Method Based on Local Feature Analysis. *The 5th Asian Conference on Computer Vision ACCV2002*. Melbourne, Australia. 23-25 January 2002

[43] I Cox, J. Ghosn, P.Yianilos, Feature-based face recognition using mixture-distance. *In: Proc. Int. Conf. Comput. Vis. Patt. Recogn*, pp. 209-216, 1996.

[44] P.S. Penev and J.J. Atick, .Local Feature Analysis: A General Statistical Theory for Object Representation,. *Network: Computations in Neural Systems*, Vol. 7, No. 3, pp. 477-500, 1996.

[45] R. Brunelli and T. Poggio. Face Recognition: Features versus Templates, *IEEE Trans. Pattern Analysis and Machine Intelligence*, Vol. 15, No. 10, pp. 1042-1052, October 1993.

[46] B.S.Manjunath, R. Chellappa, and C.v.d. Malsburg. A feature based approach to face recognition. *Proc. IEEE Conf. Comput. Vis Patt. Recogn*, pp. 373-378, 1992.

[48] A. Pentland, B. Moghaddam, and T. Starner. View-Based and Modular Eigenspaces for Face Recognition. *Proc. IEEE Computer Society Conf. Computer Vision and Pattern Recognition*, pp. 84-91, 1994.

[47] Wiskott, L., & von der Malsburg, C. (1996). Face recognition by dynamic link matching. In J. Sirosh, R. Miikkulainen, & Y. Choe (Eds.), *Lateral interactions in the cortex: structure and function* (Chap. 11) [Electronic book]. Austin, TX: UTCS Neural Networks Research Group. Available from http://www.cs.utexas.edu/users/nn/web-pubs/htmlbook96/.

[49] Laurenz Wiskott, Jean-Marc Fellous, Norbert Krüger,Christoph von der Malsburg. Face recognition by elastic bunch graph matching. *IEEE Trans. Pattern Analysis and Machine Intelligence*, Vol. 19, No. 7, pp. 775–779, 1997.

[50] A. V. Nefian and M. H. Hayes. Hidden Markov models for face recognition. In *Proceedings IEEE International Conference on Acoustics, Speech and Signal Processing (ICASSP)*, pp. 2721–2724, Seattle, May 1998.

[51] Hazim Kemal Ekenel and Rainer Stiefelhagen. Local Appearance based Face Recognition Using Discrete Cosine Transform. *Proceedings of the 13th European Signal Processing Conference (EUSIPCO)*, Antalya, Turkey, 2005.

[52] H. K. Ekenel, R. Stiefelhagen. Local Wavelet Analysis For Face Recognition.

[53] A. Pentland, B. Moghaddam, and T. Starner. View-Based and Modular Eigenspaces for Face Recognition. *Proc. IEEE Computer Society Conf. Computer Vision and Pattern Recognition*, pp. 84-91, 1994.

[54] P. S. Penev and J. J. Atick. Local feature analysis: A general statistical theory for object representation. *Network: Computation in Neural Systems,* Vol. 7, No. 3, pp. 477-500, 1996.

[55] A. Bronstein, M. Bronstein, and R. Kimmel. Expression-invariant 3d face recognition. In *Audio & Video-based Biometric Person Authentication (AVBPA)*, Vol. LNCS-2688, pp. 62–70, 2003.

[56] X. He, S. Yan, Y. Hu, P. Niyogi, and H.-J. Zhang. Face recognition using laplacianfaces. *IEEE Trans. Pattern Anal. Mach. Intell.*, Vol. 27, No. 3, pp. 328-3410, March 2005.

[57] P. J. Phillips, H. Moo, S. A. Rizvi, and P. J. Rauss. The FERET evaluation methodology for face recognition algorithms. *IEEE Trans. Pattern Anal. Mach. Intell.,* Vol. 22, No. 10, pp. 1090–1104, October 2000.

[58] H. Cevikalp, M. Neamtu, M. Wilkes, and A. Barkana. Discriminative Common Vectors for Face Recognition. *IEEE Trans. Pattern Analysis and Machine Intelligence*, Vol. 27, No. 1, pp. 4-13, January 2005.

[59] A. Levin and A. Shashua. Principal Component Analysis Over Continuous Subspaces and Intersection of Half-Spaces", *Proc. of the European Conference on Computer Vision (ECCV),* Copenhagen, Denmark, May 2002.

References

[60] S. Z. Li, X. W. Hou, H. J. Zhang, Q. S. Cheng. Learning Spatially Localized, Parts-Based Representation. *IEEE Int. Conf. on Computer Vision and Pattern Recognition*, Hawaii, December 11-13, 2001

[61] A. Martinez and A.C. Kak, .PCA versus LDA. *IEEE Trans. Pattern Analysis and Machine Intelligence*, Vol. 23, No. 2, pp. 228-233, February 2001.

[62] T. Shakunaga and K. Shigenari. Decomposed Eigenface for Face Recognition under Various Lighting Conditions. *IEEE Int. Conf. on Computer Vision and Pattern Recognition,* Hawaii, Dec. 11-13, 2001.

[63] J. Yang, Y. Yu, and W. Kunz. An Efficient LDA Algorithm for Face Recognition. *The sixth International Conference on Control, Automation, Robotics and Vision*, Singapore, 2000

[64] W. Zhao, R. Chellappa, and P. J. Phillips. Subspace Linear Discriminant Analysis for Face Recognition. *Technical Report CAR-TR-914*, Center for Automation Research, University of Maryland, 1999.

[65] I.T. Jolliffe. Principal Component Analysis. Springer, 2nd edition, 2002.

[66] Önsen TOYGAR and Adnan ACAN. Face Recognition Using PCA, LDA And ICA Approaches On Colored Images. *Istanbul University – Journal Of Electrical & Electronics Engineering*. Vol. 3, No. 1, pp. 735-743 .2003

[67] J. R. Beveridge, D. Bolme, B. A. Draper, and M. Teixera. The CSU face identification evaluation system. *Machine Vision and Applications*, 2004.

[68] Michihiro Uenohara and Takeo Kanade. Use of fourier and Karhunen-Loeve decomposition for fast pattern matching with a large set of template. IEEE Transactions On Pattern Analysis And Machine Intelligence, Vol. 19, No. 8, pp. 891-898, August 1997.

[69] M. Kirby and L. Sirovich. Application of the Karhunen-Loeve procedure for the characterization of human faces. *IEEE Trans. Pattern Analysis and Machine Intelligence*, Vol. 12, No. 1, pp. 103-108, 1990.

[70] L. Sirovich and M. Kirby. Low-Dimensional Procedure for the Characterization of Human Faces. *Journal of the Optical Society of America A*, Vol. 4, pp. 519-524, 1987.

[71] C. Liu and H.Wechsler. Gabor Feature Based Classification Using the Enhanced Fisher Linear Discriminant Model for Face Recognition. *IEEE Trans. Image Processing*, Vol. 11, No. 4, pp. 467-476, 2002.

[72] M. Turk and A. Pentland. Eigenfaces for recognition. *J. of Cognitive Neuroscience*, Vol. 3, pp. 71-86, 1991.

[73] M.A. Turk, A.P. Pentland, Face recognition using eigenfaces. *Proceedings of the International Conference on Pattern Recognition*, pp. 586-591, 1991.

[74] M.A. Grudin. On Internal Representations in Face Recognition Systems. *Pattern Recognition*, Vol. 33, No. 7, pp. 1161-1177, 2000.

[75] J. Yang, Y. Yu, and W. Kunz. An Efficient LDA Algorithm for Face Recognition. *The sixth International Conference on Control, Automation, Robotics and Vision*, Singapore, 2000.

[76] K. Kim. Face recognition using principle component analysis. *Tutorial*, University of Maryland, College Park.

[77] Rahul Garg and Varun Gulshan. PCA: Face Recognition, Overview. October 29 2005.available at *www.cs.washington.edu/homes/rahul/data/reportPCA.pdf*

[78] P.S. Penev and L. Sirovich. The Global Dimensionality of Face Space. *Proc. Fourth IEEE Int'l Conf. Automatic Face and Gesture Recognition*, pp. 264-270, Grenoble, France, March 26-30 2000.

References

[79] L. Wiskott1z, Jean-Marc Fellous, Norbert Kr□uger1, Christoph von der Malsburg. Face Recognition by Elastic Bunch Graph Matching. *In Intelligent Biometric Techniques in Fingerprint and Face Recognition*, eds. L.C. Jain et al., publ. CRC Press, ISBN 0-8493-2055-0, Chapter 11, pp. 355-396, 1999.

[80] Kramer, M.A. Nonlinear principle component analysis using auto-associative Neural networks. *American Institution Chemical Engineering Journal*, Vol. 32, No. 2, 1991

[81] Marian Stewart Bartlett, Javier R. Movellan, and Terrence J. Sejnowski, Face Recognition by Independent Component Analysis. *IEEE transactions on neural networks*, Vol. 13, No. 6, pp. 1450- 1463, November 2002.

[82] Yang, M., Ahuja, N., Kriegman, D. Face recognition using kernel Eigenfaces. In *Proceedings of International Conference of Image Processing*. Vol. 1, pp. 37-40, 2000.

[83] Jian Yang, David Zhang, Senior Member, Alejandro F. Frangi, and Jing-yu Yang. Two-Dimensional PCA: A New Approach to Appearance-Based Face Representation and Recognition. *IEEE transactions on pattern analysis and machine intelligence*, VOL. 26, NO. 1, pp 131-137, January 2004.

[84] J. Yang and J.Y. Yang. From image vector to matrix: a straightforward image projection technique-IMPCA vs. PCA. *Pattern Recognition*, Vol. 35, pp. 1997-1999, 2002.

[85] D. Zhang and Z.-H. Zhou. (2D) 2PCA: Two-directional two-dimensional PCA for efficient face representation and recognition. *Neurocomputing*, Vol. 69, pp. 224-231, 2005.

[86] D. Zhang, Z.-H. Zhou and S. Chen. Diagonal principal component analysis for face recognition, *Pattern Recognition*, Vol. 39, pp 140-142, 2006.

[87] S. Chen, Y. Zhu, D. Zhang, and J.-Y. Yang. Feature extraction approaches based on matrix pattern: MatPCA and MatFLDA. *Pattern Recognition Letter*, Vol. 26, pp. 1157-1167, 2005.

[88] H. Kong, L. Wang, E. K. Teoh, X. Li, J.-G. Wang and R. Venkateswarlu. Generalized 2D principal component analysis for face image representation and recognition. *Neural Networks*, Vol. 18, pp. 585-594, 2005.

[89] W. Zuo, D. Zhang, and K. Wang. Bidirectional PCA with assembled matrix distance metric for image recognition. *IEEE Transactions on Systems*, Man and Cybernetics, Part B, Vol. 36, pp. 863-872, 2006.

[90] Ho, T.K. The random subspace method for constructing decision forests. *IEEE Transactions on Pattern Analysis and Machine Intelligence*, Vol. 10, No. 8, pp. 832-844, 1998.

[91] N. Nguyen, W. Liu and S. Venkatesh. Random Subspace Two-Dimensional PCA for Face Recognition. Department of Computing, Curtin University of Technology, WA 6845, Australia. available at http://impca.cs.curtin.edu.au/pubs/2007/conferences/nguyen_liu_venkatesh_pcm07.pdf.

[92] S. Shan, B. Cao, Y. Su, L. Qing, X. Chen, and W. Gao. Unified Principal Component Analysis with Generalized Covariance Matrix for Face Recognition. *IEEE*, 2008.

[93] X. Jiang. Asymmetric Principal Component And Discriminant Analyses For Pattern Classification. *IEEE transactions on pattern analysis and machine intelligence*, Vol. 31, No. 5, pp 931- 937, May 2009.

[94] P.N. Belhumeur, J.P. Hespanha, and D.J. Kriegman, .Eigenfaces vs. Fisherfaces: Recognition Using Class Specific Linear Projection. *IEEE Trans. Pattern Analysis and Machine Intelligence*, Vol. 19, No. 7, pp. 711- 720, July 1997.

[95] J. Lu, K.N. Plataniotis, and A.N. Venetsanopoulos. Face Recognition Using LDA-Based Algorithms. *IEEE Trans. Neural Networks*, Vol. 14, No. 1, pp. 195-200, January 2003.

[96] H. Yu and J. Yang. A Direct LDA Algorithms for High-dimensional Data with application to Face Recognition. *Pattern Recognition*, Vol. 34, pp. 2067-2070, 2001.

[97] R.Huang, Q.S.Liu, H.Q.Lu and S.D.Ma. Solving the Small Sample Size Problem of LDA. *In the proc. of Int. Conf. Pattern Recognition*, Vol. 3, pp 29-32, Quebec, Canada, August 2002.

References

[98] Juwei Lu, K.N. Plataniotis, A.N. Venetsanopoulos. Regularized discriminant analysis for the small sample size problem in face recognition. Pattern Recognition Letters 24 pp. 3079–3087, 2003

[99] L.-F. Chen, H.-Y.M. Liao, M.-T. Ko, J.-C. Lin and G.-J. Yu. A New LDA-Based Face Recognition System which can Solve the Small Sample Size Problem. *Pattern Recognition*, Vol. 33, pp. 1713-1726, 2000.

[100] Q. Liu, X. Tang, H. Lu, and S. Ma. Face Recognition Using Kernel Scatter-Difference-Based Discriminant Analysis. IEEE Transactions On Neural Networks, Vol. 17, No. 4, pp 1081-1085, July 2006.

[101] X. Wang, X. Tang. Dual-Space Linear Discriminant Analysis for Face Recognition. *Proceedings of the 2004 IEEE Computer Society Conference on Computer Vision and Pattern Recognition (CVPR'04).*

[102] Liu CJ, Wechsler H. Enhanced fisher linear discriminant models for face recognition. In: *Proceedings of international conference on pattern recognition*, pp. 1368-1372, 1998.

[103] X. Wang and X. Tang. Random Sampling LDA for Face Recognition. *Proc. IEEE Computer Society Conf. Computer Vision and Pattern Recognition*, Vol. 2, pp. 259-265, 2004.

[104] K. Fukunaga, *Introduction to Statistical Pattern Recognition*, 2nd ed. New York: Academic Press, 1990.

[105] C. Liu and H. Wechsler. Face recognition using Evolutionary pursuit. *Appears in the fifth European conference on computer vision, ECCV'98*, university of Freiburg, Germany, June 2-6, 1998.

[106] K. Etemad and R. Chellappa. Discriminant analysis for recognition of human face images. *J. Opt. Soc. Am. A*/ Vol. 14, No. 8, pp. 1724-1733, August 1997

[107] J. Ye. Generalized low rank approximations of matrices. in the Proceedings of the Twenty-First International Conference on Machine Learning (Outstanding Student Paper), Banff, Alberta, Canada, pp. 887-894, 2004.

[108] X. He, D. Cai, and P. Niyogi. Tensor subspace analysis. In *Neural Information Processing Systems*, pp. 499-506, December 2005.

[109] G. Golub and C. Van Loan. *Matrix Computations*, 3rd edition. Johns Hopkins, Baltimore, 1996.

[110] Thaahirah S. M. Rasied, Othman O. Khalifa and Yuslina Binti Kamarudin. Human Face Recognition Based on Singular valued Decomposition and Neural Network. *GVIP 05 Conference*, CICC, Cairo, Egypt, 19-21 December 2005.

[111] Y. H. Wang, T. N. Tan and Y. Zhu. Face Verification Based on Singular Value Decomposition and Radial Basis Function Neural Network. *National Laboratory of Pattern Recognition (NLPR)*, Institute of Automation, Chinese Academy of Sciences.

[112] S. Noushath, A. Rao, and G. Hemantha Kumar. SVD based algorithms for robust face and object recognition in robot vision and application. *24th international symposium on automation & robotics in construction (ISARC) construction automation group IIT*. Madras. pp 473-477, 2007.

[113] Tat-Jun Chin, K. Schindler, and D. Suter. Incremental Kernel SVD for Face Recognition with Image Sets. *Proceedings of the 7th International Conference on Automatic Face and Gesture Recognition (FGR'06) IEEE*, 2006.

[114] Chou-Hao Hsu. Chaur-Chin Chen. SVD-Based Projection for Face Recognition. *IEEE EIT Proceedings*, pp 703-706, 2007.

[115] R. Tjahyadi, W. Liu, and S. Venkatesh. Application of the DCT Energy Histogram for Face Recognition. *Submitted to the Proceedings of the 2nd International Conference on Information Technology for Application (ICITA)*, pp. 305- 310, 2004.

References

[116] Willie L. Scott, II. Block-level discrete cosine transform coefficients for autonomic face recognition. PhD thesis. *Louisiana State University and Agricultural and Mechanical College*, USA, May 2003.

[117] S. Wong. Energy Compaction by Orthonormal Transform. *EE392c Project Report*, December 1997.

[118] Z. Pan and H. Bolouri. High Speed Face Recognition Based on Discrete Cosine Transforms and Neural Networks. *Technical report, Univ. of Hertfordshire*, September 27 1999.

[119] Vinayadatt V. Kohir and U. B. Desai. Face Recognition Using A DCT-HMM Approach. *IEEE*, pp. 226-231, 1998.

[120] Y.Chen. Y.Zhao. Face Recognition Using DCT and Hierarchical RBF Model. IDEAL 2006, LNCS 4224, pp. 355–362, 2006.

[121] J. Nagi, S. K. Ahmed, and F. Nagi. A MATLAB based Face Recognition System using Image Processing and Neural Networks. In *Proc. of 4th International Colloquium on Signal Processing and its Applications*, pp. 83-88, 2008.

[122] S. A. Khayam. The Discrete Cosine Transform (DCT): Theory and Application. *Technical Report WAVES-TR-ECE802.602, Michigan State University*, 2003.

[123] J.Nagi1, S. Khaleel Ahmed, and F. Nagi. Pose Invariant Face Recognition using Hybrid DWT-DCT Frequency Features with Support Vector Machines. In *Proceedings of the 4th International Conference on Information Technology and Multimedia at UNITEN (ICIMU')*, Malaysia, pp. 99 - 104, 2008.

[124] L. Ma, Y. Xiao, K. Khorasani, and R. K. Ward. A new facial expression recognition technique using 2D DCT and k-means algorithm. In *Proc. International Conference on Image Processing*, pp. 1269-1272, October 2004.

[125] L. Ma and K. Khorasani. Facial expression recognition using constructive feedforward neural networks. *IEEE Transactions on Systems, Man and Cybernetics*, Part B, Vol. 34, No. 3, pp. 1588 -1595, June 2004.

[126] Y. Chen, S. Jiang, and A. Abraham. Face Recognition Using DCT and Hybrid flexible Neural Tree. *In Proc. of the International Conference on Neural Networks and Brain*. pp. 1459-1463, 2005.

[127] M. Hassan, I. Osman, and M. Yahia. Walsh-Hadamard Transform for Facial Feature Extraction in Face Recognition. *International Journal of Computer and Information Science and Engineering*, Vol.1, No. 3, pp 167- 171, 2007.

[128] M. Hajiarbabi, J. Askari, S. Sadri, and M. Saraee. Face Recognition using Discrete Cosine Transform plus Linear Discriminant Analysis. *Proceedings of the World Congress on Engineering*, Vol I WCE 2007, London, U.K, July 2 - 4, 2007.

[129] J. Choi, Y. Chung, K. Kim, and J. Yoo. Face Recognition Using Energy Probability in DCT Domain; *IEEE*. pp. 1549-1552. ICME, 2006.

[130] James S. Walker. *A Primer On Wavelets And Their Scientific Applications.* 2nd edition. Taylor & Francis Group, LLC, 2008.

[131] H.K. Ekenel and B. Sankur. Multiresolution Face Recognition. *Image and Vision Computing*, Vol. 23, No. 5, pp. 469-477, 2005

[132] G.C. Feng, P.C. Yuen, D.Q. Dai. Human face recognition using PCA on wavelet subband. *SPIE Journal of Electronic Imaging*, Vol. 9, No.2, pp. 226–233, 2000.

[133] C. Garcia et al. Wavelet packet analysis for face recognition. *Image and Vision Computing*, Vol. 18, No.4, pp. 289-297, 2000.

[134] Dao-Qing Dai and P. C. Yuen. Wavelet-Based 2-Parameter Regularized Discriminant Analysis for Face Recognition. *Proc. AVBPA Int'l Conf. Audio-and Video-Based Biometric Person Authentication*, pp. 137-144, June, 2003.

References

[135] Bai-Ling Zhang, Haihong Zhang, Shuzhi Sam Ge, Face Recognition by Applying Wavelet Subband Representation and Kernel Associative Memory. *IEEE Transactions On Neural Networks*, Vol. 15, No. 1, pp. 166-177, January 2004.

[136] V.Perlibakas. Face Recognition Using Principal Component Analysis and Wavelet Packet Decomposition. *INFORMATICA*, Vol. 15, No. 2, pp. 243–250, 2004.

[137] Chao-Chun Liu, Dao-Qing Dai and H. Yan. Local Discriminant Wavelet Packet Coordinates for Face Recognition, *Journal of Machine Learning Research* 8, 1165-1195, 2007.

[138] B. Li, Y. Liu. When Eigenfaces are combined with Wavelets. *Knowledge-Based Systems*, Vol. 15, No. 5-6, pp. 343-347, 2002

[139] R. Hassanpour, A. Shahbahrami, and S. Wong. Adaptive Gaussian Mixture Model for Skin Color Segmentation. *Proceedings Of World Academy Of Science*, *Engineering And Technology*, Vol 31 ISSN 1307-6884, July 2008.

[140] D. Chai and K. N. Ngan .Face segmentagion using skin-color map in videophone applications. *IEEE Trans. on Circuits and System for video Technology*, Vol. 9, No.4, pp. 551-564, 1999.

[141] B. Ulery, A. Hicklin, C. Watson, W. Fellner, and P. Hallinan. Studies of biometric fusion. *Technical Report NISTIR* 7346, NIST, September 2006.

[142] Arun Ross and Anil K. Jain. Multimodal Biometrics: An Overview. *Appeared in Proc. of 12th European Signal Processing Conference (EUSIPCO)*, Vienna, Austria, pp. 1221-1224, September 2004.

[143] A. Ross, K. Nandakumar, and A. K. Jain. *Handbook of Multibiometrics*. 1st edition, Springer, New York, USA, 2006.

[144] M. Tistarelli, Stan Z. Li, and R. Chellappa. *Handbook of Remote Biometrics for Surveillance and Security*. Advances in Pattern Recognition. Springer-Verlag London, April 2009.

[145] S. Prabhakar and A. K. Jain. Decision-level fusion in fingerprint verification. Pattern Recognition 35 pp. 861–874, October 2002.

[146] Arun Ross. An Introduction To Multibiometrics. Appeared in *proceeding of the 15 th European signal processing conference (EUSIPCO)*,(Poznan, Poland), September 2007.

[147] K. I. Chang, K. W. Bowyer, and P. J. Flynn. Face recognition using 2D and 3D facial data. In *Proc. Of Workshop on Multimodal User Authentication*, (Santa Barbara, CA), pp. 25-32, December 2003.

[148] A. Kumar, D. C. M. Wong, H. C. Shen, and A. K. Jain. Personal verification using palmprint and hand geometry biometric. In *Proc. of 4th Int'l Conf. on Audio and Video-based Biometric Person Authentication (AVBPA)*, (Guildford, UK), pp. 668-678, June 2003.

[149] X. Chen, P. J. Flynn, and K. W. Bowyer. IR and Visible light face recognition. *Computer Vision and Image Understanding*, Vol. 99, No 3, pp. 332–358, September 2005.

[150] A. Kong, J. Heo, B. Abidi, J. Paik, and M. Abidi. Recent advances in visual and infrared face recognition – a review. *Computer Vision and Image Understanding*, Vol. 97, No. 1, pp. 103–135, January 2005.

[151] G. Bebis, A. Gyaourova, S. Singh, and I. Pavlidis. Face recognition by fusing thermal infrared and visible imagery. *Image and Vision Computing* 24, 727–742, January 2006.

[152] H.Chang, A.Koschan, M.Abidi, Seong G. Kong, and Chang-Hee Won. Multispectral Visible and Infrared Imaging for Face Recognition. *IEEE*, 2008.

[153] Zhihong Pan, Glenn Healey, Manish Prasad, and Bruce. Tromberg. Face recognition in hyperspectral images. *IEEE Transactions on Pattern Analysis and Machine Intelligence*, Vol. 25, No. 12, pp. 1552–1560, December 2003.

[154] G. L. Marcialis and F. Roli. Fingerprint verification by fusion of optical and capacitive sensors. *Pattern Recognition Letters*, Vol. 25, No. 11, pp. 1315–1322, August 2004.

References

[155] Arun Rossa; Anil Jaina, James Reismanb. A hybrid fingerprint matcher. Pattern Recognition 36, pp. 1661-1673, 2003.

[156] X. Lu, Y. Wang, A.K. Jain, Combining classifiers for face recognition, in: Proceedings of the ICME 2003, Baltimore, MD, pp. 13-16, July 6-9 2003.

[157] Seong G. Kong, Jingu Heo, Besma R. Abidi, Joonki Paik, and Mongi A. Abidi. Recent advances in visual and infrared face recognition—a review. *Computer Vision and Image Understanding*, Vol. 97, No. 1, pp. 103-135, January 2005.

[158] Z. Wu, L. Cai, and H. Meng. Multi-level Fusion of Audio and Visual Features for Speaker Identification. *International Conference on Biometrics, ICB 2006*, Lecture Notes in Computer Science(LNCS), Vol. 3832, pp. 493- 499, 2005.

[159] J. Jang, K. R. Park, J. Son, and Y. Lee. Multi-unit Iris Recognition System by Image Check Algorithm. In *Proceedings of International Conference on Biometric Authentication (ICBA)*, pp. 450–457, Hong Kong, July 2004.

[160] M.C. Cheung, M.W. Mak, and S.Y. Kung, Multi-Sample Data-Dependent Fusion of Sorted Score Sequences for Biometric verification. *In Proc. of the IEEE Conference on Acoustics Speech and Signal Processing (ICASSP04),* Montreal, Canada, pp. 229-232, 2004.

[161] U. Uludag, A. Ross, and A. K. Jain. Biometric template selection and update: A case study in fingerprints. *Pattern Recognition*, Vol. 37, No. 7, pp.1533–1542, July 2004

[162] M.C. Cheung, K.K. Yiu, M.W. Mak, and S.Y. Kung, Multi-Sample Fusion with Contrained Feature Transformation for Robust Speaker Verification. *In Proc. of the IEEE Conference on Acoustics Speech and Signal Processing (ICASSP04),* Montreal, Canada, pp. 1813-1816, 2004

[163] S. Abdul, S. Dzati, A. Ramli, and A. Hussain. A Comparative Study on Multi-Sample Fusion Schemes to Enhance Spectrographic Speaker Verification. *6th WSEAS International Conference on Circuits, Systems, Electronics, Control & Signal Processing*, Cairo, Egypt, 335-340, December 29-31, 2007.

[164] E. S. Bigun, J. Bigun, B. Duc, and S. Fischer. Expert conciliation for multimodal person authentication systems using bayesian statistics. In *First International Conference on Audio and Video-Based Biometric Person Authentication (AVBPA)*, pp. 291-300, Crans-Montana, Switzerland, March 1997.

[165] R. Brunelli and D. Falavigna. Person identification using multiple cues. *IEEE Transactions on Pattern Analysis and Machine Intelligence*, Vol. 17, No. 10, pp. 955-966, October 1995.

[166] Amit Kale, Amit K. RoyChowdhury and Rama Chellappa. Fusion Of Gait And Face For Human Identification. In *IEEE International Conference on Acoustics, Speech, and Signal Processing (ICASSP)*, pp. (V-901) - (v-904), 2004.

[167] Souheil Ben-Yacoub, Yousri Abdeljaoued, and Eddy Mayoraz. Fusion of Face and Speech Data for Person Identity Verification. *IEEE Transactions On Neural Networks*, Vol. 10, No. 5, pp. 1065-1074, September 1999.

[168] S. Ribaric and I. Fratric. A Biometric Identification System Based on Eigenpalm and Eigenfinger Features. *IEEE Transactions On Pattern Analysis And Machine Intelligence*, Vol. 27, No. 11, pp. 1698-1709, November 2005.

[169] Chang, K., et al. Comparison and combination of ear and face images in appearance based biometrics. *IEEE Transactions On Pattern Analysis And Machine Intelligence*, Vol. 25, No. 9, pp. 1160-1165, September 2003.

[170] Dr. Hana'a, and M. Salman. Fusion Face And Palmprint For Human Recognition Via Spectral Eigenvector. *Engineering &Technical Journal*, Vol.27, No.4, pp 788-798, 2009.

[171] A. Pentland, B. Moghaddam, and T. Starner. View-Based and Modular Eigenspaces for Face Recognition. *Proc. IEEE Computer Society Conf. Computer Vision and Pattern Recognition*, pp. 84-91, 1994.

References

[172] A. Rattani and M. Tistarelli. Robust Multi-Modal And Multi-Unit Feature Level Fusion Of Face And Iris Biometrics. *Technical Report* No. CVL -2008-003, December 2008.

[173] A. Ross, S. Shah, and J. Shah. Image versus feature mosaicing: A case study in fingerprints. In *Proceedings of SPIE Conference on Biometric Technology for Human Identification III*, pages 620208–1 – 620208–12, Orlando, USA, April 2006.

[174] R. Singh, M. Vatsa, A. Ross, and A. Noore. Performance enhancement of 2D faces recognition via mosaicing. In *Proceedings of the 4th IEEE Workshop on Automatic Identification Advanced Technologies (AuotID)*, pp. 63-68, Buffalo, USA, October 2005.

[175] Y.-L. Zhang, J. Yang, and H. Wu. A Hybrid Swipe Fingerprint Mosaicing Scheme. In *Proceedings of Fifth International Conference on Audio- and Video- Based Biometric Person Authentication (AVBPA)*, pages 131-140, Rye Brook, USA, July 2005.

[176] K. Choi, H. Choi, and J. Kim. Fingerprint Mosaicking by Rolling and Sliding. In *Proceedings of Fifth International Conference on Audio- and Video-Based Biometric Person Authentication (AVBPA)*, pp. 260-269, Rye Brook, USA, July 2005.

[177] A. K. Jain and A. Ross. Fingerprint Mosaicking. In *IEEE International Conference on Acoustics, Speech, and Signal Processing (ICASSP)*, Vol. 4, pp. 4064-4067, Orlando, Florida, May 2002.

[178] Y. S. Moon, H. W. Yeung, K. C. Chan, and S. O. Chan. Template Synthesis and Image Mosaicking for Fingerprint Registration: An Experimental Study. In *IEEE International Conference on Acoustics, Speech, and Signal Processing (ICASSP)*, Vol. 5, pp. 409-412, Montreal, Canada, May 2004.

[179] N. K. Ratha, J. H. Connell, and R. M. Bolle. Image Mosaicing For Rolled Fingerprint Construction. In *Proceedings of Fourteenth International Conference on Pattern Recognition (ICPR)*, Vol. 2, pp. 1651-1653, Brisbane, Australia, August 1998.

[180] A. Ross and R. Govindarajan. Feature Level Fusion Using Hand and Face Biometrics. *Appeared in Proceeding of SPIE Conference on Biometric Technology for Human Identification II*, Vol. 5779, pp.196-204, Orlando, USA, march 2005.

[181] J.Gan. Y.Liang. A Method for Face and Iris Feature Fusion in Identity Authentication .*IJCSNS International Journal of Computer Science and Network Security*, Vol.6 No.2B, pp135-138, February 2006.

[182] A. Kumar and D. Zhang. Personal Authentication using Multiple Palmprint Representation. *Pattern Recognition*, Vol. 38, No. 10, pp. 1695-1704, October 2005.

[183] A. Ross and R. Govindarajan. Feature Level Fusion Using Hand and Face Biometrics. In *Proceedings of SPIE Conference on Biometric Technology for Human Identification II*, Vol. 5779, pp. 196-204, Orlando, USA, March 2005.

[184] J. Jang and H. Kim. Score-level Fusion in Multiple Biometrics using Non-linear Classification. *10th Intl. Conf. on Control, Automation, Robotics and Vision*. Hanoi, Vietnam, 17–20 Dec 2008.

[185] A. Ross, K. Nandakumar, and A. K. Jain. *Handbook of Multibiometrics*. 1^{st} edition, Springer, New York, USA, 2006.

[186] S. C. Dass, K. Nandakumar, and A. K. Jain. A Principled approach to score level fusion in multimodal biometric systems. In *Proceedings of Fifth International Conference on Audio and Video-based Biometric Person Authentication (AVBPA)*, pp1049-1058, Rye Brook, USA, July 2005.

[187] A. K. Jain, K. Nandakumar, and A. Ross. Score normalization in multimodal biometric systems. *Pattern Recognition*, Vol. 38, No.12, pp. 2270-2285, December 2005.

References

[188] P. Verlinde and G. Cholet. Comparing decision fusion paradigms using k-NN based classifiers, decision trees and logistic regression in a multi-modal identity verification application. In *Proceedings of Second International Conference on Audio- and Video-Based Biometric Person Authentication (AVBPA)*, pp. 188-193, Washington D.C., USA, March 1999.

[189] J. Daugman. Combining Multiple Biometrics. Available at http://www.cl.cam.ac.uk/users/jgd1000 /combine/combine.html, 2000.

[190] L. Lam and C. Y. Suen. Application of majority voting to pattern recognition: An analysis of its behavior and performance. *IEEE Transactions on Systems, Man, and Cybernetics, Part A: Systems and Humans*, Vol. 27, No. 5, pp. 553-568, September 1997.

[191] L. Xu, A. Krzyzak, and C. Y. Suen. Methods for combining multiple classifiers and their applications to handwriting recognition. *IEEE Transactions on Systems, Man, and Cybernetics*, Vol. 22, No. 3, pp. 418-435, 1992.

[192] Y. S. Huang and C. Y. Suen. Method of combining multiple experts for the recognition of unconstrained handwritten numerals. *IEEE Transactions on Pattern Analysis and Machine Intelligence*, Vol. 17, No. 1, pp. 90-94, January 1995.

[193] C.Wang, Y.Li, H.Zhang, L.Wang. Multi-Modal Biometric Verification Based on FAR-score Normalization. IJCSNS International Journal of Computer Science and Network Security, Vol.8 No.4, pp. 250-254, April 2008.

[194] X. Lu, Y. Wang, A.K. Jain, Combining classifiers for face recognition, in: Proceedings of the ICME 2003, Baltimore, MD, pp. 13-16, July 6-9 2003.

[195] M. Indovina, U. Uludag, R. Snelick, A. Mink and A. Jain. Multimodal Biometric Authentication Methods: A COTS Approach. In Proc. MMUA Workshop on Multimodal User Authentication, pp. 99-106, (Santa Barbara, CA), December 2003.

[196] J.R. Beveridge, K. She, B. Draper, and G.H. Givens, A nonparametric statistical comparison of principal component and linear discriminant subspaces for face recognition, *Proc IEEE Conf Computer Vision and Pattern Recognition*,
Kauai, HI, December, 2001a, pp. 535–542.

[197] P. Navarrete, J. Ruiz-del-Solar. Analysis and Comparison of Eigenspace-Based Face Recognition Approaches. *International Journal of Pattern Recognition and Artificial Intelligence*, Vol. 16, No. 7, pp. 817-830, November 2002.

[198] W. Zhao, R. Chellappa, A. Krishnaswamy. Discriminant Analysis of Principal Components for Face Recognition. *Proc. Of the 3rd IEEE International Conference on Automatic Face and Gesture Recognition*, 14- 16 April 1998, Nara, Japan, pp. 336-341

[199] Nadjet Radji, Dr Dalila Cherifi, Dr.H.Benterzi. Face Recognition using PCA and WPD in YCbCr Color Space. ISSSPA'09, Oran, ALGERIE, 3-7 October, 2009.